The impact of glucose on *Staphylococcus aureus* virulence

by

Amelia Carole Stephens

Bachelor of Science, University of Maryland, 2016

Submitted to the Graduate Faculty of the

School of Medicine in partial fulfillment

of the requirements for the degree of

Doctor of Philosophy

University of Pittsburgh

2022

UNIVERSITY OF PITTSBURGH

SCHOOL OF MEDICINE

This dissertation was presented

by

Amelia Carole Stephens

It was defended on

September 7, 2022

and approved by

Vaughn S. Cooper, Professor, Department of Microbiology and Molecular Genetics

Jennifer Bomberger, Associate Professor, Department of Microbiology and Molecular Genetics

John F. Alcorn, Professor, Department of Pediatrics

Nara Lee, Assistant Professor, Department of Microbiology and Molecular Genetics

Dissertation Director: Anthony R. Richardson, Associate Professor, Department of Microbiology and Molecular Genetics

The impact of glucose on *Staphylococcus aureus* virulence

Amelia Carole Stephens, PhD

University of Pittsburgh, 2022

Staphylococcus aureus is a dangerous human pathogen capable of causing a variety of infections, from minor skin and soft tissue infections to life-threatening invasive infections such as endocarditis, osteomyelitis, and bacteremia/sepsis. Garnering more information on how this pathogen is so infectious in so many environments is key to understanding how severe infections can be treated. The rise of antibiotic resistance makes this knowledge even more important, as methicillin-resistant *S. aureus* (MRSA) is pervasive in the community today. Historically, focus on *S. aureus* pathogenesis has been on the production of toxins and proteases by the bacterium during infection. In the past few decades, a rising appreciation for other aspects of pathogenesis has arisen; for example, investigation of how bacterial metabolism has been shaped by the host immune system. This dissertation will focus on how carbon source metabolism, specifically, the metabolism of glucose, results in alterations to *S. aureus* pathogenesis in the following areas: 1) the impact of glucose on virulence factor expression in a hyperglycemic host environment; 2) the impact of metabolic regulators of carbon metabolism on virulence factor expression; 3) the impact of glucose on gene expression under host immune stress and the connection to phosphate transport; and 4) the impact of glucose on *ldh1* expression and the downstream effects this expression has on immune response resistance. These insights are collectively discussed and their contribution in the context of understanding *S. aureus* pathogenesis is presented.

Table of Contents

List of Tables

List of Figures

Preface

This dissertation would not have been possible if not for the help, mentorship, and support of many individuals. I would first like to thank Kelly Hurley, for her hours of troubleshooting help and for being a constant companion for the last five years. Thanks to Dr. Lance Thurlow and Dr. Srijon Bannerjee for helping with the animal and cell culture experiments. I would also like to acknowledge Dr. Anthony Richardson for being a fantastic mentor and friend for the last five years. I can attribute my love for bacterial genetics and metabolism to his enthusiasm and support throughout my PhD. I would like to thank Dr. Jennifer Bomberger and Dr. Vaughn Cooper for being wonderful mentors to me as well. You always have an open door and a willing ear with any questions or concerns I have. Thanks as well to Dr. John Alcorn and Dr. Nara Lee – you have all made up the best and most supportive committee I could have asked for. Many thanks as well to Kristin DiGiacomo, who always had the answers I needed.

I have so many people who supported me on my way here. Allison Haas, my lunch buddy for five years, I could not have gotten through tough times without you there for commiseration. Pam Brigleb and Alex Wells, I love our group chat more than anything – but Pam, get an iPhone. Maggie Vesper, best roommate I could have asked for. Angel, Rollo, and Loaf, who never fail to cheer me up with Ws. To my family, thank you for your patience and understanding these last five years. Mom, yes, I will call you more now. Sarah, I loved being distracted by helping you plan your wedding. Abby, I can't wait to live near you again. Dad, your positive notes are a ray of sunshine in my life. Finally, and most important, to my partner, Collin McCourt – thank you for being the understanding, calm, patient, caring, and supportive person that I needed you to be. And thank you equally for the reality checks you give me when I need them. Love you all.

1.0 Introduction

The versatility of *Staphylococcus aureus* as a pathogen lies in its variety. The variety of environments it can infect, the variety of virulence factors it creates, and the variety of cellular metabolism processes it possesses. In this introduction, this variety will be addressed to present context for the pathogenesis discussed the remainder of this thesis.

1.1 *Staphylococcus aureus* as a pathogen

S. aureus has been a pervasive pathogen in human history, causing infection in records as early as the Greek times, but was first cultured in the 1880s(*1*). The hallmark of *S. aureus* as a culturable bacteria is the golden color of its colonies, the result of the pigment Staphyloxanthin(*2*). This golden color earned the species its name – *aureus* being derived from the Latin for gold. The bacterium is a Gram-positive coccus, staining dark purple under Gram staining procedure and have a round or spherical shape. The bacteria are known to cluster together, the result of all the adhesins expressed by the bacteria, and these "grape-like clusters" are where the Staphylococci get their name from. The Staphylococcal species are distinguished from other Gram-positive cocci, like Streptococci, by not only their clustering morphology but by their expression of certain hallmark genes, such as catalase. Staphylococci are remarkably halotolerant and can grow as facultative anaerobes(*3*). Most Staphylococcal species are commensal organisms, living in harmony with the host and other microflora. This includes the other opportunistic pathogen *Staphylococcus epidermidis*. *S. epidermidis* lacks many of *S. aureus* virulence factors but can cause an infection

in an immuno-compromised host(*4*). *S. aureus*, on the other hand, can cause infections in a healthy host, on both a small and large scale (see 1.1.1.)(*2, 3*). While *S. aureus* is considered a commensal in some individuals, colonization by *S. aureus* is often seen as a risk factor for infections by *S. aureus*(*5*). Therefore, we deem it reasonable to hypothesize that *S. aureus* has not evolved to be a commensal organism, but to be a pathogen(*6*). The types of infections, as well as factors contributing to *S. aureus* infections, will be addressed in this section of the introduction.

1.1.1 *S. aureus* infections

S. aureus is an important human pathogen causing a range of diseases from mild, treatable skin and soft tissue infections to more invasive, difficult-to-manage conditions such as endocarditis and osteomyelitis(*7, 8*). In this section, the different presentations of *S. aureus* infections will be addressed.

1.1.1.1 Skin infections

The most common presentation of *S. aureus* infection is the skin and soft tissue infection. These infections can vary in severity, from a small lesion or impetigo to a chronic wound infection, or even the dangerous presentation necrotizing fasciitis(*8*). The most common presentations can change depending on the characteristics of the group being evaluated. Small children most commonly present with impetigo, a small boil-like lesion that will progress to a more crusted form over time. Impetigo is generally non-threatening and self-resolving. In adult patients, minor infections are more likely to present as folliculitis, a subcutaneous presentation, resulting in a furuncle or boil, or as a purulent cutaneous abscess, a more open wound, similar to the models used by our lab in this dissertation. Different risk factors can contribute to the frequency and

severity of these disease presentations. For example, individuals with diabetes, HIV, or immunosuppressive conditions are more likely to contract serious, recurring abscesses compared to their heathy counterparts(*9–11*). These individuals are also more susceptible to rare, dangerous infection progressions, such as necrotizing fasciitis, a condition where the skin becomes necrotic(*8*). This infection requires rapid response by healthcare professionals and still results in high mortality rates. Differences in epidemiology around *S. aureus* SSTIs is also present. Age and race both play a role in predilection to *S. aureus* infections (*12–14*). *S. aureus* is also the most common bacteria isolated from infected surgical sites, linking *S. aureus* healthcare associated settings (*15, 16*).

The burden of *S. aureus* SSTIs on the healthcare system is large and has been growing in the new century(*12, 14, 17, 18*). For all SSTIs that require hospitalization, culturable samples from over 80% of them contain *S. aureus*, and about half of these of these are MRSA (See section 1.1.1.6)(*13*). MRSA infections are associated with longer and more expensive hospital stays, sometimes requiring more than just antibiotics to treat(*19–21*). Overall, the cost of SSTIs to the US healthcare system has reached an estimated $13 billion in 2015, including emergency department and ambulance care(*18*). The CDC estimates the healthcare costs of MRSA infections as upwards of $1.5 billion dollars(*22*).

1.1.1.2 Bacteremia

One of the more dangerous presentations that can occur alongside a severe SSTI is bacteremia(*8*). This occurs when bacteria exit the abscess and enter the bloodstream. This is one of the most common ways that the presentations discussed below of *S. aureus* infections can occur. The bloodstream transports the bacteria from the skin infection to other sterile tissues, where *S. aureus* is able to thrive. Bacteremia can present alongside sepsis, a dangerous inflammatory

response by the immune system to bacteremia. The most critical result of *S. aureus* bacteremia and the subsequent septic response by the immune system is increased coagulation of the blood, which can result in tissue damage as these clots become caught in the narrow blood vessels of organs (*23*).

Similar to SSTIs, rates of *S. aureus* bacteremia have increased in the 21st century(*24–26*). MRSA rates have increased with the emergence of USA300 (See section 1.1.1.6), and MRSA accounts for approximately 50% of bacteremia infections(*26*, *27*). Mortality is approximately 14%(*26*, *27*) early in infection and can increase as high as 30% if the infection drags on for 1-3 months(*25*, *28*, *29*). MRSA infections often have more severe outcomes than their MSSA counterparts(*27*, *30*). Age is an risk factor for developing *S. aureus* bacteremia(*25*), as are conditions like diabetes(*31*), and having an foreign device implant(*26*). Overall, *S. aureus* bacteremia is a severe disease presentation that can lead to further infection in disseminated tissues as described below.

1.1.1.3 Endocarditis

Infective endocarditis (IE) is defined as an infection of the endothelium of the heart – often, the heart valves(*32*). Individuals who have damaged or artificial heart valves are more prone to IE infections, and IE is often associated with hospital-acquired infections(*33–35*). IE can be developed from bacteremia, intravenous drug use, or surgical infection(*24*, *35*). Once established, the bacteria present in the heart can result in sustained bacteremia and assist bacterial dissemination to other tissues. Like other infections with *S. aureus* as a major cause, IE incidence has been rising since 2000(*8*, *36*). In this time, between 30-50% of IE cases are caused by *S. aureus*, making it the pathogen most responsible for IE infections(*36–38*). Again, MRSA infections are associated with worse outcomes than MSSA infections, and result in a greater burden to the healthcare system as

they are more difficult to treat (*21*). IE treatment involves intravenous antibiotics, and, in over 50% of cases, surgery (*24*, *33*, *35*, *39*). Outcomes for *S. aureus* IE are poor, with up to a 20-30% mortality rate(*24*).

1.1.1.4 Osteomyelitis

Osteomyelitis is defined as the infection of the bone, and is predominantly caused by *S. aureus*, in 30-60% of cases(*8*). It can result from trauma to the bone, surgery, or in individuals with predisposed conditions with modified vasculature, such as diabetes(*8*, *40–42*). Fascinatingly, *S. aureus* infection can trigger remodeling of the bone tissue, sequestering the bacteria in aggregates and making it even more difficult for the immune system and systemic treatments to reach the infection site(*41*, *43*). Treatment for osteomyelitis infections includes systemic and targeted antibiotic treatment, and, in some severe cases, surgery or amputation (*8*, *41*, *42*). Chronic osteomyelitis is common, with recurrence rates of over 30%(*8*, *40*, *42*).

1.1.1.5 Pneumonia

Bacterial pneumonia is the infection of the lung by a bacterial pathogen. Community acquired (CAP) and hospital acquired pneumonia (HAP) have historically been considered separately, with *S. aureus* infections more likely to be in the latter category. With the emergence of the USA300 clone (see section 1.1.1.6), however, CAP became increasingly associated with *S. aureus*(*8*). Over 40% of cases of HAP can be attributed to *S. aureus*, making it an important pneumonia pathogen(*8*). *S. aureus* is also associated with ventilator associated pneumonia, which can have extremely poor outcomes for hospitalized patients, with over a 55% mortality rate(*8*, *44*). CAP is most often acquired through inhalation, as it is highly associated with colonization of the nares(*8*, *45*). CAP can also be established through bacteremia spread, as addressed above, making

it a dangerous location for bacterial dissemination(*45*). It can also follow influenza infection, as the decimated landscape of the lungs by influenza results in an optimal environment for *S. aureus* colonization(*45*). HAP is more often associated with elderly populations, whereas CAP can present in almost any age group(*8*, *45*). Both HAP and CAP can result in high mortality levels of up to 50%(*8*, *45*). Again, MRSA infections prove to be associated with higher healthcare costs and increased poor outcomes compared to MSSA infections (*8*, *44*, *45*). Likelihood of contracting MRSA pneumonia increases with previous antibiotic treatment, nasal carriage, and presence of MRSA in the hospital(*8*, *45*, *46*). Treatment involves courses of varying antibiotics and can require intubation of the patient if lung function declines(*8*, *44*, *45*, *47*).

1.1.1.6 MRSA and USA300 emergence

The difference between methicillin resistant *S. aureus* strains (MRSA) and methicillin sensitive *S. aureus* strains (MSSA) is straightforward. MRSA strains contain a mobile genetic element called an SCC*mec*, or a Staphylococcal Chromosomal Cassette with *mec*(*48*). The defining gene in SCC*mec* is *mecA*, which confers methicillin resistance through the production of penicillin binding proteins (PBP2a). There are eight types of SCC*mec*, referred to as I – VIII(*49*). The SCC*mec* acquired by a strain can help designate how related MRSA strains are. Another way to identify the relatedness of MRSA strains is through a process known as multi-locus sequence typing (MLST), which involves the sequencing of SNPs in seven housekeeping genes to determine relatedness into sequence types (STs)*(50)*. STs can then be grouped into clonal complexes (CCs) to more broadly define relatedness(*50*, *51*). Alternatively, to group Staphylococcoccal infections, one can use pulsed-field gel electrophoresis (PFGE) to create a unique banding pattern of the genome, resulting in the well-known USA subtypes 100-1200(*52*).

As mentioned above, at the onset of the 21st century, there was a shift in MRSA pathogenesis. Previously, MRSA cases had been rarer, with many MSSA infections still being a major source of *S. aureus* infections. MRSA was also almost exclusively associated with hospital associated infections(*53*). In the mid-1990s, however, there was a rise in community acquired MRSA (CA-MRSA) cases. Initially, these cases were caused by a variety of clonal complexes, including CC1 and the pulse-field type USA400(*54*). In the early 2000s, however, a sweep occurred where these USA400 clones were exclusively replaced by a single MRSA clone. These cases all belonged to CC8, containing SCC*mec*-IV, and molecularly typed as USA300(*54*). By 2005, CA-MRSA was considered epidemic in the United States(*53*, *55*). The complete genome of this circulating CA-MRSA clone was sequenced in early 2006, and named FPR3757, and is commonly called USA300(*56*). They found that this strain contained not only Panton-Valentine leukotoxin (see below, section 1.1.2.1), but also a large genetic element named the arginine catabolic mobile element, or ACME. ACME is present in several *S. epidermidis* strains, but not in other *S. aureus* strains(*56*). It contains an arginine deiminase pathway that is constitutively expressed, as well as an oligopeptide permease system, both of which were hypothesized to play a role in *S. aureus* growth and, therefore, infectivity. By 2005, USA300 was causing over 80% of CA-MRSA cases(*57*). Proteomics performed on USA300 showed that it produces more exoproteins, such as toxins and proteases (see 1.1.2.1) than a USA400 strain(*58*). Studies also found that USA300 strains were directly more infectious than their USA400 counterparts(*59*). Over time, this hypervirulence was shown to be the result of overactivity of the Agr system (see section 1.1.2.2)(*60*). It also was found that ACME played a role in increased *S. aureus* survival and pathogenesis, but the locus that made USA300 methicillin resistant, also known as *SCCmec*, is dispensable for pathogenesis. Therefore, the fact that this predominant clone was MRSA was

simply unfortunate – the methicillin resistance did not play a role in bacterial survival outside of antibiotic treatment(*61*). The ACME cassette was also shown to contain a gene known as *speG*, which confers resistance to polyamines, abundant molecules in skin tissue that are capable of killing *S. aureus*(*62*, *63*). To date, the mechanism behind polyamine killing and *speG*-conferred resistance is unknown. The ACME arginine deiminase system Arc was also shown to support *S. aureus* growth, contributing to acid tolerance in the skin(*63*). While we have some understanding as to why USA300 has emerged as a prominent CA pathogen – its hypervirulence and increased growth rate – we do not fully understand these factors. The overactivation of the Agr system in this clone has never been explained, and USA300 cases are still rampant in the U.S. today.

1.1.2 *S. aureus* virulence factors

It has long been appreciated that the coordinated expression of a diverse array of virulence traits including toxins, proteases and immunosuppressive factors is critical for the pathogen to cause disease(*64*). The variety of virulence factors produced by *S. aureus* is a large part of what makes it such a dangerous pathogen. These virulence factors can be separated into two categories – those that directly cause damage to the host, such as toxins and proteases, and those that allow the pathogen to evade detection and killing by the host immune system. These sets of virulence factors allow the bacteria to 'attack' and 'defend', respectively, and will be covered in this section.

1.1.2.1 Attack

The most prominent toxin synthesized by *S. aureus* during an infection is α-toxin, also known as Hla or alpha-hemolysin. This toxin was reported as early as the 1950s, as doctors and scientists noticed the dermonecrotic properties of *S. aureus* infections(*65*, *66*). The toxin was

isolated in the 1960s(*67*), and the toxic effects on a variety of hosts were quickly noted. Very little was understood about how the toxin functioned, however. It wasn't until the 1980s that the mechanism behind α-toxin toxicity was discovered(*68*). α-toxin and many other bacteria toxins are pore-forming toxins, which essentially 'poke holes' in the membrane of a cell, compromising the integrity of the cell and causing the cell to release its contents. A large number of studies have been performed investigating the targets of α-toxin, but it wasn't until the 2010s that the binding receptor of α-toxin, ADAM-10, was identified(*69–71*). ADAM-10 is present on most cells, but especially on red blood cells (RBCs), resulting in the hemolysis that is characteristic of *S. aureus.* Another key function was subsequently identified for the functionality of α-toxin, which is its role in targeting adherens junctions of the epithelium(*72*). These junctions between cells are key for epithelial integrity, and when α-toxin breaks them apart, the epithelial layer is breached and *S. aureus* can spread its infection more efficiently(*73*, *74*). Studies have also shown that the interaction between ADAM-10 and α-toxin will trigger inflammation by immune cells(*75*), resulting in highly inflamed environments, which cause more tissue damage than they have an effect on *S. aureus* growth (See section 1.2.5). α-toxin has been shown to play a prominent role in infection, an insight that will be reflected in chapter 2 of infection(*76*). Importantly, it has been shown to be a key mediator in USA300 skin infection pathogenesis, our primary model of infection(*77*). Overall, α-toxin is an important factor in *S. aureus* pathogenesis and makes for an excellent indicator of virulence.

Similar to α-toxin, the phenol soluble modulins are small pore-forming toxins that are capable of causing great damage to a cell. They work efficiently against immune cells and expressed under most infection conditions. Initially described in 2007, the PSMs are located in a single locus and consist of four short (~20 aa) and two long (~40 aa) small proteins known as the

α and β PSMs, respectively(*78*). A separate locus contains a related gene, but this has been previously reported and named δ-toxin(*79*). The PSMαs are important for neutrophil targeting and lysis, making them important for *S. aureus* survival, as neutrophils are at the front of the immune response to *S. aureus*(*78*). As the PSMs are present in both pathogenic and commensal Staphylococci, their role in *S. aureus* evolution has been questioned(*80*, *81*). In *S. aureus*, they are distinct from other toxins and virulence factors as they are encoded directly in the genome and are directly regulated by Agr (see section 1.1.3.1), whereas most other toxins are encoded on pathogenicity islands or other mobile genetic elements and are controlled by Rot (see section 1.1.3.1). It is hypothesized that the PSMs play a role as a surfactant in Staphylococcal spreading and colonization, as well as in biofilm formation for environmental survival(*80*, *81*). They have been shown to play a role in *S. aureus* infection(*78*), however, and are a good indicator of Agr activity and virulence(*81*).

The *S. aureus* leukotoxins are two-component pore forming toxins that involve two different proteins that come together to form a pore in the membrane of a cell(*82*, *83*). There are four different bi-valent toxins, all of which have activity against neutrophils, and only two have activity against RBCs(*82*). The first leukotoxin is known as γ-hemolysin, and was defined as early as the 1970s(*84*). The larger group was not defined until later in the 1990s(*85*) and consist of LukED, LukAB or LukGH, and Panton-Valentine Leukotoxin (PVL). LukED and γ-hemolysin are the two toxins with activity against RBCs. LukED, LukAB, and γ-hemolysin are present in nearly all *S. aureus* strains, their preservation indicates they are important for infection(*86*, *87*). Indeed, several studies have shown a role for each of these toxins in infection(*88*–*91*). The exception, and a major cause of debate in the field, is PVL. Discovered almost a century ago(*92*), it is only present in a fraction of *S. aureus* strains. However, it is present in the hypervirulent USA300 strain(*93*).

For a time, the research community believed that PVL contributed to USA300's hyper-infectivity. However, no conclusive role has been drawn in connection of PVL to USA300 infections, and its role remains unclear(*82*, *83*, *94*). Overall, however, the leukotoxins remain an important aspect of the *S. aureus* virulence arsenal.

The final toxin group that will be addressed here are the superantigens, including Toxic shock syndrome toxin 1 (TSST-1) and the staphylococcal enterotoxins. Superantigens (SAgs) are a class of bacterial toxins that are capable of indiscriminately activating T-cells, causing widespread inflammation. These toxins bind to the T-cell receptor and the MHCII molecule in a non-peptide specific manner, eliciting a T cell response when there should be none across many T cells. The resulting cytokine storm can cause widespread damage. While these SAgs are not relevant in all forms of disease, they have been known to contribute to *S. aureus* food poisoning, as well as the well-known toxic-shock syndrome (TSS) from tampons in the late 1980s(*83*, *95*).

S. aureus encodes several different proteases that play a role in virulence. These include V8 (or SspA), a serine protease first isolated in the 1970s, aureolysin, a metalloprotease, and several cystine proteinases, including the staphopains, (or ScpA/SspB)(*96–101*). They play several key roles in infection, from processing extracellularly secreted virulence factors to contributing directly to pathogenesis as well(*102*). They can play a role in nutrient acquisition, being essential for growth when peptides are the only carbon source present(*103*). Aureolysin is known to contribute to the cleavage of antimicrobial peptides and compliment proteins, helping evade immune responses(*104–106*). The proteases secreted by *S. aureus* are known to be activated extracellularly in a cascade that has one protease cleaving and activating another protease(*101*, *107*). They also play a role in cleaving secreted virulence factors from the *S. aureus* cell surface, such as the fibrinogen binding proteins, facilitating a switch from an adhesive to an invasive

infection(*108*, *109*). They are also involved in toxin activity, having an extracellular effect on both α-toxin and PSMα processing and stability(*110*, *111*).

In addition to these exogenous proteases, *S. aureus* has the unique ability to secrete proteases that will play a role in the coagulation of blood, known as Coagulase and von Willebrand factor binding protein (vWbp)(*112–114*). Coagulase binds to the terminal end of prothrombin, a clotting agent in the blood, and inducing a conformational change that will activate clotting via the cleavage fibrinogen into fibrin(*114–116*). This ability of coagulase and vWbp to cause bind and process fibrinogen and activate clotting is important for infection, and can cause downstream effects on abscess formation and sepsis(*117*). In fact, coagulase is considered such a defining part of *S. aureus* pathogenesis that *S. aureus* is often distinguished from other Staphylococci, including *S. epidermidis*, by referring to these other species as coagulase-negative Staphylococci or CoNS.

Finally, and potentially most importantly for *S. aureus* infection, we have the surface binding proteins. These are the set of proteins expressed by *S. aureus* that allow for adhesion to host cell surfaces and subsequent establishment of infection. These proteins are all anchored to the cell wall by the actions of SortaseA, an important factor in cell wall protein secretion(*118*). Most prominent among these cell-wall anchored (CWA) proteins are the MSCRAMMs – ‘Microbial Surface Components Recognizing Adhesive Matrix Molecules’ (*119*). This broad category refers to proteins that interact with the host extracellular matrix (ECM), allowing for adhesion of the bacteria to its infection site. All the MSCRAMMs contain two IgG-like folding domains, but can be divided into two categories(*119*, *120*). The first is proteins that are similar in structure to and employ a dock lock ligand (DLL) mechanism for adhesion. This includes proteins such as clumping factors A and B (ClfA/B), SdrC family proteins, and Fibrinogen binding proteins A and B (FnBPA/B). These proteins contain a hydrophobic trench that will bind their target, and a then

a conformational change will trigger a lock in place, firmly attaching the bacteria to its ligand. There are also the collagen binding proteins that bind their substrate in a way called the collagen hug, such as the collagen binding protein Cna. These proteins again have a conformational change upon binding their ligand, but they twist around the thicker collagen fiber, holding it firmly in place. These methods of binding are more thoroughly reviewed elsewhere(*119*, *120*), but nevertheless, MSCRAMMs play an important role in *S. aureus* infection. They have a diverse range of binding targets in the ECM, from fibrinogen to collagen to elastin(*121*). Outside of the MSCRAMM family, but still considered CWA proteins involved in adhesion, are IsdA, an iron-acquisition protein that promotes nasal colonization and IsdB, which binds to integrins(*120*). SraP is a cadherin like protein that can help bind to platelets and other sialyated proteins on cell surfaces(*122*). Overall, adhesive factors are vital for infection, as the SortaseA mutant is unable to establish an infection in the host(*123*), and therefore must be considered an important part of the *S. aureus* virulence arsenal.

1.1.2.2 Defend

The most well-known protein involved in *S. aureus* immune evasion is protein A, or SpA. SpA is a CWA capable of being secreted that bind the Fc portion of IgG antibodies(*121*, *124–126*). Antibodies are secreted by the adaptive immune system to help neutralize and opsonize (prime for phagocytosis) bacteria. This opsonization occurs when the Fab portion of the antibody binds to the bacteria, and the immune cells can then recognize the Fc portion and phagocytose the bacterium(*127*). By expressing a protein that will nonspecifically bind the Fc region of the antibody, *S. aureus* is able to disguise itself from phagocytosing cells because the “wrong” portion of the antibody will be sensed by the immune system. The role of SpA has been extensively studied and reviewed, and its role in *S. aureus* immune evasion is considered essential(*126*, *127*). *S. aureus*

has been identified as having more than one of these antibody-binding proteins, with this redundancy again indicating the important role of these proteins in infection(*128*).

In addition to antibody opsonization, another important immune factor that *S. aureus* must evade is the complement system. This cascade of proteins that are secreted by immune cells will bind to the surface of the bacteria, resulting in opsonization as well as creating pores in the bacterial cell wall in an attempt to kill the bacteria(*129*). *S. aureus* has several complement evading proteins. Staphylokinase is another bacterial secreted protease that will cleave plasminogen, a component found in the blood, into plasmin, a protease that will assist *S. aureus* in degrading bound complement factors(*124*, *130*). Aureolysin, described above, will also degrade host complement factors. Some CWA proteins, such as Efb, will bind extracellular complement proteins to prevent their cleavage and activation of the complement cascade(*124*, *131–133*). The secreted protein Ecb (Extracellular complement binding protein) will bind C3b, a key part of the complement cascade, and prevent its activation(*124*, *134*, *135*). C3b is also a key opsonin, and its binding will prevent recognition from phagocytes. Finally, and potentially most important, we have SCIN, or staphylococcal complement inhibitor, which will bind to the complement convertases, resulting in the halting of all complement pathway progression(*124*, *133*, *136*).

Another role of complement is chemotaxis, or the attraction of other immune cells to the site of infection(*129*). Neutrophils and macrophages will also excrete other chemo-attractants, or chemokines, in an effort to increase host defenses(*137*). Again, *S. aureus* has several factors to help mitigate chemo-attractants. CHIPS, or chemotaxis inhibitory protein of staphylococcus, is a secreted protein that will interfere with the receptors for chemokines produced by complement(*124*, *136*, *138*). The secreted protease staphlyopain cleaves the receptors of chemokines like CXCR2 from the surface of immune cells(*124*). FLIPr-like is a secreted protein

that directly competes with the chemokine FLIPr, allowing for decreased immune cell recruitment, activation, and phagocytosis(*124*).

Capsules are an element used by many bacteria to avoid detection by the immune system. They are a collection of secreted polysaccharides that are anchored to the cell wall and coat the outside of the bacterium, making it more difficult for the immune system to detect common antigens like peptidoglycan(*139*). There is a large amount of variation in the capsular polysaccharide, with some being more commonly associated with infection than others(*140*). Since capsular polysaccharide takes a huge effort to produce, some strains do not make it at all, relying instead on other immune evasion factors. This includes the predominant MRSA strain USA300(*141*).

Another element that can be used to disguise the bacteria from the immune system is the formation of biofilm. Bacteria will secrete a variety of polysaccharides and other molecules to form a dense extracellular matrix (ECM) that will, again, hide common cell-surface associated factors that could be recognized by the immune system(*142*). *S. aureus* biofilms are most commonly associated with the production of a thick ECM made up majorly of PIA (polysaccharide intercellular adhesin), and PIA has been identified as an important virulence factor in some situations(*142–144*). However, it is becoming increasingly appreciated that biofilms can form without PIA production, saving the cell energy(*142, 144*). The hypervirulence of USA300 is often negatively associated with biofilm production, for reasons explored below (section 1.1.3) (*145*).

Finally, an important way that the immune system targets bacteria is though the production of immune radicals, a process known as oxidative burst(*146, 147*). These immune molecules, including reactive oxygen species (ROS) like superoxide and reactive nitrogen species (RNS) like nitric oxide (NO), will target iron-sulfur clusters in proteins (*147*). The proteins that most

commonly come under target by ROS/RNS are often involved in metabolism, like TCA cycle enzymes and the electron transport chain, although lipids and DNA are also known to be affected by ROS and RNS(*147*). The overall damage caused to the cell by these immune radicals can be fatal, and *S. aureus* must overcome their presence in order to survive in the host(*148*). To overcome metabolic impacts, the bacterium will shift its metabolic strategy, which will be covered in section 1.2. To mitigate damage, however, to DNA and the cell in general, *S. aureus* must be able to detoxify these compounds. It does this by creating several molecules that will assist in detoxification. *S. aureus* expresses two superoxide dismutases, or Sods, SodA and SodM. The differences in these are addressed in 1.2.1, but they both detoxify the superoxide created by oxidative burst(*149*). While most bacteria encode some form of Sod, *S. aureus* is rather unique in the fact that it expresses two different Sods(*150*). Indeed, sodM is only found in *S. aureus*, not in other CoNS(*151*). Also important for superoxide and other ROS is the pigment produced by *S. aureus* known as staphyloxanthin. This pigment is what gives *S. aureus* the characteristic golden color that it is named for, but it is also vital for superoxide quenching(*152*, *153*). Another reactive oxygen species that can be damaging to bacteria is hydrogen peroxide (H_2O_2), and *S. aureus* encodes a catalase to convert hydrogen peroxide into water and oxygen(*154*). This is a hallmark of Staphylococci and is often used in diagnostic testing(*155*). Finally, NO detoxification is performed by Hmp, a flavohaemoprotein that is, again, vital for *S. aureus* infection(*148*).

Of course, the proteases and toxins described in 1.2.1 play a role in pathogen defense as well. The proteases secreted by *S. aureus* are important not only for complement inactivation, as described above, but for the breakdown of anti-microbial peptides that are secreted by immune cells(*124*). The toxins mentioned above are critical upon phagocytosis, as they are needed for cell lysis from the inside as well as the outside of the immune cell. The superantigens of *S. aureus*

often have a dual role involved in blocking of the toll-like receptors (TLRs) as well as chemokine receptors (CXCRs)(*124*). The variety of roles played by so many different virulence factors makes it easy to understand how *S. aureus* is such a dangerous pathogen.

1.1.3 *S. aureus* virulence factor regulation

The large variety of virulence factors that are required for *S. aureus* infection take a huge amount of energy to make. This is because of the variety and quantity of the proteins synthesized for infection. As a result, careful coordination is needed to make sure that energy is not wasted in the synthesis of virulence factor production.

Synthesis of these virulence factors occurs in two different phases. The first phase is the expression of the proteins required for colonization. These include the MSCRAMMS and other CWA proteins, coagulases, and PIA, as well as some immune evasion factors like SpA. The second phase occurs once the infection site has been established and involves the production of toxins and proteases to release nutrients from host cells and defend against infiltrating immune cells. The onset of the second phase also involves the repression of many proteins involved in the first phase, like SpA. This switch in protein expression is strongly guided by the Agr quorum sensing system.

1.1.3.1 Agr

The Accessory Gene Regulatory system, or Agr system, is the main regulator of *S. aureus* virulence(*156*). Homologs of this system are in closely related Staphylococci, as well as almost all related Firmicutes(*157*). The key difference lies in the Agr regulon, or proteins whose expression is under the control of this system. Those other species only have a few proteins under Agr regulation – instead, almost every virulence factor in *S. aureus* is somehow regulated by Agr. The

virulence factors discussed in 1.1.2 are mostly unique to *S. aureus* and have been carefully coordinated to only be expressed when advantageous to the cell. Quorum sensing systems are responsible for coordinating gene expression in a growth-phase dependent manner(*158*). In an infection context, this means using bacteria population density to activate and repress different virulence factors. By coordinating the expression of its virulence factors under the Agr system, *S. aureus* ensures that no energy will be wasted making extraneous toxins or proteases when there are not enough bacteria around to defend the infection from the immune system. Instead, the bacterium will produce MSCRAMMS and other adhesive factors while avoiding the immune system with the help of SpA production to establish an infection niche. Then, when the bacteria have replicated to a high enough cell density, the Agr system will be activated. This will allow for a shift away from the initial phase of infection and into the second phase, where toxins and proteases will be produced in mass for the survival of the now-dense group of bacteria.

The Agr system consists of four proteins – AgrBDCA(*159, 160*). AgrB is a transmembrane protein that will process and secrete the AgrD peptide into extracellular space. At this point, this peptide is referred to as auto-inducing peptide, or AIP. The AgrD peptide is short and linear, whereas AIP is even shorter, consisting of only 9-11 amino acids, and contains a circular loop called a thiolactone. The AIP will interact with the AgrC protein, a transmembrane histidine kinase that is part of the AgrAC two-component system (TCS). In traditional TCS fashion, once AIP binds to the AgrC HK, the protein will auto-phosphorylate and then pass this phosphate on to the AgrA response regulator. AgrA is a DNA-binding protein that will upregulate gene expressions at promotors that include the AgrA binding sequence. These include the *agrBDCA* locus itself, as well as the neighboring promotor for RNAIII. The AgrA regulon also includes the promotor of the

PSMα locus, making RNAIII and these small proteins excellent reporters for AgrA transcriptional activity(*161*).

The sequence of AgrD, as it is so short, is the most variable part of the Agr system. In fact, *S. aureus* strains can be separated by the type of AIP they are producing. There are four different AIPs, known as AIP-I, AIP-II, AIP-III, and AIP-IV(*160*). The binding pocket of the AIPs on AgrC also exhibits variation, and different AIPs cannot cross activate each system. Most AIPs will actually inhibit binding of a cognate AIP to its AgrC locus, so only one AIP type will be dominant locally in the infection site. This allows for clonal bacteria to flourish and inhibits intraspecies competition.

Although the Agr regulon describe above is small, the majority of virulence factors are still regulated by Agr. This is not through direct binding of AgrA to their promotors, however. It is mostly through the role of the small RNA known as RNAIII(*162*). A small portion of this RNA encodes for δ-hemolysin, but the major consequences of RNAIII expression are on other virulence factors. The most well categorized function of RNAIII is its effect on the Repressor of Toxins, or Rot, expression(*163–165*). The Rot RNA is generally stable, but when RNAIII is present in the cytoplasm, it can interact with the Rot RNA to repress translation and destabilize the RNA, resulting in rapid Rot RNA degradation and then subsequent depression of the Rot operon once the Rot protein is overturned(*165*, *166*). Rot strongly represses the expression of most of the toxins in the *S. aureus* genome, and its absence results in rapid transcription of toxin loci, allowing the bacteria to produce the toxins needed for infection(*163*, *164*). RNAIII has other roles in virulence factor expression as well. For example, it stabilizes the *hla* transcript by base pairing with the 5' end of the transcript and exposing the ribosome binding site(*167*), and it blocks translation of and destabilizes the *spa* transcript(*168*, *169*), changing the most highly expressed virulence transcript

from a defensive to an offensive protein. The coordination of virulence factor expression by quorum sensing is one of the most important aspects of *S. aureus* virulence, as it helps define the phases of infection by population density.

1.1.3.2 SaeRS

The *S. aureus* exoprotein expression regulator system SaeRS is an important two-component system (TCS) that integrates environmental signals with virulence factor expression. Two component systems are a mechanism through which a bacterium can sense its environment and make changes to its gene expression as a result(*170*). They typically consist of a receptor histidine kinase, or HK, that will bind some environmental signal on the exterior of the bacterium and induce a conformational change, resulting in the phosphorylation of the interior portion of the HK. This phosphorylated HK will pass this phosphate group on its cognate response regulator (RR), a DNA-binding protein that is activated upon phosphorylation. Once activated, the RR will bind to a specific sequence on the DNA, typically upstream of a gene, and either repress or activate expression of said gene, thus integrating extracellular cues with gene expression. TCSs are important for distinguishing when bacterial genes should or should not be expressed, especially helpful in specifying metabolic conditions or indicating when a toxic substance is present. The SaeRS TCS was reported to have synergy in gene expression with the Agr system as early as 2003(*171*). SaeRS responds to the presence of immune molecules, including neutrophil-produced AMPs and calprotectin, a molecule plentiful in neutrophil cytoplasm(*172–174*). The expression of SaeRS is quite complicated and is beyond the scope of this introduction(*171–173*). What remains important, however, is that the SaeRS regulon and the Agr regulon have a decent amount of overlap(*172*, *175*, *176*). SaeRS has been shown to have significant impacts of the expression of coagulase, *hla*, the superantigens, and several CWAs(*172*). SaeRS is also known to synergize with

Rot to regulate the expression of some toxins(*177*). The importance of SaeRS is emphasized by studies that show attenuation of *saeRS* locus mutants(*60, 178*). Overall, the ability to integrate the environmental signals produced by immune cells with toxin and virulence factor production is important for *S. aureus* infection.

1.1.3.3 Other regulatory proteins

An important family of regulatory proteins in *S. aureus* are the Sar, or staphylococcal accessory regulatory proteins. Most important of these in virulence regulation is SarA, which has a direct impact on Agr transcription(*179, 180*). This results in a large impact on virulence factor expression and attenuation of a *ΔsarA* strain(*181*).

Another important SarA family regulator is MgrA, which plays a role in *S. aureus* biofilm formation and clumping factor regulation(*180*). The expression of MgrA is highly impacted by ArlRS, a TCS that responses to the autolytic response of *S. aureus*(*180, 182*). ArlRS, in conjunction with Agr and Sae, coordinates the expression of virulence factors with metabolite presence; specifically, pyruvate(*183*).

While this is not an exhaustive list of the regulators of virulence in *S. aureus*, the major players have been highlighted. In further chapters, the Agr system will be a major focus of this dissertation.

1.2 *Staphylococcus aureus* metabolism

While the role of the virulence factors discussed above has long been noted, it has more recently been established that metabolic adaptation to different host environments and to the host

immune response is equally critical for the success of the pathogen(*184*). Several global metabolic regulators (*e.g.* CodY and CcpA) have both direct and indirect effects on the activity of global virulence and quorum sensing regulons (see Chapter 3). The intertwining of virulence and metabolic regulatory networks underscores the interdependence of metabolic adaptation to the host immune response with the elaboration of virulence traits for the pathogen to successfully cause disease and transmit to a new host. This section summarizes recent developments (in the past ~5 years) in both organic and inorganic cellular metabolism that have been shown to be critical for *S. aureus* to cause disease. The optimization and alteration of these metabolic pathways in the face of host nitric oxide (NO) production is critical for the success of the pathogen and will be discussed as well. As always, a better understanding of the metabolic adaptations mounted by this pathogen against the host immune response (*e.g.* NO production) may one day lead to the development of antimicrobial agents, which are desperately needed to treat invasive *S. aureus* infections.

Table 1:Metabolism genes 'essential' for S. aureus NO resistance. Genes that were significantly underrepresented in the output of a Tn-Seq experiment conducted in the presence of NO.

Locus	Gene	Description	Role
SAUSA300_2060	*atpA*	F0F1 ATP synthase subunit alpha	Respiration
SAUSA300_2064	*atpB*	F0F1 ATP synthase subunit A	Respiration
SAUSA300_2057	*atpC*	F0F1 ATP synthase subunit epsilon	Respiration
SAUSA300_2058	*atpD*	F0F1 ATP synthase subunit beta	Respiration
SAUSA300_2063	*atpE*	F0F1 ATP synthase subunit C	Respiration
SAUSA300_2062	*atpF*	F0F1 ATP synthase subunit B	Respiration
SAUSA300_2059	*atpG*	F0F1 ATP synthase subunit gamma	Respiration
SAUSA300_2061	*atpH*	F0F1 ATP synthase subunit delta	Respiration
SAUSA300_0963	*qoxA*	quinol oxidase, subunit II	Respiration
SAUSA300_0962	*qoxB*	quinol oxidase, subunit I	Respiration
SAUSA300_0961	*qoxB*	quinol oxidase, subunit III	Respiration
SAUSA300_0960	*qoxD*	quinol oxidase, subunit IV	Respiration
SAUSA300_0984	*ptsI*	phosphoenolpyruvate-protein phosphotransferase	Glucose Fermentation
SAUSA300_0759	*gpmI*	phosphoglyceromutase	Glucose Fermentation
SAUSA300_1644	*pyk*	pyruvate kinase	Glucose Fermentation
SAUSA300_0235	*ldh1*	L-lactate dehydrogenase	Glucose Fermentation
SAUSA300_1442	*srrA*	respiratory response protein, SrrA	Regulatory
SAUSA300_1441	*srrB*	respiratory response protein, SrrB	Regulatory
SAUSA300_1148	*codY*	transcriptional repressor CodY	Regulatory
SAUSA300_1682	*ccpA*	catabolite control protein A	Regulatory
SAUSA300_0234	*hmp*	putative flavohemoprotein	Immune Radical Defense
SAUSA300_1513	*sodA*	Fe/Mn family superoxide dismutase	Immune Radical Defense
SAUSA300_0839	*nfu*	Fe-S Biogenesis protein	Fe-S Homeostasis
SAUSA300_0491	*cysK*	cysteine synthase A	Fe-S Homeostasis
SAUSA300_0618	*sitA*	ABC transporter substrate-binding protein	Fe Acquisistion
SAUSA300_0620	*sitB*	ABC transporter ATP-binding protein	Fe Acquisistion
SAUSA300_0619	*sitD*	ABC transporter permease	Fe Acquisistion
SAUSA300_0635	*fhuG*	ferrichrome transport permease fhuG	Fe Acquisistion

1.2.1 Inorganic Metabolism

The acquisition of inorganic nutrients from the surrounding environment is vital for *S. aureus* survival and pathogenesis. This includes metals such as iron, manganese, and zinc, as well as other important molecules such as potassium and phosphate.

1.2.1.1 Iron

Iron is a vital ingredient for bacterial metabolism. It serves as a cofactor in many metabolic enzymes, particularly those in the TCA cycle and electron transport chain. Thus, the ability to

obtain iron plays an important role in *S. aureus* infection. Indeed, mutations in iron transporters SitABC and FhuG showed fitness defects in the presence of nitric oxide (Table 1). Siderophores are also known to be key factors in iron acquisition during infection. Recent work has shown that siderophore production is heterogenous within the host, where some abscesses exhibit iron limitation while others do not(*185*, *186*). Similar heterogeneity is shown for other metals as well, such as manganese (Mn) and zinc (Zn). Another method of iron acquisition for *S. aureus* is the ability to make and capture heme, an essential cofactor for respiration as well as detoxification of $NO\cdot$ and H_2O_2 via the flavohemoprotein (Hmp) and catalase (Kat), respectively. As heme acquisition has been thoroughly reviewed elsewhere(*187–189*), we will only address a few recent discoveries relating heme to virulence and metabolism. IsdB, the hemoglobin receptor for *S. aureus*, plays a key role in extracting heme from the host. A recent study has shown that the *S. aureus isdB* gene has evolved parallel to human hemoglobin, creating a high binding affinity and better heme acquisition(*190*). Finally, a role has been demonstrated for the (p)ppGpp stress response in controlling high intracellular iron levels(*191*). A mutant unable to produce (p)ppGpp has increased intracellular free iron levels, as well as elevated ROS levels and toxicity to the cell. This study implies that the (p)ppGpp stress response reduces respiratory chain activity, helping to regulate ROS and free iron levels in stressed bacteria.

1.2.1.2 Manganese

One of the ways the body helps control infection is by sequestering essential nutrients, which can include metals like Mn. This process, known as nutritional immunity, makes it difficult for bacteria to obtain essential nutrients. One of the ways the body sequesters Mn is via the protein Calprotectin (Cp), which binds Mn and Zn with a high affinity(*192*). *S. aureus* can overcome Mn starvation using the two-component system ArlRS(*193*, *194*) by shifting the metabolism of the cell

from glycolysis to amino acid catabolism. This is reliant on the sensor kinase ArlS and the response regulator ArlR(*195*). Also important for resistance is the expression of the Mn importer, MntABC. This importer works at a variety of pH values and is important for surviving in the presence of Cp and other immune effectors(*196, 197*). Mn is essential for survival of *S. aureus* as an important cofactor in proteins involved in cellular metabolism. For example, a Mn-dependent phosphoglycerate mutase, GpmI, is a critical glycolysis enzyme. Accordingly, *S. aureus* expresses a metal independent isozyme (GpmA) for survival under nutritional immunity(*198*). Additionally, Mn can help resist the effects of superoxide secreted by the immune system. The superoxide dismutase SodM can use either iron or Mn as a cofactor, while SodA is dependent on Mn(*199*). The latter was shown to be required for full NO·-resistance in *S. aureus* (Table 1). Having two SODs allows *S. aureus* flexibility in metal acquisition under nutritional immunity. The mutations allowing for these metal specificities is being studied alongside the evolutionary trajectories of SODs(*200*). The expression of the Mn-dependent SODs is tightly regulated, being controlled by RsaC, a non-coding RNA transcribed with the Mn importer MntABC(*201*). Considering these findings, Mn clearly plays an important role in *S. aureus* virulence. For example, excess dietary Mn can promote endocarditis infection(*202*). If too much Mn if present in the bloodstream, it can accumulate in the heart tissue where it is available to *S. aureus*, which will use this Mn to help protect from superoxide stress from neutrophils via SodA/M. However, like any metal, too much Mn is toxic to the cell. Therefore, *S. aureus* must also contain a way to detoxify excess Mn in the cell. At high levels of intracellular Mn, the repressor MntR will shut off MntABC and activate expression of MntE, which functions as an Mn exporter, maintaining Mn homeostasis and allowing for continued bacterial survival and virulence(*203*).

1.2.1.3 Zinc

One of the most interesting findings in the field of *S. aureus* and metal preference is the recent discovery of the zincophore Staphylopine. First reported in 2017, Staphylopine is a siderophore-like molecule secreted by the CntE system, allowing for highly efficient acquisition of zinc in the host, despite the overwhelming presence of host zinc sequestration Cp(*204*). Work in this field has defined Staphylopine synthesis(*205, 206*) by the *cntKLM* genes in the *cnt* operon(*207*). These results indicate that internal concentrations of metals can impact metallophore production. As previously stated, the CntE exporter secretes Staphylopine, which can sequester zinc, and return it to the cell chaperoned by CntA, an extracytoplasmic binding protein. The CntBCDF transporter can import the CntA/Staphylopine complex into the cell(*208*). Several groups have demonstrated that this export/import process is essential for metal homeostasis, as deletion of *cntA* or *cntKLM* is detrimental to pathogen survival in the host(*204*), yet deletion of *cntE* is toxic to the cell(*209, 210*). It was demonstrated that the *cnt* locus is regulated by Fur and iron availability, as well as Zur, a ncRNA responsible for sensing zinc availability, keeping tight control over the expression of Staphylopine(*211*). Finally, bioinformatic analysis of a variety of bacterial species indicates that, while discovered in *S. aureus*, this zincophore system is not unique and is likely to be present in extremely diverse bacteria(*212*).

1.2.1.4 Copper

Copper, an essential metal, has long been known also to have a negative effect on bacterial growth. In recent years, a few new factors in *S. aureus* copper resistance have been discovered. In the mobile element ACME harbored by USA300 strains, the *copBL* or *copXL* operon protects from copper toxicity, in addition to known copper protection elements such as *copA* and *copZ.* All four of these genes are induced by copper and regulated by CsoR. CopZ is a copper binding chaperone

and CopA is an ATPase copper exporter. CopB seems to be similar to CopA and also effluxes copper from the cell. CopL is a membrane-associated surface-exposed lipoprotein that binds copper tightly. The newly described copper binding site is important for CopL's ability to protect against copper toxicity. These newly described *copBL* genes are present in several other species, including other Staphylococcal species(*213*, *214*). This system has been shown to be important in infection models(*215*). Additionally, a transposon screen of a *copAZBL* mutant identified the manganese transporter MntABC as having an impact on copper import(*216*). A defective MntABC transport system resulted in decreased accumulation of copper, indicating that this transporter may be a mechanism by which Cu(II) is able to enter the cell, wherein it is reduced into the more toxic form, Cu(I). Finally, a mass-spectrometry analysis of *S. aureus* cells exposed to copper stress details the many changes that occur in the bacterium under copper exposure, including a marked increase in glycolytic flux(*217*). This study also detailed the association of copper with glycolytic protein GapA, reducing the protein's enzymatic activity under copper stress.

1.2.1.5 Potassium

While the field of *S. aureus* metabolism understands how potassium transport functions, the wider impact of potassium uptake on metabolism is only beginning to be understood. A key study shows that environments with limiting potassium (K+), metabolism is shifted away from the electron transport chain and towards the Pta-AckA(*218*). This could be due to a shift in intracellular pH that occurs upon lessened K+ import in exchange for H+ ions. This shift results in lower ATP, which may result in decreased Agr activity (see below). Furthermore, K+ import has also been shown to be regulated by the second messenger cyclic di-AMP. This signaling molecule was shown to bind to the KtrA subunit of both Ktr K+-importers and inhibit its ability to bring in K+(*219*).

1.2.1.6 Sulfur

In addition to metals, bacteria must be able to acquire all other vital inorganic nutrients while causing infection in the host. One of these essential ingredients is sulfur, commonly found in the form of cystine (or cysteine, the reduced form), which serves as a redox buffer in the bloodstream. *S. aureus* has two cystine transporters, TcyABC and TcyP that have been shown to play an active role in cystine import during infection(*220*). This study produced a thoroughly studied role for each transporter in cystine acquisition and demonstrated that TcyP plays a role in liver and heart infections. Other studies in recent years have defined how the sulfur from cystine then plays a vital role in the cell, being incorporated into iron-sulfur clusters that are key for metabolic enzyme activity. The SufCDSUB biosynthetic system was demonstrated to be important for survival in human neutrophils, with a sufD mutant demonstrating markedly reduced survival compared to WT strains in neutrophils(*221*). Furthermore, cysteine and Fe-S homeostasis were shown to be important for NO-resistance; specifically, mutants in cysK and nfu showed fitness defects in the presence of the immune radical (Table 1). Another iron-sulfur cluster assembly factor, SufT, plays an important role in iron-sulfur cluster assembly when cells experience lipoic acid stress – SufT appears to be important for the iron-sulfur clusters needed for lipoic acid synthesis(*222*). This study also presented a new role for a previously undefined protein domain, DUF59. Studies have also been conducted to gain an understanding of how reactive sulfur species (RSS) impact *S. aureus* fitness and virulence. While high levels of RSS can be toxic, low levels can be used as a signaling mechanism. A study conducted using proteomics to determine which proteins are altered by RSS showed an impact on sulfur metabolism and virulence factor production. The latter was through the modification of several SarA-family regulators, such as MgrA, which have an impact on virulence factors expression and GAPDH activity(*223*). This

implies a broad role for RSS in managing metabolism and virulence in *S. aureus*. The link between RSS and virulence factors was also elaborated by demonstrating that the per- and polysulfide sensor CstR regulates toxin expression(*224*). Additionally, hydrogen sulfide can react with reactive nitrogen species such as NO, resulting in the intermediate HNO, which can interact with RSS modifications to further impact the expression of genes relating to metal availability and sulfur signaling(*224*).

1.2.1.7 Phosphate

Phosphate is an important inorganic nutrient that must be acquired during infection, yet little is known about how *S. aureus* acquires it. Recent studies have defined the roles of the three phosphate transporters – PstSCAB, PitA, and NptA – in infection, demonstrating that each phosphate transporter has a niche where it helps *S. aureus* thrive(*225*). NptA was the only transporter that was sufficient on its own to support systemic infection, indicating this transporter is especially key for *S. aureus* virulence. A follow-up study showed that the two-component system, PhoPR, is important for expression of PstSCAB and NptA, and is key for growth in phosphate limited environments, including *in vivo*. While inorganic phosphate is not freely available in the host, several methods by which *S. aureus* can obtain inorganic phosphate have been defined. First, *S. aureus* secretes a protein GlpQ, which can cleave glycerol-3-phosphate from wall teichoic acids of other coagulase-negative *Staphylococcal* species, which can then be imported as a phosphate and carbon source(*226*). GlpQ does not affect the WTAs of *S. aureus*, indicating this is a competitive mechanism, and the expression of *glpQ* is increased under phosphate limitation stress. Additionally, the secreted phosphatase PhoB can release inorganic phosphates from host derived organophosphates, including amino acids, sugars, and nucleotides found in cell debris at infection sites(*227*). These inorganic phosphates are then brought into the

cell by the transporters discussed above. These two different methods of phosphate acquisition are likely vital for infection. Interestingly, Mn limitation is more toxic to *S. aureus* when *pstSCAB* is overexpressed, indicating a link between metal homeostasis and phosphate homeostasis(*228*).

1.2.2 Organic Metabolism

Staphylococcus aureus can use a variety of carbon/energy sources that are abundant in the human host. Primarily, *S. aureus* has evolved to use carbohydrates, peptides or free amino acids, organic acids, and/or fatty acids as carbon/energy sources.

1.2.2.1 Carbohydrates

By far, *S. aureus* has dedicated much more genetic material towards encoding proteins and enzymes involved in the catabolism and transport of carbohydrates. The major mode of carbohydrate transport in *S. aureus* is the PhosphoTransfer System, or PTS system. Briefly, PTS systems are composed of three subunits: EIIA, EIIB, and EIIC. The EIIA and EIIB subunits are involved in direct phosphorylation of the incoming sugar using the Histidine-Containing Phosphocarrier Protein (Hpr) as the donor, whereas the EIIC subunit acts as a carbohydrate specific transporter. Each sugar that can be utilized by *S. aureus* is imported by its own cognate PTS transport system. *S. aureus* encodes 19 individual PTS subunits, allowing the pathogen to transport and catabolize ~14 unique carbohydrate moieties ranging from glucose, mannose, and fructose to mannitol and maltotriose(*229*). Most of the utilizable carbohydrates for *S. aureus* are brought in via dedicated PTS systems, as mutation of *ptsH* (encoding Hpr, the universal PTS phosphodonor) eliminates growth on all but three sugars(*229*). The use of carbohydrates as carbon/energy sources leads to the accumulation of the glycolytic intermediate, fructose 1-,6-bisphosphate (FBP). This

metabolite signals to both CcpA (Carbon Catabolite Protein A) and the central glycolytic regulator GapR to maximize glycolytic gene expression and repress TCA cycle genes. Consequently, when consuming sugar, most of the carbon is excreted as acetate via the *pta-ackA* pathway for maximal energy yield(*230*). The TCA cycle is only used later, when the sugar is exhausted, and the acetate is used for energy(*231*). Interestingly, the sugar most efficiently used by *S. aureus* is the major sugar in our bloodstream, glucose. *S. aureus* has three dedicated glucose PTS systems (GlcA, GlcB and GlcC), a PTS-independent glucose transporter (GlcU, requiring the function of glucokinase, *glcK* for generation of glucose-6-phosphate), and a glucose-6-phosphate transporter (UhpT)(*229*, *232*). Of these, only *glcB*, *glcU* and *uhpT* are found in most coagulase-negative species. The fact that *S. aureus* encodes four dedicated glucose transporters speaks to the importance of this sugar to this pathogen. Mutants that specifically lack the ability to import glucose alone show specific growth defects under non-respiratory conditions including growth in the presence of NO(*229*). Indeed, we suggest that the presence of glucose acts as a "signal" to *S. aureus* that it is no longer on the surface of the skin where glucose is scarce, but rather in deeper tissue, with access to serum glucose. Furthermore, many patients with poorly controlled diabetes suffer from severe recurrent *S. aureus* infections (See Chapter 2). Therefore, the steady rise in MRSA incidence in the US over the past several decades, which was attributed to evolving hypervirulent clones, may in fact be partially due to the parallel rise in diabetes incidences over the same time period, creating a population particularly susceptible to this pathogen.

1.2.2.2 Amino Acids

S. aureus elaborates an impressive array of proteases that are capable of degrading abundant skin proteins (*e.g.* filaggrin and collagen) into peptides and free amino acids that can be consumed for carbon/energy(*233*). The main method of peptide import is via the Opp-3 ABC

transporter, though there are well documented transporters for individual amino acids as well(*233–235*). The main three families of amino acids that can be fully catabolized for energy are those that feed into ketoglutarate, oxaloacetate and pyruvate. Indeed, *S. aureus* can efficiently break down proline, arginine, glutamate (and presumably glutamine), and, to a lesser extent, histidine, all of which enter the TCA cycle at ketoglutarate (via GudB)(*236*). Similarly, aspartate (and presumably asparagine) can be shuttled into the TCA cycle through oxaloacetate (via AspA and AsnA). Finally, alanine, serine, glycine, and threonine can be used to generate pyruvate, which in turn is converted to acetate and excreted via Pta/AckA(*236*). Branched chain and aromatic amino acids are not readily catabolized, nor are cysteine and methionine; however, the latter two can be used as sulfur sources (see above). Instead, these amino acids can be imported and directly incorporated into protein.

1.2.2.3 Fatty Acids

S. aureus can import free fatty acids from the environment, though it has been reported that the pathogen does not oxidize free fatty acids(*237*). However, its genome does harbor a full pathway for fatty acid β-oxidation (SACOL0211-0215). Since the pathogen lacks genes encoding isocitrate lyase and malate synthase, it doesn't possess the glyoxylate shunt. Thus, while fatty acid oxidation can serve as a source of energy, they cannot feed into gluconeogenesis. However, recent studies have shown that *S. aureus* can incorporate exogenous fatty acids into its phospholipid repertoire(*238*). Therefore, in a way, this pathogen can use fatty acids as an indirect carbon source. One caveat is that certain unsaturated fatty acids can be toxic when incorporated, putatively due to membrane peroxidation(*239*). Indeed, inactivating fatty acid kinase (FakA) eliminates exogenous fatty acid incorporation and limits the toxicity of unsaturated fatty acids such as linoleic or oleic acids(*240*). *S. aureus* also encodes a lipase (*geh*) that allows the pathogen to extract fatty

acids from host phospholipids(*241*). This facilitates the use of human low-density lipoproteins (LDLs) as a fatty acid source for *S. aureus*(*242*).

1.2.2.4 Organic Acids

Generally, *S. aureus* doesn't consume many organic acids: almost none of the TCA cycle intermediates can serve as carbon/energy sources, likely due to lack of dedicated transporters. However, malate, lactate, and pyruvate can serve as carbon/energy sources and acetate can serve as an energy source (again, because of the lack of the glyoxylate shunt, acetate cannot serve as a carbon source). Malate can be oxidized to oxaloacetate by Mqo, a membrane bound malate:quinone oxidoreductase. This requires active respiration, so in conditions with limited respiratory activity (see below) malate cannot serve as a carbon/energy source. L-lactate can be utilized via one of the two cytosolic lactate dehydrogenase or by the membrane associated lactate:quinone oxidoreductase (Lqo)(*243*). D-lactate can only be utilized by the cytosolic dehydrogenase Ddh. Pyruvate can be consumed via Pyruvate Dehydrogenase, Pyruvate-Formate Lyase or via quinone-dependent Pyruvate Oxidase(*244*).

1.2.3 Respiration versus Fermentation

Like many bacteria, *S. aureus* harbors a branched respiratory chain and is capable of respiring on several terminal electron acceptors (oxygen, nitrite, nitrate and some in strains, nitric oxide) (Figure 1). Only cytochrome aa_3 and the nitrate reductase can serve as coupling sites by directly pumping protons across the membrane. The other reductases can only contribute to membrane potential via Q-loops (reducing quinone on the cytoplasmic face of the membrane and then oxidizing it with the concomitant release of protons on the extra cellular face of the

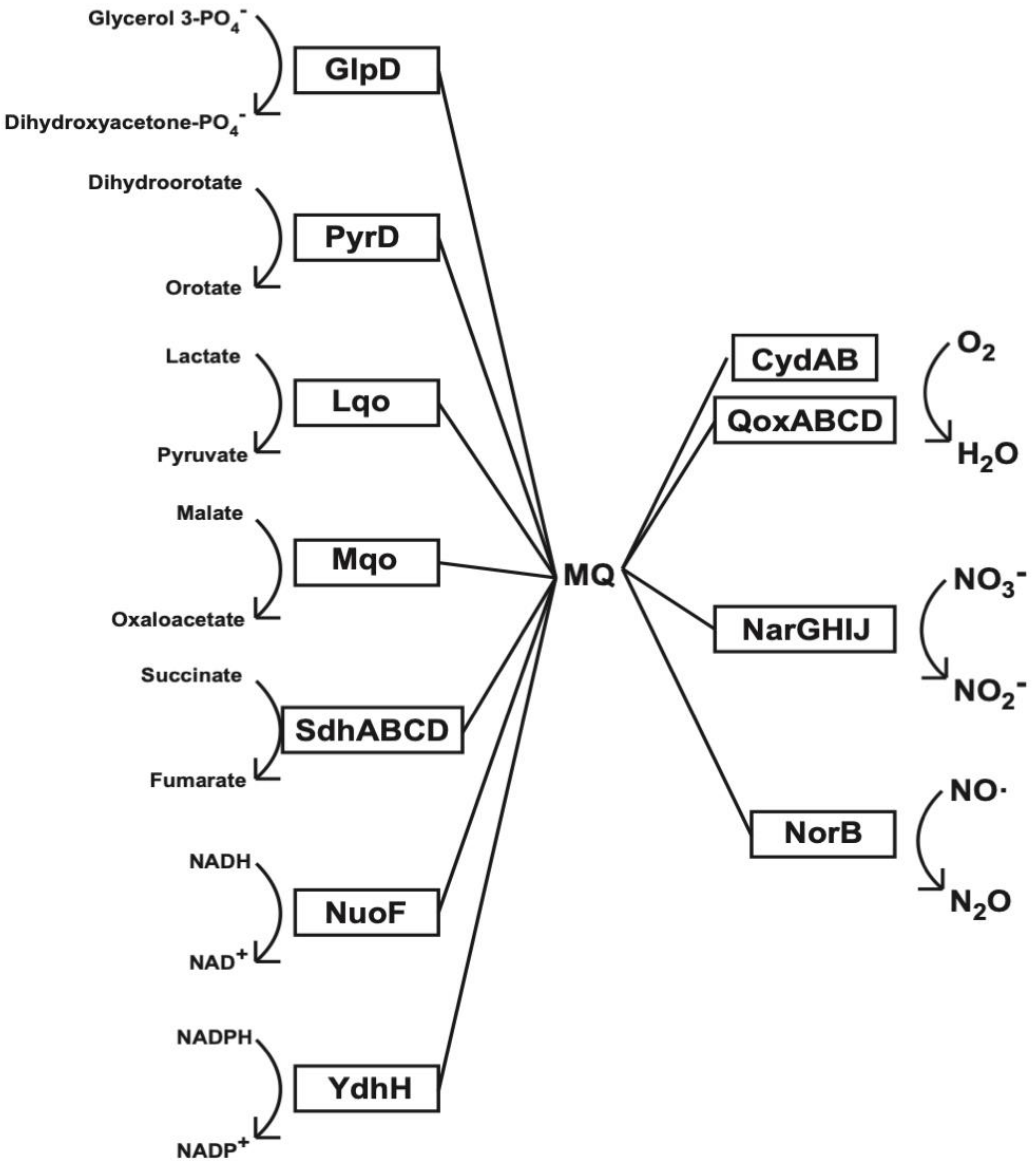

Figure 1: *S. aureus* respiration options. Like many pathogens, *S. aureus* has several options for electron acceptors at the end of the ETC. These include oxygen, nitrite, and NO, as displayed above on the right. *S. aureus* also has several donors to the ETC; not only NADH and NADPH, but succinate, malate, lactate, glycerol-phosphate, and dihydroorotate can donate electrons to the ETC (as seen above on the left). All electrons must pass through meniquinone, however.

membrane). *S. aureus* only produces one form of quinone (menaquinone) and has several reductases/dehydrogenases that can feed electrons into respiration (Figure 1). The SrrAB TCS controls respiratory flux, presumably by sensing the reduced state of the menaquinone pool. Overly reduced menaquinone pools signal for the heightened production of cytochromes, nitrate reductase, heme, and nitric oxide detoxification, as well as iron-sulfur cluster repair systems(*245*). Respiring *S. aureus* can utilize all the above-mentioned carbon/energy sources with little or no restrictions. However, if no external electron acceptor is available (or if respiration is inhibited by host immune radicals, see below), *S. aureus* possesses robust fermentative capacities beyond those of most coagulase-negative Staphylococci(*246*). When *S. aureus* grows fermentatively on its preferred carbon/energy source (*e.g.* glucose) it produces primarily lactate and formate and, to a lesser extent, ethanol and butanediol(*247*). Both the L- and D-isomers of lactate are made and are the most abundant excreted fermentative end-product. To maintain protonmotive force, the bacteria must hydrolyze ATP and run the F_1F_0 ATPase in reverse to extrude protons(*248*). This leads to alkalinization of the cytosol to a pH ~8.5, which happens to be the pH optimum for all three lactate dehydrogenases(*249*). The major regulator that controls the expression of genes encoding fermentative enzymes is the Rex repressor(*250*). Normally, Rex binds DNA and prevents expression of fermentative genes. However, when NADH builds up resulting from halted respiration, it binds to Rex leading to a conformational change and a loss of DNA binding ability(*251*). The de-repression of fermentative enzymes leads to the rebalancing of redox potential in the cell. Interestingly, the Rex regulon is far larger in *S. aureus* than most other coagulase-negative species. Consequently, *S. aureus* grows much better than its coagulase-negative relatives under strictly fermentative conditions(*246*). The only caveat is that in order to grow fermentatively, *S. aureus* must have a utilizable carbohydrate present(*252*). This does not include sugar alcohols,

which are too reduced to support strictly fermentative growth. *S. aureus* cannot ferment amino acids or organic acids, with the exception of pyruvate. Additionally, the requirement for carbohydrates is much more drastic under fermentative conditions than during respiration. Respiring *S. aureus* consume 3 g of glucose to generate a gram of biomass (dry weight), whereas fermenting bacteria require four times as much(*229*). Hence, the acquisition of additional glucose transporters to a species that is capable of rapid growth under fermentative conditions provides the pathogen with an evolutionary advantage over its coagulase-negative relatives.

1.2.4 *Staphylococcus aureus* Nitric Oxide Resistance

S. aureus is capable of thriving in the presence of considerable amounts of the immune radical, nitric oxide (NO). In broth culture, *S. aureus* can continue to replicate in the presence of ~1 mM NO, a concentration roughly 10 times greater than the bacterium would encounter in the host(*148*). *S. aureus* does possess NO-detoxification mechanisms, in that all strains harbor a flavohemoprotein encoded by *hmp* and some strains (mostly belonging to the CC30 clade) possess an additional NO-reductase, Nor. However, neither enzyme is more active or more expressed in *S. aureus* than any other Staphylococcal species, so this cannot account for this level of NO-resistance(*148*). Rather, *S. aureus* has metabolically evolved to induce a physiologic state that is inherently resistant to the effects of NO. Under high level NO ($\geq$ 50 μM), such as that encountered via direct contact within host macrophages or neutrophils(*253*, *254*), *S. aureus* relies primarily on glycolysis. In fact, in tissue culture, *S. aureus* residing within macrophages relies entirely on glycolysis, with gluconeogenesis being dispensable. This was demonstrated by the extreme survival defect of a Δ*pyk* mutant, which cannot perform glycolysis, in macrophages and no phenotype for a Δ*pckA* mutant, which can run glycolysis normally, but cannot perform

gluconeogenesis. However, upon inhibition of host NO·-production using the iNOS inhibitor, L-NIL, it was demonstrated that the Δ*pyk* mutant survived just as well as the WT and the Δ*pckA* mutant(*252*). This suggested that there are a variety of nutrient resources within a macrophage, but due to host NO·-production, *S. aureus* relies entirely on glycolysis.

1.2.4.1 Expanded Rex Regulon

The primary target of NO as far as growth and metabolism are concerned is cellular respiration and the TCA cycle, due to their heavy reliance on ferrous iron (Figure 2). Therefore, *S. aureus* shifts into heterolactic fermentation in the presence of NO with a heavy reliance on metal-independent glycolysis. In *S. aureus,* but not other species, glycolysis is able to proceed during NO stress due to the expanded Rex regulon. There are upwards of 38 predicted and confirmed genes directly regulated by the Rex repressor in *S. aureus*. In contrast, *S. epidermidis* barely has 16, while *S. saprophyticus* has less than 10(*246*). Consequently, these coagulase negative species grow poorly under strict fermentative conditions or in the presence of NO. Many of the genes in the Rex regulon of *S. aureus* are simply missing from these CoNS genomes. This includes *ldh1*, encoding the most dominant lactate dehydrogenase under NO-stress(*148*). In fact, Ldh1 is responsible for roughly 90% of the excreted L-lactate during NO-stress. In 2012, however, a new species of *Staphylococcus* was described that was a closer relative of *S. aureus* than is *S. epidermidis. Staphylococcus simiae* was isolated from the feces of the South American Squirrel monkey and its genome was published(*255*). Curiously, it has most of the Rex regulated genes that *S. aureus* possesses, including *ldh1*. Consequently, it too can grow well anaerobically, and it is also NO resistant. Moreover, in *S. aureus,* overexpressing Rex essentially shuts off the regulon, even in the presence of NO or anaerobiosis(*246*). Over-expression of Rex has no effect on aerobic

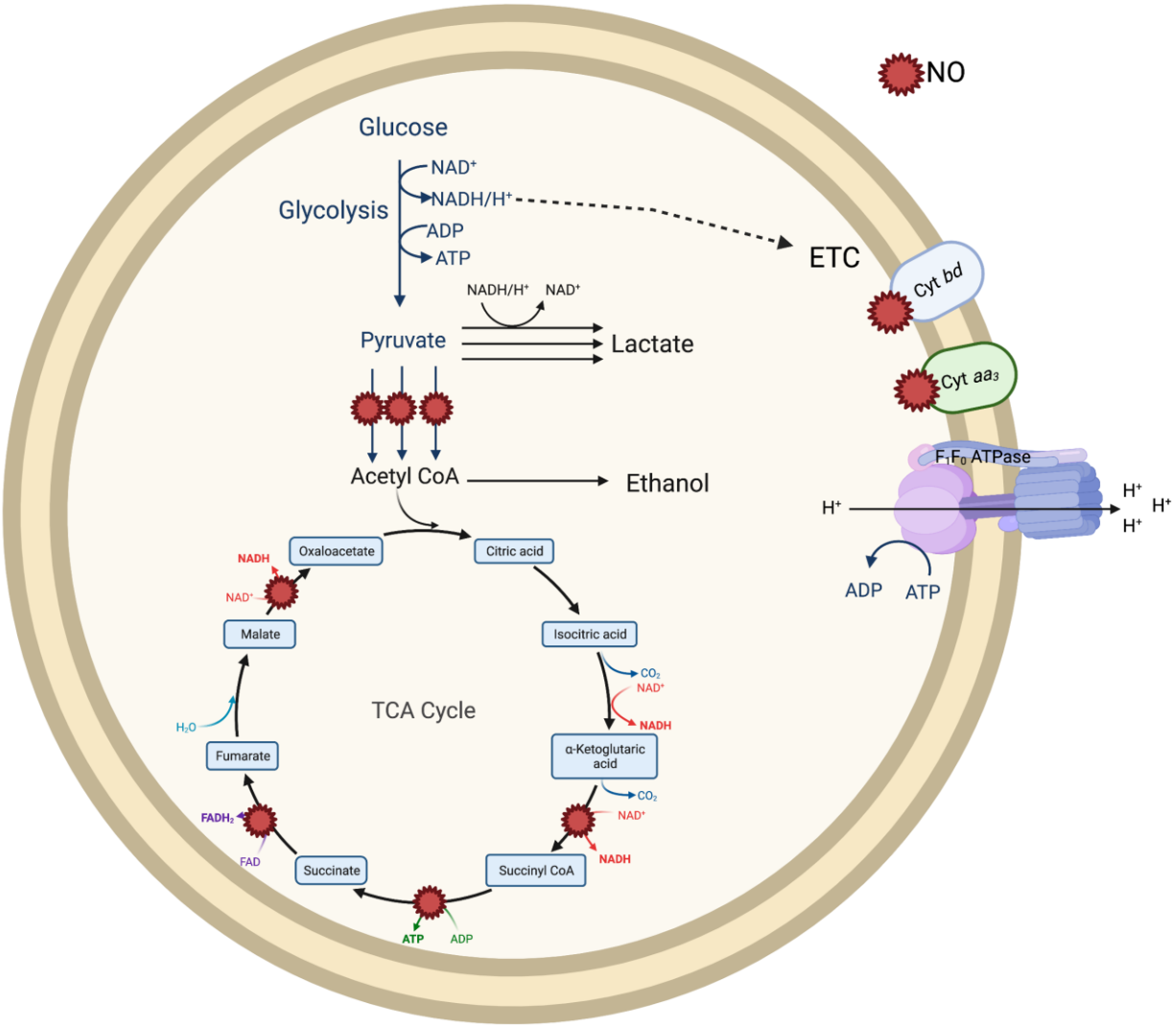

Figure 2: Metabolic Targets of Nitric Oxide. NO can target several areas of metabolism in the cell. Proteins that are particularly susceptible to NO include α-ketoglutarate dehydrogenase, succinate dehydrogenase and succinyl-COA synthestase in the TCA cycle, as well as malate-quinone oxidase and the cytochromes in the ETC. Pyruvate dehydrogenase, pyruvate synthase, and pyruvate formate-lyase, all of which convert pyruvate the acetate, are blocked by NO, leading to a buildup of pyruvate and NADH, resulting in a need for Ldh1 to convert pyruvate to lactate for maintain redox balance. Created with biorender.com.

growth, but anaerobic and NO-resistant growth are completely inhibited. These two observations suggest that the expanded Rex regulon in *S. aureus* (and *S. simiae*) is necessary and sufficient for NO-resistance. It appears the expanded Rex regulon originally may have evolved to accommodate efficient colonization of the anaerobic primate gut by the last common ancestor between the two species. However, *S. aureus* uses the trait to thrive in the face of host immune radicals that are highly inhibitory of respiration.

1.2.4.2 Intersection of Rex and SrrAB Regulons

Two genes that are under the control of Rex in *S. aureus,* but that are not controlled by Rex in *S. simiae,* encode the two-component system SrrAB (See above). Consequently, NO induces the expression of SrrAB to much higher levels in *S. aureus.* In turn, the expression of SrrAB regulated genes, including NO detoxification and cytochromes, are much higher in *S. aureus* upon exposure to NO. The means that *S aureus* is capable of respiring under moderate NO levels that are far and away above that which *S. simiae* can(*246*). Thus, the intersection of the SrrAB and Rex regulons represents an adaptation to host NO made specifically by *S aureus*. Indeed, *S. simiae* possesses no virulence factors or antibiotic resistance determinants, suggesting it has no pathogenic potential. Therefore, if the Rex regulon becomes activated, it is likely that the bacterium has entered the anaerobic primate gut, so overexpression of NO-detoxification or cytochrome genes would not have any benefit. In contrast, when the Rex regulon becomes activated in *S aureus*, it's likely due to the host inflammatory response. Therefore, high-level expression of NO-detoxification and cytochrome genes would have immediate benefits; namely, the chance to resume respiration in areas with moderate NO levels, such as those distal to infiltrating immune cells. This opens up metabolic opportunities to *S. aureus* that would not be available to other species. Specifically, if moderate respiratory flux is possible, *S. aureus* can grow

in the absence of glucose, provided there is access to the combination of lactate and peptides. Interestingly, under moderate NO stress, *S. aureus* cannot thrive on either nutrient alone, only in combination(*256*). This is due to the fact that the bacterium uses lactate via Lqo to generate energy through acetogenesis. This energy is used in turn to drive amino acid uptake and gluconeogenesis. This is all made possible by the fact that overexpression of NO detoxification and cytochrome genes afford moderate respiratory activity in *S. aureus* alone.

1.2.4.3 Host/Pathogen Immunometabolism

The fact that *S. aureus* has evolved to link virulence with glucose consumption is underscored by the fact that isolates from asymptomatic long term skin colonization augment TCA cycle activity to be successful catabolizing skin organic, amino, and fatty acids(*257*). A similar TCA-augmentation is observed in long-term lung colonization in patients with cystic fibrosis, another host site with limited access to glucose(*258*). Obviously, the normal level of TCA cycle activity is not optimized for such metabolism, since *S. aureus* is metabolically programmed to favor glycolysis and virulence. The ability of *S aureus* to continue the high-flux metabolism glycolysis in the presence of NO has direct and indirect effects on host cellular metabolism. The high need for glucose during NO stress invokes a metabolic stress on the host, leading to Hif-1α induction and IL-1β production in hypoxic keratinocytes(*259*). It also induces mitochondrial stress, leading to the production and secretion of itaconate that has immunometabolic effects on both the host and the bacterium(*260*). Furthermore, the massive amount of excreted lactate from *S. aureus* biofilms has profound effects on the host immune response, in that it leads to alterations in chromatin acetylation, resulting in excess immunosuppressive IL-10 secretion(*261*).

1.3 Concluding Remarks

The collection of virulence factors and immune evasion strategies presented in this introduction heavily indicates that *S. aureus* has not evolved to be a simply commensal organism. Indeed, it is quite reasonable to hypothesize that *S. aureus* is a pathogen that lies in wait on the surface of the skin, rather than a commensal who stumbled into an environment where it just so happens to cause infection. The following dissertation will discuss how *S. aureus* has evolved to live on the surface of the skin like other Staphylococci, but has uniquely developed the ability to recognize when it has left the skin surface and infiltrated into deep tissues through the sensing of glucose. Glucose is not commonly present on the skin surface, but *S. aureus* is incredibly reactive to its presence, as demonstrated in this dissertation. We hypothesize that *S. aureus* has evolved to respond to the presence of glucose as a signal it is in a tissue where it might cause infection, allowing for greater replication and survival of the bacteria. The signal of glucose causes a cascade of downstream effects, from expression of virulence factors (Chapters 2 and 3), to maintenance of nutrient homeostasis (Chapter 4), to expression of metabolic schemes that allow for escape from the immune system (Chapter 5). Taken together, these sets of genes are what allow *S. aureus* to be such a successful pathogen in such a variety of environments.

2.0 Lack of nutritional immunity in diabetic skin infections promotes *Staphylococcus aureus* virulence

Elevated blood/tissue glucose is a hallmark feature of advanced diabetes, and people with diabetes are prone to more frequent and invasive infections with *Staphylococcus aureus*. Phagocytes must markedly increase glucose consumption during infection to generate and oxidative burst and kill invading bacteria. Similarly, glucose is essential for *S. aureus* survival in an infection and competition with the host, for this limited resource is reminiscent of nutritional immunity. Here, we show that infiltrating phagocytes do not express their high-efficiency glucose transporters in modeled diabetic infections, resulting in a diminished respiratory burst and increased glucose availability for *S. aureus*. We show that excess glucose in these hyperglycemic abscesses significantly enhances *S. aureus* virulence potential, resulting in worse infection outcomes. Last, we show that two glucose transporters recently acquired by *S. aureus* are essential for excess virulence factor production and the concomitant increase in disease severity in hyperglycemic infections.

2.1 Introduction

The incidence of diabetes is rapidly increasing, with some estimates predicting more than 590 million afflicted people by 2035(*262*). Several complications are associated with diabetes, including increased risk of infection(*263*). One of the most common infections in individuals with diabetes are skin and soft tissue infections (SSTIs) that often manifest as foot ulcers(*263*, *264*).

SSTIs in people with diabetes are often polymicrobial; however, *Staphylococcus aureus* is the most commonly isolated pathogen from diabetic SSTIs(*9*, *265*). Moreover, *S. aureus* SSTIs more frequently result in invasive infections, including endocarditis, osteomyelitis, and sepsis in patients with diabetes(*264*, *265*). Many studies have revealed defects in both innate and adaptive immunity that are attributed to the diabetic state and contribute to the severity of infections. These include decreased reactive oxygen species (ROS) production by neutrophils and suppressed T cell function; however, the mechanisms for suppressed immunity are not known (*266*–*269*). While immune suppression in diabetic infections has been described numerous times, to our knowledge, there have been few studies that address how hyperglycemia in diabetic infections influences the virulence potential of bacterial pathogens. To cause disease, *S. aureus* must produce several secreted virulence factors including, but not limited to, α-hemolysin (Hla), phenol-soluble modulins (PSMs), and various proteases. Most of these virulence factors are unique to *S. aureus* and not found in other staphylococcal species(*255*, *270*). In addition, for full virulence, *S. aureus* must metabolically adapt to immune radical laden and hypoxic environments within sites of inflammation. This trait too distinguished *S. aureus* from most other species of staphylococci. One unifying feature of maximized virulence factor production and respiration-independent fermentation in *S. aureus* is that both require access to abundant carbohydrates, specifically glucose. Accordingly, *S. aureus* has evolved an expanded glycolytic capacity, highlighted by the acquisition of two additional glucose transporters: GlcA and GlcC(*229*). While these two phosphotransferase system (PTS)–dependent glucose transporters are found in the genomes of virtually every *S. aureus* clone, they are largely absent from coagulase-negative staphylococcal species(*229*).

Several bacterial species rely on quorum sensing to monitor cell density and regulate the expression of a spectrum of genes, including virulence factors. In *S. aureus*, the accessory gene regulator (Agr) is the primary quorum sensing system responsible for inducing the transcription of several virulence factors(*159*, *161*, *271*). The Agr operon consists of four genes, an autoinducing peptide (AIP) encoded by *agrD*, the peptide transporter/processor *agrB*, the receptor histidine kinase *agrC*, and the response regulator *agrA*. During growth, AIP accumulates in the environment and is sensed by AgrC, which subsequently auto-phosphorylates and passes its phosphoryl group to AgrA. Phosphorylated AgrA acts as a transcriptional activator that induces the transcription of many virulence factors, including the PSMs and the Agr operon itself, as well as RNAIII, which is responsible for full expression of toxins(*162*, *165*). A recent study showed that the adenosine 5′-triphosphate (ATP)–binding domain of *S. aureus* AgrC has reduced affinity for ATP relative to other sensor kinases, requiring up to 10 times more intracellular ATP for full AgrC activity(*157*, *272*). This study further suggested that linkage between Agr activity and intracellular ATP levels affords *S. aureus* the ability to "sense" the energy status of the cell via the Agr system. Thus, toxin production in *S. aureus* is controlled by bacterial density and a positive energy status. Here, we show that exacerbated disease severity in a murine model of diabetes can be attributed to two aspects of this metabolic state: innate immune dysfunction and hyperglycemia. We used a streptozotocin (STZ)–induced hyperglycemia to model particular aspects of diabetes. Namely, by specifically killing β-cells of the pancreas, STZ induces insulin-dependent hyperglycemia within 48 to 72 hours following injection. Subsequent inoculation with *S. aureus* allowed for assessing the effects of hyperglycemia on virulence factor production and disease outcomes while avoiding the confounding effects of advanced age and obesity associated with other murine models of diabetes. Given the poor immune output of phagocytes from STZ-treated animals, *S. aureus* is

able to reach much higher bacterial densities than in the abscesses from untreated euglycemic animals. In addition, we show that the lack of glucose consumption by phagocytes from STZ-treated mice partly explains the previous observations of diminished respiratory burst. The lack of glucose consumption by these phagocytes coupled with total body hyperglycemia results in an infection environment that is replete with the excess glucose. We show that the excess glucose in infections of STZ-treated animals maximizes *S. aureus* virulence factor production in an Agr-dependent fashion. Furthermore, our results demonstrate that mutants defective in glycolysis are limited in virulence factor production and cannot cause severe lesions in hyperglycemic infections. Last, we show that the evolved expansion of glycolytic capacity in *S. aureus* is required for excessive invasiveness in hyperglycemic SSTIs. Specifically, we show that the recent acquisition of *glcA* and *glcC* by *S. aureus* is essential for full toxin production and virulence potential in hyperglycemic SSTIs.

2.2 Results

2.2.1 Infiltrating phagocytes do not consume glucose or generate and oxidative burst in hyperglycemic infections

We used an STZ-induced diabetic mouse model to compare the severity and invasiveness of *S. aureus* SSTIs between hyperglycemic and euglycemic (untreated) mice. Mice were injected subcutaneously with 10^7 colony-forming units (CFUs) of *S. aureus* and were assessed 7 days after infection for weight loss, lesion size, bacterial burdens within the abscess, and dissemination to peripheral organs. Our results show that hyperglycemic STZ-treated mice develop more severe

infections than their untreated counterparts in every measured metric. STZ-treated mice displayed increased lesion size, excessive weight loss, elevated bacterial burden in the infected abscess, and increased dissemination to peripheral organs (Fig. 3, A to E, and fig. 24, A to C). This is consistent with other diabetic SSTI models with *S. aureus.* People with diabetes are known have innate immune defects that contribute to infection severity. The most common innate immune defect described in diabetic infections is the lack of an oxidative burst consisting of ROS and nitric oxide (NO) generated by macrophages and neutrophils(*269*). When activated, innate immune cells undergo a substantial metabolic reprogramming reminiscent of Warburg metabolism where glycolysis is significantly increased with pyruvate being converted to lactate instead of being fluxed through the tricarboxylic acid (TCA) cycle(*273*). The rapid influx of glucose needed for oxidative burst necessitates the expression of high-affinity glucose transporters encoded by *SCL2A1* and *SCL2A3,* commonly referred to glucose transporter-1 and -3 (GLUT-1/-3)(*274*). To determine the importance of host glucose utilization to *S. aureus* immunity, we deprived RAW 264.7 macrophages of glucose and expectedly found that the absence of glucose prevents macrophages from generating an oxidative burst and attenuates their ability to kill *S. aureus in vitro* (fig. 25, C and D). Immunohistochemistry (IHC) performed on infected tissues revealed that immune cells in both untreated and STZ-treated mice expressed inducible NO synthase (iNOS); however, similar to what has previously been described, we observed almost no evidence of oxidative burst in abscess tissues from STZ-treated animals by the absence of nitro-tyrosine adducts that are only formed in the presence of high levels of ROS and NO (Fig. 3, F and G). Furthermore, we observed that iNOS-positive infiltrating cells at the infection site in untreated mice stained brightly for GLUT-1 and GLUT-3; however, we detected neither in infected tissue from STZ-treated animals even though infiltrating cells were present (Fig. 3H and fig. 24, A and

B). We subsequently infected LysM/Cre GLUT-1 knockout (KO) mice that do not express GLUT-1 on macrophages or neutrophils to confirm that maximum host glucose utilization is necessary for oxidative burst and control of *S. aureus* infections. Similar to what we observed in diabetic mice, IHC from GLUT-1 KO mice showed no GLUT-1 expression concomitant with the absence of nitrotyrosine adducts (fig. 26, A to D). In addition, GLUT-1 KO mice displayed increased bacterial burdens in the abscess and increased dissemination to peripheral organs, albeit to a lesser extent than in STZ-treated mice (fig. 26, E and F). Thus, with all other aspects of insulin signaling intact, the limited host glycolytic flux in GLUT-$1^{-/-}$ mice results in reduced ability to control *S. aureus* infections.

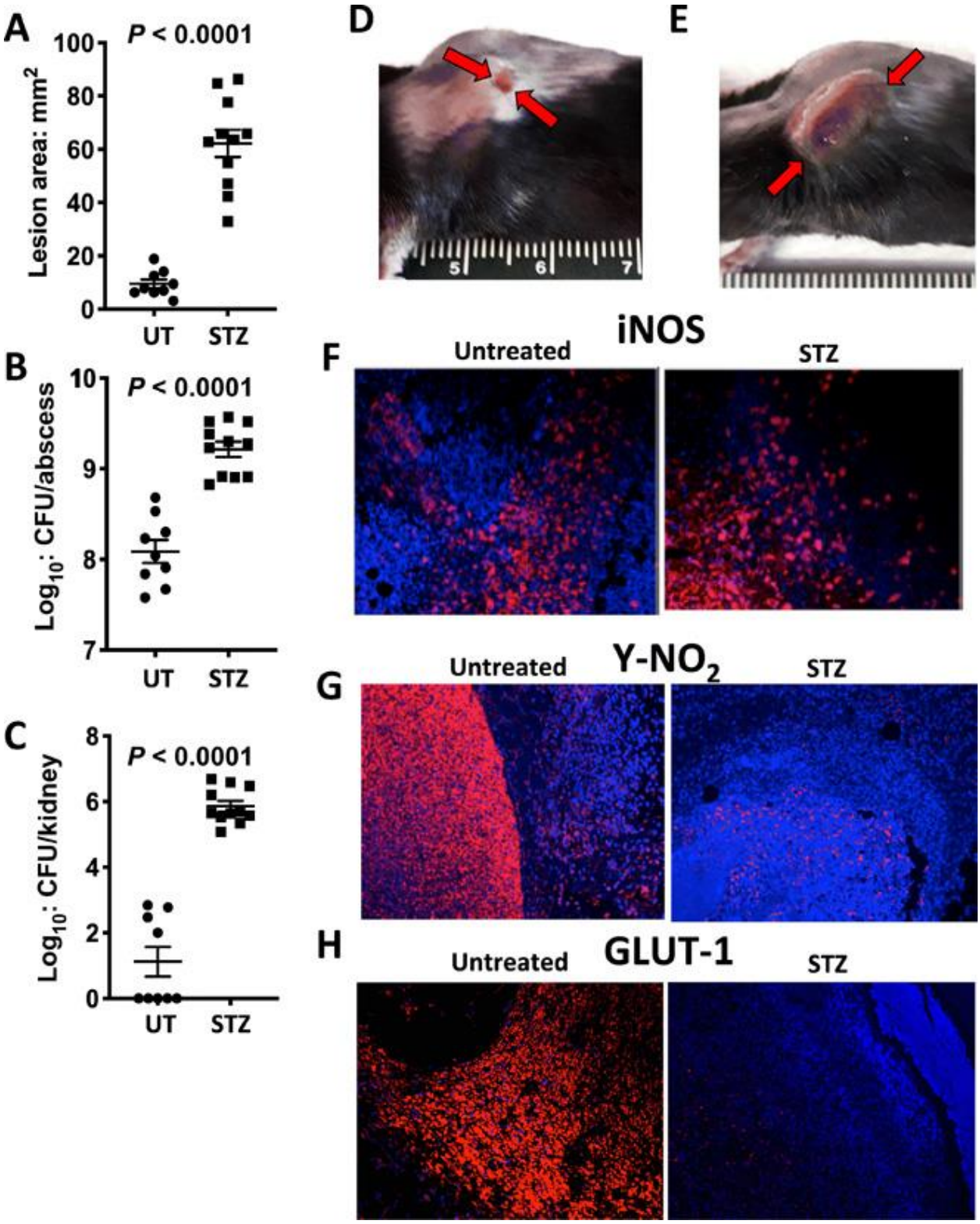

Figure 3: Diminished oxidative burst in hyperglycemic abscesses correlates with worse infection outcomes.

Untreated (N=9 and N=11) and STZ-treated (N=11 and N=8) mice were infected with $1x10^7$ CFU of the USA300

MRSA strain LAC. WT infected STZ-treated mice have a larger dermonecrotic lesion, (A) increased abscess burden (B), and increased dissemination to the kidney (C) compared to similarly infected untreated mice. Pictures of dermonecrotic lesions from an untreated mouse (red arrows) (D), and a STZ-treated mouse (E) show enhanced dermonecrosis in hyperglycemic infection. Immunohistochemistry (IHC) was performed on tissues from untreated and STZ-treated infections using antibodies against iNOS, nitrotyrosine (Y-NO_2), or GLUT-1 (red) and counterstained with DAPI (blue). Tissues from both untreated and STZ-treated mice show iNOS staining (F). However, while untreated mice exhibit robust Y-NO_2 staining, this adduct is largely absent in tissue from STZ-treated animals (G) Similarly, tissues from untreated mice show robust GLUT-1 staining that is mostly absent in tissue from STZ-treated animals (H). Photo credit: Lance Thurlow, University of Pittsburgh.

2.2.2 The Agr two-component system is essential for invasive hyperglycemic infections and requires glucose for activation

Our results show that STZ-treated mice develop more severe infections than their untreated counterparts in every measured metric. STZ-treated animals exhibit elevated blood glucose (≥300 mg/dl compared with ~100 mg/dl in untreated animals), which translates into significantly elevated tissue glucose levels (>4-fold) at the site of infection (Fig. 4A). Furthermore, others and we observed that glucose promotes Agr-mediated toxin production by *S.* aureus(*275*, *276*). The Agr-regulated RNAIII is responsible for maximal toxin and protease expression. The presence of glucose is known to enhance Agr activity when grown in buffered conditions(*276*). We cultivated *S. aureus* in chemically defined media (CDM) supplemented with glucose (PNG) or casamino acids (PNCAA) to determine whether glucose preferentially activated RNAIII transcription using an RNAIII yellow fluorescent protein (YFP) fusion. Our results confirm a significant increase in RNAIII-driven YFP in strains grown in PNG compared with PNCAA (Fig. 4, B and C).

In *S. aureus*, the Agr two-component system is required for virulence factor production and is attenuated in numerous animal models including SSTIs(*277*). Given the above results, we infected untreated and STZ-treated mice with wild-type (WT) LAC and the LAC *agr*A::Tn, and consistent with other studies, we show that the *agrA*::Tn strain is attenuated in normal mice in terms of weight loss, lesion size, bacterial burden in the skin, and dissemination to peripheral organs (Fig. 4, D to F, and fig. 28, A to C). We also show that the *agrA*::Tn strain is attenuated compared with WT in hyperglycemic STZ-treated mice, as there is no lesion formation with the *agrA*::Tn (Fig. 4D and fig. 28, D to F). This is despite the increased bacterial burden observed in the skin of the STZ-treated mice infected with *agrA*::Tn (Fig. 4E). The increased burden in STZ-treated animals likely stems from the immune dysregulation and weak oxidative/nitrosative burst described in Fig. 3 and by others(*267*, *269*).

Several virulence factors have been shown to directly contribute to disease severity in murine SSTI models including alpha-toxin (Hla) and a myriad of secreted proteases. Hla is known to be responsible for the majority of dermonecrosis associated with *S. aureus* SSTIs(*77*). In addition, in an SSTI, *S. aureus* grows in a biofilm-like aggregate that, in STZ-treated mice, is consistently able to disseminate to peripheral organs. The proteases produced by *S. aureus* potentiate biofilm dispersal, with aureolysin (aur) being the most active(*278*). We used a Δ*hla* mutant and an isogenic mutant that lacked all protease production (ΔPro) to determine the contribution of each to invasive infection in hyperglycemic mice. Mice infected with Δ*hla* had decreased lesion size and decreased dissemination to peripheral organs in both untreated and STZ-treated mice as compared with the WT-infected counterparts (fig. 29, A to F). While Δ*hla* exhibited marked reduction in abscess burden in untreated mice, it was still able to reach the elevated burdens of WT infections in the STZ-treated animals (fig. 29C). Unlike the Δ*hla* mutant,

the ΔPro mutant was not attenuated in lesion size or abscess burden in untreated mice; however, ΔPro was attenuated in STZ-treated mice, as it produced smaller lesion sizes and decreased dissemination compared with WT-infected mice despite normal bacterial burdens (fig. 28, A to F). The increased bacterial burden observed in the skin of STZ-treated mice infected with the Δ*hla*, ΔPro, and the *agrA*::Tn can most likely be attributed to immune deficiency associated with the lack of insulin signaling. However, these data suggest that hyperglycemic STZ-treated mice are not completely permissive to invasive *S. aureus* infection in that full disease severity and dissemination require virulence factors under the control of Agr.

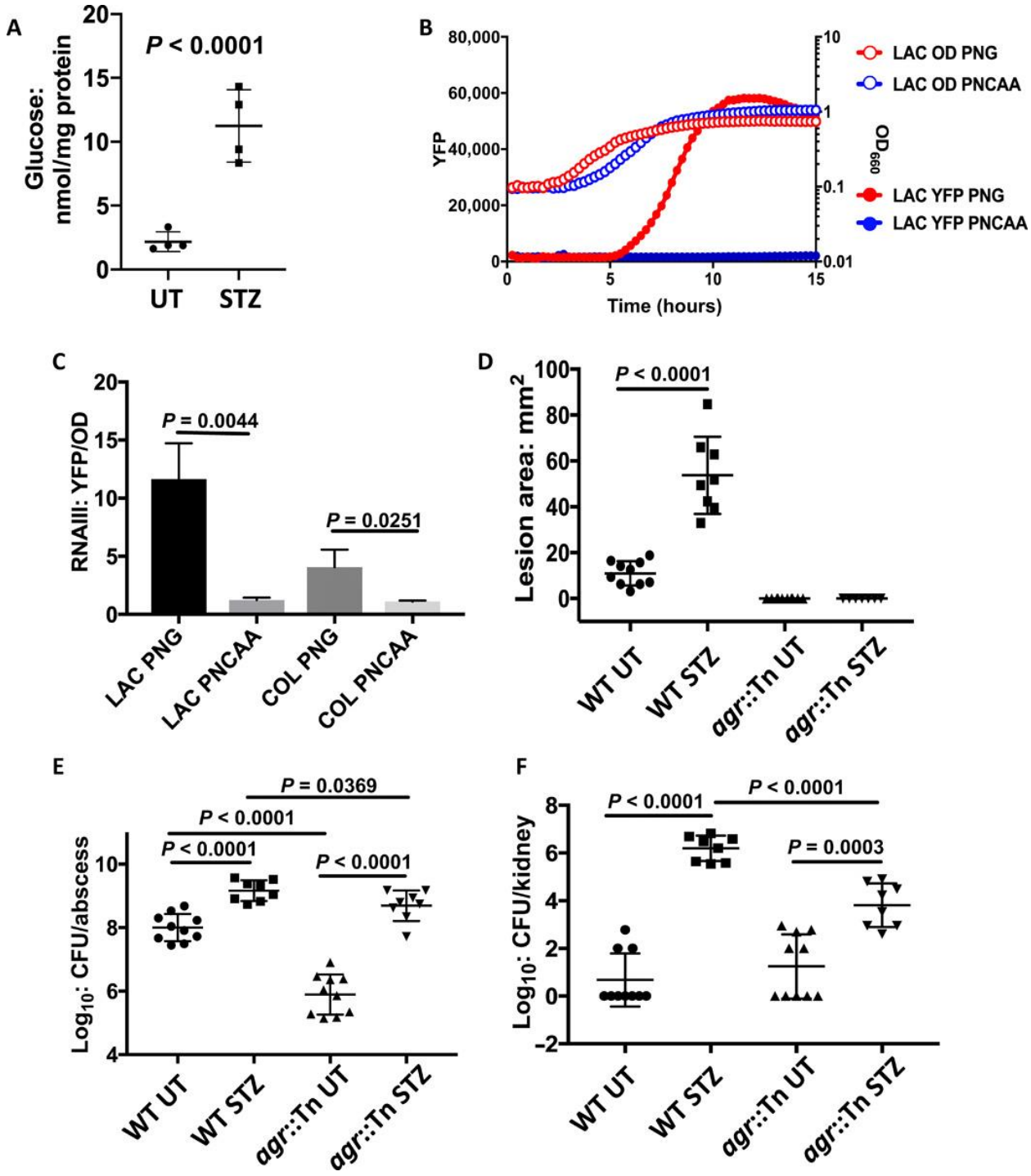

Figure 4: Agr is required for invasive infections in hyperglycemic mice and requires glucose for activation.

Glucose levels were measured in abscesses from untreated and STZ-treated animals and normalized to protein levels. Abscesses from STZ-treated animals had significantly higher glucose levels than those from untreated animals (A). *S. aureus* strain LAC harboring a plasmid with YPF linked to the RNAIII promoter (filled symbols)

were grown in PNG (red symbols) or PNCAA. (blue symbols) (B). Flouresence is only observed in strains grown in PNG (left axis) (B). Relative RNAIII:YFP fluoresence normalized to OD 660 at 10 hrs shows greater induction of RNAIII in strains LAC and COL grown in PNG (n=3) (C). Normal (N=9 and N=11) and diabetic (N=11 and N=8) mice were infected with $1x10^7$ CFU of the USA300 MRSA strain LAC or LAC agr::Tn (n=10 for untreated and N=8 for STZ-treated). Neither treated nor STZ-treated of mice infected with *agr*::Tn form necrotic lesions, (D). The *agr*::Tn abscesses had lower bacterial burdens than WT infect mice in both untreated and STZ-treated mice; however, the reduced burden in STZ-treated mice was not as striking (E). STZ-treated mice infected *agr*::Tn had significantly less dissemination to the kidneys compare to STZ-tretaed mice infected with WT LAC (F).

2.2.3 Glycolysis is required for maximal ATP generation and *S. aureus* virulence factor production

S. aureus grown in chemically defined media supplemented with glucose (PNG) preferentially activated RNAIII transcription compared with media supplemented with casamino acids (PNCAA) (Fig. 4B). In addition to increased RNAIII transcript in PNG, we observed an elevated transcription of *hla*, *psmα*, and *aur* in *S. aureus* grown in PNG and overproduction of Hla secreted into the media (Fig. 5, A and B, and fig. 29, B to D). The mere presence of glucose, however, is not enough to maximize virulence factor production. Mutants unable to efficiently use glucose consistently exhibited reduced *hla* expression. The glycolytic mutants Δ*pfkA* and Δ*pyk* exhibited reduced Hla excretion despite the presence of glucose (Fig. 5, D and E). In addition, mutants with complete and partial defects in converting glucose to glucose-6-phosphate (*ptsH*^{H15A}/*glcK* and *ptsH*^{H15A}, respectively; fig. 29) also produced significantly less Hla and were severely attenuated in both untreated and STZ-treated mice (fig. 30). *ptsH*^{H15A} is an allele that cannot import any carbohydrates via any PTS system but is still able to engage carbon catabolite protein A (CcpA) for carbon catabolite regulation. The mutant can still use glucose via the non-

PTS GlcU permease, but this requires glucose kinase (GlcK) to generate glucose-6-phosphate in order for carbon to enter into upper glycolysis (fig. 29).

The mechanism behind the glucose-stimulated virulence factor production in *S. aureus* has never been formally defined. However, given the reduced affinity of AgrC for ATP (K_M = ~1.5 mM, ~1 order of magnitude above other histidine kinases), phosphorylation of AgrA would require high intracellular ATP levels(*157*). Our results show that *S. aureus* grown in PNG contain roughly twice as much intracellular ATP compared with the PNCAA grown counterparts (Fig. 5C). We determined that intracellular ATP concentrations in PNG range between 0.8 and 1 mM, just under the K_M of AgrC for ATP, suggesting that further reduction in ATP pools (e.g., growth in PNCAA) may significantly hinder Agr activity. In further support of the role of ATP levels in modulating toxin production, reducing the efficiency of ATP generation from glucose catabolism also reduced virulence factor expression. In the presence of glucose and oxygen, *S. aureus* uses overflow metabolism where glucose is primarily metabolized to acetate (fig. 27). This pathway provides *S. aureus* the ability to rapidly generate two additional ATP per glucose molecule. *S. aureus* uses the phosphotransacetylase (Pta)–acetate kinase (AckA) pathway to generate acetate and ATP (fig. 29)(*230*). Although not as marked as Δ*pfkA* or Δ*pyk*, our results show that compared with WT, growth of the Δ*ackA* mutant in PNG resulted in less ATP production and decreased Hla production compared with WT (Fig. 5, G to I). Thus, despite being able to fully catabolize glucose, the decreased energy yield in the Δ*ackA* mutant reduced Agr activity, resulting in decreased disease severity in both euglycemic and hyperglycemic animals (Fig. 5, K and L, and fig. 31). Agr activity in the form of Hla excretion was linearly correlated with the level of intracellular ATP in all of the mutants tested [coefficient of determination (R^2) = 0.7], suggesting that Agr activity is tightly linked with the energy state of the cell (Fig. 5J).

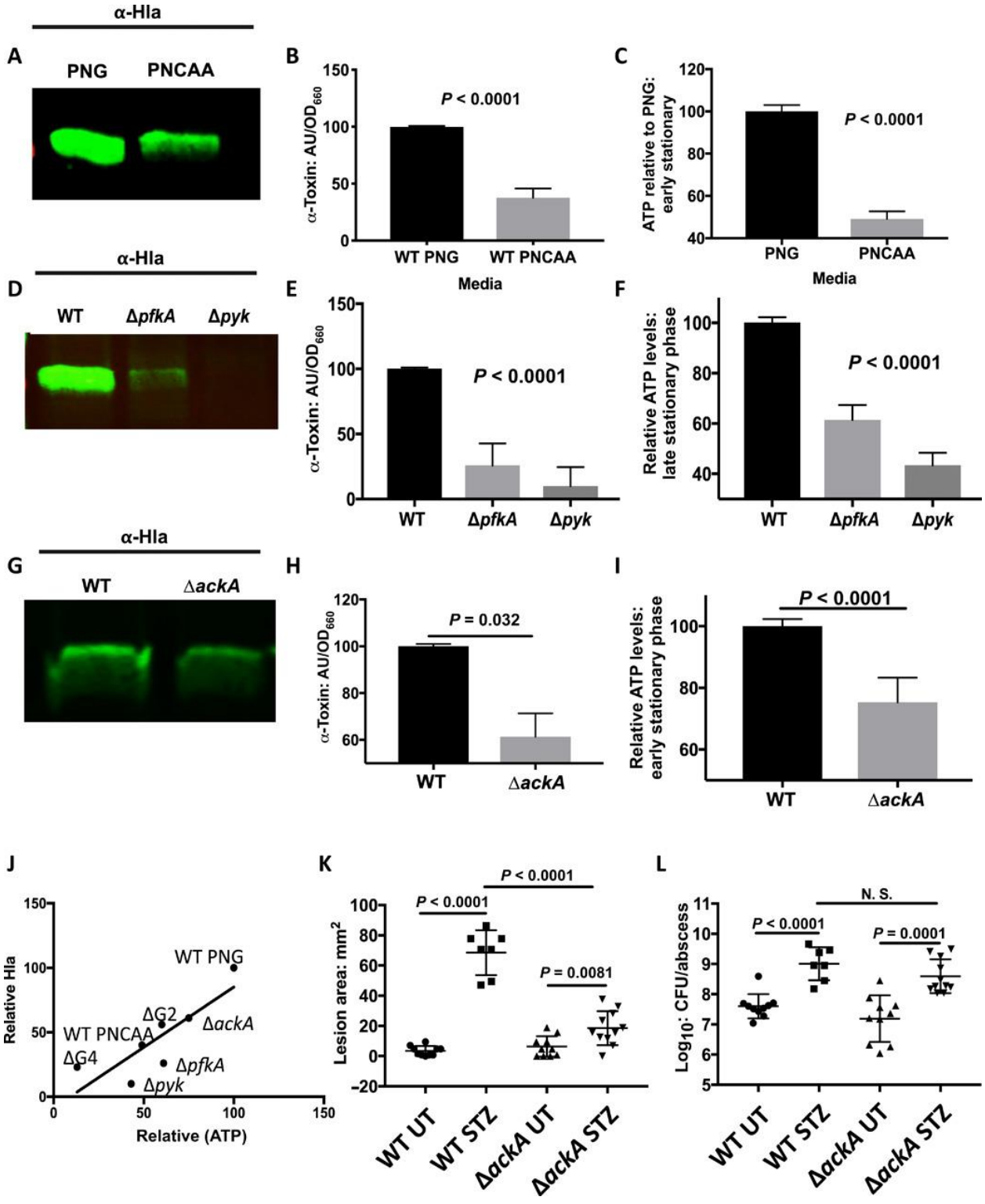

Figure 5: Toxin production by *S. aureus* requires ATP generation from glycolysis. Representative western blot showing α-hemolysin in spent media from LAC grown in PNG (left) or PNCAA (right) (A). Quantification α-hemolysin normalized to OD 660 in LAC grown in PNG or PNCAA (n=3) (B). Quantification of intracellular ATP

normalized to OD660 relative to LAC grown in PNG versus PNCAA (n=3) (C). Representative α-hemolysin western blots from culture supernatants from LAC (left), LAC *Δpfk*A (center) and LAC *Δpyk* (right) grown in PNMix (D). Quantification of western blots from LAC, LAC *Δpfk*A, and LAC *Δpyk* (n=3) (E). Quantifiction of intracellular ATP normalized to OD660 relative to LAC (F). Representative α-hemolysin western blots of culture supernatant from LAC (left) and LAC *ΔackA* (right) grown in PNG (G). Quantification α-toxin western blots from LAC and LAC *ΔackA* (n=3) (H). Quantification of intracellular ATP normalized to OD660 relative to LAC (n=3) (I). Regression analysis revealed a significant correlation between normalized intracellular ATP and the amount of normalized excreted Hla (R2= 0.7, non-zero slope, p = 0.019) (J). Untreated and STZ-treated mice were infected with 10^7 CFU of WT LAC or LAC *ΔackA* (WT UT n=10, WT STZ n=7, *ΔackA* UT n=10, *ΔackA* STZ n=11). Untreated mice infected with WT or *ΔackA* have similar lesion sizes (K). STZ-treated mice infected with *ΔackA* have significantly larger lesion sizes than similarly infected untreated mice infected, but smaller lesion sizes than STZ-treated mice infected with WT (K). STZ-treated mice infected with WT have significantly increased bacterial burden in the subcutaneous abscess compared to similarly infected untreated mice (L). STZ-treated mice infected with *ΔackA* have significantly increased bacterial burden in the subcutaneous abscess compared to similarly infected untreated mice (L). There is no significant difference in abscess burden in STZ-treated mice infected with WT or *ΔackA* (L).

2.2.4 Excess glucose in hyperglycemic infections disproportionately potentiates *S. aureus* virulence over fitness

Phlorizin is a competitive inhibitor of the sodium/glucose cotransporters 1 and 2 (SGLT 1 and 2) in the kidney and lowers blood glucose levels by inhibiting glucose reabsorption. We treated mice with phlorizin 1 day before and throughout infection with *S. aureus*. Phlorizin treatment reduced blood glucose to below 200 mg/dl in 7 of 10 treated mice. The phlorizin-treated mice with lower blood glucose had markedly smaller lesion sizes and lower organism burdens and exhibited reduced dissemination to peripheral organs than their hyperglycemic (STZ alone treated)

counterparts (Fig. 6, A to F). In addition, using quantitative real-time polymerase chain reaction (PCR), we show that transcripts of *hla*, *psmα,* and *aur* are significantly elevated in hyperglycemic infections compared with untreated controls (Fig. 6G). However, in phlorizin-treated animals, we observe that transcripts of *hla*, *psmα,* and *aur* are reduced to levels observed in euglycemic untreated mice (Fig. 6G). This suggests that the stark reduction in disease severity in phlorizin-treated mice is incongruent with the mere ~half-log reduction in organism burden, despite being statistically significant. Rather, the improved infection outcome from phlorizin treatment results partly from the reversal of excessive virulence factor production in hyperglycemic mice.

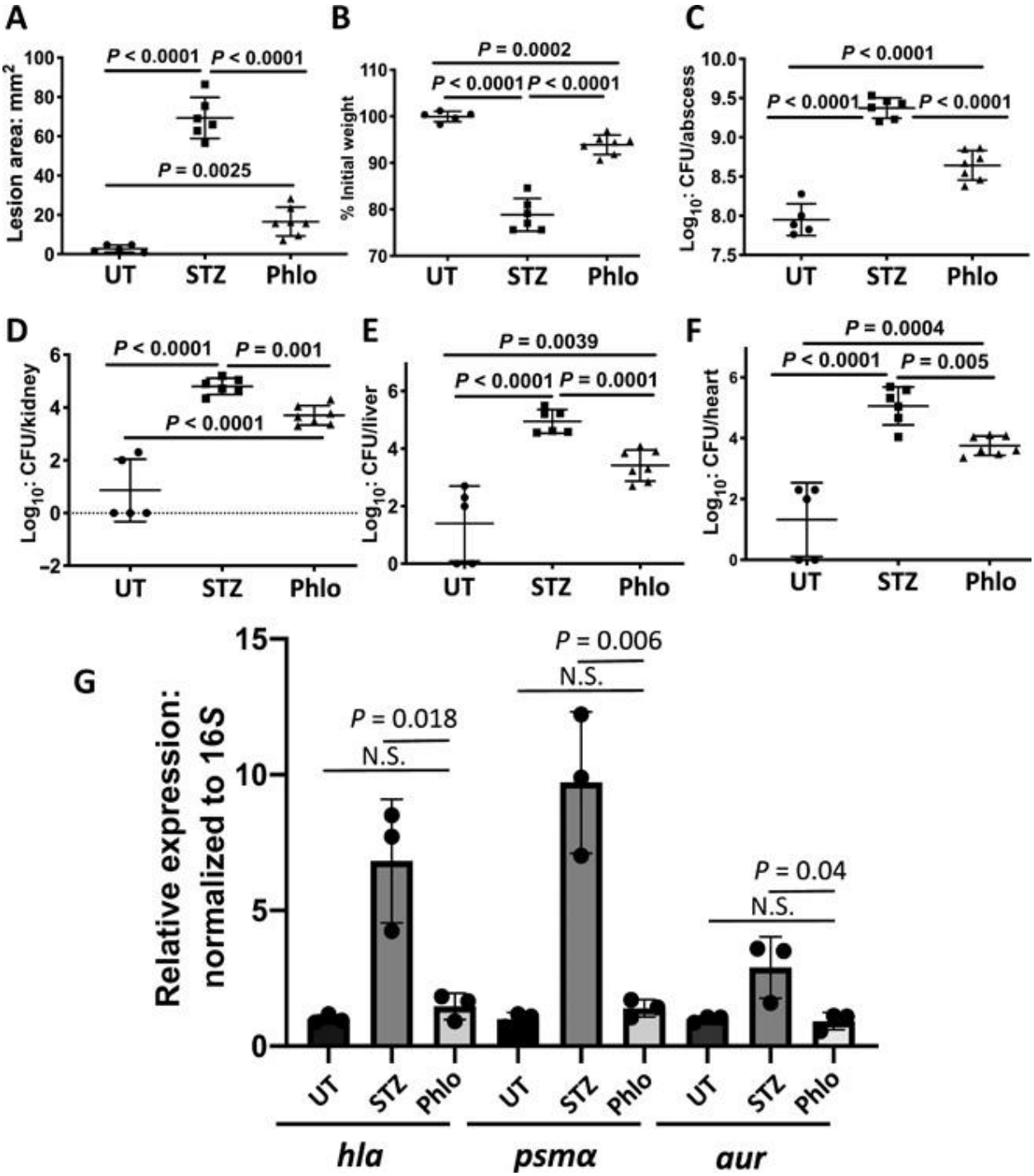

Figure 6: Reducing blood glucose in hyperglycemic mice with phlorizin reverses infection severity. Mice were treated with phlorizin one day prior to infection and throughout the course of infection to lower blood glucose levels without influencing insulin signaling. STZ-treated mice treated with phlorizin had smaller lesions than mice treated with STZ alone, but larger lesions than untreated mice (A). Infected STZ-treated mice display significant weight loss that is reversed with phlorizin (B). STZ-treated mice that were further treated with phlorizin display lower

abscess burdens than mice treated with STZ-alone, but higher burdens than untreated mice (B). Phlorizin treatment resulted in decreased dissemination to the peripheral organs in STZ-treated mice including the kidneys (D), liver (E), and heart (F). Quantitative real-time PCR *S. aureus* isolated from untreated, STZ-treated, and dual STZ-phlorizin abscesses showed significantly increased expression ($p < 0.05$) of *hla*, *psmα*, and *aur* in STZ-treated mice that is reversed by phlorizin (G).

2.2.5 Evolutionarily acquired glucose transporters are essential for full toxin production and virulence potential in diabetic mice

In support of the notion that the primary effect of excess glucose in diabetic infections is to exacerbate virulence factor production, we infected untreated and STZ-treated animals with an *S. aureus* mutant devoid of glucose transport. Unlike Δ*pfkA* or Δ*pyk* mutants, which cannot use any carbohydrate, the ΔG4 mutant (lacking all four glucose transporters: *glcA, glcB, glcC,* and *glcU*) is specifically defective in glucose utilization(*229*). We observed decreased ATP levels concomitant with decreased Hla accumulation in media and decreased transcript levels of *hla*, *psm*-α, and *aur* when ΔG4 was grown in CDM with both glucose and casamino acid carbon/energy sources (PNMix) (Fig. 7, A to D). This translates into reduced lesion sizes and dissemination to peripheral organs in both untreated and STZ-treated animals (Fig. 7, F and G, and fig. 32). Even at day 3, when abscess sizes are largest, we see no observable skin lesion in ΔG4-infected STZ-treated animals (fig. 32E). This decreased disease severity cannot be fully explained by reduced organism burdens, particularly in the case of hyperglycemic animals in which the ΔG4 was still overabundant by ~2 logs compared with untreated mice (Fig. 7G). Rather, real-time PCR performed on WT and ΔG4 isolates from hyperglycemic abscesses showed markedly decreased transcription of *hla*, *psm*-α, and *aur* in the ΔG4 strain (Fig. 7E). Thus, mutants that are unable to capitalize on excess blood glucose in hyperglycemic tissue cause markedly reduced disease

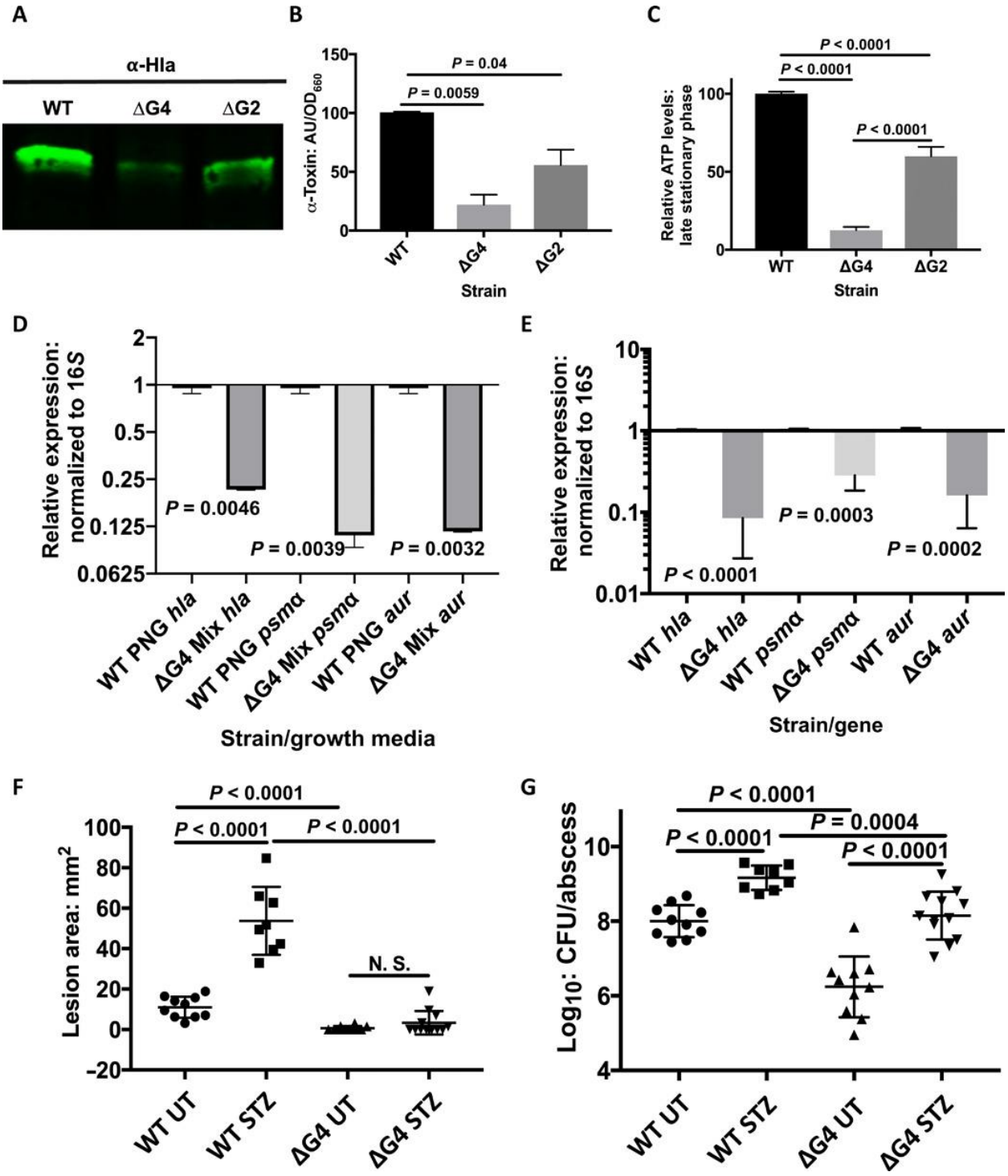

Figure 7: Glucose transporters are essential for ATP and toxin production. Representative α-hemolysin western blot from supernatants of WT LAC, LAC ΔG4 (lacking all glucose transporters), and LAC ΔG2 (lacking the recently acquired GlcC and GlcA transporters) grown in PNG (A). Quantification of α-hemolysin western blots (n=3) showing significantly decreased α-hemolysin production by LAC ΔG2 and LAC ΔG4 compared to WT LAC (B).

The LAC ΔG4 (lacking all glucose transporters) and LAC ΔG2 have reduced intracellular ATP compared to WT LAC when grown in PNG (C). Quantitative real-time PCR from WT LAC and LAC ΔG4 grown in PNG shows significant decreases in *aur, psmα*, and *hla* transcripts in LAC ΔG4 (n=3) (D). Quantitative real-time PCR from WT LAC and and LAC ΔG4 isolated from STZ-treated mice showed reduced transcript levels of *hla, psmα,* and *aur* in LAC ΔG4 (E). Day seven lesion sizes measured from untreated mice infected with LAC ΔG4 were virtually undetectable and abscesses in STZ-treated mice infected with LAC ΔG4 also rarely had small lesions (F). LAC ΔG4 is attenuated in untreated and STZ-treated mice compared to WT LAC, but has higher CFU in STZ-treated animals (G).

severity with only a modest reduction in organism burden.

Glycolysis is essential for both the full virulence capacity of *S. aureus* and the ability of the host to mount an effective immune response against invading pathogens. Consequently, the host uses two dedicated, high-affinity glucose transporters (GLUT-1 and GLUT-3) to support active inflammatory phagocyte activity. Similarly, two of the four *S. aureus* glucose transporters, GlcA and GlcC, are recent additions to the genome, as they are absent in all but two other staphylococcal species and overly contribute to glucose transport (Fig. 8A)(*229*). We deleted *glcA* and *glcC* (ΔG2) to determine the contribution of these recently acquired, highly active glucose transporters to S. aureus toxin production and virulence. Although not as robust as the ΔG4 mutant, the ΔG2 mutant had decreased intracellular ATP levels and decreased Hla production (Fig. 7, A to C). The ΔG2 mutant was moderately attenuated in untreated euglycemic mice but achieved WT levels of abscess burden hyperglycemic abscesses (Fig. 8C). However, STZ-treated mice infected with ΔG2 exhibited decreased weight loss, smaller lesion sizes, and reduced dissemination compared with WT infections (Fig. 8, B to D, and fig. 33). Thus, for *S. aureus* to fully benefit from elevated blood glucose in hyperglycemic animals, it must express these two newly acquired, highly active glucose PTS systems.

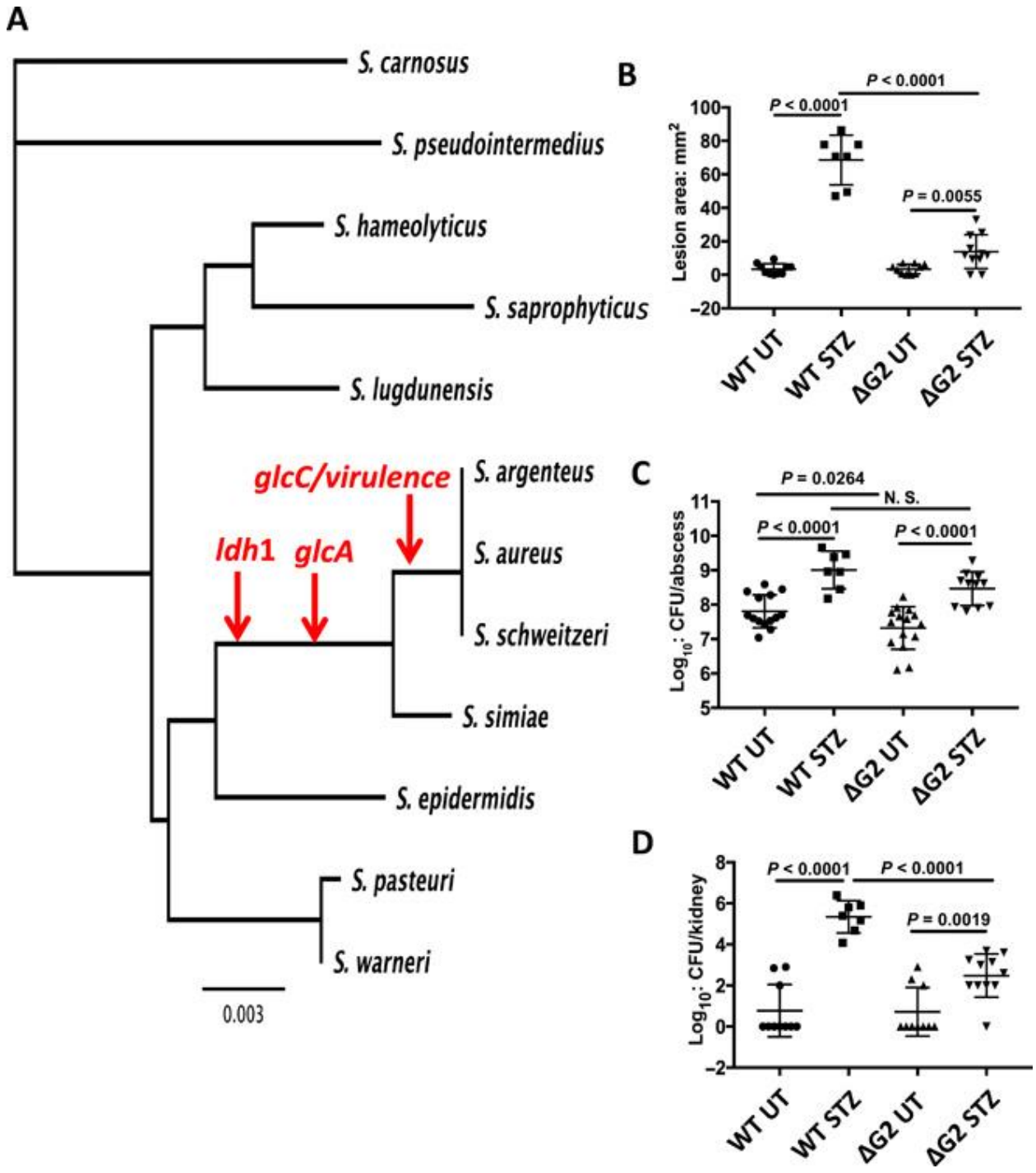

Figure 8: The evolutionary acquisition of glucose transporters by *S. aureus* coincides with acquisition of virulence factors. A phylogenetic tree based on 16S ribosomal DNA sequences showing the relation of *S. aureus* to other Staphylococcal species. Red arrows show where *S. aureus* and other related species evolutionarily acquired lactate dehydrogenase 1 (*ldh1*), glucose transporter A (*glcA*), glucose transporter C (*glcC*), and virulence factors

including α-, β- and γ-hemolysins (A). Untreated and STZ-treated mice were infected with 1 x 10^7 CFU of WT and ΔG2 (n=10 WT UT, n=7 8 WT STZ, n=10 ΔG2 UT and n=11 ΔG2 STZ). STZ-treated mice infected with WT had larger lesion sizes than untreated mice infected. STZ-treated mice infected with ΔG2 had smaller lesion sizes than WT infected STZ-treated mice. (B). STZ-treated mice infected with WT or ΔG2 had significantly higher abscess bacterial burdens than their untreated infected controls (C). STZ-treated mice infected with WT displayed increased dissemination to the kidneys compared to similarly infected untreated mice (D). STZ-treated mice infected with ΔG2 had increased dissemination to the kidneys compared to similarly infected untreated mice (D).

2.3 Discussion

Individuals with diabetes are prone to more frequent and invasive SSTIs, with *S. aureus* being the most common pathogen isolated from diabetic wounds(*10*, *263*, *265*). Previous studies have proposed that decreased respiratory burst produced by innate immune cells might be the underlying cause of increased infection severity; however, the mechanisms for suppressed immunity are not known(*267–269*). Upon stimulation, infiltrating phagocytes adopt a metabolic strategy whereby high glycolytic flux is redox balanced via lactate production. The excess requirement for glucose acquisition is met by the induction of high-affinity glucose transporters, GLUT-1 and GLUT-3, on infiltrating phagocytes (Fig. 3H and fig. 25A)(*274*). The ability to transition into this metabolic state is critical for immune output since any interference with phagocyte glucose import precludes an effective oxidative burst and bacterial clearance (figs. 25, C and D, and 26, E and F)(*273*). We previously showed that *S. aureus* has evolved a similar metabolic strategy through the genetic acquisition of two highly active glucose transporters (*glcA* and *glcC*; Fig. 8A and fig. 29A) and a highly active lactate dehydrogenase (*ldh1*) to resist immune radicals such as NO(*229*). This "metabolic mimicry" affords *S. aureus* the ability to thrive

at sites of inflammation, provided that it has adequate access to glucose. However, over time, the supply of glucose is diminished by the ever-increasing populations of infiltrating phagocytes, eventually leading to the resolution of the SSTI and bacterial clearance (Fig. 3, A to C)(*279*). In STZ-treated hosts, however, this coordinated immunometabolic response is completely dysfunctional, as infiltrating phagocytes do not express GLUT-1 or GLUT-3 and do not elicit a respiratory burst (Fig. 3, F to H, and fig. 25, A and B). The lack of robust immune radical production has been previously observed in multiple diabetic models of infection; however, a role in glucose transport was never implicated. In addition, we observed a sixfold increase in glucose in abscesses from STZ-treated animals compared with those from untreated mice even though there is only about a fourfold increase in blood glucose (Fig. 4A). This suggests that competition for glucose at the infection site is another form of nutritional immunity reminiscent of the host scavenging transition metals such as iron, zinc, and manganese, all of which have been shown to directly contribute to *S. aureus* clearance in resolving SSTIs(*280, 281*). Moreover, only people with diabetes that have poor glycemic control [HB1Ac (glycated hemoglobin) > 8.5] are at a heightened risk for developing severe MRSA SSTIs, suggesting that sustained hyperglycemia is a driving force in infection susceptibility(*282*). This raises the question of how decreased nutritional immunity and the concomitant increase in tissue glucose contribute to invasive infection in diabetic SSTIs.

The Agr system controls the expression of several *S. aureus* virulence factors and requires glucose for activation (Fig. 4, B and D). The sensor kinase AgrC belongs to the HPK-10 family of histidine kinases with variations at key conserved Asp residues. The Asp to Asn variation results in roughly a 10-fold reduction in affinity toward ATP for AgrC compared with other families of two-component systems(*157*). The K_M for canonical histidine kinases is well below the

intracellular ATP concentrations found in all conditions tested here (K_M = ~100 μM range), and therefore, activity would not be affected by the energy state of the cell. In contrast, the low affinity of AgrC toward ATP allows for the coordination of cell density signals with that of the energy state of the cell. Given that *S. aureus* has evolved to maximize energy production via glycolysis, this links Agr activity to the availability of glucose, which is overly abundant in the abscesses of STZ-treated animals (Fig. 4A). However, linking Agr activity to the availability of an organism's preferred energy source may be important for proper responses to stimuli by HPK-10 family members beyond virulence, as many are found in nonpathogenic bacteria.

In an SSTI, *S. aureus* grows in a biofilm-like aggregate that is able to disseminate to peripheral organs in STZ-treated mice. Our results show that STZ-treated mice develop more severe infections by every measurable metric and that this phenotype requires the Agr TCS (Fig. 4, D to F, and fig. 27). Agr-regulated proteases and Hla contribute equally to invasive infection in diabetes. The expression of proteases, primarily aureolysin, is essential for *S. aureus* biofilm dissemination, while Hla is required for SSTI lesion formation (fig. 26). In hyperglycemic mice, the *hla* mutant was more attenuated in lesion formation than the protease mutant, but both mutants were similarly attenuated in dissemination (fig. 28). During the course of an SSTI, the host generates an abscess wall consisting of mostly collagen and fibronectin around the infected tissue. This creates an environment devoid of glucose while simultaneously preventing the spread *S. aureus* to neighboring tissues(*279*). Since collagen is one of the substrates readily hydrolyzed by Aur, one could envision in a hyperglycemic SSTI that the overabundant expression of proteases would continually degrade the primary components of the abscess wall while simultaneously promoting dissemination of the biofilm-like aggregate. Moreover, increased Hla expression accelerates dermonecrosis and lesion growth, thereby preventing the host from properly walling

off the abscess. This scenario potentially explains why both Hla and proteases are necessary for invasive infection in STZ-treated mice.

We contend that immune dysfunction in STZ-treated animals primarily results in increased bacterial burdens, whereas elevated tissue glucose is responsible for increased *S. aureus* virulence factor production. For instance, ΔG4 mutants are still able to attain nearly the same elevated skin burdens in STZ-treated mice given their inherent immune dysfunction. However, the ΔG4 mutant does not cause lesions or disseminate, since it cannot capitalize on the excess tissue glucose in hyperglycemic SSTIs (Fig. 7, F and G, and fig. 32, B to D). We also observe a similar phenotype with the Agr mutant, in that bacterial numbers increase in abscesses from STZ-treated mice, but there is no corresponding increase in dermonecrosis or dissemination (Fig. 4, D to F). Furthermore, phlorizin treatment, which lowers blood glucose without restoring insulin signaling or full immune function, completely abrogated excessive virulence factor production and significantly reduced abscess lesion area without lowering organism burdens by even a log (Fig. 6). Thus, the diabetic state results in two deficiencies that directly affect the outcome of *S. aureus* SSTIs: reduced immune output that allows for bacterial overgrowth and limited nutritional immunity resulting in excess glucose, which directly stimulates Agr-dependent virulence.

The recent acquisition of the glucose transporters GlcA and GlcC significantly contributes to *S. aureus* virulence, particularly in hyperglycemic tissues (Fig. 8, B to D, and fig. 33, F to H). These two PTS transporters are highly active and support the ability of *S. aureus* to battle the host's nutritional immunity strategy, at least for a while before the increasing immune infiltrate overwhelms the competitive abilities of invading bacteria. In STZ-treated animals, a ΔG2 mutant, which has the same glucose transport ability of *Staphylococcus epidermidis*, cannot take advantage of the excess tissue glucose and largely resembles an infection with a ΔG4 mutant completely

devoid of glucose transport. Furthermore, the most recent acquisition of GlcC coincided with the acquisition of several toxins, including α-, β-, and γ-hemolysins (Fig. 8A). Staphylococcus *schweitzeri* and *Staphylococcus argenteus* both have *glcA* and *glcC,* as well as all three hemolysins and several proteases (Fig. 8A). In contrast, *Staphylococcus simiae* lacks *glcC* and does not encode any hemolysins or nearly as many proteases. Not much is known about *S. schweitzeri*, but *S. argenteus* was initially classified as *S. aureus* until further analysis revealed it to be a unique species(*283*). Furthermore, *S. argenteus* is an emerging pathogen in Southeast Asia with several isolates coming from patients with diabetes(*284*). Whether metabolic evolution preceded or succeeded the acquisition of virulence is still unknown. However, the correlation of the two supports the role of host glucose as a signal to *S. aureus* that it is no longer on the skin surface (where carbohydrates are scarce), but rather in deeper tissue replete with serum glucose. Consequently, this signal results in the pathogen modulating both virulence and metabolism. Moreover, two other Gram-positive pathogens that are readily killed by immune radicals, *Streptococcus pyogenes* and *Enterococcus* spp., are associated with invasive infections in patients with diabetes(*10*). Much like *S. aureus*, both of these pathogens link glucose availability to virulence factor production(*285*, *286*). This suggests that several organisms that cause invasive infections in people with severe diabetes are evolutionarily predisposed to take advantage of immune suppression and the availability of excess glucose(*285*, *286*).

The reasons why people with diabetes are prone to more frequent and invasive infections have remained elusive. One obvious reason for increased infection frequency in individuals with diabetes is immune suppression, as several commensal bacteria are frequently isolated from diabetic wounds but do not cause invasive infections. Here, we show that the lack of GLUT-1/-3 expression on infiltrating phagocytes from STZ-treated, insulin-deficient animals correlate with

their inability to mount an effective oxidative burst and clear the infection. However, the mechanism explaining the requirement of effective insulin signaling for phagocyte GLUT-1/-3 expression remains unknown. That said, we can now begin to understand why patients with diabetes suffer specifically from *S. aureus* infections so frequently. Our results show that the evolutionary coupling of expanded glycolytic capacity with toxin production in *S. aureus* and suppressed host nutritional immunity allows this pathogen to take advantage of the unique infection environment associated with advanced diabetes, resulting in more severe infections. Furthermore, these data suggest that the development of specific inhibitors of bacterial glycolytic enzymes would be beneficial for treating infections in people with diabetes(*287*).

2.4 Materials and methods

2.4.1 Bacterial strains and growth conditions

The bacterial strains used in this study are listed in table 2. *S. aureus* strain LAC was used in *in vitro* and *in vivo* studies. *S. aureus* was grown in the brain heart infusion (BHI) for mouse infection studies. For *in vitro* studies, *S. aureus* was grown in CDM supplemented with glucose (PNG), casamino acids (PNCAA), or both (PNMix) at 37°C with shaking at 250 revolutions per minute (rpm) as previously described(*243*). Bacteria were enumerated by plating for viable CFUs on BHI agar plates.

Table 2: Strains used in Chapter 2

Strain	Description	Source
LAC	Methicillin Resistant Clinical *S. aureus* Isolate	
SF8300	Methicillin Resistant Clinical *S. aureus* Isolate	
COL	Methicillin Resistant Clinical *S. aureus* Isolate	
AR1038	*S. aureus* LAC pDB59	(*288*)
AR1048	*S. aureus* COL pDB59	(*229*)
AR1198	*S. aureus* LAC Δ*agrA*::Tn	(*248*)
AR0776	*S. aureus* SF8300 Δ*pfkA*	(*252*)
AR0891	*S. aureus* LAC Δ*pyk*::Erm^R	(*252*)
AR1698	*S. aureus* LAC Δ*ackA*::Km^R	(*252*)
AR1290	*S. aureus* LAC ΔG2: Δ*glcA*::Km^R, Δ*glcC*::Sp^R	(*229*)
AR1297	*S. aureus* LAC ΔG4: Δ*glcA*::Km^R, Δ*glcB*::Er^R, Δ*glcC*::Sp^R, Δ*glcU*::Tc^R	(*229*)
AR1320	*S. aureus* LAC ptsH-H15A	(*229*)
AR1321	*S. aureus* LAC ptsH-H15A/Δ*glk*::Tn	(*229*)
AR1356	*S. aureus* Protease	(*289*)
AR1759	*S. aureus* Δ*hla*	

2.4.2 Animal studies

Animal experiments were approved by the University of Pittsburgh Animal Care and Use Committee (protocol nos. 16027663 and 15127428). Investigators were not blinded, and studies were not randomized. No statistical method was used to predetermine sample size. C57BL/6J mice

were obtained from Jackson Labs (Bar Harbor, ME). Mice were maintained on a 14-hour light cycle and housed five mice per cage. Mice were checked daily during infection studies. Veterinary care was provided 7 days a week. Studies used female mice between 8 and 12 weeks old.

2.4.3 Quantitative real-time reverse transcription PCR

Infected abscesses were carefully dissected and were homogenized in 500 μl of TRIzol reagent (Ambion, Carlsbad, CA). Total RNA was purified from homogenates using a PureLink RNA mini kit (Invitrogen, Carlsbad, CA) following the manufacturer's directions. Quantitative real-time reverse transcription (RT) PCR was performed with a SensiFAST SYBR no-ROX one-step kit (Bioline, Taunton, MA) using 50 ng of RNA/reaction and primers. Primers used are listed in Table 3. Reaction conditions were specified by Bioline and performed with a MyIQ thermocycler (Bio-Rad, Indianapolis, IN). All transcript levels were normalized to 16S.

Table 3: Primers used in Chapter 2

Name	Sequence
16S Fwd	TGATCCTGGCTCAGGATGA
16S Rev	TTCGCTCGACTTGCATGTA
Hla Fwd	ACAATTTTAGAGAGCCCAACTGAT
Hla Rev	TCCCCAATTTTGATTCACCAT
Aur Fwd	GCGTAAAGCGTCTCCCTCTTTTC
Aur Rev	GTGATGGTGATGGTCGCACATTC
Psmα Fwd	TATCAAAAGCTTAATCGAACAATTC
Psmα Rev	CCCCTTCAAATAAGATGTTCATATC

2.4.4 Western blot

Western blots for α-hemolysin were performed on clarified culture supernatants. Cultures were grown in the appropriate CDM to an $OD_{660} \approx 5.0$, and a 1 ml volume of culture was removed for analysis. A 20 μl aliquot of culture was used for bacterial enumeration by dilution plating. Supernatants were clarified by centrifugation at 12,000 rpm for 5 min. Clarified supernatants were boiled, and ≈30 μl was loaded on a 12% SDS polyacrylamide gel and subsequently transferred to a nitrocellulose membrane. Membranes were blocked using LI-COR blocking buffer (LI-COR, Omaha, NE) and probed with anti–α-hemolysin antibody (Abcam, Cambridge, MA) overnight at 4°C. Membranes were washed and incubated with IRDye 800CW secondary antibodies (LI-COR). Membranes were imaged using a LI-COR Odyssey infrared imager, and band densities were quantified using Image Studio version 4.0 (LI-COR). Band intensities were normalized to CFU.

2.4.5 Mouse infections

Diabetic mice were generated by intraperitoneal injection of STZ (Sigma-Aldrich) at a dose of ≈225 mg/kg. Mouse blood glucose was analyzed 3 days after STZ treatment using a glucometer. Only mice with a blood glucose level >300 mg/dl were used as hyperglycemic mice. Mice that did not become hyperglycemic following STZ administration were not used for further studies. For the phlorizin studies, phlorizin was administered twice daily at 400 mg/kg (in 10% ethanol, 15% dimethyl sulfoxide, and 75% saline) by subcutaneous injection on the flank of the mouse without infection. Phlorizin was administered 1 day before infection and every day through the course of infection. Mice that had blood glucose levels about 300 mg/dl after phlorizin treatment were not included in subsequent analysis. Subcutaneous infections were performed as previously

described(*63*). Bacteria were grown overnight in BHI, washed 3× with phosphate-buffered saline (PBS) and enumerated by dilution plating. Washed bacteria were stored overnight in PBS at 4°C. Bacteria were subsequently adjusted to a concentration of 5×10^8 in PBS, allowing for a 20 μl injection to equal 1×10^7 CFU. Mice were anesthetized with 2,2,2-tribromoethanol followed by shaving of the left flank. *S. aureus* in 20 μl was injected subcutaneously at $\approx 1 \times 10^7$ CFU. Mice were euthanized on day 7 after inoculation, and tissues were collected for glucose content, RNA isolation, or bacterial enumeration.

2.4.6 Glucose quantification

Abscess tissues were carefully dissected away from healthy tissues and were homogenized in 500 μl of radioimmunoprecipitation assay buffer (Boston BioProducts). Abscess homogenates were subsequently centrifuged twice at 12,000g for 15 min, and protein content from the clarified supernatants was quantified using a bicinchoninic acid assay (Thermo Fisher Scientific). Glucose from clarified supernatants containing equivalent amounts of protein was quantified using the glucose assay kit from EMD Millipore (Billerica, MA) following the manufacturer instructions.

2.4.7 Quantification and statistical analysis

Statistical method and sample size (n) are indicated in the figure legends. For *in vivo* studies, n represents the number of mice or tissues per group. For *in vitro* studies, n represents the number of biological replicates. Statistical analysis was performed using Prism 7 (GraphPad) software. A two-tailed Student's t-test was performed on the means of all parametric data. Statistical significance was defined as $P < 0.05$. Error bars on figures show SEM.

2.4.8 Intracellular ATP assays

Cultures grown (5 ml) to an OD_{660} of interest in PN + carbon source (0.5% glucose, 1% casamino acid, or a mix of glucose and CAA). Strains were washed three times in PBS and diluted 1:100. Intracellular ATP concentrations were determined using a Promega BacTiter-Glo assay kit (Promega Corporation, Madison, WI) following the manufacturer's instructions. Sample luminescence was determined using a Synergy H1 microplate reader (BioTek, Winooski, VT).

2.4.9 YFP reporter

RNAIII-YFP promoter fusion was previously described(*288*). Samples were inoculated in indicated media, and growth curves were generated on a Tecan Infinite M200 (software, Magellan V7.2). Samples were shaken with amplitude of 1, continuously at 37°C, read every 15 min, OD_{660} (no. of flashes, 25), YFP emission at 485, excitation at 535, and gain at 100. Graphs were generated using Prism 7.

2.4.10 Immunohistochemistry

IHC was performed on tissues as previously described(*290*). In brief, abscess tissues were fixed in 10% formalin, paraffin embedded, sectioned (10 μm), and stained with hematoxylin and eosin by the University of North Carolina Histopathology Core Facility or by the histology lab facility in the McGowan Institute for Regenerative Medicine at the University Pittsburgh School of Medicine. For immunofluorescence staining, unstained sections were deparaffinized using a graded series of xylene and ethanol washes followed by heat-mediated antigen retrieval for 20 min

in 10-mM sodium citrate buffer (pH 6). Specimens were blocked for 1 hour in 10% serum from the host species of the secondary antibody and subsequently incubated overnight with primary antibodies. Primary antibodies against GLUT-1 and GLUT-3 were obtained from Biorbyt (Cambridge, UK). The nitrotyrosine antibody was obtained from Millipore (Temecula, CA). Primary antibodies were detected with the use of biotinylated secondary antibodies followed by incubation with Alexa Fluor 594–conjugated streptavidin (Jackson ImmunoResearch, West Grove, PA). Stained sections were mounted in ProLong Antifade Gold reagent with DAPI (Invitrogen, Grand Island, NY). Samples were viewed with an Olympus BX60 fluorescence microscope. iVision Software v.4.0.0.0 (BioVision Technologies, New Minas, Nova Scotia) was used for image collection.

2.4.11 Macrophage assays

RAW 264.7 macrophages were suspended in RPMI 1640 (catalog no. 11875-093; Gibco) supplemented with fetal bovine serum (FBS) (10%) and at a concentration of $1\times10_6$ cells/ml, seeded into the wells of a 48-well plate at 0.5 ml per well, and incubated for 18 hours at 37°C. The cells were then activated via incubation in RPMI 1640 plus lipopolysaccharide (LPS) (100 ng/ml) and interferonγ (IFN-γ) (20 ng/ml) for 1 hour at 37°C and then spin inoculated in RPMI 1640 alone with *S. aureus* (opsonized in Hanks' balanced salt solution plus 10% mouse serum with active complement at 37°C for 30 min) at a multiplicity of infection of 10:1 (*S. aureus*/RAW 264.7). Following incubation of the RAW 264.7 cells with *S. aureus* for 30 min at 37°C, the cells were washed twice with PBS and then incubated in RPMI 1640 plus gentamicin (100 μ g/ml) for 1 hour at 37°C. The infected RAW 264.7 cells were then washed twice with PBS, after which certain wells were treated with 0.01% Triton X-100 to induce RAW 264.7 cell lysis for bacterial

enumeration (time zero), while the remaining infected RAW 264.7 cells were incubated in RPMI 1640 plus gentamicin (12 μg/ml) at 37°C for an additional 12 hours. Experiments involving glucose titration used RPMI 1640 without glucose (catalog no. 11879-020; Gibco) that was supplemented with FBS (10%). Oxidative burst was measured using Dihydrorhodamine 123 (DHR) (Cayman Chemical, Ann Arbor, MI). DHR is a cell-permeable fluorogenic probe that measures intracellular peroxynitrite formation. For DHR experiments, RAW 264.7 at a concentration of $2 \times 10_6$ cells in 1 ml of media in a six-well plate were incubated for 24 hours at 37°C in the presence or absence of glucose. Following the 24-hour incubation, cells were washed and incubated in fresh media containing LPS (100 ng/ml), IFN-γ (20 ng/ml), and 10 μM DHR for 1 hour. Following incubation, cells were washed three times in PBS and resuspended in 200 μl of PBS in a 96-well plate, and fluorescence was measured using a Tecan Infinite M200 Pro microplate reader following the manufacturer's instructions.

3.0 Mechanisms Behind the Indirect Impact of Metabolic Regulators on Virulence Factor Production in *Staphylococcus aureus*

Staphylococcus aureus is a human skin pathogen capable of causing invasive infections in many tissues in the human body. The host of virulence factors, such as toxins and proteases, available to *S. aureus* contribute to its diverse disease presentations. The majority of these virulence factors are under the control of the Agr quorum sensing system. The interaction between the Agr system and some well-established metabolic regulators has long been noted, but no mechanism has been provided as to these indirect interactions. In this study, we examine the connection between Agr and CcpA, a regulator of central carbon metabolism with a known positive impact on Agr function. We further investigated the interaction of Agr and CodY, a regulator of amino acid metabolism and a member of the stringent response with a known negative impact on Agr function. We show that though there are alterations in intracellular amino acid levels in each of these mutants that are consistent with their effect on Agr, there does not seem to be a direct impact on the translation of the Agr system itself that contributes to the altered expression observed in these mutants. Given the changes in cellular metabolism in a Δ*ccpA* mutant, we find reduced levels of intracellular ATP even in the presence of glucose. This reduction in ATP, combined with the reduced affinity of the AgrC sensor kinase for ATP, explains the reduction in Agr activity long observed in Δ*ccpA* strains.

3.1 Introduction

Staphylococcus aureus is a Gram-positive bacterial pathogen that typically colonizes the skin and nares of heathy humans(*5, 291*). In some cases, however, *S. aureus* can cause manageable disease such as skin and soft tissue infections (SSTIs); it can also progress to more invasive and difficult to manage presentations, such as endocarditis, osteomyelitis, and bacteremia(*292–294*). Invasive disease often occurs after the skin barrier or mucosal surface has been breached, allowing *S. aureus* access to a more nutritionally rich environment, especially serum glucose(*295*). Once in this environment, *S. aureus* is provided with the benefit of more nutrients, increased growth, and enhanced virulence factor production, allowing *S. aureus* the chance to establish an active infection.

Quorum sensing is an important aspect of infection for most bacterial species. It involves the ability of the bacteria to sense the cell density of its own species in the immediate area, as well as the presence of other bacterial species. In *S. aureus,* quorum sensing is mediated by the Accessory gene regulatory (Agr) system(*180*). This system consists of the *AgrBDCA* locus. AgrD, a small peptide, is processed and secreted by AgrB and released into the extracellular environment as auto-inducing peptide, or AIP. AIP signals back to the bacteria in the vicinity by binding to the AgrC sensor kinase, which auto-phosphorylates and passes that phosphate on to the AgrA response regulator. AgrA then engages transcription at certain promotors, including the Agr locus itself and the neighboring RNAIII promotor. RNAIII is a ~1kb sRNA that encodes the toxin *hld,* but also has pleiotropic effects on the transcript levels of many different virulence factors. These include toxins (α-toxin and leukotoxins) and proteases (*e.g.* aureolysin) capable of causing severe tissue damage, which have long been established as important for *S. aureus* infection(*73, 100, 296*). The regulation of these virulence factors has been extensively studied, and a general understanding of

regulation of the Agr system is widely accepted. However, some aspects of regulation are still unknown, including how metabolic regulators interact with the Agr system.

CcpA (carbon catabolite protein A) is a vital transcriptional regulator for carbon catabolite repression (CCR), the regulation scheme bacteria use to optimize which carbon source they utilize(*297*). For *S. aureus*, the carbon source optimized by CCR is glucose. Glucose transporters and glycolysis genes are upregulated by CcpA, and genes relating to the catabolism of other carbon sources (such as amino acids) are repressed. However, in *S. aureus*, CcpA has been shown to activate genes outside of its canonical regulon. For instance, it has a positive indirect effect on *ldh1*, which is also important for infection(*298*). This effect only occurs when in the presence of glucose; a Δ*ccpA* mutant consuming amino acids does not exhibit this regulation. Additionally, CcpA has a positive impact of Agr function(*275*, *276*, *299*). Again, this effect is dependent on glucose and is indirect. Despite a virulence defect in Δ*ccpA* being reported as early as 2006, no explanation of the mechanism behind decreased Agr activity in Δ*ccpA* strains has been provided.

CcpA is not the only metabolic regulator with an effect on Agr function. CodY has been reported to have an indirect negative effect on Agr function, with only speculation as to how this effect is exerted(*300–303*). CodY responds to levels of branch chain amino acids (BCAAs) and intracellular GTP, becoming activated by low BCAA or GTP levels(*304*). One way GTP is exhausted is through insufficient amino acid concentrations leading to high levels of uncharged tRNA, activating the stringent response and the concomitant synthesis of ppGpp(p), resulting in lowered GTP levels(*305*, *306*). BCAAs are the most commonly encoded amino acids in most genomes, and their abundance is tightly linked to the overall amino acid content of the cell. Once reduced BCAAs or GTP levels are sensed by CodY, it becomes inactive and derepresses genes related to amino acid synthesis and transport, aiming to increase intracellular amino acid

concentrations(*305*, *306*). A Δ*codY* mutant has been shown to have increased RNAIII levels and downstream toxin levels, indicating that the absence of CodY regulation somehow increases Agr signaling and activation(*303*). While no explanation has been proven, it has been theorized that increased intracellular amino acid pools in a Δ*codY* mutant due to increased synthesis and transport could result in improved translation of common transcripts in the cell, including *agrBDCA*, resulting in increased Agr signaling and activity(*302*).

With increasing rates of Methicillin-Resistant *S. aureus* (MRSA) infections in the US(*22*), understanding the different mechanisms *S. aureus* uses to control Agr activity and the subsequent production of virulence factors is vital. The dominant MRSA clone circulating in the USA since the early 2000s is the USA300 clone, which exhibits hyperexpression of virulence factors for unknown reasons(*56–58*, *60*, *94*). Understanding any interactions between virulence and the metabolic state of *S. aureus* could be key to developing new ways to target MRSA infections. One aspect of this interaction is the poor affinity of the response regulator AgrC to ATP, which exhibits a K_M ~10x lower than that of a typical sensor kinase (*157*). This makes the Agr system highly dependent on the energy state of the cell. To this end, the effect of serum glucose on *S. aureus* disease outcomes has been increasingly appreciated (*307*). Specifically, increased serum glucose present in individuals with diabetes presents a more abundant energy source to *S. aureus* infections, allowing the bacteria to increase glycolytic flux and, in turn, cellular ATP levels. This results in increased levels of virulence factor production per bacterium in diabetic mice as compared to non-diabetic mice. These diabetic animals experienced overall worsened infections, and these infections were mitigated when key glycolytic genes were knocked out in *S. aureus.* While that study demonstrated how ATP is linked to Agr and glycolysis, this study aimed to go one step further, and investigate how the genetic regulators of metabolism link to Agr activation.

3.2 Results

3.2.1 A *ΔccpA* strain is attenuated in a diabetes mouse model

We infected WT C57BL/6 mice subcutaneously with 10^7 CFU WT *S. aureus* LAC and the isogenic Δ*ccpA* strain and mice were monitored daily for weight loss over 7 days. At day 7, mice were sacrificed and analyzed for lesion size and CFU burden at the site of infection and in peripheral organs. Our results show that the Δ*ccpA* strain was attenuated in this infection model compared to WT LAC (Figure 9), displaying decreased lesion area and CFU in both the abscess and disseminated tissues. We also conducted identical infections on mice treated with streptozotocin (STZ) to induce an insulin-dependent diabetic state (via killing of pancreatic β-cells). In this model, which has been characterized as being more susceptible to LAC SSTIs(*307*), we found significant attenuation of the Δ*ccpA* strain in all measures analyzed (Figure 9). We note that the attenuation seen in the animals infected with the Δ*ccpA* strain is more severe than with any other glycolytic or Δ*agrA* mutant tested in our lab(*307*), with full clearance of the bacteria from ~50% of the infected mice and very low bacterial burden in the others. The abscess also never fully ruptures and becomes necrotic, indicating a much less severe infection than WT infected animals. This indicated to us that CcpA is key for infection, even in conditions where the host is immunocompromised and there is excess glucose available to *S. aureus.*

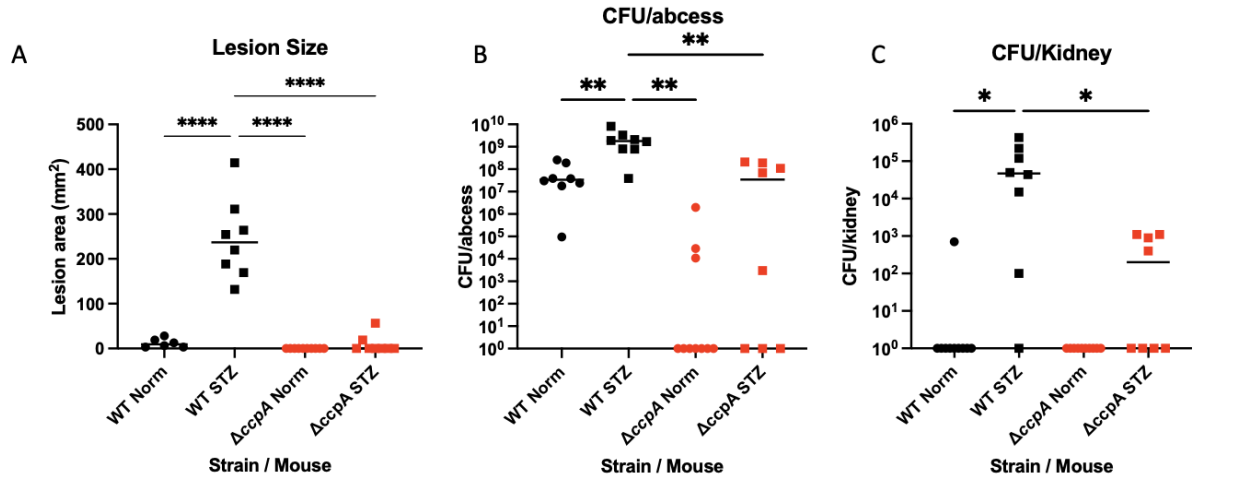

Figure 9: Deletion of *ccpA* results in severely attenuated infections in both normal and diabetic animals.

Untreated and STZ treated mice were subcutaneously infected with 1 x 10^7 CFU WT *S. aureus* LAC and the isogenic Δ*ccpA* mutant (n=8 for each category). STZ treated mice infected with WT LAC showed larger lesion area (A) and higher bacterial burdens in the abscess and in the kidney (B, C). Mice infected with the Δ*ccpA* mutant exhibited attenuated infection and lowered metrics in all categories (A-C) in both untreated and STZ treated animals. Statistics: One-way ANOVA with Tukey's multiple comparisons; * = $p < .05$, ** = $p < .01$, **** = $p < .0001$

3.2.2 The *ΔccpA* strain has reduced Agr activity

The Agr regulon is known to be important for virulence in animals, as it controls the expression of most toxins and proteases in *S. aureus*, either directly or indirectly(*180*). We tested the effect of the deletion of *ccpA* on transcription (Figure 10A) and translation (Figure 10B-C) of the toxins and proteases affected by Agr. We used RT-PCR to determine the expression level of the phenol-soluble modulin-α (psmα) toxin in WT LAC grown in TSB with and without glucose, as well as in the Δ*ccpA* strain. Expression of psmα is directly controlled by AgrA binding to the psmα promotor, making the expression of these toxins an excellent metric for AgrA activity. We found that the expression of psmα in the Δ*ccpA* strain grown in TSB + glucose was reduced to the

level of WT LAC grown in TSB – glucose (Figure 10A). At the protein level, we analyzed the supernatants of overnight culture of WT LAC grown in TSB +/- glucose, as well as Δ*ccpA* in TSB +/- glucose, for α-toxin levels. α-toxin is one of the most post-transcriptionally regulated proteins by RNAIII, making it a good way to measure the effects of post-transcriptional regulation by the Agr system. We performed a Western blot on the supernatants of WT LAC and Δ*ccpA* and found a reduction of α-toxin protein in the supernatants of a Δ*ccpA* strain in conditions with and without glucose (Figure 10B-C). These two pieces of data, take together, indicate a reduction of Agr activity in a Δ*ccpA* strain.

While the CcpA protein mediates the consumption of glucose, there are other metabolic mediators that can affect the levels of metabolites in bacterial cells. One such regulator is CodY, which represses amino acid synthesis. The CodY regulon would be derepressed in a Δ*codY* strain, possibly resulting in increased production and transport of amino acids. We also investigated the effects of a Δ*codY* mutation on Agr activity, and found, as previously reported, that Agr activity is increased, at both the transcription and translational level (Figure 10A-C).

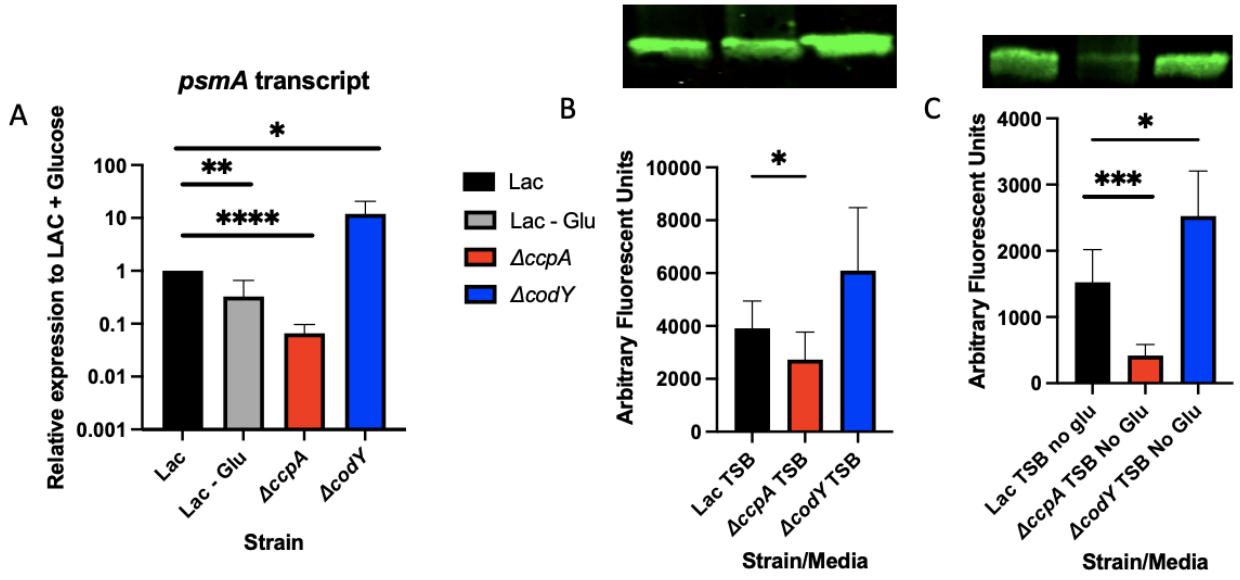

Figure 10: Δ*ccpA* and a Δ*codY* mutants have opposing effects on virulence factor expression. Cultures of WT LAC, Δ*ccpA*, and Δ*codY* were grown to mid-exponential phase (OD_{660} = ~3-4) and samples were taken for RNA extraction. QRT-PCR was performed on these for expression of *psmA* normalized to *rpoD* (A) (n=3). The same cultures were also grown overnight in TSB with (B) or without (C) glucose and their supernatants were run on an SDS-PAGE gel for Western blot stained for a-hemolysin (B, C) (n=5). Statistics: (A) unpaired t-test; * = p<.05, ** = p < .01, **** p < .0001 (B) paired t-test; * = p < .05 (C) unpaired t-test; * = p < .05 *** = p < .001

3.2.3 Several amino acids are limited in a *ΔccpA* strain and overabundant in a Δ*codY* strain

Knowing that a Δ*ccpA* mutant under-expresses and the Δ*codY* mutant over-expresses the Agr regulon, we considered common factors between these two strains. Both mutations are likely to have an impact on amino acid pools; with amino acids being consumed for energy in a Δ*ccpA* mutant and excess amino acids being produced/imported by a Δ*codY* mutant. HPLC was used to quantify the amino acid levels present intracellularly in WT LAC and isogenic Δ*ccpA* and Δ*codY* mutants. We found elevated levels of all amino acids in a Δ*codY* mutant, as compared to WT LAC grown in the same conditions (Figure 34), but only a few amino acids were significantly reduced

in a Δ*ccpA* mutant (Figures 11, 34). These included arginine, threonine, and glycine, all of which are known to be catabolized by *S. aureus* for energy, especially in a Δ*ccpA* mutant(*235*).

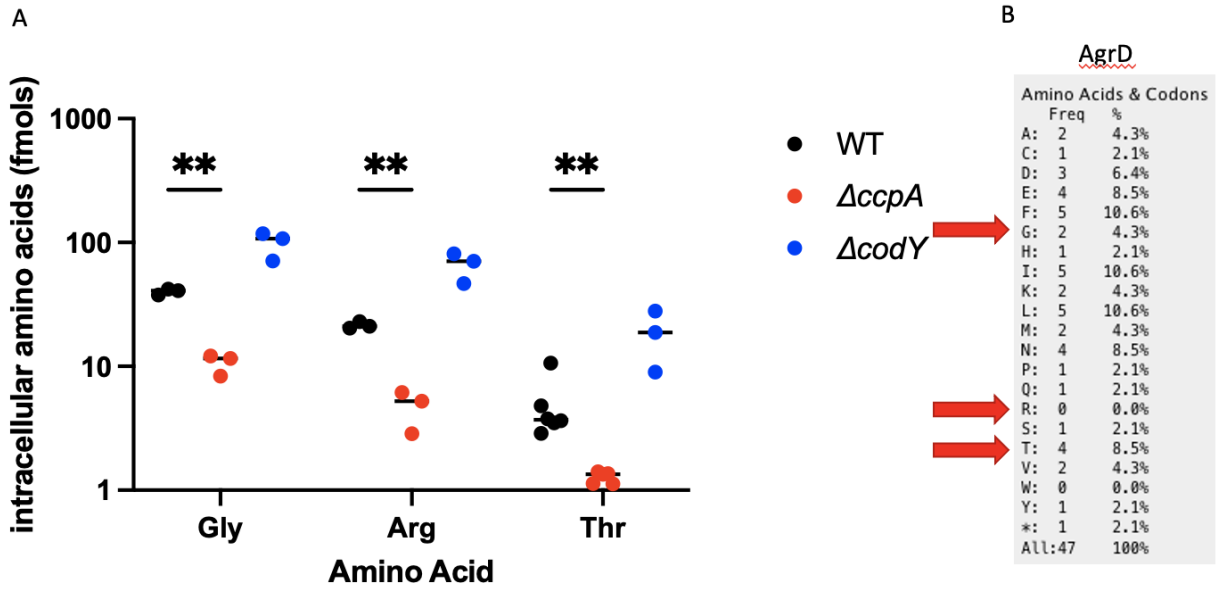

Figure 11: Intracellular levels of key amino acids are altered in a Δ*ccpA* and Δ*codY* mutant. Cell-free extracts were created from cultures of WT LAC, Δ*ccpA* and Δ*codY* grown to mid-exponential phase to determine intracellular amino acid levels (n=3). Levels of glycine, arginine, and threonine were significantly altered from WT levels in both a Δ*ccpA* and a Δ*codY* mutant (A). Glycine and threonine are both present in the AgrD peptide (B). Statistics: mixed-effects model with Dunnett's multiple comparisons test. ** = $p < .01$

3.2.4 Amino acid pools and AgrD translation is not responsible for the reduced Agr activity in a Δ*ccpA* strain

Threonine and glycine are both present in the AgrD peptide (Figure 11). Previous studies have hypothesized that excess amino acid pools in a Δ*codY* mutant could affect the translation of the Agr locus, especially AgrD(*302*). Increasing the availability of amino acids could allow for the AgrD peptide to be translated more efficiently from its abundant transcript in a quorum-active cell. To test this hypothesis, we used a reporter strain of LAC expressing YFP under the RNAIII

promotor (LAC YFP::RNAIII), a promotor directly activated by AgrA, to determine Agr activity. We grew this strain in minimal defined media containing glucose (PNG) and added supernatants from LAC, Δ*ccpA*, and Δ*codY* strains grown overnight. If Δ*codY* produced more AgrD peptide than LAC, more AIP would be present in the supernatants of Δ*codY* cultures. Additionally, if the lowered pools of threonine and glycine present intracellularly in a Δ*ccpA* strain could impact AgrD translation, lower levels of AIP would be present in these supernatants. Adding these exogenous supernatants prior to quorum activation in the LAC YFP::RNAIII strain will allow the AIP present in these supernatants to induce Agr activity, which will be reflected in YFP levels (observed in Figure 12). YFP levels can be compared to those of a no supernatant control, which will only exhibit YFP induction by its natural Agr system. Differences in YFP production at an early enough timepoint will indicate differences in exogenously added AIP. As a negative control, we included overnight supernatants from a strain that lacks AgrA, which cannot properly synthesize AIP and exhibits YFP production at the same level as the no supernatant (Figure 12). This indicates differences in AIP production by these strains.

However, as the Agr system is positively autoregulated, any impairment in transcription will be observed at the translational level. That is, if the impact of either of these regulators is at the transcriptional level, we would still see a difference in AIP production downstream. Considering this, we cannot be sure that there is a defect in translation of AgrD in a Δ*ccpA* mutant. Attempts to quantify the levels of AgrD transcript resulted in C_t values too low to truly determine differences in AgrD transcription. To rectify this issue, we created a plasmid in which the *agrBD* gene is under a constitutive promotor, referred to as p*lgt-agrBD.* By transforming this plasmid into a WT LAC, Δ*ccpA,* Δ*codY,* and Δ*agrA* background, we can equilibrate the transcript levels of AgrBD in each of these strains. This allows us to observe the effects of translation specifically on

each strain's supernatant AIP levels when added to the LAC YFP::RNAIII strain in an experiment identical to above. Upon the introduction of p*lgt-agrBD* into our strains of interest, we observed a similar level of YFP induction in WT, Δ*agrA*, and Δ*ccpA* supernatants (Figure 13). Expressing p*lgt-agrBD* in a Δ*agrA* background is expected to yield similar AIP levels to WT – indeed, there should be no differences in the transcript level or translation of AgrBD in either strain, as AIP production is no longer under Agr control. Surprisingly, the Δ*ccpA* strain supernatant also appeared to induce YFP to both WT and Δ*agrA* levels, indicating that there is no translational defect in AgrD production and that the defect in Agr activation seen in a Δ*ccpA* mutant is likely at the transcriptional level. The induction of YFP by Δ*codY*, however, trends towards significance (Figure 13), indicating that there may be increased translation of AgrD transcript by a Δ*codY* mutant, possibly due to the excess intracellular amino acids observed in Figure 11.

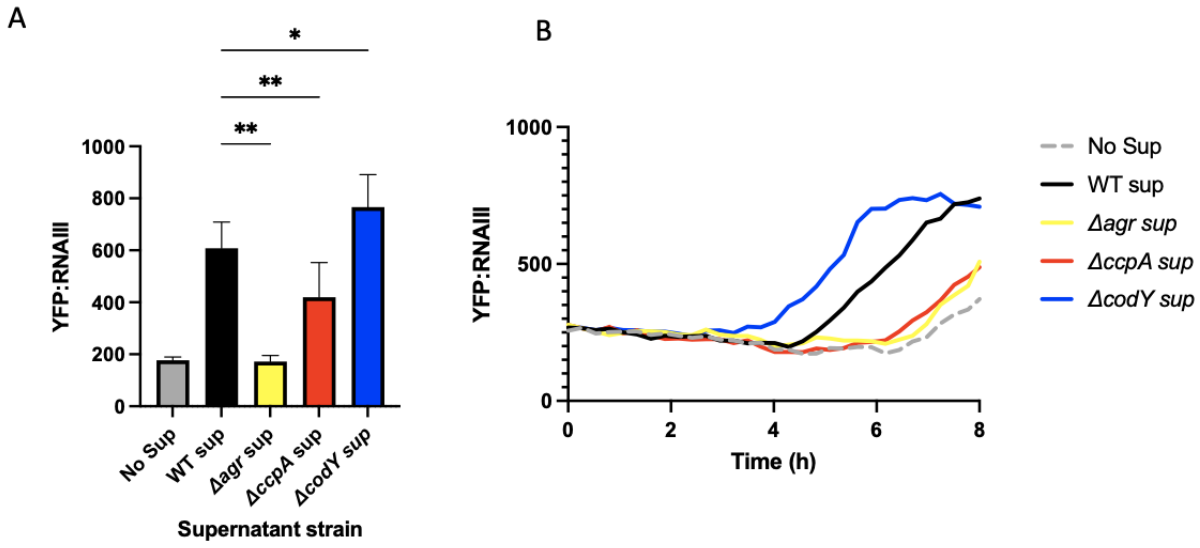

Figure 12: Supernatants from Δ*ccpA* and Δ*codY* mutants have opposing effects on the stimulation of an RNAIII::YFP reporter strain. Supernatants were removed from overnight cultures of WT LAC, *ΔccpA*, *ΔcodY*, and *ΔagrA* strains. These were added to fresh cultures of WT LAC harboring a pYFP::RNAIII reporter plasmid. Averages of peak expression levels at hour 6 are shown in (A) (n=5-6), a representative curve is shown in (B). Statistics: mixed-effect analysis with Tukey's multiple comparisons; * = p <.05, ** = p < .01

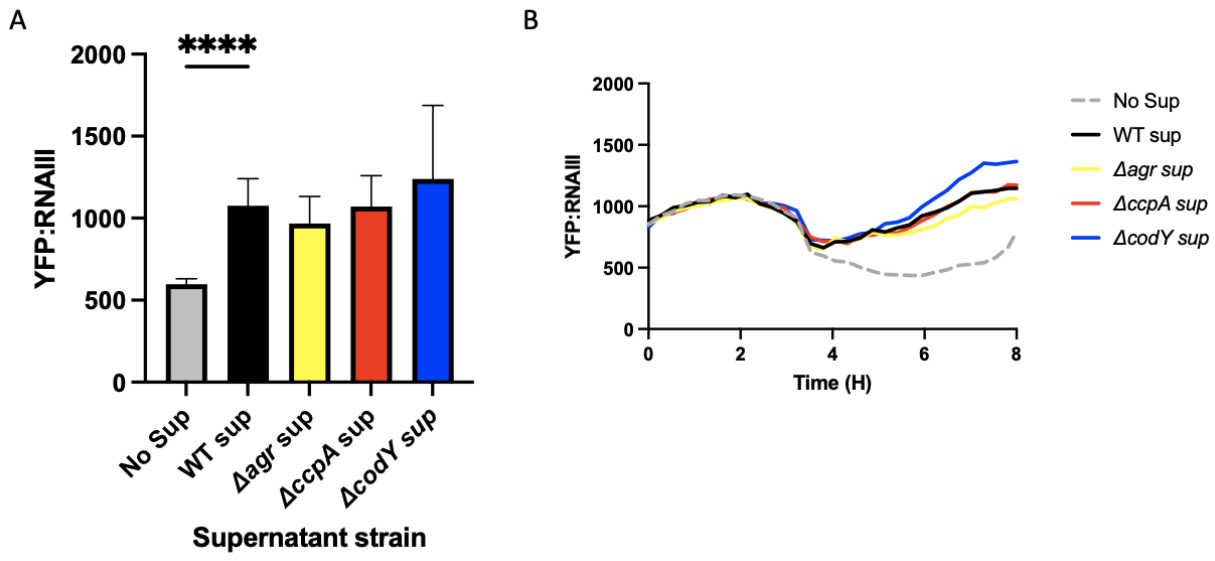

Figure 13: Constitutive expression of AgrBD equalizes RNAIII::YFP stimulation across all mutants.

Supernatants were removed from overnight cultures of WT LAC, Δ*ccpA*, Δ*codY*, and Δ*agrA* strains harboring p*lgt::agrBD*. These were added to fresh cultures of WT LAC harboring a pYFP::RNAIII reporter plasmid. Averages of peak expression levels at hour 6 are shown in (A) (n=5-6), a representative curve is shown in (B). Statistics: mixed-effects model with Dunnett's multiple comparisons test. **** = $p < .0001$

3.2.5 A *ΔccpA* strain has decreased ATP in the presence of glucose as compared to WT

To determine what could be having an impact on Agr transcription in a Δ*ccpA* mutant, we turned to the hypothesis investigated in Chapter 2(*307*). We have shown that WT *S. aureus* consuming different carbon sources in minimal defined media has differing levels of ATP and α-toxin production (WT LAC grown in CDM with glucose vs casamino acids). As stated previously, because a Δ*ccpA* mutant is unable to efficiently consume glucose, it preferentially consumes amino acids. Therefore, we hypothesized that the intracellular ATP levels in a Δ*ccpA* mutant would be similar to those in WT LAC grown in the absence of glucose. Quantification of ATP in WT LAC grown in TSB +/- glucose as compared to a Δ*ccpA* mutant grown in TSB + glucose shows that

Δ*ccpA* ATP levels are similar to that of WT grown without glucose, despite glucose being present in the media (Figure 14). Indeed, there appears to be strong similarities between the levels of virulence factor expression as shown in Figure 10 and the ATP levels demonstrated in Figure 14. Finally, we see similar ATP levels between WT and Δ*codY* strains, showing that no excess ATP is produced by a Δ*codY* mutant and that ATP levels alone cannot explain the elevated Agr activity observed by the Δ*codY* mutant.

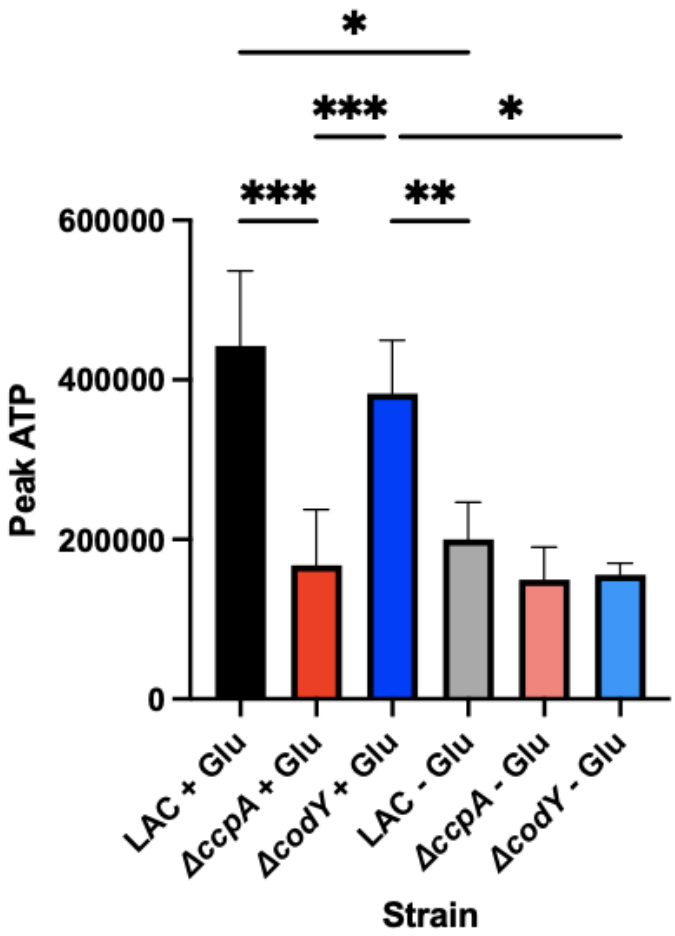

Figure 14: ATP levels in a Δ*ccpA* mutant reflect those of WT LAC grown in the absence of glucose. ATP levels were determined in cultures of WT LAC, Δ*ccpA* and Δ*codY* strains grown in TSB with and without glucose. Statistics: Mixed effects model with Tukey's multiple comparison test(n=4-5). * = $p < .05$,** = $p < .01$, *** = $p < .001$

3.3 Discussion

During infection of a host, the *S. aureus* bacterium must fight against the host for limited resources to replicate and cause an active infection. While canonically considered nutrients are metals (like iron, zinc, manganese, etc…), this idea of 'nutritional immunity' can be expanded to almost any metabolite that a bacterium needs to live – including carbon sources like glucose, amino acids, inorganic phosphate, and so on. A major role of the toxins and proteases so heavily featured when discussing *S. aureus* virulence factors is to release these important molecules, including amino acids from extracellular proteins broken down by proteases, and nutrients released from host cells lysed by toxins. Considering this role of these virulence factors, logic implies that there should be an impact on their production by metabolic regulators. Indeed, for the past few decades, it has been understood that metabolic transcriptional regulators, such as CcpA and CodY, impact virulence factor production. However, little mechanism for how these regulatory systems interact has been provided.

CcpA plays a key role in carbon catabolite repression, the method that bacteria use to determine if their optimal carbon source is present to consume. For *S. aureus*, that carbon source is glucose, and the consumption process is glycolysis. CcpA directly activates genes related to glycolysis and directly represses genes related to the consumption of gluconeogenic substrates. Therefore, CcpA activates the optimal carbon catabolism process, which leads to optimized levels of ATP. The ATP from glycolysis itself and additionally from the AckA overflow pathway contribute to increased intracellular ATP concentrations(*230*). Additionally, as glucose is an important precursor for several macromolecules and essential processes in the cell, in the absence of glucose *S. aureus* would need to run the process of gluconeogenesis, an energy expensive process that consumes ATP directly. CcpA also represses this pathway, so in the absence of this

important regulator, not only is glycolysis not entirely active, but energy is also being consumed to run gluconeogenesis, even though glucose may be present already in the environment. All this 'waste' of ATP, on top of inefficient ATP generation, leads to the deficit in ATP seen in Figure 6 between WT LAC growing in the presence and absence of glucose, as well as between the *ΔccpA* mutant and WT. This lowered ATP pool leaves less energy available for other processes, including the synthesis of virulence factors. We propose that the reason these virulence factors are under the control of the Agr system is not simply because of quorum, but because the Agr system is uniquely influenced by the energy state of the cell. The Agr system has a low affinity for ATP (*157*), and there must be optimal ATP levels in the cell to gain full activation of the Agr system. Energy cannot be wasted on extraneous virulence factors in an energy stressed environment any more than it can be wasted on synthesizing these factors in the absence of quorum sensing. Combining these two influences of the environment into one signaling system that contributes significantly to infection is no doubt evolutionarily important for *S. aureus*. This lowered affinity for ATP is present in all low GC+ bacteria that possess an Agr-like quorum sensing system, indicating that this specialization is not something that *S. aureus* has evolved, but rather a larger phenomenon in this family of bacterial species that allows the bacterium to place synthesis of extraneous factors under the control of an energy-optimized system.

CodY is also a transcriptional regulator that reacts to stress from nutrient limitation. Specifically, CodY reacts to lowered levels of BCAAs and GTP. Both of these can become limiting in an infection environment, and the subsequent de-repression of the Agr system by CodY could be useful in obtaining the amino acids that act as a stress signal through CodY. However, CodY reacts weakly with the Agr and RNAIII promotor, leading to questions about how CodY affects gene expression. In one of the most thorough studies performed on CodY and Agr to date(*302*),

the authors posit that increased intracellular amino acid pools present via the increased transport and synthesis of amino acids in a Δ*codY* strain could result in the increased translation of the AgrD peptide, which could in turn lead to increased Agr signaling. We showed that the Δ*codY* strain does, in fact, produce more AIP than its WT counterpart. Additionally, while there does seem to be a trend towards increased AIP in the supernatants of a Δ*codY* strain with the autoinduction of the Agr system nullified by constitutive expression of the *agrBD* locus, this trend is not significant. This could be due to the fact that the constitutive expression of *agrBD* under the *lgt* promotor results in enough excess *agrBD* transcript that the differences in amino acids observed in Figure 3 may not be enough to cause extra translation of these transcripts as compared to WT. However, here we can confidently eliminate an effect of Δ*codY* on ATP levels as the means of controlling Agr activity, as a Δ*codY* mutant has increased Agr activity in the presence and absence of glucose despite different intracellular ATP levels (Figure 14). Further investigation into this hypothesis may be required. We did show, however, that unlike in a Δ*ccpA* mutant, deleting Δ*codY* does not affect ATP levels; thus, another explanation for the effect of CodY is needed.

The intersection of metabolism and virulence is a growing area of interest for researchers investigating a number of pathogens; especially pathogens like *S. aureus*, that are capable of colonizing the host asymptomatically as well as causing devastating disease. The concept of metabolic signals being a trigger for virulence activation has become more popular as researchers realize how important metabolism is to bacterial pathogens. In this study, we are able to shed light on how two different metabolic transcriptional regulators indirectly affect the expression of virulence factors vital for infection. Further study in this field may reveal exactly how important it is for *S. aureus* to link its survival in the host with its ability to cause infection and metabolize nutrients present underneath the environment it typically colonizes.

3.4 Materials and methods

3.4.1 Bacterial strains and growth

The strains used in this study are listed in Table 4. All *S. aureus* strains are derivatives of USA300 clone LAC. For infection studies, strains were grown in BHI (BD Biosciences). For all other studies, strains were grown in TSB or TSB without glucose (BD Biosciences), or in minimal defined media (PN) with .5% glucose (PNG) or 1% amino acids (PNCAA) supplemented as a carbon source(*308*) at 37°C shaking at 250 RPM with a 10:1 flask:medium ratio to ensure aerobic cultures. The Δ*ccpA* and Δ*codY* mutants were created using homologous recombination and the *E. coli* harbored PBTK* or PBTT* plasmids, respectively, as previously described(*298*). Plasmids used in the study were engineered by restriction enzymes in the pOS1 background under the constitutive promotor *lgt.* Antibiotic marked mutations and plasmids were moved into fresh backgrounds using phi-11 phage transduction(*309*). Antibiotic makers for *S. aureus (E.coli)* are as follows: Kanamycin 25 mg /mL, Tetracycline 5 mg /mL, Chloramphenicol 20 mg /mL, and Ampicillin (50 mg/mL).

Table 4: Strains used in Chapter 3

Strain Name	Strain Description	Source
WT LAC	Methicillin-Resistant Clinical *S. aureus* Isolate	
AR1749	*S. aureus* LAC Δ*ccpA::*Kan	This Study
AR1128	*S. aureus* LAC Δ*codY*::Tet	(*310*)
AR1198	*S. aureus* LAC Δ*agrA*::Tn	(*252*)
AR1038	*S. aureus* LAC pYFP::RNAIII	(*290*)
AR1750	*S. aureus* LAC plgt::*agrBD*	This Study
AR1751	*S. aureus* LAC Δ*ccpA::*Kan plgt::*agrBD*	This Study
AR1752	*S. aureus* LAC Δ*codY*::Tet plgt::*agrBD*	This Study
AR1753	*S. aureus* LAC Δ*agrA*::Tn plgt::*agrBD*	This Study

3.4.2 Mouse Infections

C57BL/6J mice of 8-12 weeks of age were intraperitoneally injected with 225 mg/kg dosages of STZ (Sigma-Aldrich). Blood glucose was assayed by glucometer (ReliOn) 3 days after treatment. Only mice with a blood glucose level >300 mg/dL proceeded in the study. Subcutaneous infections were performed as previously described(*63*). Briefly, bacteria were grown in BHI, washed three times with PBS, plated for enumeration, and stored at 4°C in PBS overnight. Bacteria were diluted to a concentration of $5x10^8$, and 20 mL were injected into mice shaved and anesthetized with 2,2,2-tribromoethanol. Mice were monitored daily for weight loss, and at day 7 mice were euthanized with CO_2 and abscesses were measured. Tissues were collected and

homogenized and plated on BHI plates for enumeration. All animal manipulations and infections were conducted under an institutionally approved and currently active IACUC protocol (# 22030607).

3.4.3 Western Blots

Bacteria for Western blots were grown overnight in TSB with or without dextrose. The following morning 1mL of culture was centrifuged at 13,000x g for 1 minute, the supernatant was removed, and heat inactivated at 70°C for 10 minutes. The supernatants were diluted 1:4 with Laemelli buffer (BioRad) with 2-mercaptoethanol (Fischer Scientific) and boiled at 99 C for 10 minutes. 40 mL of boiled supernatant was loaded onto a Mini Protean TGX 12% gel (BioRad) and run on a Mini Trans-Blot apparatus (BioRad) for 90 minutes at 150 V with a Chameleon Duo Pre-Stained Protein ladder (LI-COR). The gel was transferred to a supported nitrocellulose .22 mm membrane (BioRad) for 60 minutes at 100 V. The membranes were blocked for 4 hours with Intercept protein-free blocking buffer (LI-COR), and then incubated overnight with the abcam mouse MAb anti-alphahemolysim antibody (ab190467) at 1 mg/mL. The following day, the membranes were washed for 10 minutes, then 5 minutes, then 5 minutes with PBS - .05% Tween (Sigma-Aldrich). The membranes were then stained with the secondary antibody IR Dye 800CW Donkey anti-mouse (LI-COR) diluted in donkey serum (Sigma-Aldrich) for 1 hour, then washed as above. The membranes were imaged on a LI-COR Odyssey machine with 7 (800) and 2 (700) gains on the fluorescent channels.

3.4.4 RNA extraction and RT-PCR

RNA extractions were performed as recently described(*246*). Briefly, ~30 mL of cells was grown in a 250 mL flask, shaking, at 37°C. At a mid-log OD (~4-3), 25 mL of culture was quenched with 50/50 ethanol/acetone at 0°C. The samples were frozen at -80°C. For extraction, the samples were thawed at 30°C and pelleted at 4,250 rpm for 10 minutes. The supernatant was discarded, and the pellet was air-dried. Upon drying, the pellet was resuspended in 250 μL of Tris-EDTA buffer. The pellet was frozen in a dry ice-ethanol bath and thawed at 60°C three times, and then bead-beat for 1 minute and rested on ice for 5 minutes. 650 μL of lysis buffer with 2-mercaptoethanol was added to the sample and the bead-beating was repeated. The samples were pelleted and 600 μL of supernatant was combined with 600 μL of 70% ethanol. The samples were then processed according to the Invitrogen Pure-link RNA mini kit. The purified samples were treated with NEB DNAse-1 for 1 hour at 37°C and then re-purified with the Pure-link RNA mini kit.

The RNA samples were quantified, and 50 ng of RNA was added to a RT-PCR reaction according to manufacturer's instructions for the Power SYBR green RNA-to C^t 1-step kit (Applied Biosystems). The machine used was a BioRad iQ5. The C^t was determined using the iQ5 software and the data was analyzed for $\Delta\Delta C^t$ based on the control gene *rpoD.* The primers used are listed in table 5.

Table 5: Primers used in Chapter 3

Primer Name	Sequence
psma_fwd_RT	TATCAAAAGCTTAATCGAACAATTC
psma_rev_RT	CCCCTTCAAATAAGATGTTCATATC
rpoD_RT.1A	AACTGAATCCAAGTGATCTTAGTG
rpoD_RT.1B	TCATCACCTTGTTCAATACGTTTG
CcpA_3'.1B	GGGGAATTCGTGCCACAATTGGAGGC
CcpA_3'.1A	GGGGAATTCAGGCATTCATCTAACGACCC
CcpA_5'.1A	GGGGGATCCAGCTGGCCGTACGAAAAAGC
CcpA_5'.1B	GGGGGATCCCGCGCTTCTCTTGCTACATC
AgrBD.1A	GGGCATATGAATTATTTTGATAATAAAATTGACCAGTTTGCC
AgrBD.1B	GGGGGATCCTCCACCTACTATCACACTCTC

3.4.5 Intracellular Amino Acid Assays

We generated cell-free extracts (CFEs) from cultures grown to mid-log OD (~3-4) and 50 mL of culture was pelleted at 4,250 RPM for 10 minutes. The supernatant was discarded, and the cells were resuspended in 5 mL of PBS and then 1 mL of PBS. The 1 mL of cells in PBS were bead-beat for 1 minute, then rested on ice for 5 minutes, three times. The supernatant of this bead-beating was removed and frozen down for analysis.

Samples were thawed and 250 mL was moved into a fresh tube. To remove protein from the sample, 62.5 mL of Tricarboxylic Acid (Sigma) was added to the CFEs and the CFEs were incubated on ice with the TCA for 10 minutes. Then the samples were centrifuged at 13,000x g

for 10 minutes. The supernatant from this sample was removed and pH balanced in a new 1.5 mL tube to a pH of 6.2-8. 20 mL of this pH balanced CFE was derivatized as according to the Waters AccQ-Tag protocol. In short, 20 mL of sample was added to 60 mL of borate buffer, and then 20 mL of "reagent A" was added to the sample. The samples were incubated at 55°C for 10 minutes, and then diluted 1:10 to a volume of 1 mL. The samples were then run on a Waters alliance HPLC machine as according to the AccQ-Tag protocol. The resulting curves were integrated using the Waters Empower software and the area under these curves was graphed. The intracellular concentration was determined for significantly different amino acids using standard curves.

3.4.6 Supernatant stimulation YFP growth curves

Cultures of LAC, *ΔccpA, ΔcodY, and ΔagrA* or each of those strains containing p*lgt::agrBD* were grown to a mid-log OD (~2) in PNG. 1 mL of cells was removed and pelleted, and the supernatants were filter sterilized through a .2 mm filter (Corning). Additionally, overnight cultures of WT LAC harboring the pYFP::RNAIII plasmid(*183*) were washed three times with PBS and diluted 1:200 in PNG. 200 mL of this culture was added to a 96-well flat-bottom plate (Costar), along with 50 mL of the supernatants prepared earlier. A no supernatant control had an additional 50 mL of PNG added. The plates were grown shaking at 37°C in a Bio-Tek Synergy HTX plate reader overnight with readings being taken every 15 minutes. Curves were analyzed by highlighting the region of time before the no supernatant control showed YFP expression and examining activation of the wells with each supernatant added. These experiments were repeated in biological and technical triplicate.

3.4.7 ATP assays

Cultures of LAC, ΔccpA, and ΔcodY diluted 1:200 from overnight cultures were grown shaking at 37°C in TSB with and without dextrose. Every hour, 100 mL of culture was removed from the culture and added to a 96-well plate containing 100 mL of BacTiter-Glo reagent (Promega). Plates were briefly shaken and then incubated for 5 minutes. The luminescent signal of each well was determined using a Bio-Tex Synergy plate reader. These experiments were done in technical duplicate and biological triplicate.

4.0 Specialized phosphate transport is essential for *Staphylococcus aureus* nitric oxide resistance

Staphylococcus aureus is a major human pathogen capable of causing a variety of diseases ranging from skin and soft tissue infections to systemic presentations such as sepsis, endocarditis, and osteomyelitis. For *S. aureus* to persist as a pathogen in these environments, it must be able to resist the host immune response, including the production of reactive oxygen and nitrogen species (*e.g.* nitric oxide, NO). Extensive work from our lab has shown that *S. aureus* is highly resistant to NO, especially in the presence of glucose. RNA-seq performed on *S. aureus* exposed to NO in the presence and absence of glucose showed a new system important for NO resistance – phosphate transport. The phosphate transport systems *pstSCAB* and *nptA* are both upregulated upon NO-exposure particularly in the presence of glucose. Both are key for phosphate transport at an alkaline pH, which the cytosol of *S. aureus* becomes under NO stress. Accordingly, the *ΔpstSΔnptA* mutant is attenuated under NO stress *in vitro* as well as in macrophage and murine infection models. This work defines a new role in infection for two phosphate transporters in *S. aureus* and provides insight into the complex system that is NO resistance in *S. aureus.*

4.1 Introduction

Staphylococcus aureus is a human skin pathogen capable of causing both mild and severe infections. Mild and manageable presentations include skin and soft tissue infections, whereas severe cases can result from spread of the infection throughout the body to cause endocarditis,

pneumonia, osteomyelitis, and/or sepsis(*292–294*, *311–313*). The diversity of infections caused by *S. aureus* is a unique facet of this bacterium's pathogenesis and can be attributed to several different causes including the wide array of toxins and proteases expressed during infection(*180*). These factors afford *S. aureus* the ability to resist antibody-mediated phagocytosis, to kill and escape from successful phagocytes and the ability to resist host immune radicals such as reactive oxygen and nitrogen species(*73*).

Our lab has extensively studied the response of *S. aureus* to host nitric oxide (NO)(*229*, *243*, *246–248*, *252*, *256*, *310*). The primary targets of host NO are transition metals such as the iron molecules in heme centers and iron sulfur clusters and cytosolic thiols such as cysteine(*314*, *315*). These motifs are over abundant in specific metabolic pathways including the TCA cycle and the electron transporter chain (ETC). Thus, *S. aureus* adopts a metabolic scheme that relies less on these pathways and more on glycolytic substrate-level phosphorylation. To achieve this, *S. aureus* requires robust import of glucose, high levels of glycolytic flux, and a highly active lactate dehydrogenase (Ldh1)(*247*, *252*). Given the importance of high flux through this pathway for growth in the presence of NO, many of the key reactions are carried out by seemingly redundant enzymes/transporters. For instance, *S. aureus* recently acquired two additional glucose transporters (*glcA* and *glcC*) to facilitate rapid uptake of glucose during infection(*229*). The pathogen also acquired an additional lactate dehydrogenase (Ldh1) to account for the redox imbalance that occurs due to NO-mediated inhibition of the ETC(*247*). Another important facet of the NO-resistant metabolic state is for the pathogen to maintain adequate inorganic phosphate levels to support the sole energy producing substrate-level phosphorylation in glycolysis. To this end, there are three systems that are used for inorganic phosphate transport in *S. aureus*(*225*). Recently, a thorough study demonstrated that there are different conditions in which each of these transporters are vital

for *S. aureus* growth(*225*). The first, and most complex, system is the PstSCAB system, an ABC transporter that uses PstS as a shuttle for inorganic phosphate(*316–318*)(*319*). This system has the highest affinity for inorganic phosphate. Secondly, the PitA system is dependent on proton-motive force and is the most common form of phosphate transport(*316, 320*)(*319*). This system is particularly important when extracellular inorganic phosphate is plentiful. Finally, the NptA system is a sodium dependent phosphate antiport system, which was recently "reacquired" by *S. aureus* from some staphylococcal relative (Figure 35)(*225, 321*).

The *ldh1* gene is controlled by a redox-sensing repressor known as Rex(*298*). Rex binds to NADH when levels get too high, causing the repressor to lose DNA binding affinity and derepressing the entire regulon. However, redox imbalance is not the only signal that affects *ldh1* expression. *ldh1* is more highly expressed during NO-stress in the presence of glucose than in its absence(*298*). This and other factors make glucose essential to *S. aureus* in the presence of host NO. However, the mechanism of glucose-dependent control of *ldh1* is entirely unknown. Typical regulators of carbon catabolite repression, like CcpA, are not responsible for the direct regulation of *ldh1* in the presence of glucose(*298*). Here we employed RNA-Seq to define the set of genes that, like *ldh1*, are induced by NO to a much higher level in the presence of glucose than in its absence. The highest differentially induced genes encoded the Pst and NptA phosphate transport systems (Figure 15), which have been shown to be required for growth under conditions we hypothesized would be relevant to NO-resistance. We also assess the importance of these transporters in the presence of host NO both *in vitro* as well as *in vivo* and show their requirement for efficient glycolytic substrate level phosphorylation and ATP production.

4.2 Results

4.2.1 Phosphate transporters are transcriptionally upregulated by NO and glucose

We conducted RNA-sequencing on samples of WT *S. aureus* strain LAC grown to early exponential phase in chemically defined media (CDM) containing two different carbon sources - 0.5% glucose, and a combination of 0.5% casamino acids and 0.5% pyruvate. RNA was isolated from each of these cultures at OD_{660} = 0.5, and the NO donor DETA/NO was added to the remaining cultures (10mM) for an additional 15 minutes. RNA was then isolated from each of these cultures. We analyzed all data sets for significantly regulated genes – that is, genes whose RPKM is more than two standard deviations removed from the average – and present them in Table S1. Figure 15A shows the relative expression of the top genes differentially regulated by NO and significantly different between CDM-G + NO and CDM-CP + NO. While *ldh1* does come out of this analysis, it is not the gene most differentially regulated. The top genes from this analysis were all related to the phosphate transport system *pstSCAB* and its regulator *phoU*. We also see the differential regulation of a few hypothetical proteins, sRNAs, and other genes (Figure 36).

S. aureus has three phosphate transport systems – *pstSCAB, nptA,* and *pitA,* all of which were assessed for expression under these conditions (Figure 15B). Using RT-Q-PCR, we validated findings from the RNA-Seq dataset. We found no difference in *pitA* expression in either medium with/out NO (Figure 37A). We also found that basal *nptA* and *pstS* expression was higher in the presence of glucose than in its absence (Figure 37B). We independently confirmed that the expression of *pstSCAB* is induced by NO to a much higher level in the presence of glucose than in the absence, while *nptA* is not induced by NO (Figure 15C). Thus, it seems as though *pstSCAB* responds to both NO and glucose, while *nptA* responds only to glucose.

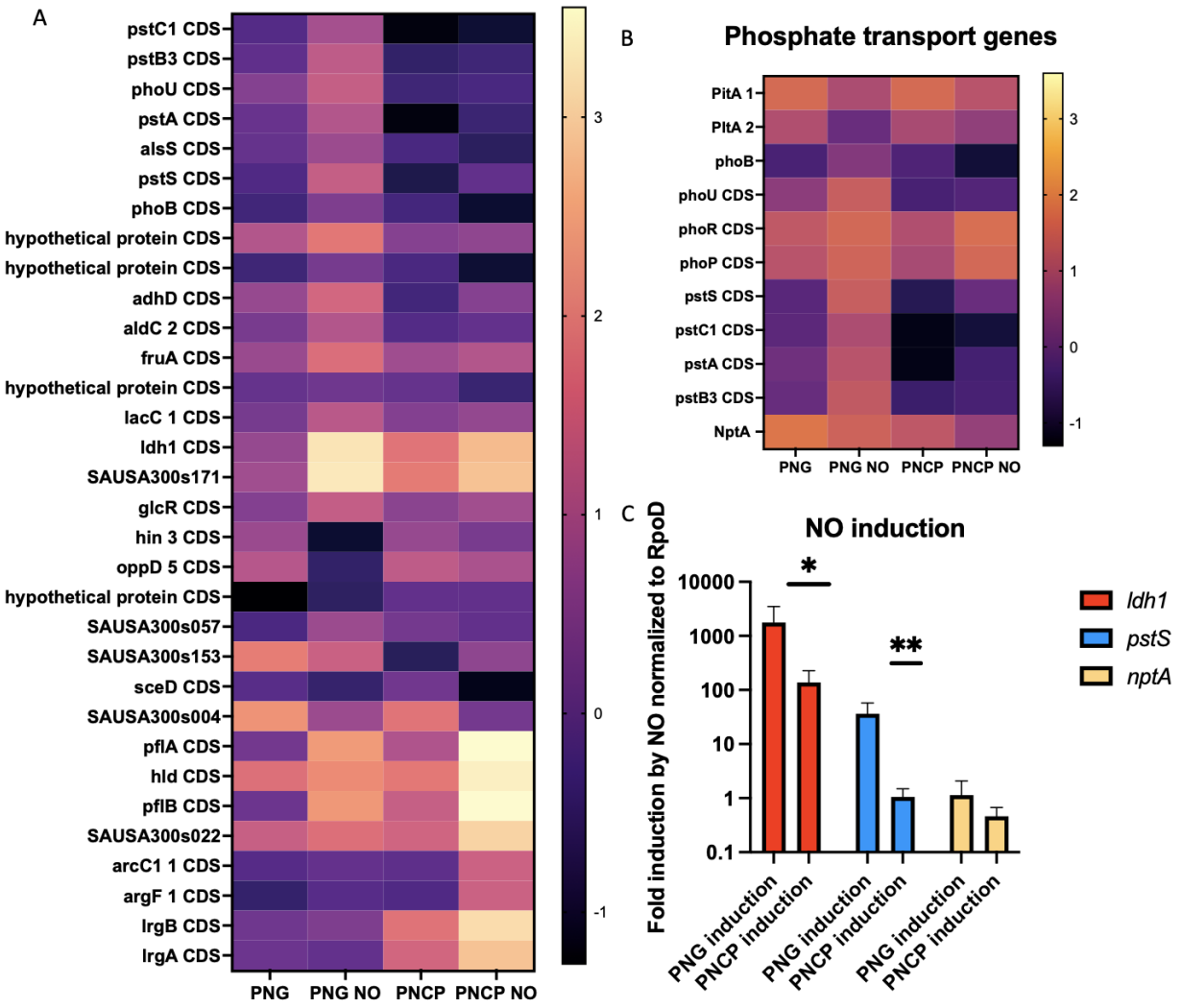

Figure 15: Phosphate transporters *pstSCAB* and *nptA* are upregulated in glucose. Cultures of WT LAC were grown to an OD of .5 and RNA samples were taken (n=2). 10mM DETA-NO was added to the remaining culture and further samples were taken after 15 minutes. The resulting RNA was sequenced, and the results were parsed for differential expression between CDM-G and CDM-CP, as well as genes that are upregulated by NO in one media or the other (A). The top results prompted us to look at phosphate transporter expression in this data set (B). We independently confirmed the expression of *pstS* and *nptA* with RT-PCR in triplicate, using *ldh1* as a control for NO induction (C). Statistics: unpaired t-tests of genes * = $p < .05$, ** = $p < .01$

4.2.2 Phosphate transporters PstSCAB and NptA are vital for growth in alkaline conditions

Based on our RNA-Seq data, we developed individual mutants in *pstS* and *nptA.* We also created a double mutant, *ΔnptAΔpstS.* A previous study characterizing the three phosphate transport systems in *S. aureus* demonstrated that there is a need for *nptA* or *pstSCAB* in high pH conditions(*225*). We grew our mutants in a low phosphate CDM + glucose at a pH of 7.4 and 8.5 and found that the double mutant *ΔnptAΔpstS* exhibited significant lag as compared to both WT LAC and the single mutant counterparts specifically under alkaline conditions (Figures 16A & B).

Our lab has previously demonstrated that the intracellular pH of a *S. aureus* strain growing in the presence of NO is ~8.5(*248*). We tested whether *S. aureus* defends the cytoplasmic pH of the cell against the external pH of the media (Figure 16C). We found that while *S. aureus* does defend against extracellular acidity (internal pH ~7 at an external pH of ~5.5), it does not defend against extracellular alkalinity (Figure 16C). Thus, at an extracellular pH of ~8.5, *S. aureus* exhibits an intracellular pH of ~8.5 – virtually identical to the internal pH of *S. aureus* in the presence of nitric oxide.

Therefore, we tested the impact of NO on our phosphate transport mutants. Grown in the same phosphate limiting CDM-glucose, with 10 mM NO donor added at inoculation of cultures, the *ΔnptAΔpstS* mutant displays a similar lag in growth as in alkaline conditions (Figure 17). Again, there is no defect in growth for the single mutants. Taken together, we conclude that the intracellular pH of *S. aureus* dictates which phosphate transporters are necessary for growth under limiting phosphate. We also find that in the presence of NO, either *pstSCAB* or *nptA* is necessary for *S. aureus* growth.

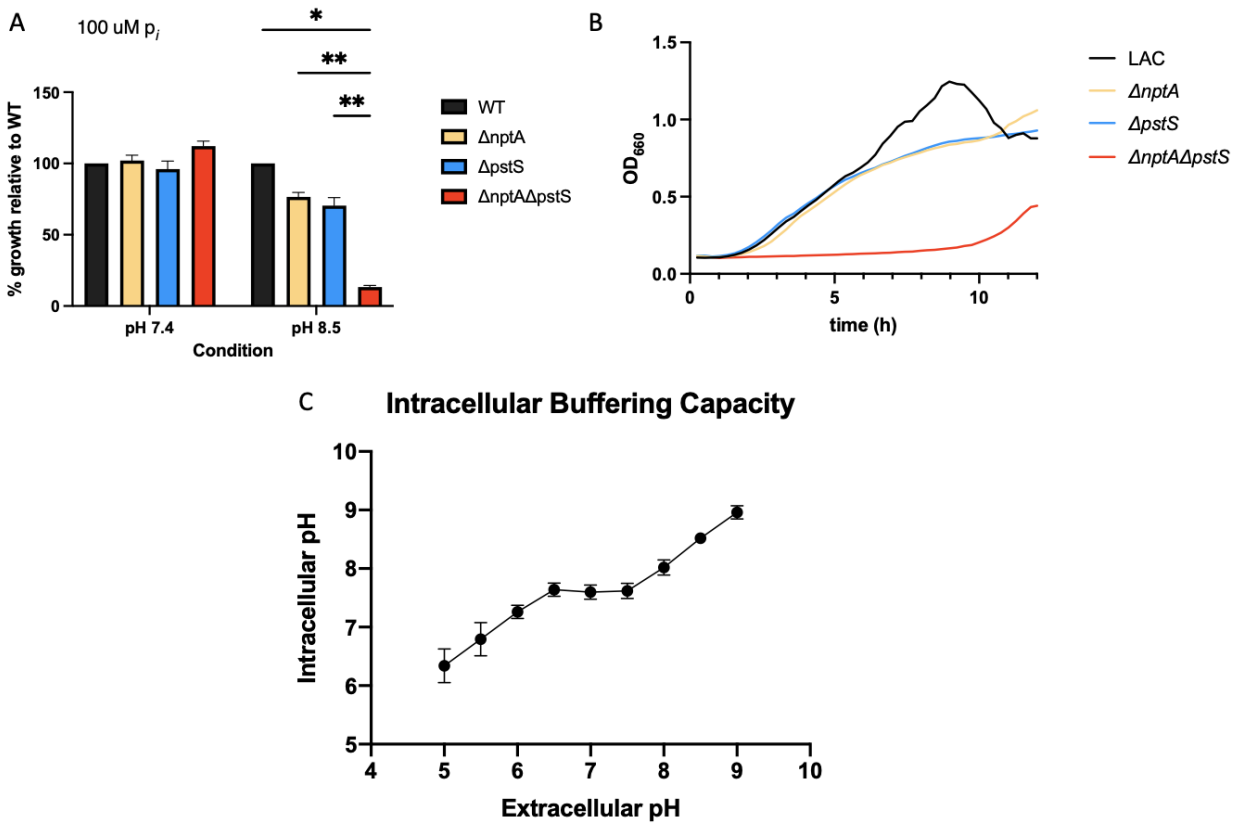

Figure 16: Phosphate transport via NptA or PstSCAB is needed for growth in alkaline conditions. WT LAC, *ΔnptA, ΔpstS* and *ΔnptAΔpstS* were grown in phosphate limiting CDM + G. The OD of these strains at 8 hours were normalized to WT LAC and graphed in (A) (n=3). A representative growth curve is in (B). The intracellular pH of LAC growing in various pH CDM + G was determined and graphed as a function of extracellular pH (C) (n=3). Statistics: 2-way ANOVA with Tukey's multiple comparisons. * = $p < .05$, ** = $p < .01$

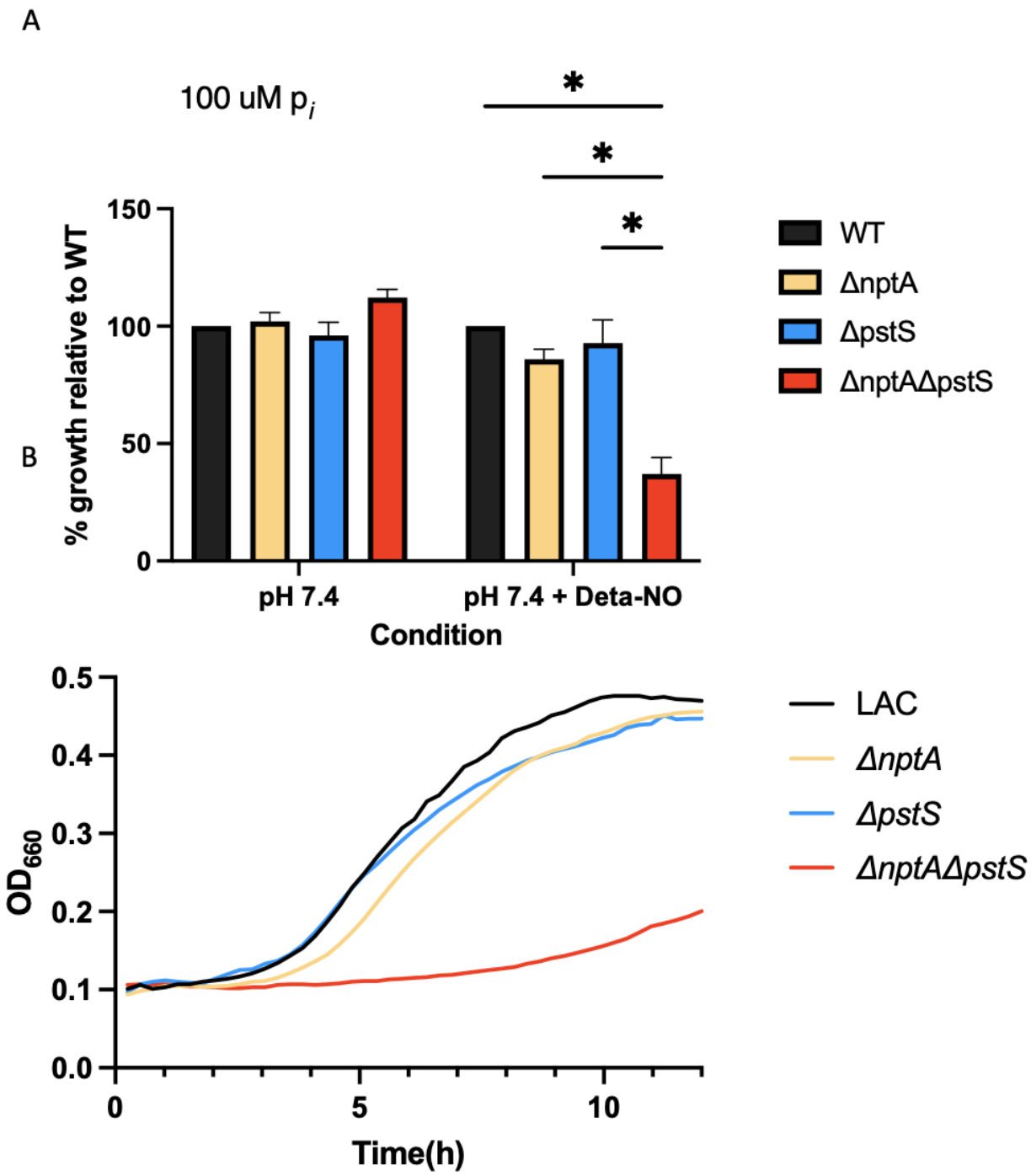

Figure 17: Phosphate transport via NptA or PstSCAB is needed for growth under NO stress. WT LAC, *ΔnptA, ΔpstS* and *ΔnptAΔpstS* were grown in phosphate limiting CDM + G and exposed to 10 mM DETA-NO from inoculation. The OD of each these strains at 8 hours were normalized to WT LAC and graphed in (A) (n=3). A representative growth curve is in (B). Statistics: 2-way ANOVA with Tukey's multiple comparisons. * = $p < .05$

4.2.3 Phosphate transport mutants have lowered ATP

While inorganic phosphate plays a role in several cellular functions in the bacterium, a major one is the formation of ATP via glycolytic substrate level phosphorylation. GAPDH incorporates inorganic phosphate into glyceraldehyde-3-PO_4^- to yield 1,3-bisphosphoglycerate. This assimilated phosphate will be used to generate ATP in the next step of glycolysis, allowing for the incorporation of exogenous phosphate into the ATP pool. GAPDH requires adequate intracellular inorganic phosphate levels to function efficiently. To this end, we tested our *ΔnptA*, *ΔpstS,* and *ΔnptAΔpstS* mutants for intracellular ATP levels in CDM + G, and phosphate limiting CDM + G at pH 7.4 and 8.5. We found that while there was no difference in ATP levels between the mutants and WT in regular CDM-glucose or pH 7.4 phosphate limiting CDM-glucose, there was a significant reduction in ATP in the *ΔnptAΔpstS* strain at a high pH (Figure 18A). Interestingly, there also appears to be a defect in ATP levels in a *ΔnptA* single mutant as well – but no phenotype was displayed in either condition by this mutant (Figures 16 and 17). We also tested the impact of NO on ATP levels in WT LAC and *ΔnptAΔpstS.* We found, again, significantly reduced ATP levels in this mutant under NO stress (Figure 18B). This link between phosphate transport and ATP levels indicates that these transporters are vital for glycolysis and the synthesis of ATP, something that is extremely important in NO stressed cells, as glycolysis becomes the primary form of energy generation under these conditions. This link is possibly the reason for the increased expression of these two phosphate transporters observed in the RNA-sequencing experiment. However, we still do not have a molecular mechanism behind the glucose-dependent expression of *pstSCAB, nptA,* or *ldh1*.

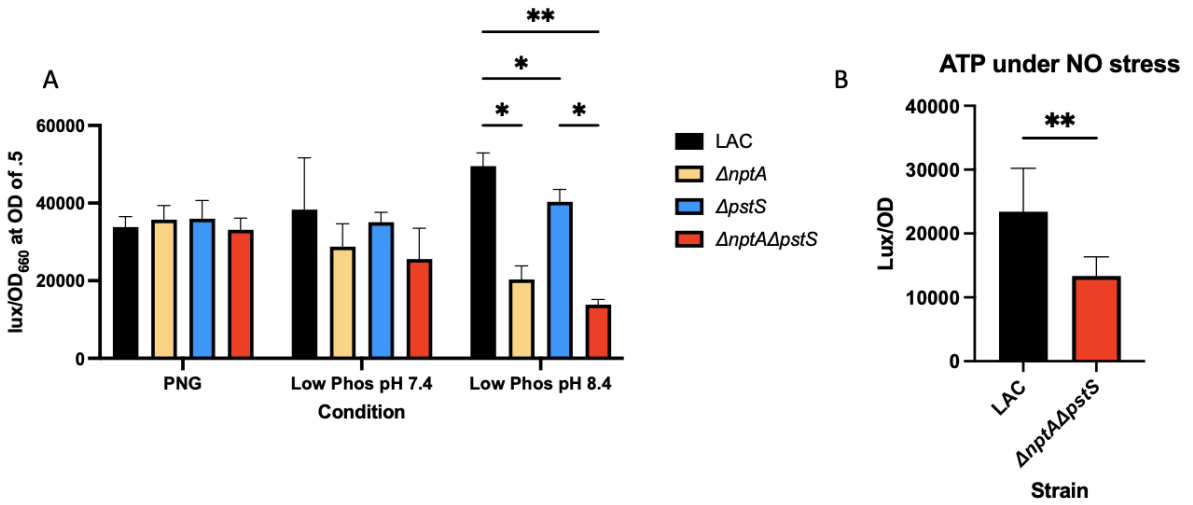

Figure 18: Intracellular ATP is lowered in a *ΔnptAΔpstS* double mutant as compared to WT. WT LAC, *ΔnptA, ΔpstS* and *ΔnptAΔpstS* were grown in various CDM + G and intracellular ATP was determined for each strain and normalized to the strain's OD_{660} at that time point. (A) shows the ATP of each strain non-phosphate limiting CDM + G, low phosphate CDM + G at pH 7.4, and low phosphate CDM + G at pH 8.5 (n=3). (B) shows the ATP of WT LAC and *ΔnptAΔpstS* grown in low phosphate CDM + G at pH 7.4 and exposed to 10 mM DETA-NO from inoculation (n=3). Statistics: (A) 2-way ANOVA with Tukey's multiple comparisons. (B) unpaired t-test, * = $p < .05$, ** = $p < .01$

4.2.4 *In vivo* phenotypes indicate PstSCAB and NptA are vital for infection

To assess the role of these phosphate transporters coupled with NO *in vivo* we performed intracellular survival assays on WT *S. aureus* LAC and the *ΔnptAΔpstS* isogenic mutant. We used promyelocytic cell line MPRO differentiated into neutrophils (Figure 19A) and RAW264.7 macrophages (Figure 19B). In each cell type, WT LAC starts to replicate after 3 hours, and has almost doubled its CFU count by 6 hours. The *ΔnptAΔpstS* mutant, however, never starts to replicate and has significantly lower CFU counts by 6 hours. We treated the RAW264.7 macrophages with the iNOS inhibitor L-NIL, known to limit inflammatory NO production. L-NIL

treatment allowed for additional outgrowth of WT LAC at later timepoints (Figure 19B). Interestingly, the addition of L-NIL also allowed for the outgrowth of *ΔnptAΔpstS* to WT levels. This included significant growth over the untreated counterpart at both 3 and 6 hours, indicating that NO causes a significant impairment in *ΔnptAΔpstS* growth in immune cells.

We also tested the ability of a *ΔnptAΔpstS* mutant to cause infection in a skin and soft tissue infection model (SSTI). We subcutaneously infected WT C57BL/6J mice with 10^7 CFU of WT LAC and the isogenic *ΔnptAΔpstS* strain. We monitored the weight loss of the mice for 7 days, and at day 7 sacrificed the mice to measure lesion area and CFU/abscess. We found significant attenuation of the *ΔnptAΔpstS* mutant in both abscess formation and CFU/abscess as compared to WT LAC, indicating a defect in virulence and survival of the *ΔnptAΔpstS* mutant (Figure 19C-D).

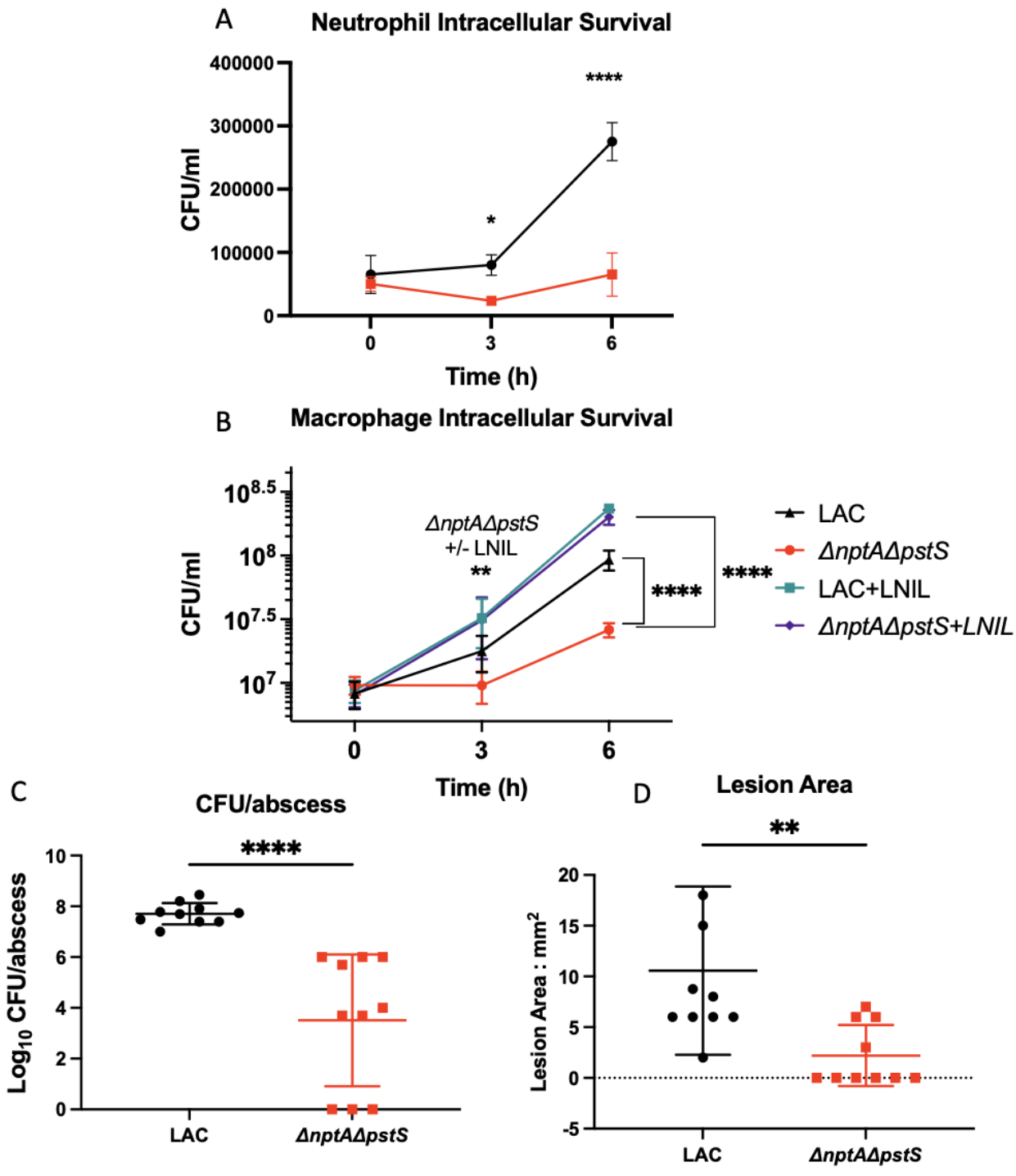

Figure 19: The *ΔnptAΔpstS* double mutant is attenuated *in vivo*. Intracellular survival assays were performed on WT LAC and the *ΔnptAΔpstS* mutant in neutrophils derived from MPRO cells (A) and RAW264.7 cells (B) (n=3). In RAW264.7 macrophages, L-NIL, an inhibitor of iNOS, was added to determine the impact of NO on intracellular survival. 6-8 week-old C57BL/6J mice were subcutaneously infected with WT LAC and the *ΔnptAΔpstS* mutant and

assayed for CFU/abscess (C) and lesion area (D) at day 7 post-infection(n=10). Statistics: (A) 2-way ANOVA with Sidak's multiple comparisons (B) 2-way ANOVA with Tukey's multiple comparisons (C, D) unpaired t-tests. * = p < .05, ** = p < .01, **** = p < .0001

4.3 Discussion

Under NO stress in a host, *S. aureus* must adapt rapidly and efficiently to a new metabolic state that is independent of the TCA cycle and ETC to survive. Our lab has characterized several aspects of this response – increased glucose transport, increased fermentation of pyruvate to lactate – and has now added another facet – increased phosphate transport. The RNA-Sequencing study published here aimed to identify aspects of the NO response that are transcriptionally dependent on glucose. The *pstSCAB* operon fell out as the most differentially regulated operon in the presence of glucose compared to its absence. Preliminary investigation into the genetic regulation of the *pstSCAB* system shows that CcpA, a carbon catabolism regulator, and PhoU, the regulatory protein downstream of the *pstSCAB* operon, are not responsible for this glucose-dependent regulation (Figure 38). Additionally, *pstSCAB* is not regulated by Rex, the redox-sensing repressor that is responsible for the NO-dependent regulation of many NO-inducible genes(*246*). Thus, further investigation into the genetic control of the *pstSCAB* operon is needed which, in tandem with *ldh*1, may reveal a global glucose-dependent regulator responsible for both *pstSCAB* and *ldh*1 expression during NO-stress. We can also test *nptA* in this analysis, as there is differential induction of *nptA* by glucose, though it is not differentially regulated under NO stress.

It is not obvious why alkaline cytosolic conditions necessitates one of these two phosphate transporters specifically. Previous reports showed their requirements in alkaline media, which we

replicated here(*225*). We also show that upon extracellular alkaline stress, *S. aureus* does not defend its cytosolic pH. This likely reflects the fact that *S. aureus* rarely naturally encounters alkaline conditions, as the surface of the skin is mildly acidic. In any event, when the extracellular pH is 8.5, the cytosolic pH of *S. aureus* will also be 8.5. We've previously shown that due to the ATP hydrolysis mode of the F_1F_0-ATPase during NO· stress, the cytosolic pH rises to ~8.5 as protons are extruded from the cell to maintain proton motive force (PMF)(*248*). In addition to contributing to PMF, this proton extrusion also raises the cytosolic pH to the optimum for all three lactate dehydrogenases, which are critical for full NO·-resistance(*249*). We predicted that this rise in cytosolic pH would also necessitate one or more of the phosphate transporters required under alkaline conditions. Indeed, *S. aureus* requires either *ptsSCAB* or *nptA* during NO-stress, likely due to the pH of the cytosol. However, the molecular mechanism behind the pH dependence of these transporters is still unknown.

The link between phosphate transport and glucose may not initially be evident, until one looks closely at the process of glycolysis. The sixth step of glycolysis, mediated by glyceraldehyde-3-phosphate dehydrogenase (GAPDH), involves the incorporation of inorganic phosphate into the GAP molecule, creating 1, 3-bisphosphoglycerate and NADH. The inorganic phosphate that was incorporated in this step is subsequently used to generate ATP from ADP in later steps of glycolysis, allowing for the incorporation of inorganic phosphate into the energy pool. Therefore, higher glycolytic flux in the cell requires more intracellular inorganic phosphate for efficient energy production.

Glycolysis is not the only metabolic process to integrate inorganic phosphate into cellular processes. Another way that inorganic phosphate is incorporated into the energy pool is via the ArcABCD system(*322*, *323*). In the absence of glucose, *S. aureus* consumes amino acids. One of

the primary amino acids consumed for energy is arginine, which is converted to citrulline via ArcA. The resulting citrulline is converted to ornithine and carbamyl phosphate by ArcB, a reaction that incorporates inorganic phosphate. The carbamyl phosphate molecule is used by ArcC, which transfers the phosphate to ADP yielding ATP. This process is vital for the integration of inorganic phosphate into the ATP pool of the cell in the absence of glucose. This is reflected in our RNA-Seq screen as well – *arcC* can be seen in Figure 15A as induced by NO in casamino acids and pyruvate specifically. This indicates, again, the vital importance of inorganic phosphate and the energy pool under NO stress, even in the absence of glucose.

Other metabolic genes of interest came up in the RNA-Seq screen. A 2,3-butanediol synthetic pathway (*alsS/aldC*) that has been documented as playing a role in NO resistance was more highly upregulated in glucose by NO than in casamino acids and pyruvate (*324*). We also see *hld*, the small toxin encoded in RNAIII, the expression of which has been demonstrated to be impacted by pyruvate (*183*). This is particularly interesting, however, because RNAIII appears to possibly be upregulated in our sample, despite the sample being taken at a low OD of .5. Finally, *lrgAB*, the two most differentially regulated genes under NO stress in casamino acids and pyruvate, have recently been demonstrated to encode pyruvate transporters in both *Staphylococcus* and *Streptococcus* species (*325*, *326*). If LrgA and LrgB are, in fact, upregulated here because they are transporting pyruvate into the cell, this could go a long way towards explaining how *S. aureus* can still resist NO when glucose is absent, but pyruvate is present.

The field has clearly shown that *S. aureus* has evolved to resist nitric oxide. This is specific to *S. aureus* and its role as a pathogen, as it does not see these levels of NO unless it has perturbed the immune system. We have shown that *ldh1* was recently acquired by *S. aureus* and its most closely related species *S. simiae* as compared to other coagulase-negative *Staphylococci* (CoNS).

This is not necessarily true of *glcA* and *glcC*, which are important glucose transporters. While *S. simiae* does encode *glcA*, it lacks a *glcC* paralog altogether(*307*). Similarly, *nptA* is absent from closely related species such as *S. epidermidis* and *S. simiae* but is present only in *S. aureus* despite being found in many more divergent staphylococcal species (Figure 35). This study shows that this transporter, NptA, is important for growth under NO stress, both *in vitro* and *in vivo*, and especially in a skin and soft tissue infection (SSTI) model and was reacquired by *S. aureus* likely because of the advantage this extra transporter confers. Other studies done with the *ΔnptAΔpstS* mutant showed a more minor level of attenuation in a systemic infection model than we observed in a SSTI model. This may reflect the fact that *S. aureus*, as a pathogen, has evolved to persist in a skin infection, not necessarily in a systemic infection. However, from these studies it is clear that, in response to host NO and host glucose, *S. aureus* coordinates the expression of various glucose and phosphate transport systems as well as highly active fermentative enzymes to elicit a metabolic state that is compatible with inflamed host tissues replete with immune radicals such as NO.

4.4 Materials and methods

4.4.1 Bacterial Strains and Growth

Strains used in this study are listed in Table 6. All mutant strains are derived from USA300 strain LAC. The *ΔnptA* strain was made as previously described, using allelic exchange via the plasmid pBTK* (*243*). Briefly, 1 kb regions from either side of the *nptA* gene were cloned into the pBTK* plasmid on either side of the kanamycin resistance cassette. This plasmid was isolated

from *E. coli* and transformed into *S. aureus* strain RN4220 (*327*). A lysate of phi-11 phage was created from this strain and used to move the modified pBTK* plasmid into LAC (*309*). The pBTK* plasmid was integrated into the LAC chromosome at the *nptA* locus via homologous recombination after the temperature sensitive plasmid was exposed to temperatures of 43°C. Excision of the remainder of the plasmid was incited by use of cyclosporin treatment. The *ΔpstS* transposon insertion mutation from the Nebraska Transposon Mutant Library from NARSA was transduced into LAC via phi-11 phage transduction. Phage transduction was also used to combine these two mutations into the *ΔnptAΔpstS* mutant. The *ΔccpA* mutant was previously described and the *ΔphoU* mutant was also from the NARSA library.

Overnight cultures were grown in BHI (BD Biosciences). For RNA-Seq experiments and RT-PCR confirmation, strains were grown in PN media supplemented with .5% glucose or .5% casamino acids and .5% pyruvate in a 50 mL culture volume in a 500 mL flask to ensure aeration (*308*). When stated, a modified version of PN was used with a defined phosphate concentration. Briefly, the PN salts were removed and replaced with a Tris buffer solution of pH 7.4. The media was then supplemented with 10 mM or .1 mM K_2HPO_4 (high and low phosphate conditions) and 10 mM NaCl. Cultures were grown in this media at an aeration ratio of 1:10 and an inoculum ratio of 1:200 from overnight cultures grown in BHI. For growth curves, a 1:200 inoculum ratio was used in a 200 μL culture in a 96-well plate and grown at 37°C shaking in a BioTek Synergy H1 plate reader. When stated, 10mM DETA-NO (Sigma) was added to cultures.

Table 6: Strains used in Chapter 4

Strain Name	Strain Description	Source
WT LAC	Methicillin-Resistant Clinical *S. aureus* Isolate	
AR1754	*S. aureus* LAC *ΔnptA::*Km	This study
AR1755	*S. aureus* LAC *ΔpstS::*Tn-Erm	This study
AR1756	*S. aureus* LAC *ΔnptA::*Km *ΔpstS::*Tn-Erm	This study
AR1749	*S. aureus* LAC Δ*ccpA::*Kan	Chapter 3
NE1316	*S. aureus* JE2 Δ*phoU*::Tn	NARSA

4.4.2 RNA extraction

RNA extractions were performed as previously described (*246*). Briefly, 25 mL of culture was quenched with 25 mL of ice-cold ethanol:acetone. Samples were stored at -80°C for no more than 4 days. On extraction, samples were thawed at room temperature and pelleted at 5,000 x g for 10 minutes. Supernatant was discarded and pellets were dried at room temperature, then resuspended in 100 µL of TE. These resuspensions were freeze-thawed in an ethanol-dry ice bath three times, thawing at 60°C each time. Samples were then bead-beat for 1 minute, rested on ice for 5 minutes. 650 µL of lysis buffer was added to the samples and bead-beating was repeated. Lysis tubes were then centrifuged at 13,000 x g for 2 minutes and supernatants were removed and combined with an equal volume of 70% ethanol. This mixture was processed with the Invitrogen Pure-link Mini RNA extraction kit. Samples were treated with DNAse-1 (NEB) for 1 hour, then repurified using the Invitrogen Pure-link Mini RNA kit. The samples were then quantified.

4.4.3 RNA-Sequencing and analysis

The RNA extracted as above was sent to the University of Pittsburgh Health Sciences Sequencing Core at Children's Hospital of Pittsburgh. The stranded total RNA library was prepared using the TruSeq Total RNA kit (Illumina). 300 ng of RNA was depleted for rRNA using bacterial target for rRNA capture, then cleaned up with AMPureXP beads, and then fragmented. Random primers initiate first and second strand cDNA synthesis. First strand cDNA synthesis used SuperScript IV. The adenylation of 3' ends was followed by adapter ligation and 12 cycles of library amplification with indexing. Amplified library was cleaned up with 45 µL AMPureXP beads. Sequencing was performed on a NextSeq500, with a MidOutput 150 Flowcell. Read length was 150 bp, loading concentration was 1.8 pM. Demultiplexing and adapter sequence trimming were performed by the Core. Samples were analyzed via alignment to the *S. aureus* LAC genome using Geneious v.8.

4.4.4 RT-PCR

50 ng of purified RNA was used in a RT-PCR reaction as according to the manufacturer's instructions for the Power SYBR green RNA-to C^t 1-step kit (Applied Biosystems). An iQ5 machine was used for RT-PCR, and the coordinating iQ5 software was used to determine the C_t. The $\Delta\Delta C_t$ was found using *rpoD* as a reference gene. Primers used are listed in Table 7.

Table 7: Primers used in Chapter 4

Primer	Sequence
NptA_5'.1A	GGGGGATCCTGTAAACGTGACCCACTTGC
NptA_5'.1B	GGGGGATCCCTTCTGTAACCGACATTTCC
NptA_3'.1A	GGGGAATTCTCCAACATTCATGGGTTGGC
NptA_3'.1B	GGGGAATTCGGTTATACAGCATTGCAGGC
rpoD_RT.1A	AACTGAATCCAAGTGATCTTAGTG
rpoD_RT.1B	TCATCACCTTGTTCAATACGTTTG
ldh1_RT.1A	AAAACATGCCACACCATATTCTCC
ldh1_RT.1B	TACTAAATCTAAACGTGTTTCTCC
PstS_RT1.A	TGGCTCATCAACAGTAGCAC
PstS_RT1.B	AAACCAGCACCTGTACCAGC
NptA_Rt1.A	TTCAAGCATCAGCAGGAGAC
NptA_Rt1.B	GTCGTACCTGAACTACTTTG
PitA_RT1.A	ATGGATTCCATGATACAGCC
PitA_RT1.B	TAAAGTTCATCACTGCTGCC

4.4.5 Intracellular pH and ATP experiments

Intracellular pH of LAC grown in CDM-G at varying extracellular pH was assayed using the pHrodo Red AM Intracellular pH Indicator Kit (ThermoFisher). Cells were grown to an OD of .2, then 200 µL of sample was washed with HEPES buffer at pH 7.4 and subsequently stained 50 nM pHrodo Red AM staining solution for 30 minutes at room temperature. Samples were

washed with HEPES buffer and read for fluorescence on a BioTek Synergy H1 plate reader. A standard curve of samples treated with 10 μM valinomycin/nigericin at pH levels 4.5, 5.5, 6.5, and 7.5 was used to convert fluorescence into pH.

Intracellular ATP was measured using the BacTiter-Glo kit (Promega). Briefly, cultures were grown in phosphate limiting CDM-G at pH 7.4, 8.5, or in the presence of DETA-NO. 100 μL samples were taken hourly and mixed with 100 μL of BacTiter-Glo reagent. The mixture was incubated for 5 minutes and then luminescence was determined using a BioTek Synergy H1 plate reader. The readings for identical ODs were compared to account for differing growth rates.

4.4.6 Preparation of bacterial strains for cell culture infections

S. aureus LAC and the isogenic *ΔnptAΔpstS* mutant were grown overnight at 37°C in BHI. Cultures were diluted 1:200 in fresh BHI and grown for another 4h at 37°C, harvested and washed 2 times with PBS. OD_{600} was measured and adjusted to ensure an MOI of 10:1. The required bacteria was opsonized with an equal volume of normal mouse serum for 20 min at 37°C followed by final dilution into infection media. Bacterial CFU was enumerated at this stage to ensure correct MOI.

4.4.7 Bacterial survival in RAW 264.7 cells

RAW 264.7 cells (ATCC TIB-71) were cultured in RPMI 1640 (Gibco 11875-093) containing 1mM sodium pyruvate and 10% FBS at 5% CO_2. Cells were plated in 12 well plates with 10^6 cells/well for 12-16h. On the day of infection, cells were treated with 100ng/ml LPS and 20ng/ml IFNγ for 6h followed by 3 PBS washes. Cells were overlaid with opsonized LAC or the

ΔnptAΔpstS mutant containing RPMI minus FBS and plates centrifuged at 200 x g for 5 min to allow efficient bacterial attachment. Plates were incubated at 37°C with 5% CO_2 for 30 min. Wells were washed 3 times with PBS and incubated with RPMI containing 20µg/ml Gentamicin for 1h. Cells were washed once with PBS and either incubated further or lysed for the 0h time point. For lysis and CFU analysis at every time point, wells were incubated for 5 min with 1% Triton X-100, serially diluted and plated on BHI agar. Colonies were counted the next day. For L-NIL treatment, 100µM L-NIL was added to the LPS IFN treatment wells and the presence of L-NIL was maintained in the media at all stages till cell lysis.

4.4.8 Bacterial survival in MPRO cells

MPRO cells (ATCC CRL-11422) were cultured in IMDM (Gibco 12440-046) containing 20% heat inactivated horse serum and differentiated in culture media containing 10µM ATRA for 72h. Differentiated MPRO cells were distributed at 10^6 cells /tube and treated with 100ng/ml LPS and 20ng/ml IFNγ for 6h. Cells were washed by centrifugation at 200 x g for 5 min and incubated with opsonized LAC or the *ΔnptAΔpstS* mutant in IMDM minus horse serum for 30 min at 37°C and 5% CO_2. Cells were washed 3 times with PBS and incubated with IMDM containing 20µg/ml Gentamicin for 1h. Cell lysis and CFU analysis was performed as described above.

4.4.9 Animal infections

S. aureus LAC and the isogenic *ΔnptAΔpstS* mutant were grown for 12-16h at 37°C in BHI. Cultures were diluted to 1:200 in fresh BHI and grown till OD_{600} reached 2.0. 1ml of each culture was harvested and washed twice with PBS. Bacterial pellets were reconstituted in 200µl of PBS

and serially diluted till 10^{10} dilution and plated on BHI agar. Colonies were counted the next day while the reconstituted bacterial cultures were stored at 4°C. Bacterial suspensions were adjusted to 5 x 10^8 /ml based on CFU enumeration.

Both male and female, 6-8 weeks old C57BL/6J mice weighing 20-25gm were used in this study. Mice were obtained from Jackson Laboratories and housed with 14h light cycles. On the day of infection, mice were weighed and 12 x body weight in µl of Avertin was administered via intraperitoneal injection. The dorsal left flank of each animal was shaved and 20µl of the bacterial suspension was injected subcutaneously using a 26G needle. Animals were monitored every day. On day 7, the mice were euthanized in a CO_2 chamber followed by cervical dislocation. The abscesses were measured, excised, and homogenized in PBS followed by serial dilution and plating on BHI agar for CFU enumeration. All animal manipulations and infections were conducted under an institutionally approved and currently active IACUC protocol (# 22030607).

5.0 Insights in *ldh1* regulation in a glucose-dependent manner

The unique ability of the pathogen *S. aureus* to adapt its metabolic scheme rapidly under immune stress is very important for infection. As immune radicals exert pressure on the bacterial cell, respiration is inhibited by ROS and RNS. To continue to grow, *S. aureus* must shift from a respiration-based to a fermentation-based energy generation strategy. This strategy employs the increased import of glucose (Chapter 2) and glycolysis for energy generation and the maintenance of redox balance by the conversion of pyruvate to lactate by lactate dehydrogenase Ldh1. Since this metabolic scheme is so highly dependent on glucose, the protein Ldh1 appears to be transcriptionally regulated by glucose. In this chapter, we will investigate transcriptional regulators that control expression of glucose-dependent genes to determine if they impact *ldh1* expression. We will show that CggR does not affect *ldh1* expression. We will also examine some unique aspects of the *ldh1* transcript, including the extended 5' untranslated-region, and their roles in Ldh1 production. We will show that the 5' UTR is not responsible for differences in transcript stability and does not interact with a top sRNA candidate for interaction known as RsaOT. Finally, we will demonstrate that while the 5' UTR has a negative impact on Ldh1 production, it is *not* responsible for the glucose-dependent induction of Ldh1. While we have further hypotheses, we cannot make any conclusions about the glucose-dependent regulation of *ldh1* at this point.

5.1 Introduction

S. aureus is a pathogen capable of infection many different environments in the human body, including the skin, heart, kidney, joints, lungs, and bloodstream(*8*). Different challenges are presented to the pathogen in each of these environments, but all of them will heavily feature encounters with the innate immune system upon initial infection(*124*). These forerunners of host defenses against infection exhibit several antimicrobial properties, prominent among them being the production of immune radicals, such as reactive oxygen and reactive nitrogen species(*328*). These radicals will interfere with different aspects of bacterial metabolism and replication, including respiration, the TCA cycle, and DNA repair(*146*). Most pathogens succumb to these life-altering changes, but *S. aureus* is unique in that it exhibits high levels of resistance to these stressors(*148*).

One of the key players in *S. aureus* immune radical resistance is the altered metabolic scheme adopted by the bacteria when NO or other immune radicals are encountered. NO inhibits the electron transport chain, resulting in an imbalance of NADH to NAD+, which is vital for glycolysis and energy generation(*146*). Additionally, the inhibition of the ETC results in lowered ATP levels, as this is an important source of ATP levels during respiration. This requires the bacteria to find another way to generate ATP and maintain the NAD+/NADH ratio, also known as redox balance.

To generate ATP under immune radical stress, *S. aureus* adopts an altered metabolic scheme focused on glycolysis for energy generation(*252*). Glucose is rapidly brought into the cell via the four glucose specific transporters, and glycolytic flux is increased(*229*). This results in an increased amount of NADH in the cell. This increase in NADH will be sensed by the redox-sensing repressor Rex(*250*). Rex will then derepress its regulon, which includes several NO resistance

genes including *ldh1*. Ldh1 is a highly efficient lactate dehydrogenase that will convert the pyruvate generated via glycolysis into lactate, converting NADH back into NAD+ and normalizing the redox state of the cell(*247*). This allows for continued energy generation via glycolysis and bacterial survival in the face of immune radicals.

The regulation of *ldh1* has been the target of this lab's research for many years. It has a very strong promotor but is strongly repressed by Rex(*298*). Thus, it is among the most highly expressed genes in the cell under Rex de-repression. Additionally, the presence of glucose has a positive effect on *ldh1* expression. In media containing glucose, *ldh1* expression is approximately a log higher than in media without glucose. Previous work has shown that this glucose-dependent effect on *ldh1* expression is not due to CcpA, a major regulator of glucose-utilization genes(*298*). While *ldh1* is expressed to a lower level in a Δ*ccpA* mutant in mixed carbon source media, when forced to consume glucose, *ldh1* expression is not lowered in a Δ*ccpA* mutant. Additionally, CcpA does not bind the promotor region of *ldh1*, like Rex does(*298*). This led the lab to conduct a screen on over 100 different mutants in genetic regulators from the NARSA library harboring a transcriptional fusion of *ldh1*. Unfortunately, none of these regulators showed significant differences in *ldh1* expression in a glucose-dependent manner (data not shown).

Another unique aspect of the *ldh1* locus is the large 5' untranslated region (5' UTR) of the gene. The start codon is 167 bp downstream of the transcriptional start site as determined by 5' RACE(*298*). The 5' UTR contains two different hairpin loops that often interfered with the RACE experiment as well. This data led to the hypothesis that the 5' UTR may play a role in the expression of *ldh1*, and translational GFP reporters with and without the UTR were created. This chapter explores the role of the 5'UTR, as well as other regulators with known impacts in glucose regulation, in *ldh1* expression and Ldh1 production.

5.2 Results

5.2.1 CggR is not responsible for the glucose-dependent transcription of *ldh1*

While the lab has previously established that CcpA, a major glycolytic regulator, is not responsible for the glucose-dependent *ldh1* expression(*298*), there are other glycolytic regulators that could be responsible. Foremost among these is CggR (or GapR), a repressor upstream of a regulon containing important glycolytic genes like *gapA, pgk,* and *eno*(*329*). Both CcpA and CggR respond to the presence of the same glycolytic intermediate FBP(*297*, *330*). A transposon in CggR would disrupt the expression of all these important glycolytic genes, so CggR is not present in the NARSA library. To determine if there could be an impact of CggR on *ldh1* expression, we started with a plasmid constitutively expression *cggR* (plgt::*cggR).* RT-PCR was performed on RNA extracted from this strain grown in PNG for *ldh1* and *gapA,* a known gene in the CggR regulon. Expression of both *ldh1* and *gapA* is slightly repressed by *cggR* overexpression (Figure 20A). This data prompted us to make a Δ*cggR* mutant.

The Δ*cggR* strain was used for RT-PCR experiments on RNA grown in PNG or PNCP and exposed to NO for 15 minutes, as in the RNA-Seq experiment featured in Chapter 4. The induction of the expression level of *ldh1* was determined in each strain, and no significant differences were found between WT LAC and the Δ*cggR* strain (Figure 20B). Additionally, the reporter strains for Ldh1 production with and without the 5' UTR were transduced into each strain and grown in PNG, with 10 mM NO donor added at OD 0.2. Again, no significant differences were found in the production of GFP between WT and Δ*cggR,* either with or without the 5' UTR of *ldh1* present

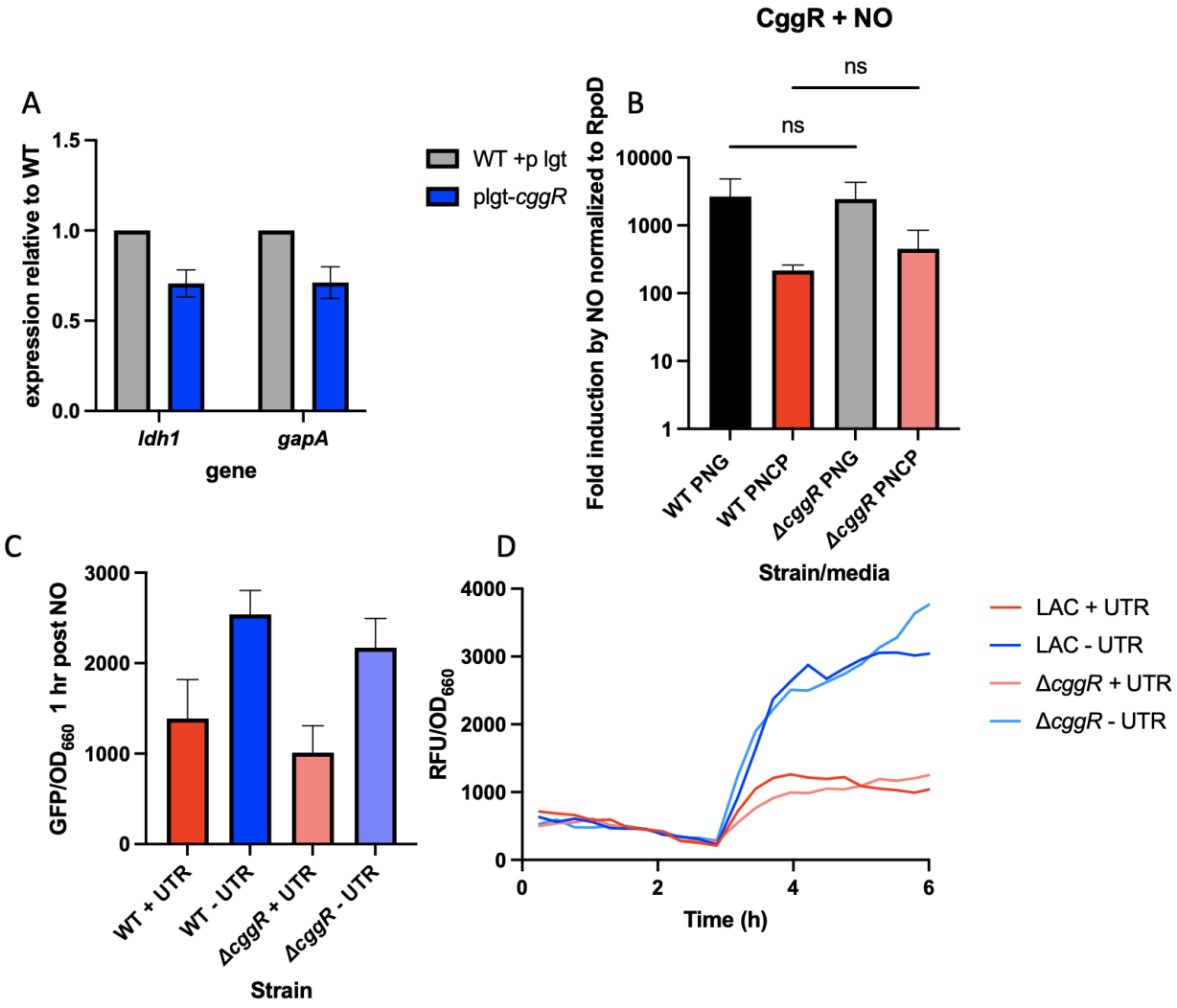

Figure 20: CggR cannot does not affect the expression of *ldh1*. RT-PCR on *ldh1* in (A) LAC harboring a *cggR* constitutive expression plasmid (n=2) or (B) LAC and the isogenic *ΔcggR* mutant (n=3). RT-PCR was also done on *gapA* in the *cggR* expression strain. Statistics: (A) Two-way ANOVA with Sidak's multiple comparisons. (B) Ordinary one-way ANOVA with Tukey's multiple comparisons. (C) GFP levels 1 hour post-NO in the *ΔcggR* mutant with the p*ldh1*::GFP plasmid with and without the *ldh1* UTR (n=3). (C) Statistics: ordinary one-way ANOVA with Tukey's multiple comparisons. (D) A representative graph from (C).

(Figure 20C and D). From this data, we conclude that CggR does not regulated *ldh1* expression or Ldh1 production. However, we do observe an increase in the production of GFP from a strain with the UTR to one without the UTR. This different remains consistent even across the *ΔcggR* mutant.

5.2.2 *ldh1* transcript stability does not depend on carbon source or the 5' UTR

In the absence of further obvious transcriptional regulator candidates, we turned to the potentiality that *ldh1* is regulated by an intrinsic characteristic of the *ldh1* RNA itself, including the 5' UTR. One way to impact transcript levels or translation of a protein in a cell is to vary the amount of time the RNA transcript is present in the cell(*331*). This is referred to as transcript stability. UTRs are known to sometimes have an impact on transcript stability(*331*, *332*). If a transcript is quickly degraded, there will be less of it present in a cell upon RNA extraction, and there will be less protein translated from it than if the transcript is degraded more slowly. To measure transcript stability, we utilize an antibiotic known as Rifampicin (Rif). Rif interferes with the RNA polymerase of bacteria, and therefore halts all transcription in the cell(*333*). By adding Rif to cultures and taking RNA from these culture at various time points post-Rif addition, we can determine how quickly transcript is degraded via RT-PCR, as there is no new transcript being made. We performed RNA stability assays *ldh1* in WT LAC grown anaerobically in the presence (PNG) and absence (PNCAA) of glucose. There was no significant difference in transcript level at 1, 5, or 10 minutes post-Rif, indicating there is little to no impact of carbon source on transcript stability (Figure 21A).

We also performed these assays on WT LAC strains harboring the p*ldh1*::GFP fusion with and without the UTR. We measured the stability of *gfp* transcript with and without the 5'UTR of *ldh1*, and found no significant differences in *gfp* transcript levels at 1, 5, and 10 minutes post-Rif

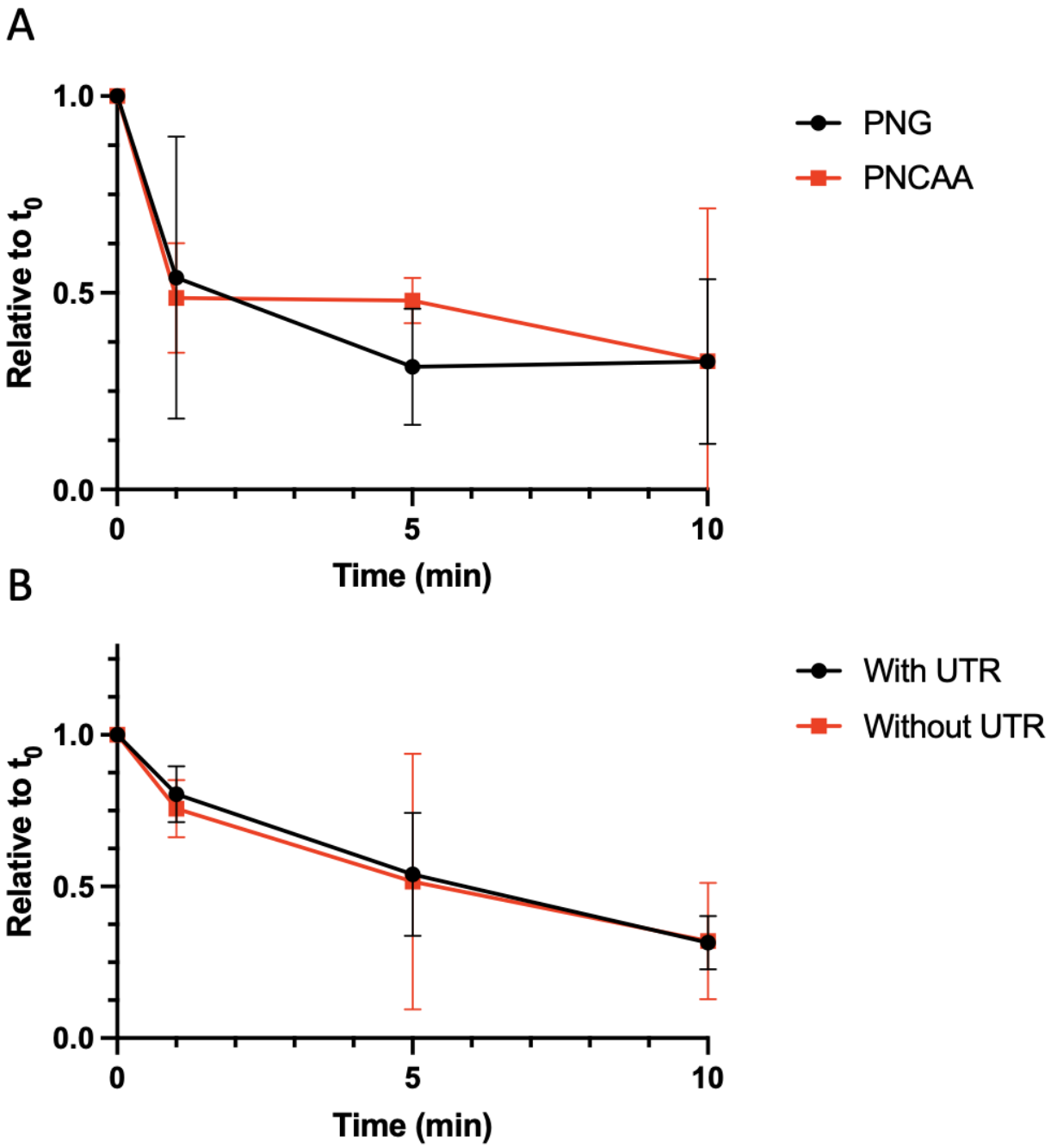

Figure 21: The stability of *ldh1* transcripts is not affected by media or UTR presence. RNA stability experiments on anaerobic cultures. Rifampicin was added to cultures at t_0, and samples were taken at 1 minute, 5 minutes, and 10 minutes after rifampicin was added (n=3). RT-PCR was performed on (A) *ldh1* in PNG and PNCAA and (B) *gfp* in strains harboring the p*ldh1::*GFP plasmid with and without the 5' UTR of *ldh1*.

(Figure 21B). This indicates that the 5'UTR of *ldh1* also has no impact on transcript stability. Therefore, we do not think that the degradation rate of *ldh1* transcripts plays a role in *ldh1* expression.

5.2.3 RsaOT has no effect on the translation of Ldh1

Having observed the strong post-transcriptional impact of the 5'UTR of *ldh1* (Figure 20), we sought to determine if a trans-acting RNA was interacting with the 5'UTR. We used a previously identified library of ~300 sRNAs in USA300 strains of *S. aureus*(*334*) to analyze our glucose and NO-dependent RNA-Seq data from chapter 4. We took the top 10 sRNAs differentially regulated by glucose and aligned them with the 5' UTR of *ldh1*. We found a region that had complementary sequence similarity with the 5' UTR of *ldh1* in the sRNA RsaOT (Figure 39). The RsaOT locus is shown in Figure 39. The sRNA known as RsaOT is immediately downstream of a protein-coding sequence of a hypothetical protein of unknown function that will be referred to as SACOL2491. We developed mutants in RsaOT, SACOL2491, and the entire locus. We additionally made a frameshifted mutant of SACOL2491. To determine if this non-coding RNA or its locus play a role in *ldh1* transcription, RT-PCR was performed on the Δ*rsaOT* and the Δ*SACOL2491* mutants grown anaerobically with or without glucose. There is no change in *ldh1* expression between WT and the mutants (Figure 22A, B). Additionally, RT-PCR was used to determine *rsaOT* expression in the ΔSACOL2491 mutant, in which *rsaOT* expression levels are lowered dramatically (Figure 22B). This data also shows that there is no difference in *rsaOT/SACOL2491* expression between glucose and no glucose conditions (Figure 22B).

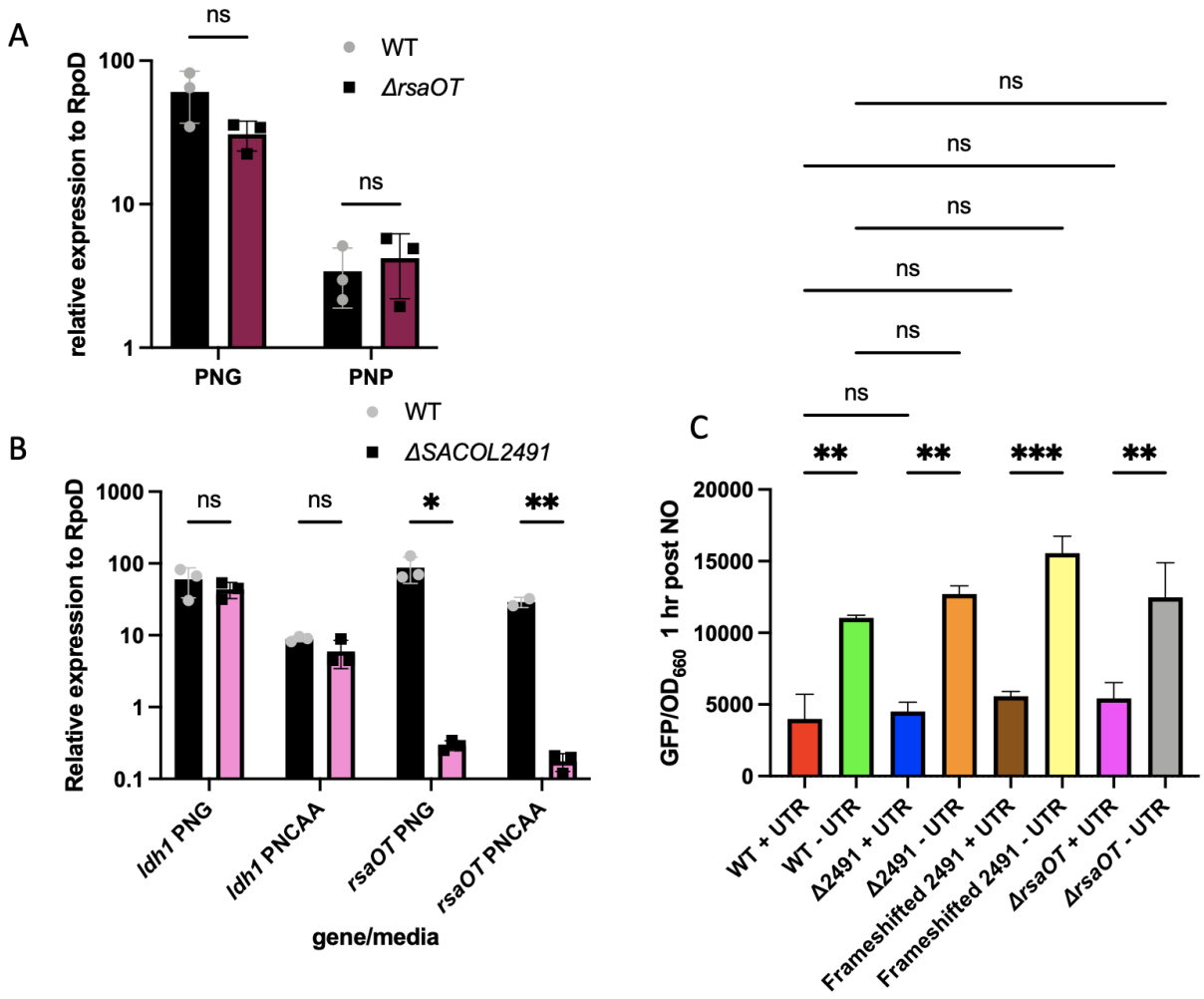

Figure 22: *rsaOT* has no impact on *ldh1* transcription or production. RT-PCR performed on (A) the *⊿rsaOT* mutant (n=3) and (B) the *⊿SACOL2491* mutant (n=3) for *ldh1* expression and in (B) *rsaOT* expression in both PNG and PNC or PNP. Statistics: Multiple t-tests; ns = non-significant, * = p<.05, ** = p<.01. There is no significant difference in *ldh1* expression between strains. (C) the GFP levels 1 hour post-NO in various *⊿rsaOT* mutants harboring the p*ldh1*::GFP plasmid with and without the UTR(n=3). Statistics: Ordinary one way ANOVA with Sidak's multiple comparisons. ** = p < .01, *** = p < .001. There are no significant alterations in GFP production between strains.

We used translational reporters with and without the 5' UTR of *ldh1* to determine if RsaOT or SACOL2491 had an impact on the post-transcriptional regulation of Ldh1 production. At first, we thought that there might be something to this regulation, as the GFP production appeared erratic between plasmids with and without the 5' UTR in the same mutant strains. Therefore, many mutants were generated. Additionally, all these mutations and the reporter plasmid were put into multiple strain backgrounds – LAC, JE2, and COL (data not shown). Results continued to appear erratic (Figure 40B, C). Upon leaving these plates on the bench top for an extended period of time, we found that some colonies appeared more yellow than others (Figure 40A). Subsequent sequencing of the GFP-containing plasmids in these strains revealed that some of these plasmids harbored known copy number mutations that increased the number of plasmids present inside the cell(*335*, *336*). This means that there are more copies of the genes to be transcribed, and the strains with the copy number mutation will express more GFP than those without it. Indeed, we found that our erratic results from all these different strains lined up with whether the colony appeared yellow or white, and therefore whether the colony had a high or low copy number plasmid. Figure 40C clearly shows the difference in GFP levels between the white and yellow colonies harboring the two plasmids.

Experiments were reconducted with this plasmid copy number issue in mind. Only unmutated plasmids were transduced into cells and plates were monitored to ensure white colonies did not turn yellow. When this was done, however, all significant differences between WT and mutants disappeared, and RsaOT and SACOL2491 clearly have no impact on GFP production (Figure 22C). This led us to conclude that despite confusing preliminary data, there is no link between RsaOT, SACOL2491, and Ldh1 production.

5.2.4 The 5' UTR of *ldh1* is not responsible for the glucose-dependent activation

To evaluate the role of the 5' UTR in *ldh1* transcription, cultures harboring the translational fusion of the *ldh1* promotor to GFP with and without the 5' UTR in PNG or PNCAA were grown to an OD of 1 and anaerobiosis was induced. Samples were taken for RNA extraction and RT-PCR was performed on the *gfp* transcript levels in the cell. There was no significant difference between the *gfp* transcript levels in samples with and without the 5' UTR, and there were markedly reduced levels of *gfp* transcript in PNCAA compared to PNG in strains harboring both constructs (Figure 23A). This led us to conclude that the 5' UTR is not responsible for the glucose-dependent transcriptional activation of *ldh1* expression.

We also used the GFP reporter strains in translational assays. We grew cultures of WT LAC harboring GFP reporter plasmids with and without the UTR in PNG and PNTL (.5% tryptone, .5% lactate). Tryptone and lactate together as a carbon source allow for continued replication of *S. aureus* under NO stress even in the absence of glucose. We added 10 mM NO donor at an OD of .2 and evaluated the induction of GFP in each condition. We consistently observe an increase in GFP levels in strains without the 5' UTR as compared to those with the 5' UTR, indicating that the 5' UTR of *ldh1* has a negative impact on translation of Ldh1 (Figure 23B). However, the ratio of GFP production between the two strains does not change depending on the carbon source in the media, again indicating that the 5' UTR is not responsible of the glucose-dependent effect on Ldh1 production (Figure 23B). We can conclude, however, that the 5'UTR of *ldh1* has a strong post-transcriptional negative impact on Ldh1 production.

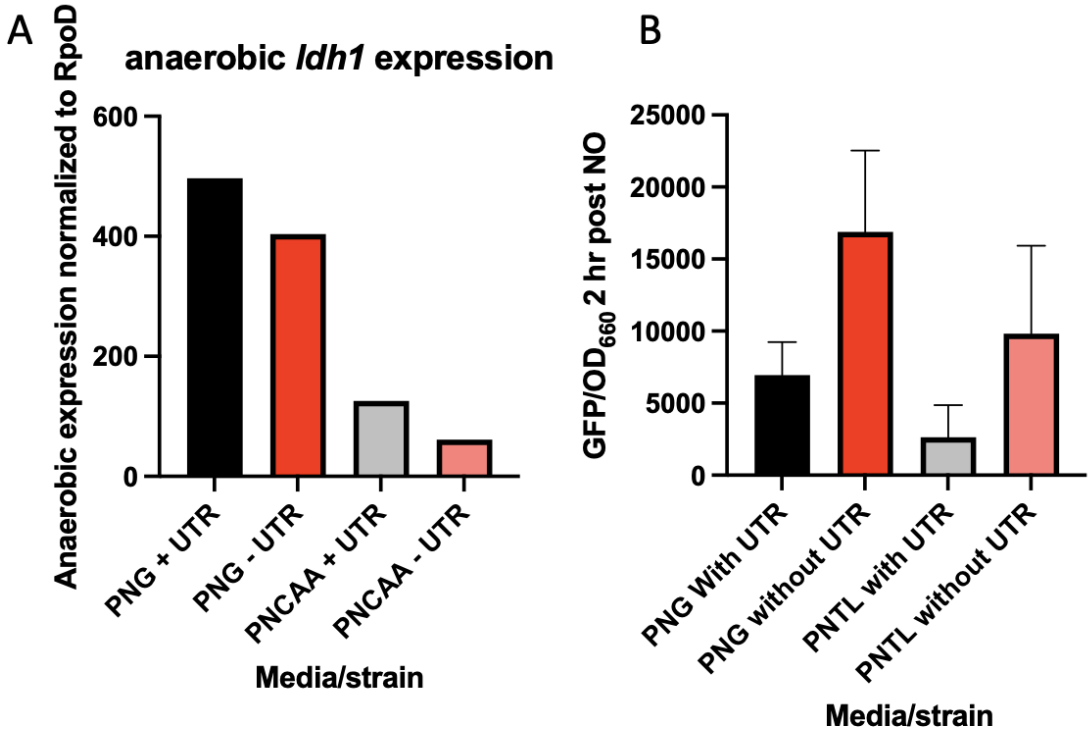

Figure 23: The 5' UTR of *ldh1* post-transcriptionally regulates Ldh1 production. (A) RT-PCR (N=1) of *gfp* in strains harboring the p*ldh1*::GFP transcriptional fusion with and without the UTR of the *ldh1* gene in both PNG and PNCAA under anaerobic conditions. (B) GFP levels 2 hours post-NO addition in PNG or PNTL in strains harboring the p*ldh1*::GFP with and without the *ldh1* UTR (n=3). Statistics: ordinary one-way ANOVA with Tukey's multiple comparisons. There are no significant differences between carbon sources.

5.3 Discussion

The altered metabolic scheme adopted by *S. aureus* under immune radical stress is vital for is survival in a variety of infection environments. Understanding this response is important for understanding how to treat *S. aureus* infections. One of the most unique aspects of this response is that the vital protein, Ldh1, is transcriptionally upregulated by glucose in an unknown manner(*298*). The ability of Ldh1 to be produced in mass quickly when the cell falls out of redox balance is key for allowing the cell to quickly change its metabolic scheme upon hinderance of the electron transport chain. This chapter has aimed to determine what may be responsible for the glucose-dependent induction of *ldh1*, whether it is a transcriptional regulator linked to glucose utilization, a trans-acting sRNA, or something intrinsic to the RNA itself.

The most prominent, not yet tested, regulator was CggR. CggR plays a role in the regulation of an operon that is key for glycolysis, including several key glycolysis genes, such as GapA. However, CggR is not known to play a role in other loci outside its own. We developed a strain overexpressing *cggR*, hoping that an excess of CggR could lead us to other promotors it may bind weaker. CggR is a repressor that will fall off its binding sequence in the presence of fructose bisphosphate (FBP), so we expected that overexpressing *cggR* will result in increased repression of its operon – an effect we did in fact observe on *gapA* expression. We also saw a similar effect on *ldh1* and thought we might have our regulator. Since the overexpression plasmid has the same origin of replication as our reporter plasmids and they cannot be co-harbored in a strain, we were prompted to create a *ΔcggR* mutant. We had to create a clean deletion of the *cggR* gene, as it is directly upstream of its operon, which is important for glycolysis and therefore cell survival. Once this mutant was obtained, we were able to test *ldh1* levels. We hypothesized that *ldh1* transcript levels in this mutant would be at 'with glucose' transcript levels in no glucose conditions, but

found that this remained untrue, and the mutation had no effect on *ldh1* levels. We also tested our GFP reporter plasmids and found no difference between WT and *ΔcggR* plasmid-containing strains. Additionally, CggR did not affect the difference between the UTR containing and UTR missing strains, indicating that there is no role of CggR in *ldh1* regulation. The effect we observed in the CggR over-expressing strain is likely an artifact of decreased glucose utilization, something we also observe in a *ΔccpA* mutant.

To determine the intrinsic stability of the RNA, we used a rifampicin assay to determine transcription levels after the inhibition of the RNA polymerase using the antibiotic rifampicin. We found that there was no inherent difference in RNA stability depending on carbon source. If the transcript had been more stable in the presence of glucose as compared to its absence, translation of Ldh1 could have been impacted. However, we found this was not the case. Additionally, we looked at a unique aspect of the *ldh1* RNA – a large, untranslated region at the 5' end of the transcript. This 5' UTR does not play a role in *ldh1* RNA stability. We did discover that the 5' UTR has a post-transcriptional effect on Ldh1 translation – when the 5'UTR is eliminated from the GFP reporter plasmid that contained the *ldh1* translational fusion, there is more GFP produced upon NO addition. However, to fully understand this effect, we will need to generate a mutant that does not have the 5' UTR of *ldh1* in the chromosome. We can then use enzyme assays to determine the amount of Ldh1 present in the cell to see if this effect on translation is true.

We considered the hypothesis that a trans-acting sRNA could be interacting with the 5' UTR and leading to alterations in the translation level of Ldh1 in the cell. Indeed, when looking at a library of 300 sRNAs, we found one with homology to the 5' UTR of *ldh1* – RsaOT (Figure 39). No role for RsaOT in cellular processes has been described, nor has there been an identified function of the hypothetical coding sequence next to RsaOT. Additionally, RsaOT was upregulated

in the absence of glucose in the RNA-Seq study conducted in chapter 4 (Figure 39). We investigated if this locus played some role in *ldh1* transcription or Ldh1 translation, and found that it did not, no matter how the locus was mutated. This indicates that this sRNA does not likely interact with the 5' UTR of *ldh1*, at least not in any impactful way. This leaves us with question – how is the UTR of *ldh1* impacting translation? We hypothesize that the stem loops in the 5'UTR of *ldh1* could be interfering with the binding of the ribosome to the Shine-Dalgarno sequence, which would initiate translation of *ldh1*. Mutating these stem loops could potentially provide insight on this hypothesis. However, in the grand scheme of the cell, this impairment of translation by the 5' UTR clearly does not lead to huge differences in Ldh1, and indeed leads to inhibition of Ldh1 production, which bodes the other question – why is the UTR present? The experiments proposed here and further investigation by other lab members may shed light on these questions.

Finally, we demonstrated that the 5' UTR is not responsible for glucose-dependent transcriptional activation. RT-PCR used to quantify transcript of GFP between plasmids with and without the 5' UTR show no differences in transcript levels between strains harboring the two plasmids, indicating that the effect of the 5' UTR is purely translational. There are also still significantly reduced levels of GFP in each strain from PNCAA to PNG, indicating that there is no role of the 5'UTR in glucose-dependent transcription and that there is still glucose-dependent activity on the promotor even at the plasmid level.

This chapter has shed light on several ways that *ldh1* is not regulated by glucose. Though we had hoped for a firm answer, eliminating several targets is still important to the process of understanding how *ldh1* is regulated by glucose. We can say that there is nothing intrinsic to the RNA that is causing this differential regulation. There remains the possibility that a sRNA is responsible for the negative regulation seen by the 5' UTR; however, the 5'UTR is not involved

in the glucose differential regulation of *ldh1*. We also identified another transcriptional regulator that is not responsible for the glucose-dependent regulation. One unexplored avenue is the role of Agr in *ldh1* transcription. As this dissertation has established, glucose catabolism activates the Agr system, so perhaps Agr somehow plays into *ldh1* regulation. Further work by future lab members will be needed and may yet provide the answers we are looking for.

5.4 Materials and methods

5.4.1 Bacterial strains

All strains used in this chapter are listed in Table 8. All data published here comes from WT LAC derived strains, unless otherwise stated. Mutants in *SACOL2491* are derived from their NARSA mutant. Mutants in *cggR, RsaOT,* the frameshifted SACOL2491, and the entire RsaOT-SACOL2491 locus were created using allelic exchange, as described above in chapter 4.4.1. Mutations were moved using phage transduction protocol. Plasmids were transferred using phage transduction protocols.

Strains were grown overnight in BHI. For most experiments, strains were grown in a chemically defined minimal media known as PN containing various carbon sources at carbon-balanced ratios. PNG - 0.5% glucose. PNCP - 0.5% casamino acids and 0.5 % pyruvate. PNTL - 0.5% tryptone and 0.5% lactate. PNCAA – 1% casamino acids. PNP – 1% pyruvate.

Table 8: Strains used in Chapter 5

Strain Name	Strain Description	Source
WT LAC	Methicillin-Resistant Clinical *S. aureus* Isolate	
AS14	WT LAC + pNAS58 (*ldh1*::GFP)	This Study
AS15	WT LAC + pNAS59 (*ldh1*-UTR::GFP)	This Study
AS101	WT LAC + plgt::*cggR*	This Study
AR1757	WT LAC ΔcggR	This Study
AR1759	AR 1757 + pNAS58 (*ldh1*::GFP)	This Study
AR1760	AR 1757 + pNAS59 (*ldh1*-UTR::GFP)	This Study
AR1628	WT LAC ΔRsaOT::Km	This Study
AS33	WT LAC ΔRsaOT::Km + pNAS58 (*ldh1*::GFP)	This Study
AS34	WT LAC ΔRsaOT::Km + pNAS59 (*ldh1*-UTR::GFP)	This Study
AS36	WT LAC ΔSACOL2491::TnErm	This Study
AS37	WT LAC ΔSACOL2491::TnErm + pNAS58 (*ldh1*::GFP)	This Study
AS38	WT LAC ΔSACOL2491::TnErm + pNAS59 (*ldh1*-UTR::GFP)	This Study
AS55	WT LAC SACOL2491 Frameshifted (f.s.)	This Study
AS56	WT LAC SACOL2491 f.s. + pNAS58 (*ldh1*::GFP)	This Study
AS57	WT LAC SACOL2491 f.s. + pNAS59 (*ldh1*-UTR::GFP)	This Study
AS83	WT LAC ΔSACOL2491locus::Erm	This Study
AS84	WT LAC ΔSACOL2491locus::Erm + pNAS58 (*ldh1*::GFP)	This Study
AS85	WT LAC ΔSACOL2491locus::Erm+pNAS59 (*ldh1*-UTR::GFP)	This Study

Table 8 continued

AR1439	WT JE2+ pNAS58 (*ldh1*::GFP)	This Study
AR1440	WT JE2+ pNAS59 (*ldh1*-UTR::GFP)	This Study
AS43	WT JE2 ΔRsaOT::Km	This Study
AS44	WT JE2 ΔRsaOT::Km + pNAS58 (*ldh1*::GFP)	This Study
AS45	WT JE2 ΔRsaOT::Km + pNAS59 (*ldh1*-UTR::GFP)	This Study
AS31	WT JE2 ΔSACOL2491::TnErm + pNAS58 (*ldh1*::GFP)	This Study
AS32	WT JE2 ΔSACOL2491::TnErm + pNAS59 (*ldh1*-UTR::GFP)	This Study
AS76	WT JE2 SACOL2491 f.s.	This Study
AS77	WT JE2 SACOL2491 f.s.+ pNAS58 (*ldh1*::GFP)	This Study
AS78	WT JE2 SACOL2491 f.s.+ pNAS59 (*ldh1*-UTR::GFP)	This Study
AS86	WT JE2 ΔSACOL2491locus::Erm	This Study
AS87	WT JE2 ΔSACOL2491locus::Erm + pNAS58 (*ldh1*::GFP)	This Study
AS88	WT JE2 ΔSACOL2491locus::Erm + pNAS59 (*ldh1*-UTR::GFP)	This Study

5.4.2 RNA extraction and RT-PCR

RNA extractions were performed as described above (Chapter 3.4.4 and 4.4.2). RT-PCR was also performed as described above (Chapter 2.4.3, 3.4.4 and 4.4.4). Primers used are listed in table 9. For anaerobic samples, cultures were grown at 37°C in a 500 mL flask in a 50 mL culture volume of the stated media until an OD of 1, at which point samples were transferred into a 50 mL

conical tube and tightly capped. Samples were left at 37°C to go anaerobic for 1 hour, and then 25 mL of culture was mixed with 25 mL of ice-cold ethanol acetone and samples were stored at -80°C until extraction. For anaerobic stability assays, cultures were left to grow anaerobically for 1 hour, at which point 25 ug/mL rifampicin was added and 25 mL of culture was taken. Remaining sample was recapped, and further samples were taken at 1, 5, and 10 minutes post-Rif addition. Samples were stored at -80°C until extraction. For NO-containing RT experiments, cultures were grown in a 500 mL flask in a 50 mL culture volume of the stated media until an OD of 0.5, at which point 25 mL of sample was taken and 10 mM DETA-NO was added to the remaining sample. 15 minutes later, the remaining sample was taken. Samples were stored at -80°C until extraction.

Table 9: Primers used in Chapter 5

Primer	Sequence
rpoD_RT.1A	AACTGAATCCAAGTGATCTTAGTG
rpoD_RT.1B	TCATCACCTTGTTCAATACGTTTG
ldh1_RT.1A	AAAACATGCCACACCATATTCTCC
ldh1_RT.1B	TACTAAATCTAAACGTGTTTCTCC
RsaOT_RT.1A	GAT GCT GAG CGT TTG TAT CAC
RsaOT_RT.1B	CAA TCA CAC TTC AAT TGC CGC
GapA_RT.1A	TCAGTGAACCAGATGCAAGC
GapA_RT.1B	GCGCCTGCTTCAATATGAGC
CggR_1.A	GGGGTCGACATTTTTGTCCCACGCGGGAC
CggR_1.B	GGGCTCGAGCTGCCATTATAATGGCCTCC
CggR_IF_1.A	GGGGGATCCTCAATATCAATATGTGCCACC
CggR_IF_1.B	GGGGGATCCTTTAACTAATTGACGGTCGCC
CggR_IF.2A	GGGGGATCCAGCACCTACAAAGCAACGTC
CggR_IF.2B	GGGGGATCCACACGAGTTTGTGTAGCGTC
CggR_Del.A	ATTTATAAATATAAGGAGGAGGTAGTAGTGTAAGAG ATAAAAAGTTTAATACTTAAA
RsaOT_5.1A	GGGGGATCCCTAATGTACCAAGTTATTCGG
RsaOT_5.1B	GGGGGATCCGGCAATAAGAACTAGTTAGTG
RsaOT_3.1A	GGGGAATTCTGGATGTGGCTTTAGTCATAC
RsaOT_3.1B	GGGGAATTCTCACATCAATCATACTATCCC
SACOL2491.1A	GTGAAATACATCACAAATCCC

Table 9 continued

SACOL2491.1B	AGTATGACTAAAGCCACATCC
RsaOT_2491_5'gibson_1.A	tagtatcgacggcccgggTTTTCTCATAATCATCACTC
RsaOT_2491_5'gibson_1.B	tgcaggtcgactctagagGGATGATGAAAAAAGGT
pBTK*_gibson_1.A	ccgggccgtcgatacta
pBTK*_gibson_1.B	ctctagagtcgacctgca
SACOL2491_fs_5.1A	GGGGAATTAGTGAATTTGATAATGTAGCTC
SACOL2491_fs_5.1B	GTCTGAGAAAATAAGCTTGCTTCAATCTATTTTCTCA TAATC
SACOL2491_fs_3.1A	GATTATGAGAAAAGAGATTGAAGCAAGCTTATTTTC TCAGAC
SACOL2491_fs_3.1B	GGGGAATTCTCTCAAGTGTCCATGACGCCC
2491_RsaOT_5.1B	GGG GGA TCC TTT TCT CAT AAT CAT CAC TCC
2491_RsaOT_5.1A	GGG GGA TCC GGA TGA TGA AAA AAG GTA TCC

5.4.3 Growth curves

Overnight cultures were grown in BHI. After 16-20 hours of growth, 1 mL of cells was removed and washed 3x with PBS. The PBS resuspended cells were added to the stated media (typically PNG) at a 1:200 ratio. 200 μL of culture was added to each well of the plate. The plate was placed in a BioTek Synergy H1 plate reader, where bacteria were grown shaking at 37°C. OD and GFP readings were taken every 15 minutes. When the average of all cells had reached an OD of 0.2, 10 mM DETA-NO was added to the cultures. The cultures grew for another 16-20 hours.

Upon termination of the growth curve, the GFP values 1 or 2 hours post-NO addition were subtracted from the GFP values at NO addition, which is graphed in the data tables above. Where relevant, a representative GFP curve is provided.

6.0 Summary and Discussion

The concept of immunometabolism, or the idea that the metabolic response to infection is a major contributor to the immune response to infection, is an emerging concept becoming more regularly appreciated by the field. Understanding that the pathogen's metabolic response is equally important to infection is a key piece of pathogenesis that has only recently been appreciated. While many pathogens are capable of consuming multiple carbon sources to produce energy, provide carbon, and keep the bacterium 'running', almost all bacteria have a favored carbon source controlled by carbon catabolite repression. For *S. aureus*, the pathogen that is the focus of this dissertation, that carbon source is glucose. *S. aureus* can consume complex carbohydrates, amino acids and peptides, organic acids and fatty acids, but the CCR system preferentially activates glycolysis and the consumption of glucose. While this knowledge has long been understood – *S. aureus* grows extremely well in any media with glucose in it – the importance of this carbon source to *S. aureus* pathogenesis has only recently been appreciated, and this thesis has aimed to take that appreciation to another level.

Previously, this lab had a developed a strong understanding of the role of glucose, glycolysis, and glucose transport in the metabolic adaptations that result from NO and immune radical stress. In this dissertation, that understanding has been broadened to apply beyond glycolysis's contribution to infection. Chapter 2 demonstrates an acutely important role for glucose in activation of the Agr system and demonstrates the importance of both the Agr system and its virulence factors, as well as the glucose transporters and utilization genes that allow for efficient Agr activation, in infection. Moreover, a key role for these systems in an immunocompromised host is demonstrated, as active infection cannot be caused even in the absence of immune radicals

unless the Agr system has been efficiently activated. The role of ATP in the activation of the Agr system is also revealed, emphasizing the importance of CCR in glycolysis and ATP generation. This chapter is vital to our understanding of *S. aureus* pathogenesis and shows how this pathogen can take advantage of the hyperglycemic environment provided as a consequence of uncontrolled diabetes.

In chapter 3, the role of CCR and metabolic regulation in infection is expanded on. This study focused on CcpA, the metabolic regulator of CCR, and CodY, a regulator of amino acid bioavailability and a member of the stringent response. These two regulators have opposing roles on the Agr system, and this study shows that CcpA affects ATP levels, resulting in adjusted activation of the Agr system, while CodY and the stringent response do not relay their affect on Agr via ATP. This is also the first time that the intracellular amino acid concentrations of a *ΔccpA* and *ΔcodY* strain have been reported, and it is clear that a *ΔccpA* strain does not always have WT levels of amino acids intracellularly, while *ΔcodY* does experience some excess intracellular amino acid levels. This demonstrates a clear role for both CcpA and CodY in maintaining intracellular amino acid balances.

Chapter 4 expands on the impact of glucose on the transcriptional environment in *S. aureus* under NO stress. Over 30 genes were differentially regulated by glucose and NO stress, and over 300 genes were differentially regulated by glucose alone. This expanded network of transcriptional regulation by glucose is vital to our understanding of the important role this carbon source plays in pathogenesis. This chapter also focuses on the role of phosphate transport in *S. aureus* under NO stress and establishes a new role for two phosphate transporters in adapting to the pH changes experienced during NO stress and infection. Garnering a better understanding of the role of glucose in gene expression is expanded upon in chapter 5, where the glucose-dependent regulation of *ldh1*

transcription is explored. Unfortunately, despite much work done in this area, an explanation of the glucose-dependent transcription observed for the past decade has not been found. Further studies, including investigation into the role the Agr system may play into *ldh1* transcriptional regulation, is needed. This chapter does show that despite unique characteristics of the *ldh1* RNA, including a long 5' UTR, there is no inherent difference in transcript stability and no role of the 5' UTR in glucose-dependent transcriptional activation. Again, more work will be required to fully understand the 5' UTR and its role in Ldh1 production.

Taken together, these conclusions provided in this dissertation contribute to our understanding of the role of glucose in *S. aureus* pathogenesis – not only in metabolic adaptation to stressors in the host environment, but in virulence factor production and activation of the Agr system. The insights provided by chapters 2 and 3 into hyperglycemic infections can provide new targets treatment of diabetic wounds, a major cause of healthcare costs and morbidity in diabetic patients. Furthermore, the implication of phosphate transporters in the schema of *S. aureus* NO resistance may provide another clear target for treatment therapies for antibiotic resistant strains of *S. aureus*. The understanding of how important metabolism is to *S. aureus* infection can change our perception of how to investigate and treat *S. aureus* infections for decades to come.

Appendix A Supplemental Figures

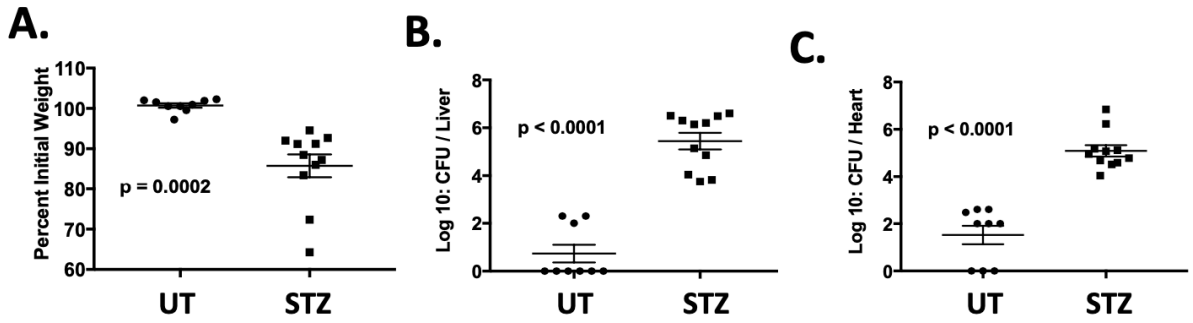

Figure 24: Hyperglycemic mice have increased bacterial dissemination to perpherial organs. UT (n=9) and STZ (n=11) mice were infected with 10^7 CFU of WT. STZ-treated mice infected with WT have significantly increased weight loss compared to untreated animals (A). Infection with WT in STZ-treated animals resulted in significantly increased bacterial dissemination to livers (B) and hearts (C) compared to similarly infected untreated mice.

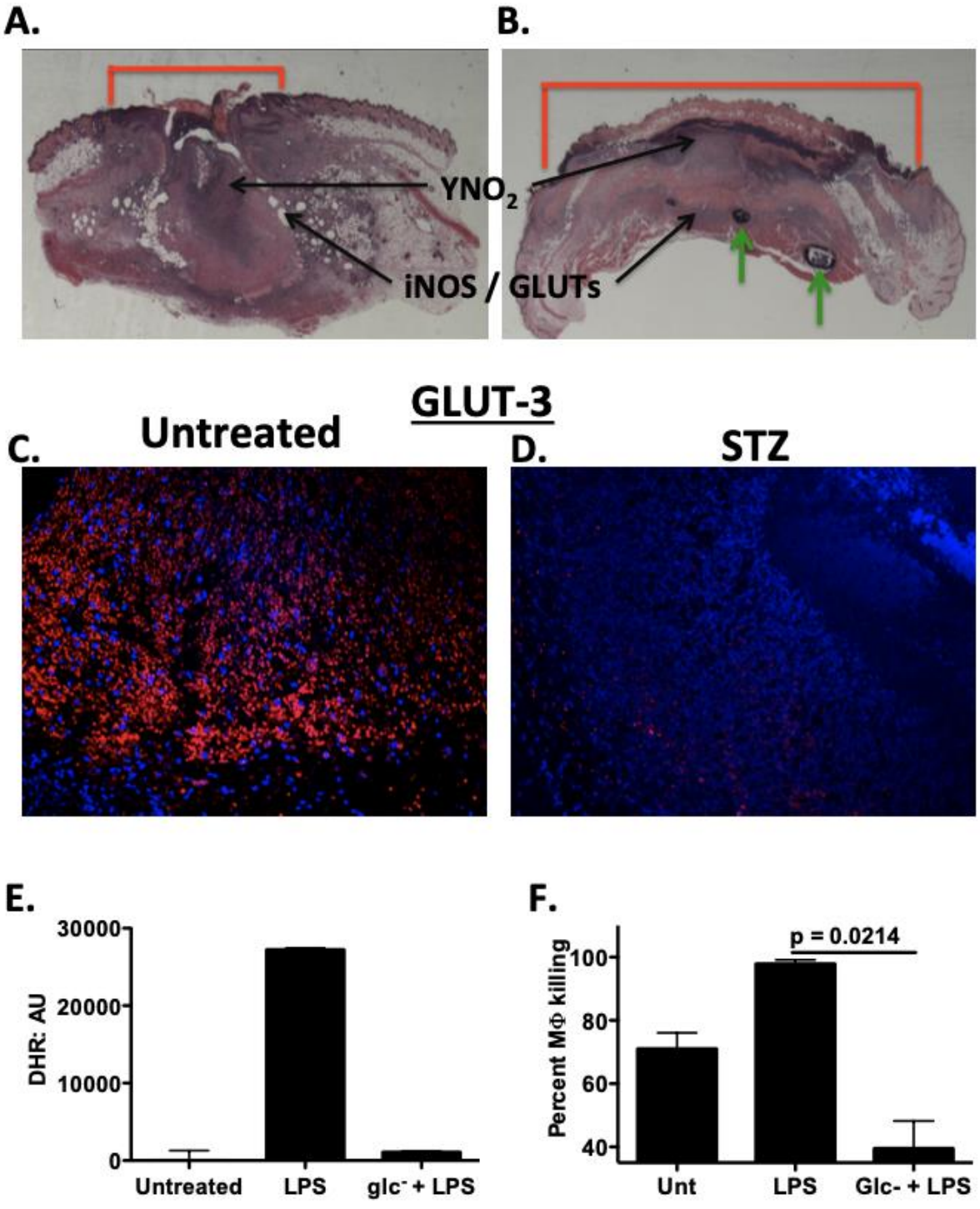

Figure 25: STZ-treated mice do not express GLUT-3. Hematoxylin and eosin stained day seven tissues from *S. aureus* infected normal (A) and streptozotocin (B) treated mice. There is increased dermonecrosis in the STZ treated infected tissues compared to normal mice (red lines). The formation of a subcutaneous abscess in the normal tissue

indicates control of tissues necrosis. In the STZ treated tissue there is no abscess formation and necrosis is observed penetrating to the ribs (green arrows) The black arrows indicate the relative areas where staining for YNO_2, iNOS, GLUT-1 and GLUT-3 was performed. Immunohistochemistry (IHC) was performed on tissues from untreated and STZ-treated mice using antibodies against GLUT-3 (red) and counterstained with DAPI (blue). GLUT-3 is highly abundant in infected tissues from untreated mice (C) but is absent from infected tissues in STZ-treated mice (D). RAW 264.7 macrophages were stimulated with LPS (100 ng/ml) and INFγ (20 ng/ml) in media containing glucose or without glucose. Dihydrorhodamine 123 was used to measure intracellular peroxynitrite formation as an indication of respiratory burst. Stimulated macrophages had robust respiratory burst in the presence of glucose, but almost no burst in the absence of glucose (E). *S. aureus* was incubated for one hour in the presence of RAW 264.7 macrophages that were either not stimulated in the presence of glucose, or stimulated with LPS and INFγ in the presence or absence of glucose. Stimulated macrophages in the presence of glucose killed more *S. aureus* than the not stimulated control (F). Stimulated macrophages in the absence of glucose had a significant reduction in bacterial killing compared to macrophages with glucose (F).

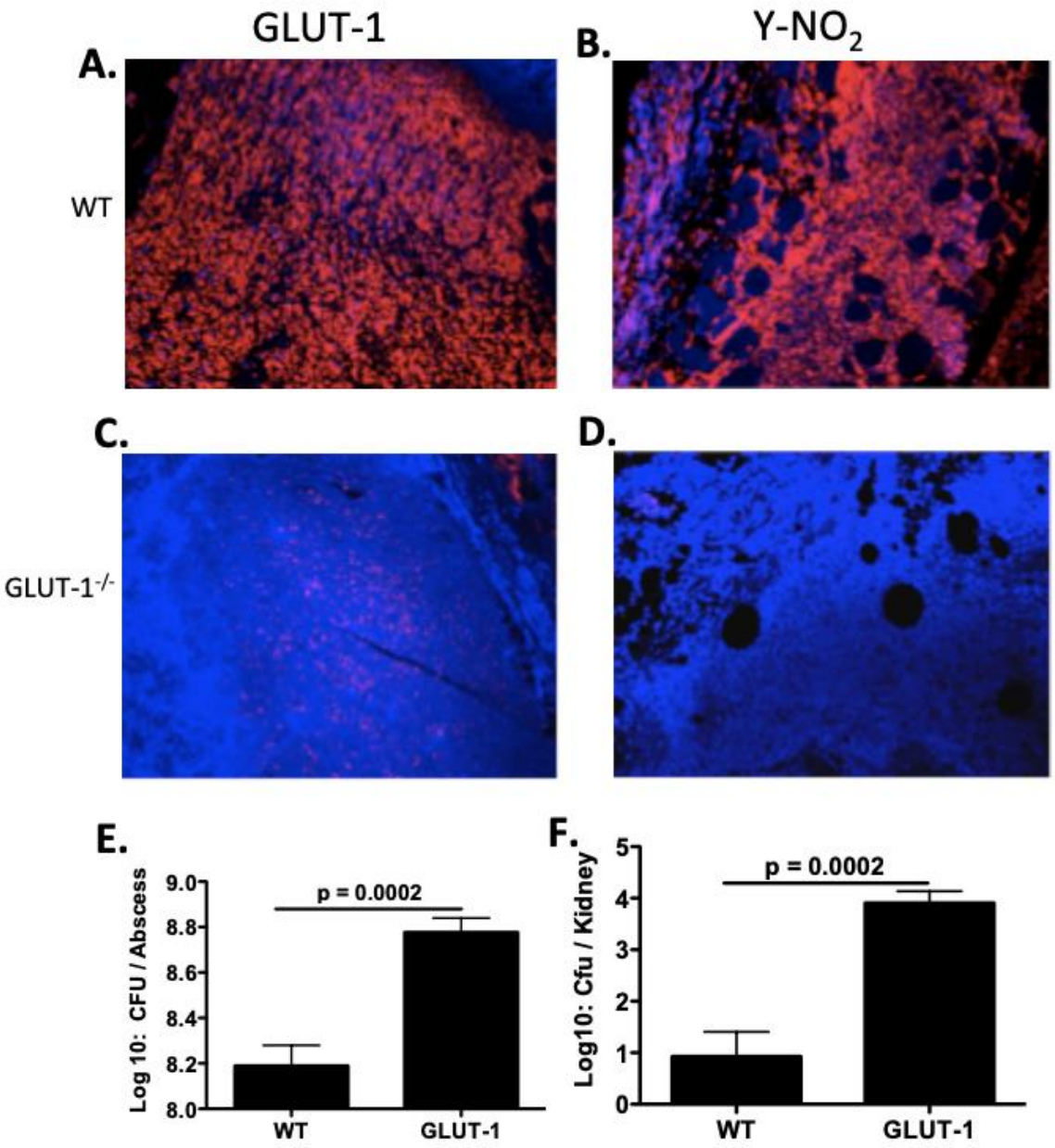

Figure 26: GLUT-1 LysM/Cre mice develop more severe *S. aureus* infections. IHC performed on infected tissues from WT and GLUT-1 LysM/Cre mice showed that WT mice had robust levels of GLUT-1 (A) and Y-NO2 (B) staining. Conversely, GLUT-1 LysM/Cre mice had virtually no signal for GLUT-1 (C) or Y-NO2 (D). Wild-type C57BL6 mice (N=9) and GLUT-1 LysM/Cre mice (N=7) were infected with 1 x 10^7 CFU of *S. aureus* LAC. GLUT-1 LysM/Cre mice had significantly higher bacterial burdens in the abscess (E) and in the kidneys (F).

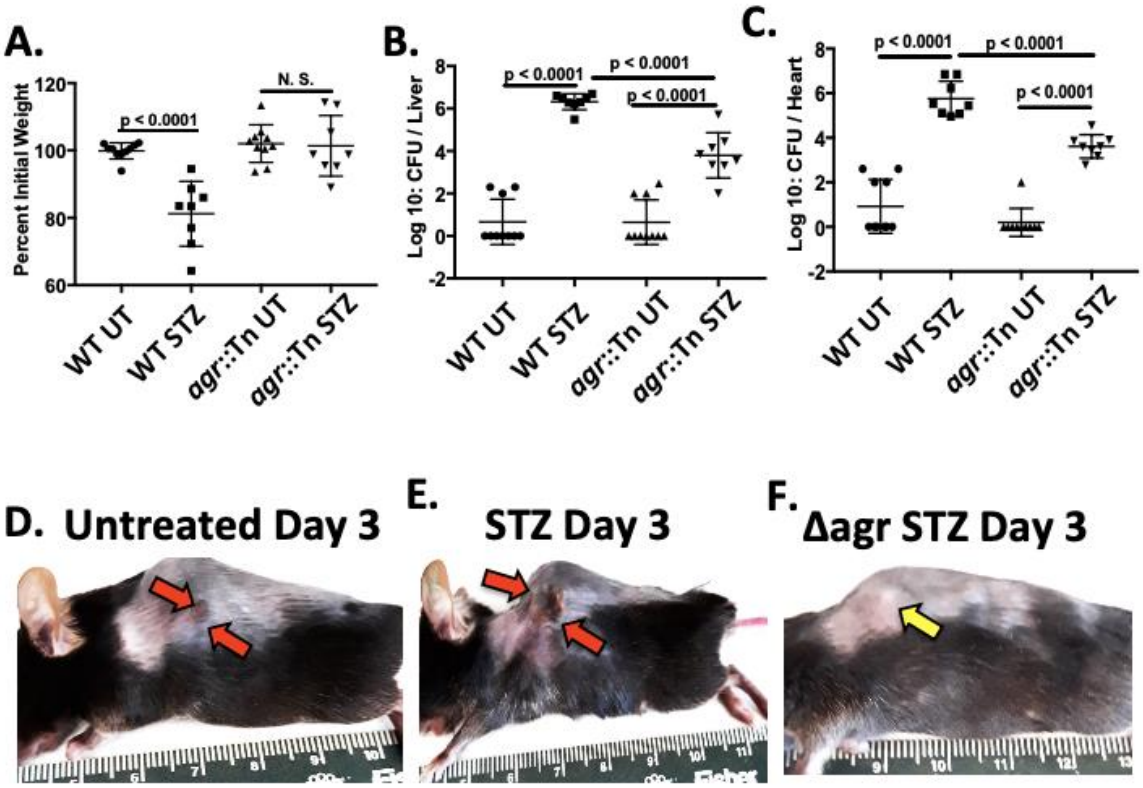

Figure 27: Increased virulence in hyperglycemic mice is mediated by Agr. STZ-treated mice infected WT displayed increased weight loss (A), increased dissemination to the liver (B) and heart (C) compared to untreated mice. While isogenic Δ*agr* mutants rarely disseminated from the abscess in untreated mice, these mutants were able to disseminate in STZ-treated animals, albeit at reduced levels compared to WT LAC (B & C). Representative photographs showing dermonecrotic lesions three days after infection from LAC WT infected untreated mouse (red arrows) (D), STZ-treated mouse (red arrows) (E), and a Δ*agr* infected STZ-treated mouse (yellow arrow) (G). Untreated mice have smaller open lesions than STZ-treated hyperglycemic mice. The Δ*agr* infected mice display a small subcutaneous abscess as shown by the small bump in the skin (Yellow arrow) that is not observable at seven days after infection. Photo credit: Lance Thurlow, University of Pittsburgh.

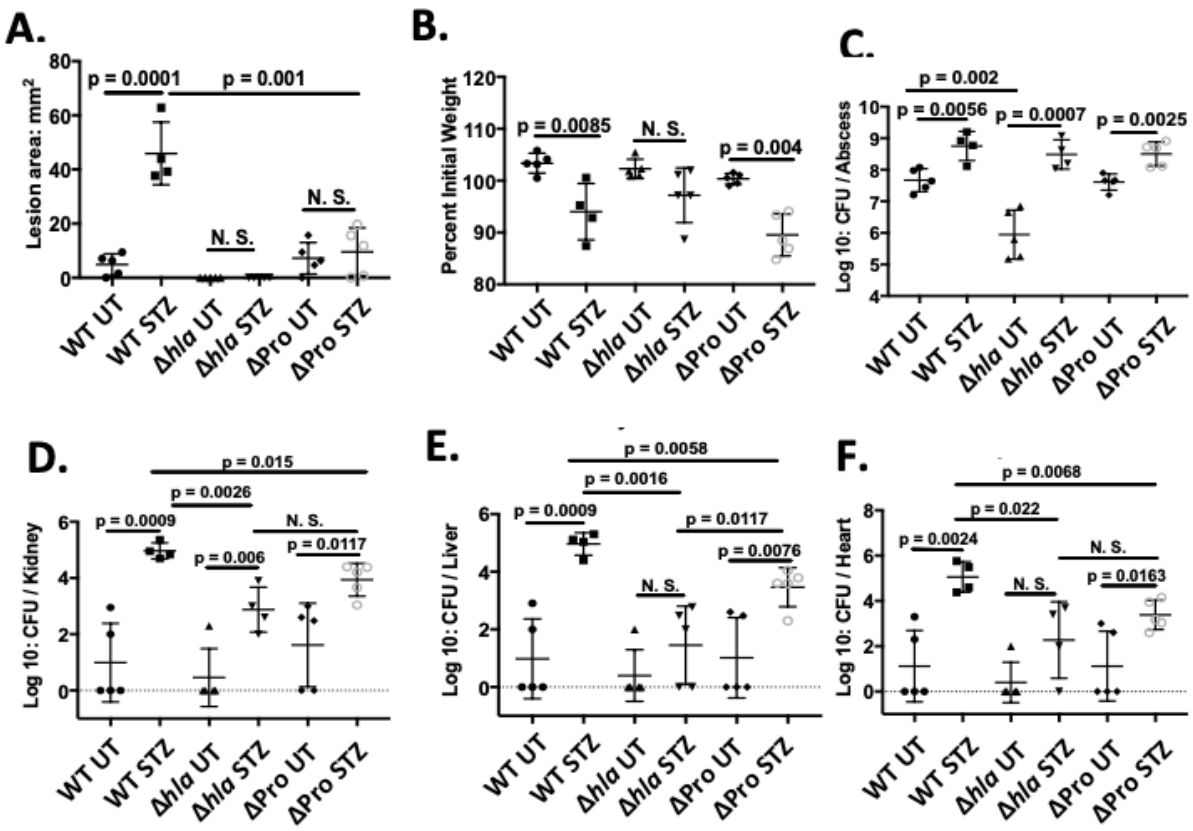

Figure 28: Proteases and α-hemolysin are still essential for invasive infections in hyperglycemic mice.

Untreated and STZ-treated mice were infected 10^7 WT, Δ*hla*, or ΔPro mutants (n=5 for all conditions). STZ-treated mice infected with WT LAC had significantly larger lesion sizes compared to all other infection combinations. Normal and hyperglycemic mice infected with LAC Δ*hla* did not have any lesions. Untreated mice infected with ΔPro had similar lesion sizes to untreated WT infected mice, but lesion sizes did not increase in hyperglycemic mice (A). STZ-treated mice infected with WT or ΔPro displayed increased weight loss compared to similarly infected untreated mice. STZ-treated mice infected with Δ*hla* did not display a significant difference in weight loss compared to similarly infected untreated animals (B). Untreated mice infected with WT had similar bacterial burdens to the same mice infected with ΔPro, but significantly higher abscess burdens than untreated mice infected with Δ*hla*. All STZ-treated mice had significantly higher abscess burdens than their untreated infected counterparts. There was no significant difference in abscess burdens between the hyperglycemic infected groups (C). STZ-treated mice infected with WT had significantly more bacterial dissemination to the kidneys than all other infection combinations (D). STZ-treated mice infected with Δ*hla* and ΔPro displayed significantly increased bacterial dissemination to kidneys

compared to similarly infected untreated mice. STZ-treated mice infected with WT had significantly more bacterial dissemination to the liver than all other infection combinations (D). STZ-treated mice infected with ΔPro displayed significantly increased bacterial dissemination to the liver compared to similarly infected untreated mice, but hyperglycemic mice infected with Δ*hla* did not (E). STZ-treated mice infected with WT had significantly more bacterial dissemination to the heart than all other infection combinations. STZ-treated mice infected with ΔPro displayed significantly increased bacterial dissemination to the heart compared to similarly infected untreated animals, but STZ-treated mice infected with Δ*hla* did not (F).

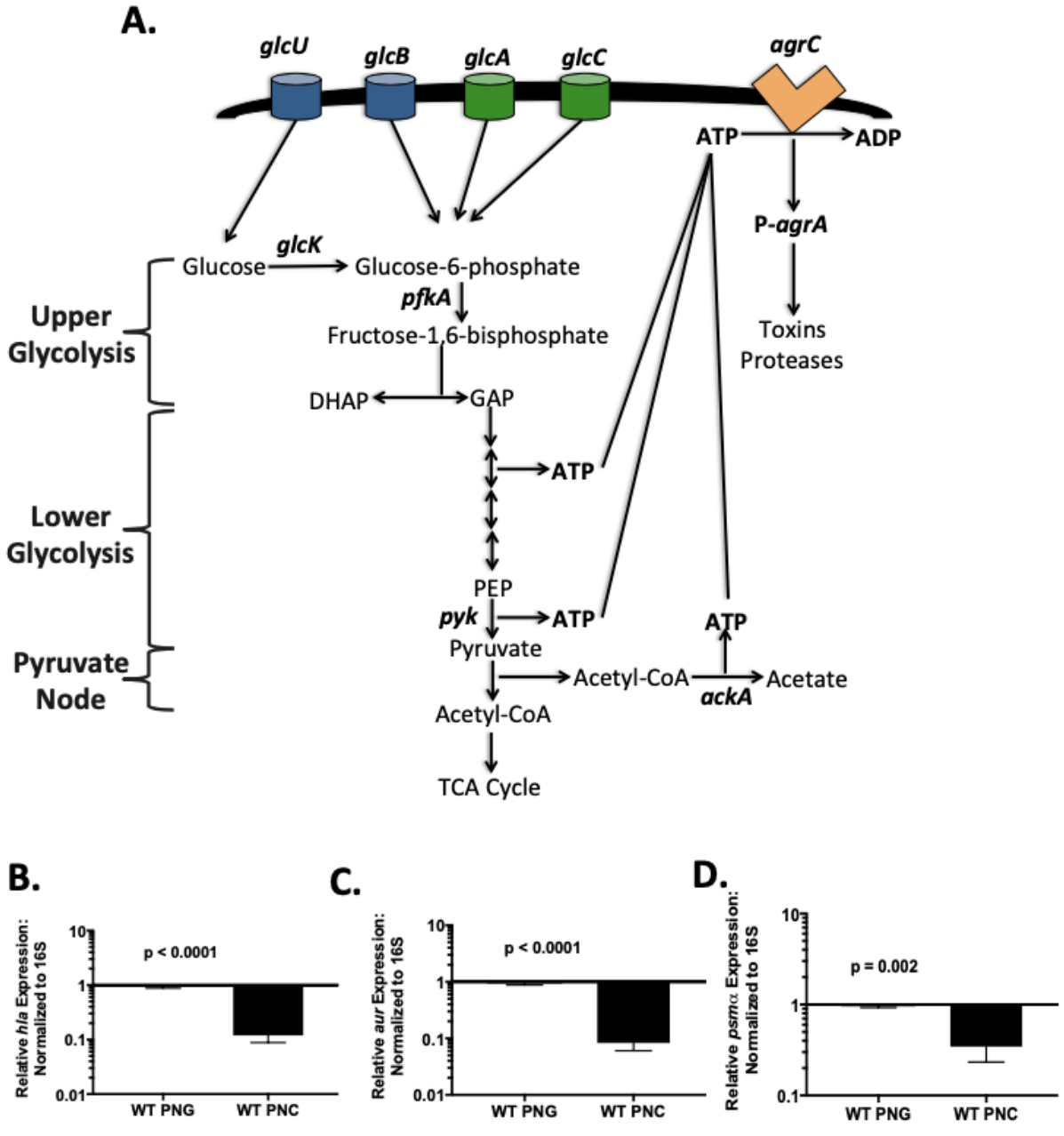

Figure 29: *S. aureus* requires glycolysis for ATP production, AgrC activation and virulence factor production. *S. aureus* imports glucose through the dedicated glucose transporters GlcB, GlcU, GlcA, and GlcC. Genes for *glcB* and *glcU* (blue) are ubiquitous among all Staphylococcal species, whereas, *glcA* and *glcC* (green) are only found in *S. aureus*. Deletions in the annotated glycolytic genes, *pfkA* and *pyk*, and the overflow metabolism gene *ackA* were used in this study. The sensor kinase, AgrC, has a unique ATP binding domain that requires high levels of intracellular ATP for full activity. In the presence of glucose, *S. aureus* will use glycolysis and overflow

metabolism to rapidly generate ATP to allow for full activation of the sensor kinase AgrC and subsequent phosphorylation of AgrA to induce transcription of several virulence factors (A). WT was grown (OD660 ≈ 5.0) in defined with glucose (PNG) or casamino acids (PNC) as a primary carbon source. Quantitative real-time PCR for α-hemolysin (*hla*), phenol soluble modulin-α (*psmα*), and aureolysin (*aur*) was performed on RNA isolated from a sample from the appropriate OD660. Our results show significantly less transcript of *hla* (B), *psmα* (C), and *aur* (D) in *S. aureus* grown in PNC compared to PNG (n=3).

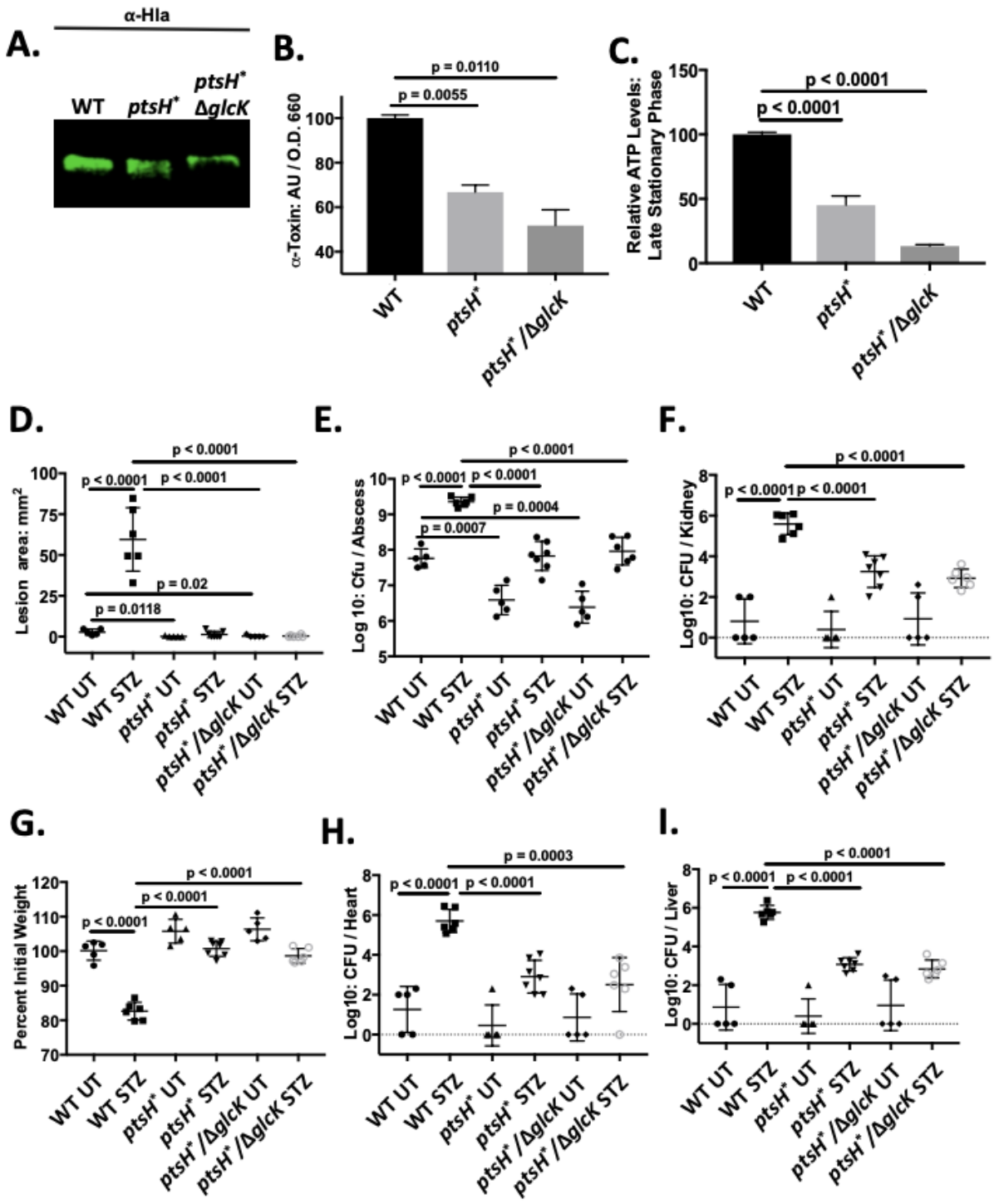

Figure 30: Sugar transport is essential for production of ATP and α-hemolysin and invasive infection. WT, ptsH-H15A (ptsH*), and ptsH-H15A/ΔglcK double mutant were grown in a chemically defined media (OD660 ≈ 5.0) with a combination of glucose and casamino acids as carbons sources. Spent supernatants were used for western

blot analysis, and an aliquot of bacteria were used for intracellular ATP analysis. Representative α-hemolysin western blot showing (from left to right) WT, ptsH*, and ptsH*/ΔglcK (A). Quantification of α-hemolysin western blots normalized to OD660 (n=3) shows decreased toxin in the supernatants of LAC ptsH* and ptsH*/ΔglcK compared to WT (B). The ptsH* and the ptsH*/ΔglcK mutants had diminished intracellular ATP compare to WT when normalize to OD660 (n=3) (C). Untreated and hyperglycemic mice were infected with 10^7 CFU of WT, ptsH*or ptsH*/ΔglcK (WT UT, n=5; WT STZ, n=6; ptsH* UT, n=5 ptsH* STZ, n=7; ptsH*/ΔglcK UT, n=5; ptsH*/ΔglcK STZ, n=6). STZ-tretaed mice infected with WT had significantly larger lesions (A), and displayed significantly more weight loss than all of the other infection combinations (G). Bacterial burdens in the abscess were significantly higher in untreated mice infected with WT compared to the ptsH* and ptsH*/ΔglcK (F). The bacterial burden in abscess in hyperglycemic mice infected with WT was significantly higher than all other infection combinations (F). STZ-treated mice infected with the ptsH* or ptsH*/ΔglcK had significantly higher abscess burdens than in similarly infected untreated mice (F). STZ-treated mice infected with WT had significantly increased bacterial dissemination to the kidneys (E), the liver (I), and the heart (H) than similarly treated mice infected with the ptsH* or ptsH*/ΔglcK.

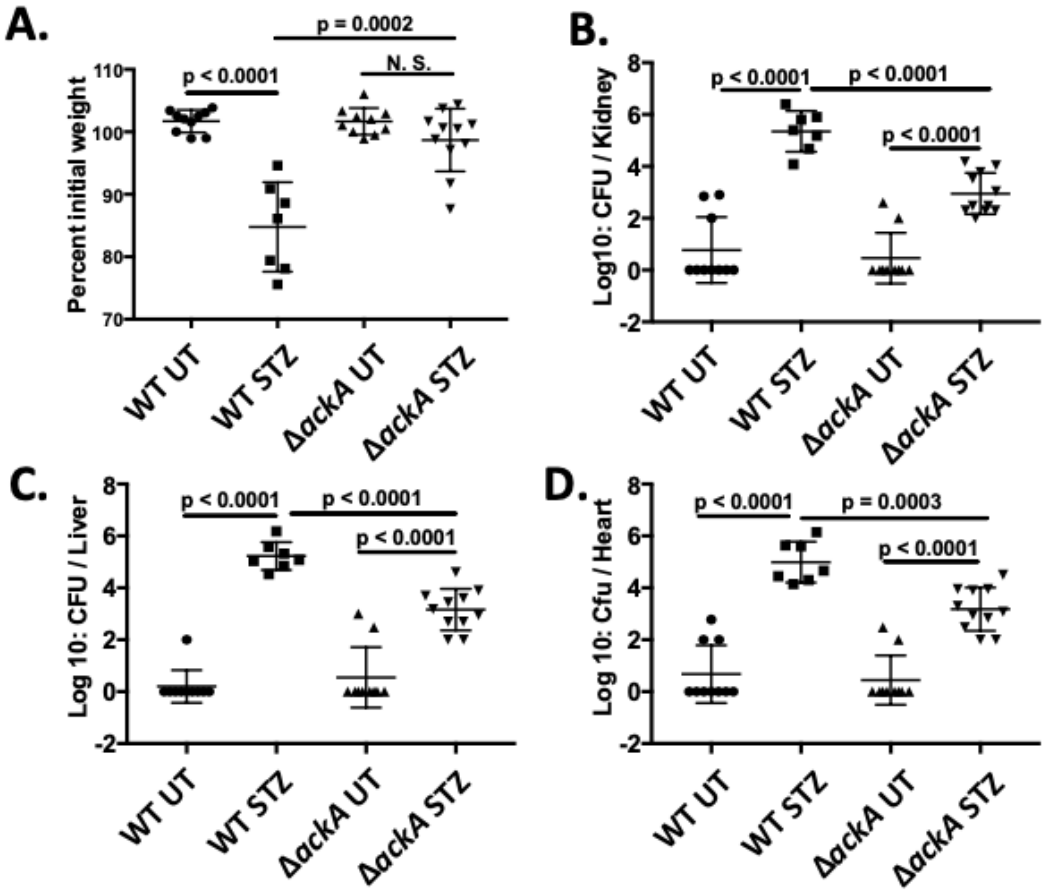

Figure 31: AckA is required for full virulence in hyperglycemic infections. Untreated and STZ-treated mice were infected with 10^7 CFU of WT Δ*ackA* (WT UT, n=10; WT STZ, n=7; Δ*ackA* UT, n=10; Δ*ackA* STZ, n=11). WT STZ mice display significant weight loss compared to WT UT and Δ*ackA* STZ (A). There is significantly more bacterial dissemination to the kidneys in hyperglycemic mice infected with WT and Δ*ackA* compared to their untreated counterparts (B). There is significantly increased dissemination to kidneys in hyperglycemic mice infected with WT compared to Δ*ackA* (B). There is significantly more bacterial dissemination to the liver in hyperglycemic mice infected with WT and Δ*ackA* compared to their untreated infected counterparts. There is significantly increased dissemination to the liver in dhyperglycemic mice infected with WT compared to Δ*ackA* (C). There is significantly more bacterial dissemination to the heart in hyperglycemic mice infected with WT and Δ*ackA* compared to their untreated infected counterparts. There is significantly increased dissemination to heart in hyperglycemic mice infected with WT compared to Δ*ackA* (D).

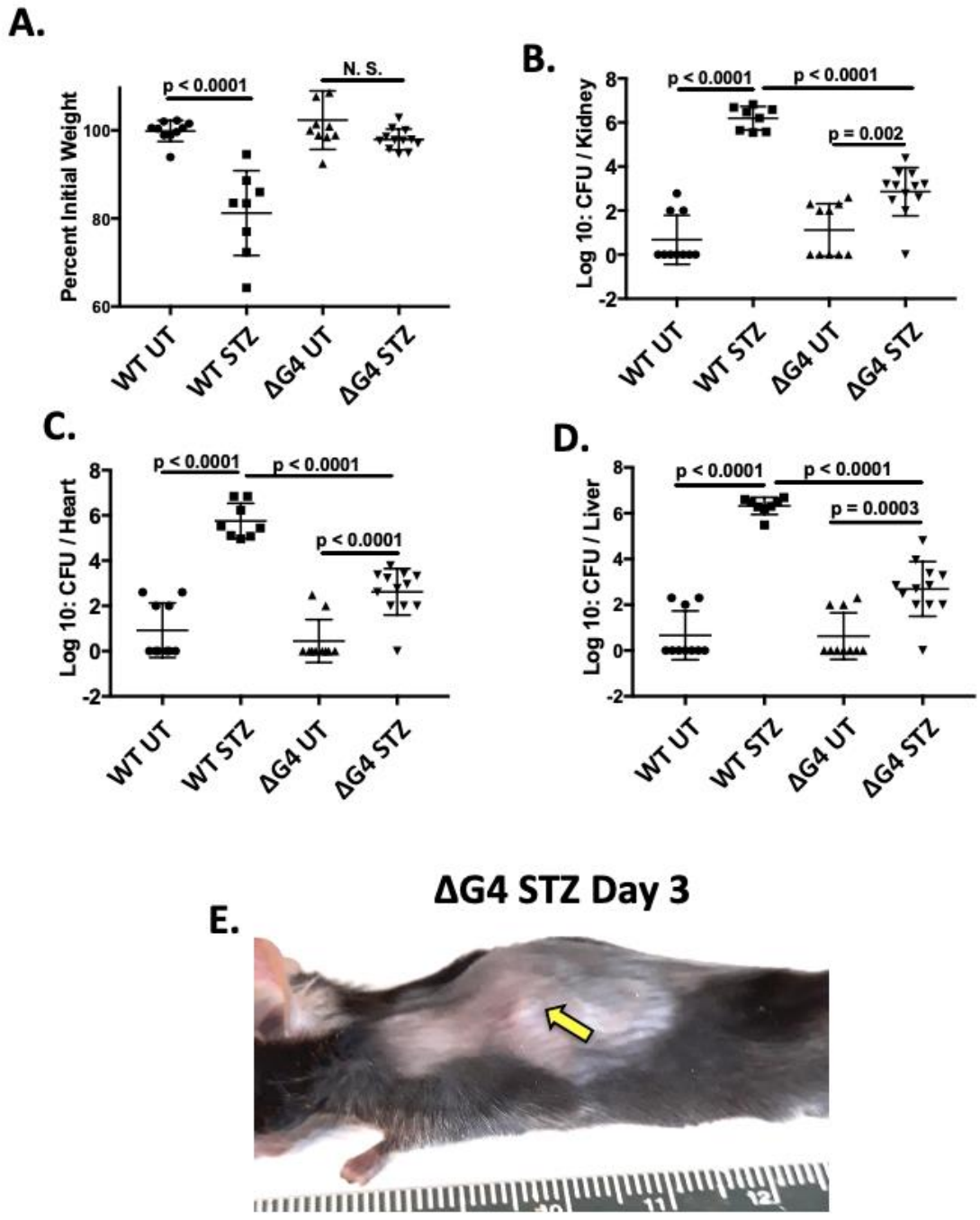

Figure 32: Glucose transporters are essential for invasive infections in hyperglycemic mice. Untreated and STZ-treated mice were infected with 10^7 CFU of WT or ΔG4 (WT UT, n=10; WT STZ, n=8; ΔG4 UT, n=10; ΔG4 STZ, n=12). Hyperglycemic mice infected with WT displayed significant weight loss compared with LAC ΔG4 UT (A). Hyperglycemic mice infected with WT and ΔG4 had significantly higher dissemination to the kidneys

compared to similarly infected untreated mice (B). Hyperglycemic mice infected with WT and ΔG4 had significantly increased bacterial dissemination to the liver compared to similarly infected normal mice (C). Hyperglycemic mice infected with WT and ΔG4 had significantly increased bacterial dissemination to the heart compared to similarly infected normal mice (D). A representative picture of a ΔG4 abscess (yellow arrow) three days after infection is comparable to a *ΔagrA* abscess at day three (Figure 32E) (E). Photo credit: Lance Thurlow, University of Pittsburgh.

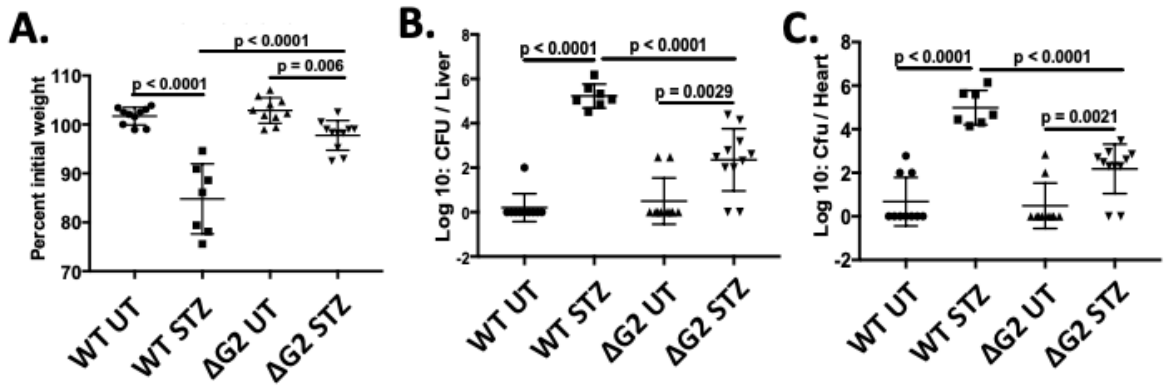

Figure 33: The glucose transporters unique to *S. aureus,* GlcA and GlcC, are essential for full virulence potential in hyperglycemic mice. Untreated and STZ-treated mice were infected with 10^7 CFU of WT or ΔG2 (WT UT, n=10; WT STZ, n=8; ΔG2 UT, n=10; ΔG2 STZ, n=11) and euthanized after seven days of infection. Hyperglycemic mice infected with WT displayed significant weight loss compared WT UT and ΔG2 UT, as well as hyperglycemic mice infected with ΔG2 (A). Hyperglycemic mice infected with WT had significantly increased bacterial dissemination to the liver and the heart compared to all other combinations (B and C). Hyperglycemic mice infected with ΔG2 had increased bacterial dissemination to the liver (B) and heart (C) compared to similarly infected untreated mice, but significantly less than WT infected hyperglycemic animals.

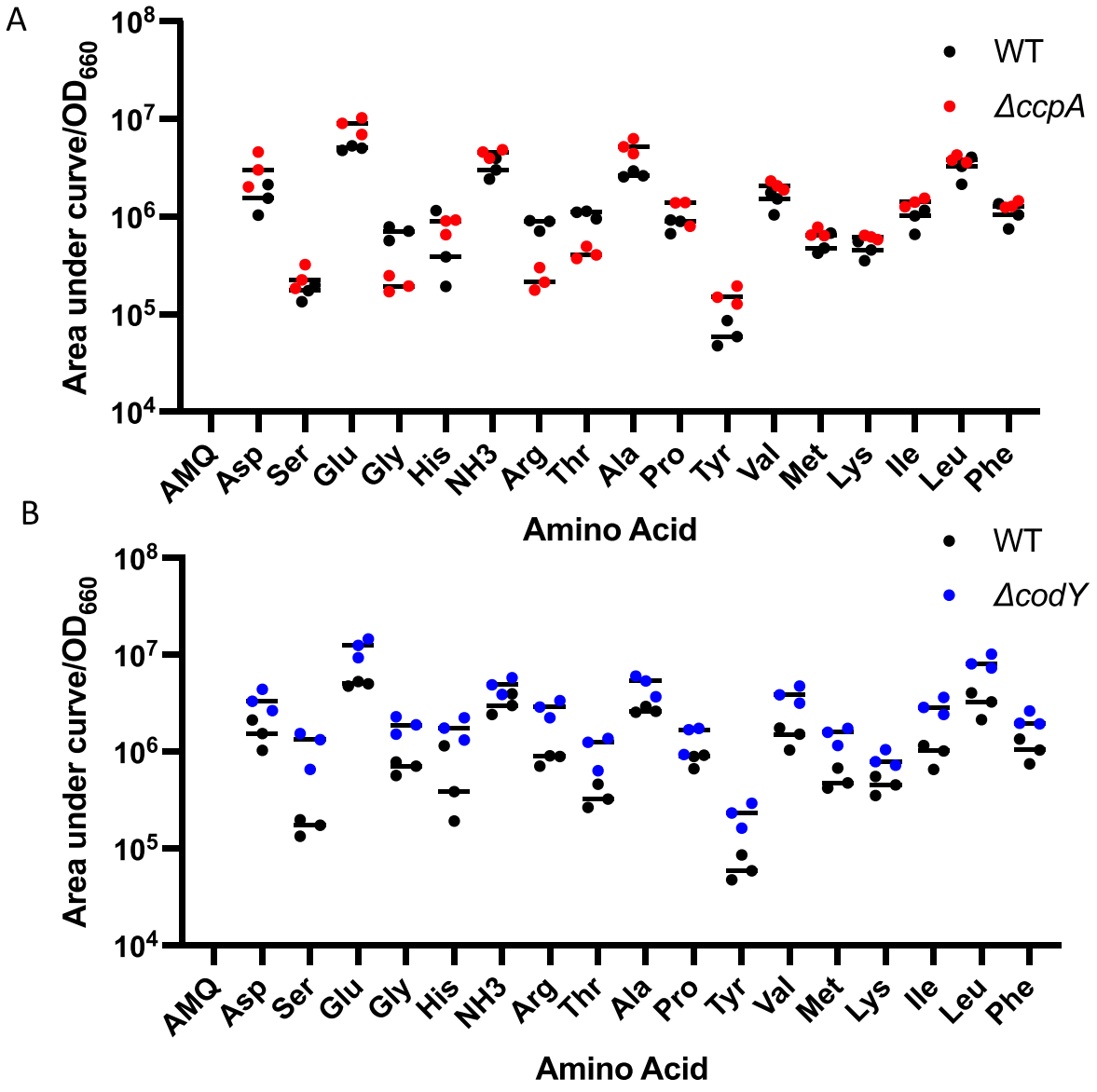

Figure 34: Analysis of intracellular amino acid levels in WT LAC, *ΔccpA* and *ΔcodY* mutants. A few amino acids (R, G and T) are under-represented in a *ΔccpA* strain (A) and all amino acids are significantly over-represented in a *ΔcodY* strain (B). Statistics: 2-way ANOVA with Sidak's multiple comparisons. Significance if $p < .05$

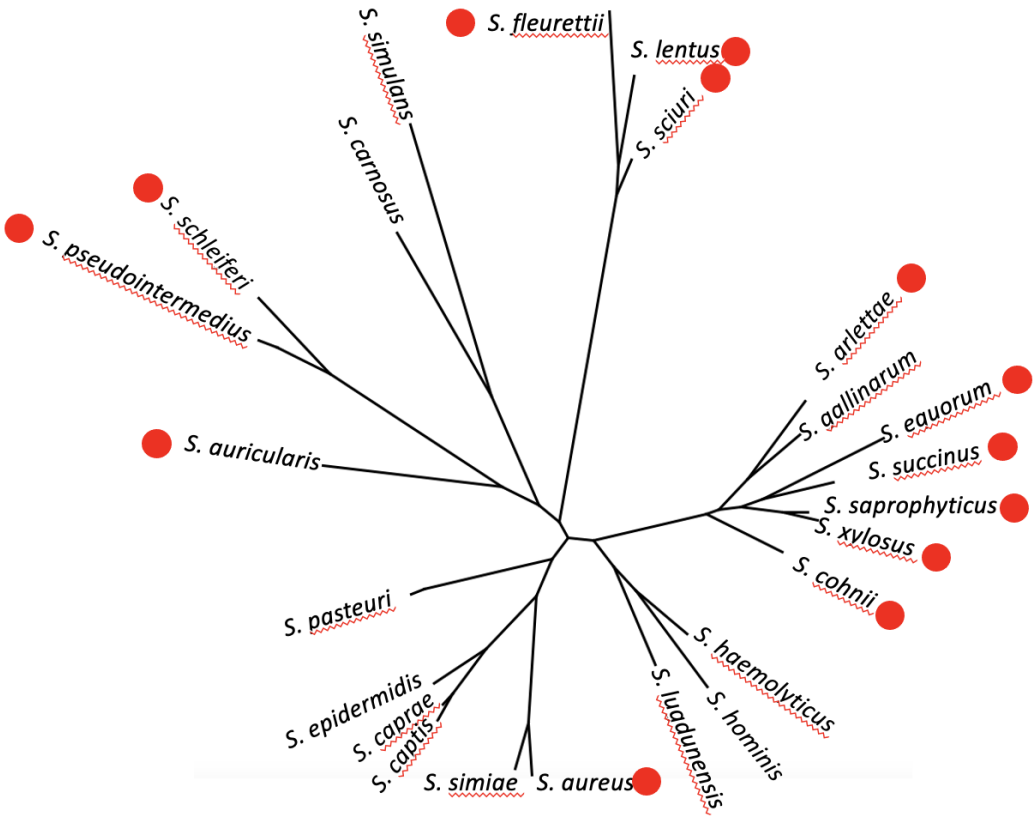

Figure 35: Phylogenetic tree of the staphylococcal species with *nptA*. Red dots denote species with an *nptA* homolog. *S. aureus* uniquely holds an *nptA* homolog among its most closely related cousins.

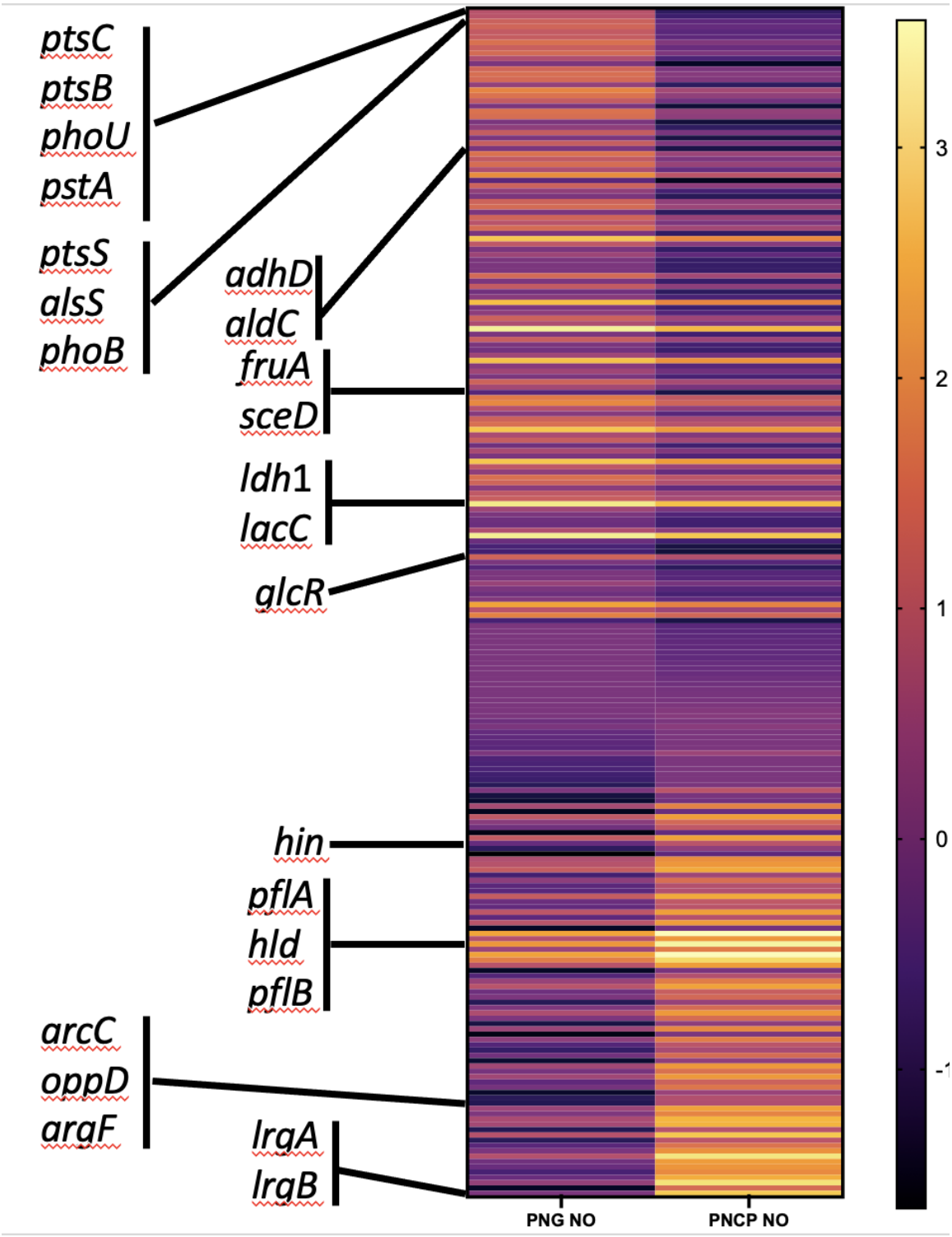

Figure 36: PNG NO to PNCP NO comparison heat map. All genes differentially expressed (with a RPKM value more than two standard deviations removed from the average) between PNG NO and PNCP NO. The genes induced by NO from Figure 1A are noted.

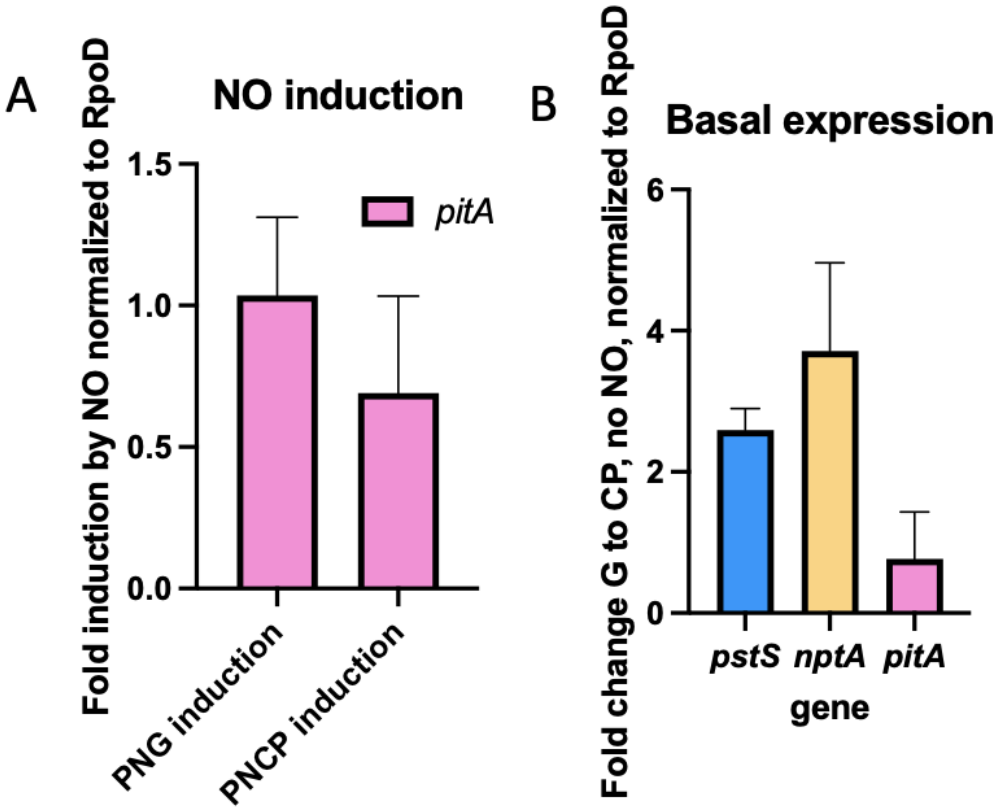

Figure 37: Expression of phosphate transporters. Q-RT-PCR was used to determine the expression of the three phosphate transporters with and without NO stress. (A) Induction of *pitA* by NO. *pitA* expression is unaffected by NO. (B) The fold change of each phosphate transporter from CDM + CP to CDM + G. *pstS* and *nptA* are ~2.5 and ~5 fold more highly expressed in CDM + G, respectively. *pitA* expression is unaffected by carbon source.

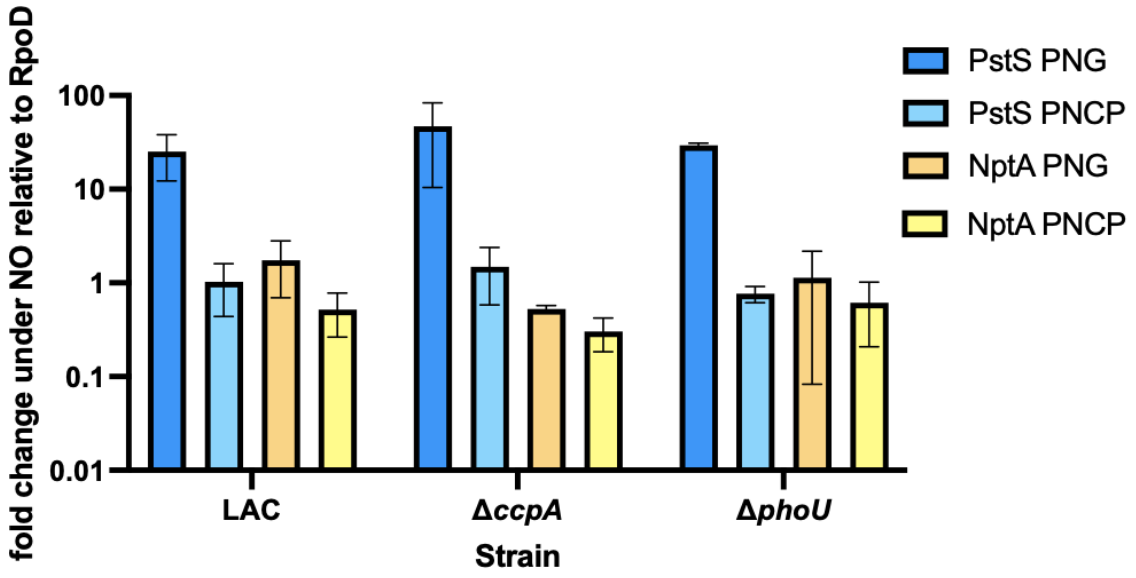

Figure 38: CcpA and PhoU do not regulate *pstS* or *nptA* expression. Q-RT-PCR was used to determine the induction of *pstS* and *nptA* in a *ΔccpA* and a *ΔphoU* background under NO stress. There were no significant differences in expression found between backgrounds.

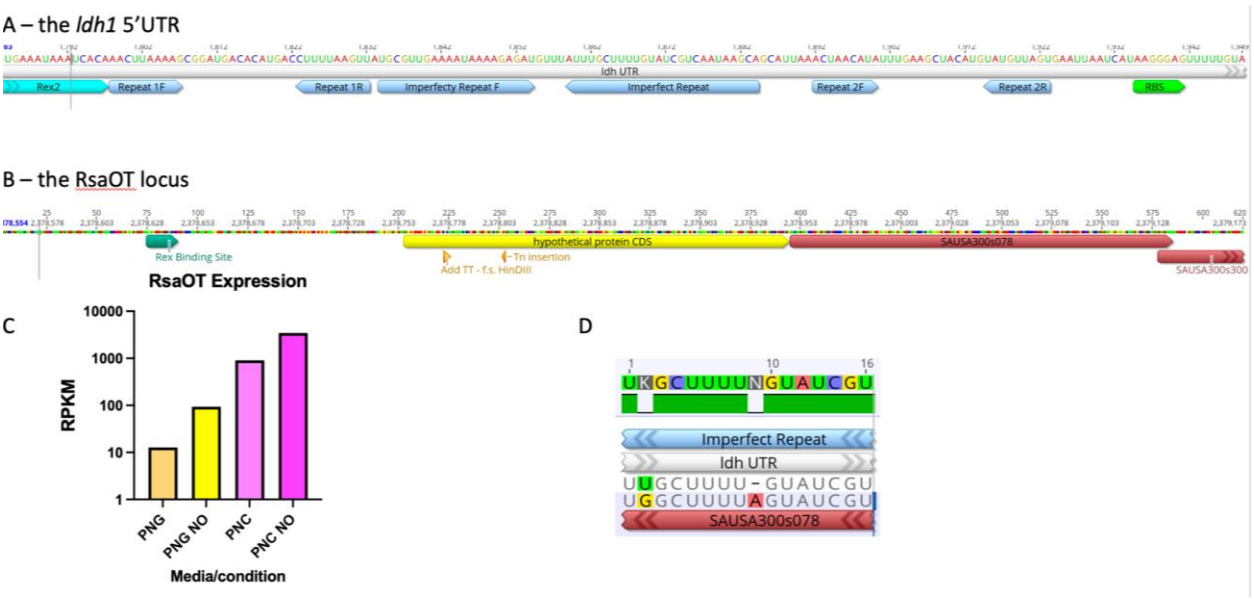

Figure 39: The RsaOT locus and the 5' UTR of *ldh1*. (A) the 5'UTR of *ldh1*, annotated with Rex and ribosome binding sites, as well as hypothesized stem-loops. (B) the SACOL2491-RsaOT locus, annotated with Rex binding sites, as well as the Tn insertion and frameshift locations. (C) Data from RNA-Seq as presented in Chapter 4 showing that RsaOT is more highly expressed in PNCP conditions than PNG, and it is induced by NO. (D) the hypothetical alignment of RsaOT and the *ldh1* 5' UTR.

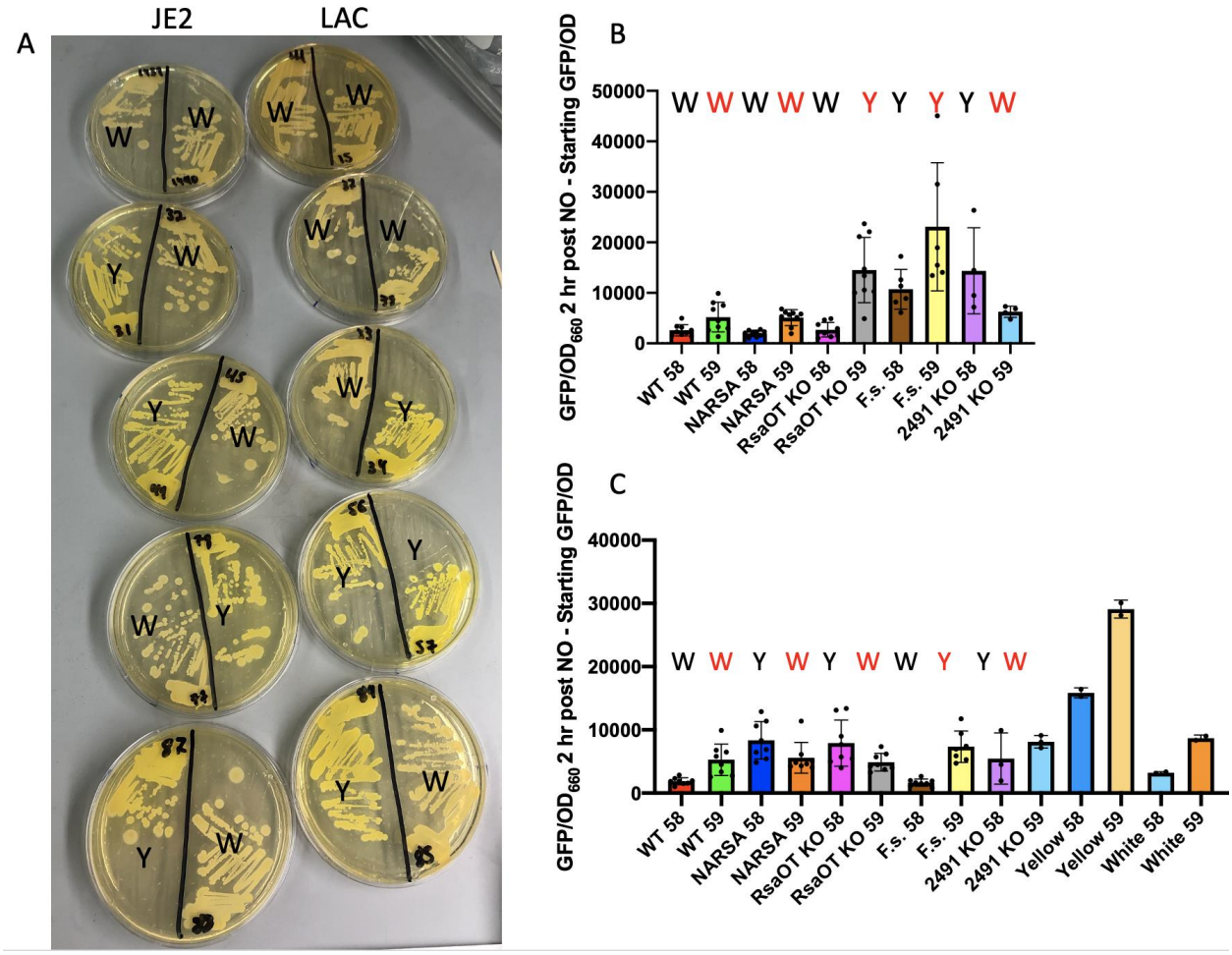

Figure 40: The reporter plasmid is prone to copy number mutations. The original strains used for the *rsaOT* experiments. (A) photographs of aged plates containing streaks of LAC and JE2 *rsaOT* mutants harboring the p*ldh1::*GFP plasmid. Plates are marked with a W for white or a Y for yellow, depending on the appearance of the strains. Photo credit: Amelia Stephens, University of Pittsburgh. (B) Original LAC *rsaOT* mutants harboring the p*ldh1*::GFP plasmid with or without the UTR. Graph shows GFP induction 2 hours post-NO. If colonies appeared yellow or white is marked. (C) Original JE2 *rsaOT* mutants harboring the p*ldh1*::GFP plasmid with or without the UTR. Graph shows GFP induction 2 hours post-NO. If colonies appeared yellow or white is marked. The final columns are yellow and white colonies with and without the UTR.

Appendix B Copyright Permissions

Chapters 2 and 3 were previously published and are presented herein in a modified form under the Creative Commons BY license *(Adv. Microbial physiology, Science Advances, Microbiology Spectrum):*

L. R. Thurlow, A. C. Stephens, K. E. Hurley, A. R. Richardson, Lack of nutritional immunity in diabetic skin infections promotes Staphylococcus aureus virulence. *Sci. Adv.* **6** (2020), doi:10.1126/sciadv.abc5569.

A. C. Stephens, L. R. Thurlow, A. R. Richardson, Mechanisms Behind the Indirect Impact of Metabolic Regulators on Virulence Factor Production in Staphylococcus aureus. *Microbiol. Spectr.*, e0206322 (2022)

Appendix C Abbreviations

ACME – Arginine catabolic mobile element

Agr – Accessory gene regulatory system

AIP – autoinducing peptide

AMPs – antimicrobial peptides

ANOVA – Analysis of variance

ATCC – American Type Culture Collection

ATP – adenosine 5'-triphosphate

ATRA – All-trans retinoic acid

BCAAs – Branched chain amino acids

BHI – brain-hear infusion broth

C – Celsius

CA – community acquired

CC – clonal complexes

CCR – carbon catabolite repression

CDM – Chemically defined media

cDNA – complementary DNA

CFE – cell-free extract

CFU – colony forming unit

CO_2 – carbon dioxide

CoNS – Coagulase negative Staphylococci

Cp – calprotectin

CWA – cell wall anchored proteins

DETA-NO – Diethylenetriamine/nitric oxide adduct

DHR – Dihydrorhodamine 123

dL – deciliters

DNA – deoxyribonucleic acid

ECM – extracellular matrix

ETC – electron transport chain

f.s. – frameshift

FBP – fructose 1,6-bisphosphate

FBS – Fetal Bovine Serum

GAP – glyceraldehyde-3-phosphate

GAPDH – glyceraldehyde-3-phosphate dehydrogenase

GFP – green fluorescent protein

GTP – guanine 5'-triphosphate

HA – hospital acquired

HEPES – 4-(2-hydroxyethyl)-1-piperazineethanesulfonic acid buffer

Hif-1α – Hypoxia inducible factor-1-alpha

HK – histidine kinase

Hla – alpha-hemolysin

HPLC – high performance liquid chromatography

IACUC – Institutional Animal Care and Use Committee

IE – infective endocarditis

IFNγ – Interferon gamma

IHC – Immunohistochemistry

IL-1β – Interleukin-1-beta

IMDM – Iscove's Modified Dulbecco's Media

iNOS – inducible nitric oxide synthase

KO – knockout

L-NIL – An inhibitor of iNOS

LPS – lipopolysaccharide

MLST – multi-locus sequence typing

mL – milliliters

mM – millimolar

mm – millimeters

MRSA – Methicillin resistant *S. aureus*

MSCRAMMs – Microbial Surface Components Recognizing Adhesive Matrix Molecules

MSSA – Methicillin sensitive *S. aureus*

NADH/NAD+ – Nicotinamide adenine dinucleotide

NARSA – Network on Antimicrobial Research in *Staphylococcus aureus*

ncRNA – non-coding RNA

ng – nanograms

NO – nitric oxide

NTML – Nebraska Transposon Mutant Library

OD – optical density

OD_{660} – optical density at 660

PBS – Phosphate buffered saline

PFGE – pulsed-field gel electrophoresis

Phlo – Phlorizin

PN media – Pattee/Neveln media, a CDM first described in 1975 in (*308*)

PNCAA – PN with casamino acids

PNG – PN with glucose

PSMs – phenol soluble modulins

PTS – phosphotransferase system

PVL – Panton-Valentine leukotoxin

RBCs – red blood cells

RNA – ribonucleic acid

RNS – reactive nitrogen species

ROS – reactive oxygen species

RPKM – reads per kilobase per million reads

RPMI – Roswell Park Memorial Institute 1640 media

RR – response regulator

RT-PCR – Real-time polymerase chain reaction

S. aureus – *Staphylococcus aureus*

SAgs – superantigens

SCC – Staphylococcal Chromosomal Cassette

SNPs – single nucleotide polymorphisms

SpA – Staphylococcal protein A

sRNA – small RNA

SSTIs – Skin and soft tissue infections

ST – sequence type

STZ – streptozotocin

TCA – tricarboxylic acid cycle

TCS – Two-component system

TE – Tris-EDTA buffer

TSB – tryptic soy broth

TSS – toxic shock syndrome

uL – microliters

uM – micromolar

USA – a PFGE based classification system for MRSA. Usually followed by 100-1200.

UT – untreated

UTR – untranslated region

WT – Wild-type

YFP – yellow fluorescent protein

ΔG2 – *S. aureus* mutant lacking *glcA* and *glcC*

ΔG4 – *S. aureus* mutant lacking all 4 glucose transporters

5’ RACE – Rapid amplification of cDNA ends

Bibliography

1. A. Ogston, Micrococcus Poisoning. *J. Anat. Physiol.* **16**, 526–567 (1882).

2. F. D. Lowy, Staphylococcus aureus infections. *N. Engl. J. Med.* **339**, 520–532 (1998).

3. T. A. Taylor, C. G. Unakal, in *StatPearls* (StatPearls Publishing, Treasure Island (FL), 2022).

4. C. Vuong, M. Otto, Staphylococcus epidermidis infections. *Microbes Infect.* **4**, 481–489 (2002).

5. A. Sakr, F. Brégeon, J.-L. Mège, J.-M. Rolain, O. Blin, Staphylococcus aureus Nasal Colonization: An Update on Mechanisms, Epidemiology, Risk Factors, and Subsequent Infections. *Front. Microbiol.* **9**, 2419 (2018).

6. R. A. Proctor, Have We Outlived the Concept of Commensalism for Staphylococcus aureus? *Clin. Infect. Dis.* **73**, e267–e269 (2021).

7. R. M. Klevens, J. R. Edwards, C. L. Richards, T. C. Horan, R. P. Gaynes, D. A. Pollock, D. M. Cardo, Estimating health care-associated infections and deaths in U.S. hospitals, 2002. *Public Health Rep.* **122**, 160–166 (2007).

8. S. Y. C. Tong, J. S. Davis, E. Eichenberger, T. L. Holland, V. G. Fowler, *Staphylococcus aureus* infections: epidemiology, pathophysiology, clinical manifestations, and management. *Clin. Microbiol. Rev.* **28**, 603–661 (2015).

9. J. Jneid, N. Cassir, S. Schuldiner, N. Jourdan, A. Sotto, J.-P. Lavigne, B. La Scola, Exploring the microbiota of diabetic foot infections with culturomics. *Front. Cell. Infect. Microbiol.* **8**, 282 (2018).

10. A. Y. Peleg, T. Weerarathna, J. S. McCarthy, T. M. E. Davis, Common infections in diabetes: pathogenesis, management and relationship to glycaemic control. *Diabetes Metab. Res. Rev.* **23**, 3–13 (2007).

11. E. Morgan, S. Hohmann, J. P. Ridgway, R. S. Daum, M. Z. David, Decreasing Incidence of Skin and Soft-tissue Infections in 86 US Emergency Departments, 2009-2014. *Clin. Infect. Dis.* **68**, 453–459 (2019).

12. G. T. Ray, J. A. Suaya, R. Baxter, Trends and characteristics of culture-confirmed Staphylococcus aureus infections in a large U.S. integrated health care organization. *J. Clin. Microbiol.* **50**, 1950–1957 (2012).

13. G. T. Ray, J. A. Suaya, R. Baxter, Incidence, microbiology, and patient characteristics of skin and soft-tissue infections in a U.S. population: a retrospective population-based study. *BMC Infect. Dis.* **13**, 252 (2013).

14. J. A. Casey, S. E. Cosgrove, W. F. Stewart, J. Pollak, B. S. Schwartz, A population-based study of the epidemiology and clinical features of methicillin-resistant Staphylococcus aureus infection in Pennsylvania, 2001-2010. *Epidemiol. Infect.* **141**, 1166–1179 (2013).

15. L. G. Miller, D. F. Eisenberg, H. Liu, C.-L. Chang, Y. Wang, R. Luthra, A. Wallace, C. Fang, J. Singer, J. A. Suaya, Incidence of skin and soft tissue infections in ambulatory and inpatient settings, 2005-2010. *BMC Infect. Dis.* **15**, 362 (2015).

16. D. M. Sievert, P. Ricks, J. R. Edwards, A. Schneider, J. Patel, A. Srinivasan, A. Kallen, B. Limbago, S. Fridkin, National Healthcare Safety Network (NHSN) Team and Participating NHSN Facilities, Antimicrobial-resistant pathogens associated with healthcare-associated infections: summary of data reported to the National Healthcare Safety Network at the Centers for Disease Control and Prevention, 2009-2010. *Infect. Control Hosp. Epidemiol.* **34**, 1–14 (2013).

17. J. A. Suaya, R. M. Mera, A. Cassidy, P. O'Hara, H. Amrine-Madsen, S. Burstin, L. G. Miller, Incidence and cost of hospitalizations associated with Staphylococcus aureus skin and soft tissue infections in the United States from 2001 through 2009. *BMC Infect. Dis.* **14**, 296 (2014).

18. G. C. Lee, N. K. Boyd, K. A. Lawson, C. R. Frei, Incidence and Cost of Skin and soft Tissue Infections In the united States. *Value Health*. **18**, A245 (2015).

19. K. S. Kaye, L. A. Petty, A. F. Shorr, M. D. Zilberberg, Current epidemiology, etiology, and burden of acute skin infections in the united states. *Clin. Infect. Dis.* **68**, S193–S199 (2019).

20. Y. Golan, Current Treatment Options for Acute Skin and Skin-structure Infections. *Clin. Infect. Dis.* **68**, S206–S212 (2019).

21. E. Y. Klein, W. Jiang, N. Mojica, K. K. Tseng, R. McNeill, S. E. Cosgrove, T. M. Perl, National Costs Associated With Methicillin-Susceptible and Methicillin-Resistant Staphylococcus aureus Hospitalizations in the United States, 2010-2014. *Clin. Infect. Dis.* **68**, 22–28 (2019).

22. Centers for Disease Control, "Antibiotic Resistance Threats in the United States (2019 AR Threats Report)" (U.S. Department of Health and Human Services, CDC, 2019).

23. J. M. Kwiecinski, A. R. Horswill, Staphylococcus aureus bloodstream infections: pathogenesis and regulatory mechanisms. *Curr. Opin. Microbiol.* **53**, 51–60 (2020).

24. H. Asgeirsson, A. Thalme, O. Weiland, Staphylococcus aureus bacteraemia and endocarditis - epidemiology and outcome: a review. *Infect Dis (Lond)*. **50**, 175–192 (2018).

25. L. Thorlacius-Ussing, H. Sandholdt, A. R. Larsen, A. Petersen, T. Benfield, Age-Dependent Increase in Incidence of Staphylococcus aureus Bacteremia, Denmark, 2008-2015. *Emerging Infect. Dis.* **25** (2019), doi:10.3201/eid2505.181733.

26. M. Souli, F. Ruffin, S.-H. Choi, L. P. Park, S. Gao, N. C. Lent, B. K. Sharma-Kuinkel, J. T. Thaden, S. A. Maskarinec, L. Wanda, J. Hill-Rorie, B. Warren, B. Hansen, V. G. Fowler, Changing Characteristics of Staphylococcus aureus Bacteremia: Results From a 21-Year, Prospective, Longitudinal Study. *Clin. Infect. Dis.* **69**, 1868–1877 (2019).

27. K. Inagaki, J. Lucar, C. Blackshear, C. V. Hobbs, Methicillin-susceptible and methicillin-resistant *Staphylococcus aureus* bacteremia: nationwide estimates of 30-day readmission, in-hospital mortality, length of stay, and cost in the United States. *Clin. Infect. Dis.* **69**, 2112–2118 (2019).

28. E. Minejima, N. Mai, N. Bui, M. Mert, W. J. Mack, R. C. She, P. Nieberg, B. Spellberg, A. Wong-Beringer, Defining the Breakpoint Duration of Staphylococcus aureus Bacteremia Predictive of Poor Outcomes. *Clin. Infect. Dis.* **70**, 566–573 (2020).

29. J. C. Lam, D. B. Gregson, S. Robinson, R. Somayaji, J. M. Conly, M. D. Parkins, Epidemiology and Outcome Determinants of Staphylococcus aureus Bacteremia Revisited: A Population-Based Study. *Infection*. **47**, 961–971 (2019).

30. A. D. Bai, C. K. L. Lo, A. S. Komorowski, M. Suresh, K. Guo, A. Garg, P. Tandon, J. Senecal, O. Del Corpo, I. Stefanova, C. Fogarty, G. Butler-Laporte, E. G. McDonald, M. P. Cheng, A. M. Morris, M. Loeb, T. C. Lee, Staphylococcus aureus bacteraemia mortality: a systematic review and meta-analysis. *Clin. Microbiol. Infect.* **28**, 1076–1084 (2022).

31. G. Cooper, R. Platt, Staphylococcus aureus bacteremia in diabetic patients. *Am. J. Med.* **73**, 658–662 (1982).

32. R. Rajani, J. L. Klein, Infective endocarditis: A contemporary update. *Clin. Med.* **20**, 31–35 (2020).

33. T. L. Holland, L. M. Baddour, A. S. Bayer, B. Hoen, J. M. Miro, V. G. Fowler, Infective endocarditis. *Nat. Rev. Dis. Primers*. **2**, 16059 (2016).

34. L. L. Vincent, C. M. Otto, Infective endocarditis: update on epidemiology, outcomes, and management. *Curr. Cardiol. Rep.* **20**, 86 (2018).

35. S. A. Hubers, D. C. DeSimone, B. J. Gersh, N. S. Anavekar, Infective endocarditis: A contemporary review. *Mayo Clin. Proc.* **95**, 982–997 (2020).

36. S. Pant, N. J. Patel, A. Deshmukh, H. Golwala, N. Patel, A. Badheka, G. A. Hirsch, J. L. Mehta, Trends in infective endocarditis incidence, microbiology, and valve replacement in the United States from 2000 to 2011. *J. Am. Coll. Cardiol.* **65**, 2070–2076 (2015).

37. N. Benito, J. M. Miró, E. de Lazzari, C. H. Cabell, A. del Río, J. Altclas, P. Commerford, F. Delahaye, S. Dragulescu, H. Giamarellou, G. Habib, A. Kamarulzaman, A. S. Kumar,

F. M. Nacinovich, F. Suter, C. Tribouilloy, K. Venugopal, A. Moreno, V. G. Fowler, ICE-PCS (International Collaboration on Endocarditis Prospective Cohort Study) Investigators, Health care-associated native valve endocarditis: importance of non-nosocomial acquisition. *Ann. Intern. Med.* **150**, 586–594 (2009).

38. A. S. V. Shah, D. A. McAllister, P. Gallacher, F. Astengo, J. A. Rodríguez Pérez, J. Hall, K. K. Lee, R. Bing, A. Anand, D. Nathwani, N. L. Mills, D. E. Newby, C. Marwick, N. L. Cruden, Incidence, microbiology, and outcomes in patients hospitalized with infective endocarditis. *Circulation*. **141**, 2067–2077 (2020).

39. V. Hoerr, M. Franz, M. W. Pletz, M. Diab, S. Niemann, C. Faber, T. Doenst, P. C. Schulze, S. Deinhardt-Emmer, B. Löffler, S. aureus endocarditis: Clinical aspects and experimental approaches. *Int. J. Med. Microbiol.* **308**, 640–652 (2018).

40. M. Dudareva, A. J. Hotchen, J. Ferguson, S. Hodgson, M. Scarborough, B. L. Atkins, M. A. McNally, The microbiology of chronic osteomyelitis: Changes over ten years. *J. Infect.* **79**, 189–198 (2019).

41. K. L. Urish, J. E. Cassat, Staphylococcus aureus Osteomyelitis: Bone, Bugs, and Surgery. *Infect. Immun.* **88** (2020), doi:10.1128/IAI.00932-19.

42. L. Giurato, M. Meloni, V. Izzo, L. Uccioli, Osteomyelitis in diabetic foot: A comprehensive overview. *World J. Diabetes*. **8**, 135–142 (2017).

43. M. I. Hofstee, G. Muthukrishnan, G. J. Atkins, M. Riool, K. Thompson, M. Morgenstern, M. J. Stoddart, R. G. Richards, S. A. J. Zaat, T. F. Moriarty, Current concepts of osteomyelitis: from pathologic mechanisms to advanced research methods. *Am. J. Pathol.* **190**, 1151–1163 (2020).

44. C. I. Pickens, R. G. Wunderink, Methicillin-Resistant Staphylococcus aureus Hospital-Acquired Pneumonia/Ventilator-Associated Pneumonia. *Semin. Respir. Crit. Care Med.* **43**, 304–309 (2022).

45. H. He, R. G. Wunderink, Staphylococcus aureus Pneumonia in the Community. *Semin. Respir. Crit. Care Med.* **41**, 470–479 (2020).

46. S.-S. Jean, Y.-C. Chang, W.-C. Lin, W.-S. Lee, P.-R. Hsueh, C.-W. Hsu, Epidemiology, treatment, and prevention of nosocomial bacterial pneumonia. *J. Clin. Med.* **9** (2020), doi:10.3390/jcm9010275.

47. M. Bassetti, L. Labate, M. Melchio, C. Robba, D. Battaglini, L. Ball, P. Pelosi, D. R. Giacobbe, Current pharmacotherapy for methicillin-resistant Staphylococcus aureus (MRSA) pneumonia. *Expert Opin. Pharmacother.* **23**, 361–375 (2022).

48. J. Liu, D. Chen, B. M. Peters, L. Li, B. Li, Z. Xu, M. E. Shirliff, Staphylococcal chromosomal cassettes *mec* (SCCm*ec*): a mobile genetic element in methicillin-resistant *Staphylococcus aureus*. *Microb. Pathog.* **101**, 56–67 (2016).

49. International Working Group on the Classification of Staphylococcal Cassette Chromosome Elements (IWG-SCC), Classification of staphylococcal cassette chromosome mec (SCCmec): guidelines for reporting novel SCCmec elements. *Antimicrob. Agents Chemother.* **53**, 4961–4967 (2009).

50. M. C. Enright, N. P. Day, C. E. Davies, S. J. Peacock, B. G. Spratt, Multilocus sequence typing for characterization of methicillin-resistant and methicillin-susceptible clones of Staphylococcus aureus. *J. Clin. Microbiol.* **38**, 1008–1015 (2000).

51. M. C. Enright, D. A. Robinson, G. Randle, E. J. Feil, H. Grundmann, B. G. Spratt, The evolutionary history of methicillin-resistant Staphylococcus aureus (MRSA). *Proc Natl Acad Sci USA.* **99**, 7687–7692 (2002).

52. L. K. McDougal, C. D. Steward, G. E. Killgore, J. M. Chaitram, S. K. McAllister, F. C. Tenover, Pulsed-field gel electrophoresis typing of oxacillin-resistant Staphylococcus aureus isolates from the United States: establishing a national database. *J. Clin. Microbiol.* **41**, 5113–5120 (2003).

53. M. Z. David, R. S. Daum, Community-associated methicillin-resistant Staphylococcus aureus: epidemiology and clinical consequences of an emerging epidemic. *Clin. Microbiol. Rev.* **23**, 616–687 (2010).

54. L. R. Thurlow, G. S. Joshi, A. R. Richardson, Virulence strategies of the dominant USA300 lineage of community-associated methicillin-resistant Staphylococcus aureus (CA-MRSA). *FEMS Immunol. Med. Microbiol.* **65**, 5–22 (2012).

55. R. J. Gorwitz, A review of community-associated methicillin-resistant Staphylococcus aureus skin and soft tissue infections. *Pediatr. Infect. Dis. J.* **27**, 1–7 (2008).

56. B. A. Diep, S. R. Gill, R. F. Chang, T. H. Phan, J. H. Chen, M. G. Davidson, F. Lin, J. Lin, H. A. Carleton, E. F. Mongodin, G. F. Sensabaugh, F. Perdreau-Remington, Complete genome sequence of USA300, an epidemic clone of community-acquired meticillin-resistant Staphylococcus aureus. *Lancet*. **367**, 731–739 (2006).

57. J. K. Johnson, T. Khoie, S. Shurland, K. Kreisel, O. C. Stine, M.-C. Roghmann, Skin and soft tissue infections caused by methicillin-resistant Staphylococcus aureus USA300 clone. *Emerging Infect. Dis.* **13**, 1195–1200 (2007).

58. C. Burlak, C. H. Hammer, M.-A. Robinson, A. R. Whitney, M. J. McGavin, B. N. Kreiswirth, F. R. Deleo, Global analysis of community-associated methicillin-resistant Staphylococcus aureus exoproteins reveals molecules produced in vitro and during infection. *Cell. Microbiol.* **9**, 1172–1190 (2007).

59. C. P. Montgomery, S. Boyle-Vavra, P. V. Adem, J. C. Lee, A. N. Husain, J. Clasen, R. S. Daum, Comparison of virulence in community-associated methicillin-resistant Staphylococcus aureus pulsotypes USA300 and USA400 in a rat model of pneumonia. *J. Infect. Dis.* **198**, 561–570 (2008).

60. C. P. Montgomery, S. Boyle-Vavra, R. S. Daum, Importance of the global regulators Agr and SaeRS in the pathogenesis of CA-MRSA USA300 infection. *PLoS ONE*. **5**, e15177 (2010).

61. B. A. Diep, G. G. Stone, L. Basuino, C. J. Graber, A. Miller, S.-A. des Etages, A. Jones, A. M. Palazzolo-Ballance, F. Perdreau-Remington, G. F. Sensabaugh, F. R. DeLeo, H. F. Chambers, The arginine catabolic mobile element and staphylococcal chromosomal cassette *mec* linkage: convergence of virulence and resistance in the USA300 clone of methicillin-resistant *Staphylococcus aureus*. *J. Infect. Dis.* **197**, 1523–1530 (2008).

62. P. J. Planet, S. J. LaRussa, A. Dana, H. Smith, A. Xu, C. Ryan, A.-C. Uhlemann, S. Boundy, J. Goldberg, A. Narechania, R. Kulkarni, A. J. Ratner, J. A. Geoghegan, S.-O. Kolokotronis, A. Prince, Emergence of the epidemic methicillin-resistant Staphylococcus aureus strain USA300 coincides with horizontal transfer of the arginine catabolic mobile element and speG-mediated adaptations for survival on skin. *MBio*. **4**, e00889-13 (2013).

63. L. R. Thurlow, G. S. Joshi, J. R. Clark, J. S. Spontak, C. J. Neely, R. Maile, A. R. Richardson, Functional modularity of the arginine catabolic mobile element contributes to the success of USA300 methicillin-resistant Staphylococcus aureus. *Cell Host Microbe*. **13**, 100–107 (2013).

64. V. Nizet, Understanding how leading bacterial pathogens subvert innate immunity to reveal novel therapeutic targets. *J. Allergy Clin. Immunol.* **120**, 13–22 (2007).

65. R. W. Brown, R. K. Scherer, A study of the necrotizing action of staphylococcic alpha toxin. *Am. J. Vet. Res.* **19**, 354–362 (1958).

66. A. Thal, W. Egner, Local effect of staphylococcal toxin; studies on blood vessels with particular reference to phenomenon dermonecrosis. *AMA Arch Pathol*. **57**, 392–404 (1954).

67. A. W. Bernheimer, L. L. Schwartz, Isolation and composition of staphylococcal alpha toxin. *J. Gen. Microbiol.* **30**, 455–468 (1963).

68. R. Füssle, S. Bhakdi, A. Sziegoleit, J. Tranum-Jensen, T. Kranz, H. J. Wellensiek, On the mechanism of membrane damage by Staphylococcus aureus alpha-toxin. *J. Cell Biol.* **91**, 83–94 (1981).

69. I. Inoshima, N. Inoshima, G. A. Wilke, M. E. Powers, K. M. Frank, Y. Wang, J. Bubeck Wardenburg, A Staphylococcus aureus pore-forming toxin subverts the activity of ADAM10 to cause lethal infection in mice. *Nat. Med.* **17**, 1310–1314 (2011).

70. N. Inoshima, Y. Wang, J. Bubeck Wardenburg, Genetic requirement for ADAM10 in severe Staphylococcus aureus skin infection. *J. Invest. Dermatol.* **132**, 1513–1516 (2012).

71. G. A. Wilke, J. Bubeck Wardenburg, Role of a disintegrin and metalloprotease 10 in Staphylococcus aureus alpha-hemolysin-mediated cellular injury. *Proc Natl Acad Sci USA.* **107**, 13473–13478 (2010).

72. L. M. Popov, C. D. Marceau, P. M. Starkl, J. H. Lumb, J. Shah, D. Guerrera, R. L. Cooper, C. Merakou, D. M. Bouley, W. Meng, H. Kiyonari, M. Takeichi, S. J. Galli, F. Bagnoli, S. Citi, J. E. Carette, M. R. Amieva, The adherens junctions control susceptibility to Staphylococcus aureus α-toxin. *Proc Natl Acad Sci USA.* **112**, 14337–14342 (2015).

73. G. Y. C. Cheung, J. S. Bae, M. Otto, Pathogenicity and virulence of Staphylococcus aureus. *Virulence*. **12**, 547–569 (2021).

74. J. Shah, F. Rouaud, D. Guerrera, E. Vasileva, L. M. Popov, W. L. Kelley, E. Rubinstein, J. E. Carette, M. R. Amieva, S. Citi, A Dock-and-Lock Mechanism Clusters ADAM10 at Cell-Cell Junctions to Promote α-Toxin Cytotoxicity. *Cell Rep.* **25**, 2132-2147.e7 (2018).

75. E. A. D. Ezekwe, C. Weng, J. A. Duncan, ADAM10 Cell Surface Expression but Not Activity Is Critical for Staphylococcus aureus α-Hemolysin-Mediated Activation of the NLRP3 Inflammasome in Human Monocytes. *Toxins (Basel)*. **8**, 95 (2016).

76. B. J. Berube, J. Bubeck Wardenburg, Staphylococcus aureus α-toxin: nearly a century of intrigue. *Toxins (Basel)*. **5**, 1140–1166 (2013).

77. A. D. Kennedy, J. Bubeck Wardenburg, D. J. Gardner, D. Long, A. R. Whitney, K. R. Braughton, O. Schneewind, F. R. DeLeo, Targeting of alpha-hemolysin by active or passive immunization decreases severity of USA300 skin infection in a mouse model. *J. Infect. Dis.* **202**, 1050–1058 (2010).

78. R. Wang, K. R. Braughton, D. Kretschmer, T.-H. L. Bach, S. Y. Queck, M. Li, A. D. Kennedy, D. W. Dorward, S. J. Klebanoff, A. Peschel, F. R. DeLeo, M. Otto, Identification of novel cytolytic peptides as key virulence determinants for community-associated MRSA. *Nat. Med.* **13**, 1510–1514 (2007).

79. J. E. Alouf, J. Dufourcq, O. Siffert, E. Thiaudiere, C. Geoffroy, Interaction of staphylococcal delta-toxin and synthetic analogues with erythrocytes and phospholipid vesicles. Biological and physical properties of the amphipathic peptides. *Eur. J. Biochem.* **183**, 381–390 (1989).

80. S. Periasamy, S. S. Chatterjee, G. Y. C. Cheung, M. Otto, Phenol-soluble modulins in staphylococci: What are they originally for? *Commun. Integr. Biol.* **5**, 275–277 (2012).

81. M. Otto, Phenol-soluble modulins. *Int. J. Med. Microbiol.* **304**, 164–169 (2014).

82. P. Yoong, V. J. Torres, The effects of Staphylococcus aureus leukotoxins on the host: cell lysis and beyond. *Curr. Opin. Microbiol.* **16**, 63–69 (2013).

83. D. Oliveira, A. Borges, M. Simões, Staphylococcus aureus Toxins and Their Molecular Activity in Infectious Diseases. *Toxins (Basel)*. **10** (2018), doi:10.3390/toxins10060252.

84. A. G. Taylor, A. W. Bernheimer, Further characterization of staphylococcal gamma-hemolysin. *Infect. Immun.* **10**, 54–59 (1974).

85. A. Rahman, K. Izaki, Y. Kamio, Gamma-hemolysin genes in the same family with lukF and lukS genes in methicillin resistant Staphylococcus aureus. *Biosci. Biotechnol. Biochem.* **57**, 1234–1236 (1993).

86. F. Alonzo, V. J. Torres, Bacterial survival amidst an immune onslaught: the contribution of the Staphylococcus aureus leukotoxins. *PLoS Pathog.* **9**, e1003143 (2013).

87. C. von Eiff, A. W. Friedrich, G. Peters, K. Becker, Prevalence of genes encoding for members of the staphylococcal leukotoxin family among clinical isolates of Staphylococcus aureus. *Diagn. Microbiol. Infect. Dis.* **49**, 157–162 (2004).

88. N. Malachowa, A. R. Whitney, S. D. Kobayashi, D. E. Sturdevant, A. D. Kennedy, K. R. Braughton, D. W. Shabb, B. A. Diep, H. F. Chambers, M. Otto, F. R. DeLeo, Global changes in Staphylococcus aureus gene expression in human blood. *PLoS ONE*. **6**, e18617 (2011).

89. I. M. Nilsson, O. Hartford, T. Foster, A. Tarkowski, Alpha-toxin and gamma-toxin jointly promote Staphylococcus aureus virulence in murine septic arthritis. *Infect. Immun.* **67**, 1045–1049 (1999).

90. F. Alonzo, M. A. Benson, J. Chen, R. P. Novick, B. Shopsin, V. J. Torres, Staphylococcus aureus leucocidin ED contributes to systemic infection by targeting neutrophils and promoting bacterial growth in vivo. *Mol. Microbiol.* **83**, 423–435 (2012).

91. A. L. Dumont, T. K. Nygaard, R. L. Watkins, A. Smith, L. Kozhaya, B. N. Kreiswirth, B. Shopsin, D. Unutmaz, J. M. Voyich, V. J. Torres, Characterization of a new cytotoxin that contributes to Staphylococcus aureus pathogenesis. *Mol. Microbiol.* **79**, 814–825 (2011).

92. P. N. Panton, F. C. O. Valentine, STAPHYLOCOCCAL TOXIN. *Lancet*. **219**, 506–508 (1932).

93. F. Vandenesch, T. Naimi, M. C. Enright, G. Lina, G. R. Nimmo, H. Heffernan, N. Liassine, M. Bes, T. Greenland, M.-E. Reverdy, J. Etienne, Community-acquired methicillin-resistant Staphylococcus aureus carrying Panton-Valentine leukocidin genes: worldwide emergence. *Emerging Infect. Dis.* **9**, 978–984 (2003).

94. B. A. Diep, M. Otto, The role of virulence determinants in community-associated MRSA pathogenesis. *Trends Microbiol.* **16**, 361–369 (2008).

95. D. Grumann, U. Nübel, B. M. Bröker, Staphylococcus aureus toxins--their functions and genetics. *Infect. Genet. Evol.* **21**, 583–592 (2014).

96. G. R. Drapeau, Y. Boily, J. Houmard, Purification and properties of an extracellular protease of Staphylococcus aureus. *J. Biol. Chem.* **247**, 6720–6726 (1972).

97. A. Björklind, S. Arvidson, Occurrence of an extracellular serineproteinase among Staphylococcus aureus strains. *Acta Pathol. Microbiol. Scand. B.* **85**, 277–280 (1977).

98. A. Banbula, J. Potempa, J. Travis, C. Fernandez-Catalán, K. Mann, R. Huber, W. Bode, F. Medrano, Amino-acid sequence and three-dimensional structure of the Staphylococcus aureus metalloproteinase at 1.72 A resolution. *Structure*. **6**, 1185–1193 (1998).

99. K. Rice, R. Peralta, D. Bast, J. de Azavedo, M. J. McGavin, Description of staphylococcus serine protease (ssp) operon in Staphylococcus aureus and nonpolar inactivation of sspA-encoded serine protease. *Infect. Immun.* **69**, 159–169 (2001).

100. L. Shaw, E. Golonka, J. Potempa, S. J. Foster, The role and regulation of the extracellular proteases of Staphylococcus aureus. *Microbiology (Reading, Engl)*. **150**, 217–228 (2004).

101. G. R. Drapeau, Role of metalloprotease in activation of the precursor of staphylococcal protease. *J. Bacteriol.* **136**, 607–613 (1978).

102. G. Pietrocola, G. Nobile, S. Rindi, P. Speziale, Staphylococcus aureus Manipulates Innate Immunity through Own and Host-Expressed Proteases. *Front. Cell. Infect. Microbiol.* **7**, 166 (2017).

103. S. L. Kolar, J. A. Ibarra, F. E. Rivera, J. M. Mootz, J. E. Davenport, S. M. Stevens, A. R. Horswill, L. N. Shaw, Extracellular proteases are key mediators of Staphylococcus aureus virulence via the global modulation of virulence-determinant stability. *Microbiologyopen*. **2**, 18–34 (2013).

104. A. J. Laarman, M. Ruyken, C. L. Malone, J. A. G. van Strijp, A. R. Horswill, S. H. M. Rooijakkers, Staphylococcus aureus metalloprotease aureolysin cleaves complement C3 to mediate immune evasion. *J. Immunol.* **186**, 6445–6453 (2011).

105. M. Sieprawska-Lupa, P. Mydel, K. Krawczyk, K. Wójcik, M. Puklo, B. Lupa, P. Suder, J. Silberring, M. Reed, J. Pohl, W. Shafer, F. McAleese, T. Foster, J. Travis, J. Potempa, Degradation of human antimicrobial peptide LL-37 by Staphylococcus aureus-derived proteinases. *Antimicrob. Agents Chemother.* **48**, 4673–4679 (2004).

106. J. Smagur, K. Guzik, M. Bzowska, M. Kuzak, M. Zarebski, T. Kantyka, M. Walski, B. Gajkowska, J. Potempa, Staphylococcal cysteine protease staphopain B (SspB) induces rapid engulfment of human neutrophils and monocytes by macrophages. *Biol. Chem.* **390**, 361–371 (2009).

107. I. Massimi, E. Park, K. Rice, W. Muller-Esterl, D. Sauder, M. J. McGavin, Identification of a novel maturation mechanism and restricted substrate specificity for the SspB cysteine protease of Staphylococcus aureus. *J. Biol. Chem.* **277**, 41770–41777 (2002).

108. M. J. McGavin, C. Zahradka, K. Rice, J. E. Scott, Modification of the Staphylococcus aureus fibronectin binding phenotype by V8 protease. *Infect. Immun.* **65**, 2621–2628 (1997).

109. F. M. McAleese, E. J. Walsh, M. Sieprawska, J. Potempa, T. J. Foster, Loss of clumping factor B fibrinogen binding activity by Staphylococcus aureus involves cessation of

transcription, shedding and cleavage by metalloprotease. *J. Biol. Chem.* **276**, 29969–29978 (2001).

110. A. K. Zielinska, K. E. Beenken, H.-S. Joo, L. N. Mrak, L. M. Griffin, T. T. Luong, C. Y. Lee, M. Otto, L. N. Shaw, M. S. Smeltzer, Defining the strain-dependent impact of the Staphylococcal accessory regulator (sarA) on the alpha-toxin phenotype of Staphylococcus aureus. *J. Bacteriol.* **193**, 2948–2958 (2011).

111. D. J. Gonzalez, C. Y. Okumura, A. Hollands, R. Kersten, K. Akong-Moore, M. A. Pence, C. L. Malone, J. Derieux, B. S. Moore, A. R. Horswill, J. E. Dixon, P. C. Dorrestein, V. Nizet, Novel phenol-soluble modulin derivatives in community-associated methicillin-resistant Staphylococcus aureus identified through imaging mass spectrometry. *J. Biol. Chem.* **287**, 13889–13898 (2012).

112. J. Bjerketorp, M. Nilsson, Å. Ljungh, J.-I. Flock, K. Jacobsson, L. Frykberg, A novel von Willebrand factor binding protein expressed by Staphylococcus aureus. *Microbiology (Reading, Engl).* **148**, 2037–2044 (2002).

113. J. Bjerketorp, K. Jacobsson, L. Frykberg, The von Willebrand factor-binding protein (vWbp) of *Staphylococcus aureus* is a coagulase. *FEMS Microbiol. Lett.* **234**, 309–314 (2004).

114. R. Friedrich, P. Panizzi, P. Fuentes-Prior, K. Richter, I. Verhamme, P. J. Anderson, S.-I. Kawabata, R. Huber, W. Bode, P. E. Bock, Staphylocoagulase is a prototype for the mechanism of cofactor-induced zymogen activation. *Nature*. **425**, 535–539 (2003).

115. P. Panizzi, R. Friedrich, P. Fuentes-Prior, K. Richter, P. E. Bock, W. Bode, Fibrinogen substrate recognition by staphylocoagulase.(pro)thrombin complexes. *J. Biol. Chem.* **281**, 1179–1187 (2006).

116. H. K. Kroh, P. Panizzi, P. E. Bock, Von Willebrand factor-binding protein is a hysteretic conformational activator of prothrombin. *Proc Natl Acad Sci USA*. **106**, 7786–7791 (2009).

117. A. G. Cheng, M. McAdow, H. K. Kim, T. Bae, D. M. Missiakas, O. Schneewind, Contribution of coagulases towards Staphylococcus aureus disease and protective immunity. *PLoS Pathog.* **6**, e1001036 (2010).

118. S. K. Mazmanian, H. Ton-That, O. Schneewind, Sortase-catalysed anchoring of surface proteins to the cell wall of Staphylococcus aureus. *Mol. Microbiol.* **40**, 1049–1057 (2001).

119. T. J. Foster, The MSCRAMM Family of Cell-Wall-Anchored Surface Proteins of Gram-Positive Cocci. *Trends Microbiol.* **27**, 927–941 (2019).

120. T. J. Foster, Surface Proteins of Staphylococcus aureus. *Microbiol. Spectr.* **7** (2019), doi:10.1128/microbiolspec.GPP3-0046-2018.

121. A. Zecconi, F. Scali, Staphylococcus aureus virulence factors in evasion from innate immune defenses in human and animal diseases. *Immunol. Lett.* **150**, 12–22 (2013).

122. K. A. Berry, M. T. A. Verhoef, A. C. Leonard, G. Cox, Staphylococcus aureus adhesion to the host. *Ann. N. Y. Acad. Sci.* (2022), doi:10.1111/nyas.14807.

123. I.-M. Jonsson, S. K. Mazmanian, O. Schneewind, T. Bremell, A. Tarkowski, The role of Staphylococcus aureus sortase A and sortase B in murine arthritis. *Microbes Infect.* **5**, 775–780 (2003).

124. K. D. Buchan, S. J. Foster, S. A. Renshaw, Staphylococcus aureus: setting its sights on the human innate immune system. *Microbiology (Reading, Engl)*. **165**, 367–385 (2019).

125. F. R. DeLeo, B. A. Diep, M. Otto, Host defense and pathogenesis in Staphylococcus aureus infections. *Infect. Dis. Clin. North Am.* **23**, 17–34 (2009).

126. H. K. Kim, V. Thammavongsa, O. Schneewind, D. Missiakas, Recurrent infections and immune evasion strategies of Staphylococcus aureus. *Curr. Opin. Microbiol.* **15**, 92–99 (2012).

127. H. Karauzum, S. K. Datta, Adaptive Immunity Against Staphylococcus aureus. *Curr. Top. Microbiol. Immunol.* **409**, 419–439 (2017).

128. L. Zhang, K. Jacobsson, J. Vasi, M. Lindberg, L. Frykberg, A second IgG-binding protein in Staphylococcus aureus. *Microbiology (Reading, Engl)*. **144 (Pt 4)**, 985–991 (1998).

129. J. V. Sarma, P. A. Ward, The complement system. *Cell Tissue Res.* **343**, 227–235 (2011).

130. M. I. Bokarewa, T. Jin, A. Tarkowski, Staphylococcus aureus: Staphylokinase. *Int. J. Biochem. Cell Biol.* **38**, 504–509 (2006).

131. T. K. Koch, M. Reuter, D. Barthel, S. Böhm, J. van den Elsen, P. Kraiczy, P. F. Zipfel, C. Skerka, Staphylococcus aureus proteins Sbi and Efb recruit human plasmin to degrade complement C3 and C3b. *PLoS ONE*. **7**, e47638 (2012).

132. L. Y. L. Lee, X. Liang, M. Höök, E. L. Brown, Identification and characterization of the C3 binding domain of the Staphylococcus aureus extracellular fibrinogen-binding protein (Efb). *J. Biol. Chem.* **279**, 50710–50716 (2004).

133. B. L. Garcia, K. X. Ramyar, D. Ricklin, J. D. Lambris, B. V. Geisbrecht, Advances in understanding the structure, function, and mechanism of the SCIN and Efb families of Staphylococcal immune evasion proteins. *Adv. Exp. Med. Biol.* **946**, 113–133 (2012).

134. H. Amdahl, I. Jongerius, T. Meri, T. Pasanen, S. Hyvärinen, K. Haapasalo, J. A. van Strijp, S. H. Rooijakkers, T. S. Jokiranta, Staphylococcal Ecb protein and host complement regulator factor H enhance functions of each other in bacterial immune evasion. *J. Immunol.* **191**, 1775–1784 (2013).

135. H. Amdahl, K. Haapasalo, L. Tan, T. Meri, P. I. Kuusela, J. A. van Strijp, S. Rooijakkers, T. S. Jokiranta, Staphylococcal protein Ecb impairs complement receptor-1 mediated recognition of opsonized bacteria. *PLoS ONE*. **12**, e0172675 (2017).

136. S. H. M. Rooijakkers, M. Ruyken, J. van Roon, K. P. M. van Kessel, J. A. G. van Strijp, W. J. B. van Wamel, Early expression of SCIN and CHIPS drives instant immune evasion by Staphylococcus aureus. *Cell. Microbiol.* **8**, 1282–1293 (2006).

137. S. L. Brandt, N. E. Putnam, J. E. Cassat, C. H. Serezani, Innate Immunity to Staphylococcus aureus: Evolving Paradigms in Soft Tissue and Invasive Infections. *J. Immunol.* **200**, 3871–3880 (2018).

138. B. Postma, M. J. Poppelier, J. C. van Galen, E. R. Prossnitz, J. A. G. van Strijp, C. J. C. de Haas, K. P. M. van Kessel, Chemotaxis inhibitory protein of Staphylococcus aureus binds specifically to the C5a and formylated peptide receptor. *J. Immunol.* **172**, 6994–7001 (2004).

139. Y. G.-Y. Chan, H. K. Kim, O. Schneewind, D. Missiakas, The capsular polysaccharide of Staphylococcus aureus is attached to peptidoglycan by the LytR-CpsA-Psr (LCP) family of enzymes. *J. Biol. Chem.* **289**, 15680–15690 (2014).

140. K. O'Riordan, J. C. Lee, Staphylococcus aureus capsular polysaccharides. *Clin. Microbiol. Rev.* **17**, 218–234 (2004).

141. D. E. Sutter, A. M. Summers, C. E. Keys, K. L. Taylor, C. E. Frasch, L. E. Braun, A. I. Fattom, M. C. Bash, Capsular serotype of Staphylococcus aureus in the era of community-acquired MRSA. *FEMS Immunol. Med. Microbiol.* **63**, 16–24 (2011).

142. N. K. Archer, M. J. Mazaitis, J. W. Costerton, J. G. Leid, M. E. Powers, M. E. Shirtliff, Staphylococcus aureus biofilms: properties, regulation, and roles in human disease. *Virulence*. **2**, 445–459 (2011).

143. H. T. T. Nguyen, T. H. Nguyen, M. Otto, The staphylococcal exopolysaccharide PIA - Biosynthesis and role in biofilm formation, colonization, and infection. *Comput. Struct. Biotechnol. J.* **18**, 3324–3334 (2020).

144. M. Zapotoczna, E. O'Neill, J. P. O'Gara, Untangling the Diverse and Redundant Mechanisms of Staphylococcus aureus Biofilm Formation. *PLoS Pathog.* **12**, e1005671 (2016).

145. H. McCarthy, J. K. Rudkin, N. S. Black, L. Gallagher, E. O'Neill, J. P. O'Gara, Methicillin resistance and the biofilm phenotype in Staphylococcus aureus. *Front. Cell. Infect. Microbiol.* **5**, 1 (2015).

146. S. S. Al-Shehri, Reactive oxygen and nitrogen species and innate immune response. *Biochimie*. **181**, 52–64 (2021).

147. F. C. Fang, Antimicrobial reactive oxygen and nitrogen species: concepts and controversies. *Nat. Rev. Microbiol.* **2**, 820–832 (2004).

148. A. R. Richardson, P. M. Dunman, F. C. Fang, The nitrosative stress response of Staphylococcus aureus is required for resistance to innate immunity. *Mol. Microbiol.* **61**, 927–939 (2006).

149. M. H. Karavolos, M. J. Horsburgh, E. Ingham, S. J. Foster, Role and regulation of the superoxide dismutases of Staphylococcus aureus. *Microbiology (Reading, Engl).* **149**, 2749–2758 (2003).

150. M. W. Valderas, M. E. Hart, Identification and characterization of a second superoxide dismutase gene (sodM) from Staphylococcus aureus. *J. Bacteriol.* **183**, 3399–3407 (2001).

151. M. W. Valderas, J. W. Gatson, N. Wreyford, M. E. Hart, The superoxide dismutase gene sodM is unique to Staphylococcus aureus: absence of sodM in coagulase-negative staphylococci. *J. Bacteriol.* **184**, 2465–2472 (2002).

152. A. Clauditz, A. Resch, K.-P. Wieland, A. Peschel, F. Götz, Staphyloxanthin plays a role in the fitness of *Staphylococcus aureus* and its ability to cope with oxidative stress. *Infect. Immun.* **74**, 4950–4953 (2006).

153. L. Xue, Y. Y. Chen, Z. Yan, W. Lu, D. Wan, H. Zhu, Staphyloxanthin: a potential target for antivirulence therapy. *Infect. Drug Resist.* **12**, 2151–2160 (2019).

154. G. L. Mandell, Catalase, superoxide dismutase, and virulence of Staphylococcus aureus. In vitro and in vivo studies with emphasis on staphylococcal--leukocyte interaction. *J. Clin. Invest.* **55**, 561–566 (1975).

155. E. W. Koneman, S. D. Allen, W. M. Janda, Diagnostic microbiology. *... : Lippincott-Raven ...* (1997).

156. P. Recsei, B. Kreiswirth, M. O'Reilly, P. Schlievert, A. Gruss, R. P. Novick, Regulation of exoprotein gene expression in Staphylococcus aureus by agr. *Mol. Gen. Genet.* **202**, 58–61 (1986).

157. B. Wang, A. Zhao, R. P. Novick, T. W. Muir, Activation and inhibition of the receptor histidine kinase AgrC occurs through opposite helical transduction motions. *Mol. Cell*. **53**, 929–940 (2014).

158. M. B. Miller, B. L. Bassler, Quorum sensing in bacteria. *Annu. Rev. Microbiol.* **55**, 165–199 (2001).

159. R. P. Novick, E. Geisinger, Quorum sensing in staphylococci. *Annu. Rev. Genet.* **42**, 541–564 (2008).

160. B. Wang, T. W. Muir, Regulation of Virulence in Staphylococcus aureus: Molecular Mechanisms and Remaining Puzzles. *Cell Chem. Biol.* **23**, 214–224 (2016).

161. S. Y. Queck, M. Jameson-Lee, A. E. Villaruz, T.-H. L. Bach, B. A. Khan, D. E. Sturdevant, S. M. Ricklefs, M. Li, M. Otto, RNAIII-independent target gene control by the agr quorum-

sensing system: insight into the evolution of virulence regulation in Staphylococcus aureus. *Mol. Cell*. **32**, 150–158 (2008).

162. R. P. Novick, H. F. Ross, S. J. Projan, J. Kornblum, B. Kreiswirth, S. Moghazeh, Synthesis of staphylococcal virulence factors is controlled by a regulatory RNA molecule. *EMBO J.* **12**, 3967–3975 (1993).

163. P. J. McNamara, K. C. Milligan-Monroe, S. Khalili, R. A. Proctor, Identification, cloning, and initial characterization of rot, a locus encoding a regulator of virulence factor expression in Staphylococcus aureus. *J. Bacteriol.* **182**, 3197–3203 (2000).

164. B. Saïd-Salim, P. M. Dunman, F. M. McAleese, D. Macapagal, E. Murphy, P. J. McNamara, S. Arvidson, T. J. Foster, S. J. Projan, B. N. Kreiswirth, Global regulation of Staphylococcus aureus genes by Rot. *J. Bacteriol.* **185**, 610–619 (2003).

165. E. Geisinger, R. P. Adhikari, R. Jin, H. F. Ross, R. P. Novick, Inhibition of rot translation by RNAIII, a key feature of agr function. *Mol. Microbiol.* **61**, 1038–1048 (2006).

166. D. Frees, K. Sørensen, H. Ingmer, Global virulence regulation in Staphylococcus aureus: pinpointing the roles of ClpP and ClpX in the sar/agr regulatory network. *Infect. Immun.* **73**, 8100–8108 (2005).

167. E. Morfeldt, D. Taylor, A. von Gabain, S. Arvidson, Activation of alpha-toxin translation in Staphylococcus aureus by the trans-encoded antisense RNA, RNAIII. *EMBO J.* **14**, 4569–4577 (1995).

168. Y. Benito, F. A. Kolb, P. Romby, G. Lina, J. Etienne, F. Vandenesch, Probing the structure of RNAIII, the Staphylococcus aureus agr regulatory RNA, and identification of the RNA domain involved in repression of protein A expression. *RNA*. **6**, 668–679 (2000).

169. E. Huntzinger, S. Boisset, C. Saveanu, Y. Benito, T. Geissmann, A. Namane, G. Lina, J. Etienne, B. Ehresmann, C. Ehresmann, A. Jacquier, F. Vandenesch, P. Romby, Staphylococcus aureus RNAIII and the endoribonuclease III coordinately regulate spa gene expression. *EMBO J.* **24**, 824–835 (2005).

170. P. Casino, V. Rubio, A. Marina, The mechanism of signal transduction by two-component systems. *Curr. Opin. Struct. Biol.* **20**, 763–771 (2010).

171. R. P. Novick, D. Jiang, The staphylococcal saeRS system coordinates environmental signals with agr quorum sensing. *Microbiology (Reading, Engl)*. **149**, 2709–2717 (2003).

172. Q. Liu, W.-S. Yeo, T. Bae, The SaeRS Two-Component System of Staphylococcus aureus. *Genes (Basel)*. **7** (2016), doi:10.3390/genes7100081.

173. T. Geiger, C. Goerke, M. Mainiero, D. Kraus, C. Wolz, The virulence regulator Sae of Staphylococcus aureus: promoter activities and response to phagocytosis-related signals. *J. Bacteriol.* **190**, 3419–3428 (2008).

174. H. Cho, D.-W. Jeong, Q. Liu, W.-S. Yeo, T. Vogl, E. P. Skaar, W. J. Chazin, T. Bae, Calprotectin Increases the Activity of the SaeRS Two Component System and Murine Mortality during Staphylococcus aureus Infections. *PLoS Pathog.* **11**, e1005026 (2015).

175. K. Rogasch, V. Rühmling, J. Pané-Farré, D. Höper, C. Weinberg, S. Fuchs, M. Schmudde, B. M. Bröker, C. Wolz, M. Hecker, S. Engelmann, Influence of the two-component system SaeRS on global gene expression in two different Staphylococcus aureus strains. *J. Bacteriol.* **188**, 7742–7758 (2006).

176. A. T. Giraudo, A. L. Cheung, R. Nagel, The sae locus of Staphylococcus aureus controls exoprotein synthesis at the transcriptional level. *Arch. Microbiol.* **168**, 53–58 (1997).

177. M. A. Benson, S. Lilo, T. Nygaard, J. M. Voyich, V. J. Torres, Rot and SaeRS cooperate to activate expression of the staphylococcal superantigen-like exoproteins. *J. Bacteriol.* **194**, 4355–4365 (2012).

178. X. Liang, C. Yu, J. Sun, H. Liu, C. Landwehr, D. Holmes, Y. Ji, Inactivation of a two-component signal transduction system, SaeRS, eliminates adherence and attenuates virulence of Staphylococcus aureus. *Infect. Immun.* **74**, 4655–4665 (2006).

179. M. G. Bayer, J. H. Heinrichs, A. L. Cheung, The molecular architecture of the sar locus in Staphylococcus aureus. *J. Bacteriol.* **178**, 4563–4570 (1996).

180. C. Jenul, A. R. Horswill, Regulation of Staphylococcus aureus Virulence. *Microbiol. Spectr.* **6** (2018), doi:10.1128/microbiolspec.GPP3-0031-2018.

181. A. K. Zielinska, K. E. Beenken, L. N. Mrak, H. J. Spencer, G. R. Post, R. A. Skinner, A. J. Tackett, A. R. Horswill, M. S. Smeltzer, sarA-mediated repression of protease production plays a key role in the pathogenesis of Staphylococcus aureus USA300 isolates. *Mol. Microbiol.* **86**, 1183–1196 (2012).

182. H. A. Crosby, N. Tiwari, J. M. Kwiecinski, Z. Xu, A. Dykstra, C. Jenul, E. J. Fuentes, A. R. Horswill, The Staphylococcus aureus ArlRS two-component system regulates virulence factor expression through MgrA. *Mol. Microbiol.* **113**, 103–122 (2020).

183. L. Harper, D. Balasubramanian, E. A. Ohneck, W. E. Sause, J. Chapman, B. Mejia-Sosa, T. Lhakhang, A. Heguy, A. Tsirigos, B. Ueberheide, J. M. Boyd, D. S. Lun, V. J. Torres, Staphylococcus aureus Responds to the Central Metabolite Pyruvate To Regulate Virulence. *MBio*. **9** (2018), doi:10.1128/mBio.02272-17.

184. A. R. Richardson, Virulence and Metabolism. *Microbiol. Spectr.* **7** (2019), doi:10.1128/microbiolspec.GPP3-0011-2018.

185. J. E. Cassat, J. L. Moore, K. J. Wilson, Z. Stark, B. M. Prentice, R. Van de Plas, W. J. Perry, Y. Zhang, J. Virostko, D. C. Colvin, K. L. Rose, A. M. Judd, M. L. Reyzer, J. M. Spraggins, C. M. Grunenwald, J. C. Gore, R. M. Caprioli, E. P. Skaar, Integrated molecular imaging reveals tissue heterogeneity driving host-pathogen interactions. *Sci. Transl. Med.* **10** (2018), doi:10.1126/scitranslmed.aan6361.

186. W. J. Perry, J. M. Spraggins, J. R. Sheldon, C. M. Grunenwald, D. E. Heinrichs, J. E. Cassat, E. P. Skaar, R. M. Caprioli, Staphylococcus aureus exhibits heterogeneous siderophore production within the vertebrate host. *Proc Natl Acad Sci USA*. **116**, 21980–21982 (2019).

187. J. E. Choby, E. P. Skaar, Heme synthesis and acquisition in bacterial pathogens. *J. Mol. Biol.* **428**, 3408–3428 (2016).

188. H. A. Dailey, T. A. Dailey, S. Gerdes, D. Jahn, M. Jahn, M. R. O'Brian, M. J. Warren, Prokaryotic heme biosynthesis: multiple pathways to a common essential product. *Microbiol. Mol. Biol. Rev.* **81** (2017), doi:10.1128/MMBR.00048-16.

189. W. Huang, A. Wilks, Extracellular heme uptake and the challenge of bacterial cell membranes. *Annu. Rev. Biochem.* **86**, 799–823 (2017).

190. J. E. Choby, H. B. Buechi, A. J. Farrand, E. P. Skaar, M. F. Barber, Molecular Basis for the Evolution of Species-Specific Hemoglobin Capture by Staphylococcus aureus. *MBio*. **9** (2018), doi:10.1128/mBio.01524-18.

191. V. N. Fritsch, V. V. Loi, T. Busche, Q. N. Tung, R. Lill, P. Horvatek, C. Wolz, J. Kalinowski, H. Antelmann, The alarmone (p)ppGpp confers tolerance to oxidative stress during the stationary phase by maintenance of redox and iron homeostasis in Staphylococcus aureus. *Free Radic. Biol. Med.* **161**, 351–364 (2020).

192. J. P. Zackular, W. J. Chazin, E. P. Skaar, Nutritional Immunity: S100 Proteins at the Host-Pathogen Interface. *J. Biol. Chem.* **290**, 18991–18998 (2015).

193. J. N. Radin, J. L. Kelliher, P. K. Párraga Solórzano, T. E. Kehl-Fie, The Two-Component System ArlRS and Alterations in Metabolism Enable Staphylococcus aureus to Resist Calprotectin-Induced Manganese Starvation. *PLoS Pathog.* **12**, e1006040 (2016).

194. P. K. Párraga Solórzano, J. Yao, C. O. Rock, T. E. Kehl-Fie, Disruption of Glycolysis by Nutritional Immunity Activates a Two-Component System That Coordinates a Metabolic and Antihost Response by Staphylococcus aureus. *MBio*. **10** (2019), doi:10.1128/mBio.01321-19.

195. P. K. Párraga Solórzano, A. C. Shupe, T. E. Kehl-Fie, The sensor histidine kinase ArlS is necessary for Staphylococcus aureus to activate ArlR in response to nutrient availability. *J. Bacteriol.*, JB0042221 (2021).

196. L. D. Handke, A. V. Gribenko, Y. Timofeyeva, I. L. Scully, A. S. Anderson, MntC-Dependent Manganese Transport Is Essential for Staphylococcus aureus Oxidative Stress Resistance and Virulence. *mSphere*. **3** (2018), doi:10.1128/mSphere.00336-18.

197. J. N. Radin, J. Zhu, E. B. Brazel, C. A. McDevitt, T. E. Kehl-Fie, Synergy between Nutritional Immunity and Independent Host Defenses Contributes to the Importance of the MntABC Manganese Transporter during Staphylococcus aureus Infection. *Infect. Immun.* **87** (2019), doi:10.1128/IAI.00642-18.

198. J. N. Radin, J. L. Kelliher, P. K. P. Solórzano, K. P. Grim, R. Ramezanifard, J. M. Slauch, T. E. Kehl-Fie, Metal-independent variants of phosphoglycerate mutase promote resistance to nutritional immunity and retention of glycolysis during infection. *PLoS Pathog.* **15**, e1007971 (2019).

199. Y. M. Garcia, A. Barwinska-Sendra, E. Tarrant, E. P. Skaar, K. J. Waldron, T. E. Kehl-Fie, A Superoxide Dismutase Capable of Functioning with Iron or Manganese Promotes the Resistance of Staphylococcus aureus to Calprotectin and Nutritional Immunity. *PLoS Pathog.* **13**, e1006125 (2017).

200. A. Barwinska-Sendra, Y. M. Garcia, K. M. Sendra, A. Baslé, E. S. Mackenzie, E. Tarrant, P. Card, L. C. Tabares, C. Bicep, S. Un, T. E. Kehl-Fie, K. J. Waldron, An evolutionary path to altered cofactor specificity in a metalloenzyme. *Nat. Commun.* **11**, 2738 (2020).

201. D. Lalaouna, J. Baude, Z. Wu, A. Tomasini, J. Chicher, S. Marzi, F. Vandenesch, P. Romby, I. Caldelari, K. Moreau, RsaC sRNA modulates the oxidative stress response of Staphylococcus aureus during manganese starvation. *Nucleic Acids Res.* **47**, 9871–9887 (2019).

202. L. J. Juttukonda, E. T. M. Berends, J. P. Zackular, J. L. Moore, M. T. Stier, Y. Zhang, J. E. Schmitz, W. N. Beavers, C. D. Wijers, B. A. Gilston, T. E. Kehl-Fie, J. Atkinson, M. K. Washington, R. S. Peebles, W. J. Chazin, V. J. Torres, R. M. Caprioli, E. P. Skaar, Dietary manganese promotes staphylococcal infection of the heart. *Cell Host Microbe*. **22**, 531-542.e8 (2017).

203. C. M. Grunenwald, J. E. Choby, L. J. Juttukonda, W. N. Beavers, A. Weiss, V. J. Torres, E. P. Skaar, Manganese Detoxification by MntE Is Critical for Resistance to Oxidative Stress and Virulence of Staphylococcus aureus. *MBio*. **10** (2019), doi:10.1128/mBio.02915-18.

204. K. P. Grim, B. San Francisco, J. N. Radin, E. B. Brazel, J. L. Kelliher, P. K. Párraga Solórzano, P. C. Kim, C. A. McDevitt, T. E. Kehl-Fie, The Metallophore Staphylopine Enables Staphylococcus aureus To Compete with the Host for Zinc and Overcome Nutritional Immunity. *MBio*. **8** (2017), doi:10.1128/mBio.01281-17.

205. Z. Luo, S. Luo, Y. Ju, P. Ding, J. Xu, Q. Gu, H. Zhou, Structural insights into the ligand recognition and catalysis of the key aminobutanoyltransferase CntL in staphylopine biosynthesis. *FASEB J.* **35**, e21575 (2021).

206. J. Zhang, S. Wang, Y. Bai, Q. Guo, J. Zhou, X. Lei, Total syntheses of natural metallophores staphylopine and aspergillomarasmine A. *J. Org. Chem.* **82**, 13643–13648 (2017).

207. C. Hajjar, R. Fanelli, C. Laffont, C. Brutesco, G. Cullia, M. Tribout, D. Nurizzo, E. Borezée-Durant, R. Voulhoux, D. Pignol, J. Lavergne, F. Cavelier, P. Arnoux, Control by Metals of Staphylopine Dehydrogenase Activity during Metallophore Biosynthesis. *J. Am. Chem. Soc.* **141**, 5555–5562 (2019).

208. M. R. Jordan, J. Wang, A. Weiss, E. P. Skaar, D. A. Capdevila, D. P. Giedroc, Mechanistic Insights into the Metal-Dependent Activation of ZnII-Dependent Metallochaperones. *Inorg. Chem.* **58**, 13661–13672 (2019).

209. C. Chen, D. C. Hooper, Intracellular accumulation of staphylopine impairs the fitness of Staphylococcus aureus cntE mutant. *FEBS Lett.* **593**, 1213–1222 (2019).

210. K. P. Grim, J. N. Radin, P. K. P. Solórzano, J. R. Morey, K. A. Frye, K. Ganio, S. L. Neville, C. A. McDevitt, T. E. Kehl-Fie, Intracellular Accumulation of Staphylopine Can Sensitize Staphylococcus aureus to Host-Imposed Zinc Starvation by Chelation-Independent Toxicity. *J. Bacteriol.* **202** (2020), doi:10.1128/JB.00014-20.

211. C. Fojcik, P. Arnoux, L. Ouerdane, M. Aigle, L. Alfonsi, E. Borezée-Durant, Independent and cooperative regulation of staphylopine biosynthesis and trafficking by Fur and Zur. *Mol. Microbiol.* **108**, 159–177 (2018).

212. J. R. Morey, T. E. Kehl-Fie, Bioinformatic Mapping of Opine-Like Zincophore Biosynthesis in Bacteria. *mSystems*. **5** (2020), doi:10.1128/mSystems.00554-20.

213. J. Purves, J. Thomas, G. P. Riboldi, M. Zapotoczna, E. Tarrant, P. W. Andrew, A. Londoño, P. J. Planet, J. A. Geoghegan, K. J. Waldron, J. A. Morrissey, A horizontally gene transferred copper resistance locus confers hyper-resistance to antibacterial copper toxicity and enables survival of community acquired methicillin resistant Staphylococcus aureus USA300 in macrophages. *Environ. Microbiol.* **20**, 1576–1589 (2018).

214. Z. Rosario-Cruz, A. Eletsky, N. S. Daigham, H. Al-Tameemi, G. V. T. Swapna, P. C. Kahn, T. Szyperski, G. T. Montelione, J. M. Boyd, The copBL operon protects Staphylococcus aureus from copper toxicity: CopL is an extracellular membrane-associated copper-binding protein. *J. Biol. Chem.* **294**, 4027–4044 (2019).

215. P. Saenkham-Huntsinger, A. N. Hyre, B. S. Hanson, G. L. Donati, L. G. Adams, C. Ryan, A. Londoño, A. M. Moustafa, P. J. Planet, S. Subashchandrabose, Copper Resistance Promotes Fitness of Methicillin-Resistant Staphylococcus aureus during Urinary Tract Infection. *MBio*. **12**, e0203821 (2021).

216. H. Al-Tameemi, W. N. Beavers, J. Norambuena, E. P. Skaar, J. M. Boyd, Staphylococcus aureus lacking a functional MntABC manganese import system has increased resistance to copper. *Mol. Microbiol.* **115**, 554–573 (2021).

217. E. Tarrant, G. P Riboldi, M. R. McIlvin, J. Stevenson, A. Barwinska-Sendra, L. J. Stewart, M. A. Saito, K. J. Waldron, Copper stress in Staphylococcus aureus leads to adaptive changes in central carbon metabolism. *Metallomics*. **11**, 183–200 (2019).

218. C. M. Gries, M. R. Sadykov, L. L. Bulock, S. S. Chaudhari, V. C. Thomas, J. L. Bose, K. W. Bayles, Potassium Uptake Modulates Staphylococcus aureus Metabolism. *mSphere*. **1** (2016), doi:10.1128/mSphere.00125-16.

219. R. M. Corrigan, I. Campeotto, T. Jeganathan, K. G. Roelofs, V. T. Lee, A. Gründling, Systematic identification of conserved bacterial c-di-AMP receptor proteins. *Proc Natl Acad Sci USA*. **110**, 9084–9089 (2013).

220. J. M. Lensmire, J. P. Dodson, B. Y. Hsueh, M. R. Wischer, P. C. Delekta, J. C. Shook, E. N. Ottosen, P. J. Kies, J. Ravi, N. D. Hammer, The Staphylococcus aureus Cystine Transporters TcyABC and TcyP Facilitate Nutrient Sulfur Acquisition during Infection. *Infect. Immun.* **88** (2020), doi:10.1128/IAI.00690-19.

221. C. A. Roberts, H. M. Al-Tameemi, A. A. Mashruwala, Z. Rosario-Cruz, U. Chauhan, W. E. Sause, V. J. Torres, W. J. Belden, J. M. Boyd, The Suf Iron-Sulfur Cluster Biosynthetic System Is Essential in Staphylococcus aureus, and Decreased Suf Function Results in Global Metabolic Defects and Reduced Survival in Human Neutrophils. *Infect. Immun.* **85** (2017), doi:10.1128/IAI.00100-17.

222. A. A. Mashruwala, C. A. Roberts, S. Bhatt, K. L. May, R. K. Carroll, L. N. Shaw, J. M. Boyd, Staphylococcus aureus SufT: an essential iron-sulphur cluster assembly factor in cells experiencing a high-demand for lipoic acid. *Mol. Microbiol.* **102**, 1099–1119 (2016).

223. H. Peng, Y. Zhang, L. D. Palmer, T. E. Kehl-Fie, E. P. Skaar, J. C. Trinidad, D. P. Giedroc, Hydrogen Sulfide and Reactive Sulfur Species Impact Proteome S-Sulfhydration and Global Virulence Regulation in Staphylococcus aureus. *ACS Infect. Dis.* **3**, 744–755 (2017).

224. H. Peng, J. Shen, K. A. Edmonds, J. L. Luebke, A. K. Hickey, L. D. Palmer, F.-M. J. Chang, K. A. Bruce, T. E. Kehl-Fie, E. P. Skaar, D. P. Giedroc, Sulfide Homeostasis and Nitroxyl Intersect via Formation of Reactive Sulfur Species in Staphylococcus aureus. *mSphere*. **2** (2017), doi:10.1128/mSphere.00082-17.

225. J. L. Kelliher, J. N. Radin, K. P. Grim, P. K. Párraga Solórzano, P. H. Degnan, T. E. Kehl-Fie, Acquisition of the Phosphate Transporter NptA Enhances Staphylococcus aureus Pathogenesis by Improving Phosphate Uptake in Divergent Environments. *Infect. Immun.* **86** (2018), doi:10.1128/IAI.00631-17.

226. A. M. Jorge, J. Schneider, S. Unsleber, G. Xia, C. Mayer, A. Peschel, Staphylococcus aureus counters phosphate limitation by scavenging wall teichoic acids from other staphylococci via the teichoicase GlpQ. *J. Biol. Chem.* **293**, 14916–14924 (2018).

227. J. L. Kelliher, A. J. Leder Macek, K. M. Grudzinski, J. N. Radin, T. E. Kehl-Fie, Staphylococcus aureus Preferentially Liberates Inorganic Phosphate from Organophosphates in Environments where This Nutrient Is Limiting. *J. Bacteriol.* **202** (2020), doi:10.1128/JB.00264-20.

228. J. L. Kelliher, E. B. Brazel, J. N. Radin, E. S. Joya, P. K. Párraga Solórzano, S. L. Neville, C. A. McDevitt, T. E. Kehl-Fie, Disruption of Phosphate Homeostasis Sensitizes Staphylococcus aureus to Nutritional Immunity. *Infect. Immun.* **88** (2020), doi:10.1128/IAI.00102-20.

229. N. P. Vitko, M. R. Grosser, D. Khatri, T. R. Lance, A. R. Richardson, Expanded Glucose Import Capability Affords Staphylococcus aureus Optimized Glycolytic Flux during Infection. *MBio*. **7** (2016), doi:10.1128/mBio.00296-16.

230. M. R. Sadykov, V. C. Thomas, D. D. Marshall, C. J. Wenstrom, D. E. Moormeier, T. J. Widhelm, A. S. Nuxoll, R. Powers, K. W. Bayles, Inactivation of the Pta-AckA pathway causes cell death in Staphylococcus aureus. *J. Bacteriol.* **195**, 3035–3044 (2013).

231. G. A. Somerville, B. Saïd-Salim, J. M. Wickman, S. J. Raffel, B. N. Kreiswirth, J. M. Musser, Correlation of acetate catabolism and growth yield in Staphylococcus aureus: implications for host-pathogen interactions. *Infect. Immun.* **71**, 4724–4732 (2003).

232. J. M. Reed, S. Olson, D. F. Brees, C. E. Griffin, R. A. Grove, P. J. Davis, S. D. Kachman, J. Adamec, G. A. Somerville, Coordinated regulation of transcription by CcpA and the Staphylococcus aureus two-component system HptRS. *PLoS ONE*. **13**, e0207161 (2018).

233. M. K. Lehman, A. S. Nuxoll, K. J. Yamada, T. Kielian, S. D. Carson, P. D. Fey, Protease-Mediated Growth of Staphylococcus aureus on Host Proteins Is opp3 Dependent. *MBio*. **10** (2019), doi:10.1128/mBio.02553-18.

234. A. Hiron, E. Borezée-Durant, J.-C. Piard, V. Juillard, Only one of four oligopeptide transport systems mediates nitrogen nutrition in Staphylococcus aureus. *J. Bacteriol.* **189**, 5119–5129 (2007).

235. C. R. Halsey, S. Lei, J. K. Wax, M. K. Lehman, A. S. Nuxoll, L. Steinke, M. Sadykov, R. Powers, P. D. Fey, Amino Acid Catabolism in Staphylococcus aureus and the Function of Carbon Catabolite Repression. *MBio*. **8** (2017), doi:10.1128/mBio.01434-16.

236. M. S. Zeden, Ó. Burke, M. Vallely, C. Fingleton, J. P. O'Gara, Exploring amino acid and peptide transporters as therapeutic targets to attenuate virulence and antibiotic resistance in Staphylococcus aureus. *PLoS Pathog.* **17**, e1009093 (2021).

237. J. B. Parsons, M. W. Frank, P. Jackson, C. Subramanian, C. O. Rock, Incorporation of extracellular fatty acids by a fatty acid kinase-dependent pathway in Staphylococcus aureus. *Mol. Microbiol.* **92**, 234–245 (2014).

238. Z. DeMars, V. K. Singh, J. L. Bose, Exogenous Fatty Acids Remodel Staphylococcus aureus Lipid Composition through Fatty Acid Kinase. *J. Bacteriol.* **202** (2020), doi:10.1128/JB.00128-20.

239. W. N. Beavers, A. J. Monteith, V. Amarnath, R. L. Mernaugh, L. J. Roberts, W. J. Chazin, S. S. Davies, E. P. Skaar, Arachidonic Acid Kills Staphylococcus aureus through a Lipid Peroxidation Mechanism. *MBio*. **10** (2019), doi:10.1128/mBio.01333-19.

240. C. N. Krute, M. J. Ridder, N. A. Seawell, J. L. Bose, Inactivation of the exogenous fatty acid utilization pathway leads to increased resistance to unsaturated fatty acids in Staphylococcus aureus. *Microbiology (Reading, Engl)*. **165**, 197–207 (2019).

241. M. W. Frank, J. Yao, J. L. Batte, J. M. Gullett, C. Subramanian, J. W. Rosch, C. O. Rock, Host Fatty Acid Utilization by Staphylococcus aureus at the Infection Site. *MBio*. **11** (2020), doi:10.1128/mBio.00920-20.

242. P. C. Delekta, J. C. Shook, T. A. Lydic, M. H. Mulks, N. D. Hammer, Staphylococcus aureus Utilizes Host-Derived Lipoprotein Particles as Sources of Fatty Acids. *J. Bacteriol.* **200** (2018), doi:10.1128/JB.00728-17.

243. J. R. Fuller, N. P. Vitko, E. F. Perkowski, E. Scott, D. Khatri, J. S. Spontak, L. R. Thurlow, A. R. Richardson, Identification of a lactate-quinone oxidoreductase in Staphylococcus aureus that is essential for virulence. *Front. Cell. Infect. Microbiol.* **1**, 19 (2011).

244. T. G. Patton, K. C. Rice, M. K. Foster, K. W. Bayles, The Staphylococcus aureus cidC gene encodes a pyruvate oxidase that affects acetate metabolism and cell death in stationary phase. *Mol. Microbiol.* **56**, 1664–1674 (2005).

245. T. L. Kinkel, C. M. Roux, P. M. Dunman, F. C. Fang, The Staphylococcus aureus SrrAB two-component system promotes resistance to nitrosative stress and hypoxia. *MBio*. **4**, e00696-13 (2013).

246. A. Dmitriev, X. Chen, E. Paluscio, A. C. Stephens, S. K. Banerjee, N. P. Vitko, A. R. Richardson, The Intersection of the Staphylococcus aureus Rex and SrrAB Regulons: an Example of Metabolic Evolution That Maximizes Resistance to Immune Radicals. *MBio*. **12**, e0218821 (2021).

247. A. R. Richardson, S. J. Libby, F. C. Fang, A nitric oxide-inducible lactate dehydrogenase enables Staphylococcus aureus to resist innate immunity. *Science*. **319**, 1672–1676 (2008).

248. M. R. Grosser, E. Paluscio, L. R. Thurlow, M. M. Dillon, V. S. Cooper, T. H. Kawula, A. R. Richardson, Genetic requirements for Staphylococcus aureus nitric oxide resistance and virulence. *PLoS Pathog.* **14**, e1006907 (2018).

249. A. E. Stockland, C. L. San Clemente, Multiple forms of lactate dehydrogenase in Staphylococcus aureus. *J. Bacteriol.* **100**, 347–353 (1969).

250. M. Pagels, S. Fuchs, J. Pané-Farré, C. Kohler, L. Menschner, M. Hecker, P. J. McNamarra, M. C. Bauer, C. von Wachenfeldt, M. Liebeke, M. Lalk, G. Sander, C. von Eiff, R. A. Proctor, S. Engelmann, Redox sensing by a Rex-family repressor is involved in the regulation of anaerobic gene expression in Staphylococcus aureus. *Mol. Microbiol.* **76**, 1142–1161 (2010).

251. K. J. McLaughlin, C. M. Strain-Damerell, K. Xie, D. Brekasis, A. S. Soares, M. S. B. Paget, C. L. Kielkopf, Structural basis for NADH/NAD+ redox sensing by a Rex family repressor. *Mol. Cell*. **38**, 563–575 (2010).

252. N. P. Vitko, N. A. Spahich, A. R. Richardson, Glycolytic dependency of high-level nitric oxide resistance and virulence in Staphylococcus aureus. *MBio*. **6** (2015), doi:10.1128/mBio.00045-15.

253. S. L. Barker, H. A. Clark, S. F. Swallen, R. Kopelman, A. W. Tsang, J. A. Swanson, Ratiometric and fluorescence-lifetime-based biosensors incorporating cytochrome c' and the detection of extra- and intracellular macrophage nitric oxide. *Anal. Chem.* **71**, 1767–1772 (1999).

254. R. Leggett, P. Thomas, M. J. Marín, J. Gavrilovic, D. A. Russell, Imaging of compartmentalised intracellular nitric oxide, induced during bacterial phagocytosis, using a metalloprotein-gold nanoparticle conjugate. *Analyst*. **142**, 4099–4105 (2017).

255. H. Suzuki, T. Lefébure, P. P. Bitar, M. J. Stanhope, Comparative genomic analysis of the genus Staphylococcus including Staphylococcus aureus and its newly described sister species Staphylococcus simiae. *BMC Genomics*. **13**, 38 (2012).

256. N. A. Spahich, N. P. Vitko, L. R. Thurlow, B. Temple, A. R. Richardson, Staphylococcus aureus lactate- and malate-quinone oxidoreductases contribute to nitric oxide resistance and virulence. *Mol. Microbiol.* **100**, 759–773 (2016).

257. K. P. Acker, T. Wong Fok Lung, E. West, J. Craft, A. Narechania, H. Smith, K. O'Brien, A. M. Moustafa, C. Lauren, P. J. Planet, A. Prince, Strains of Staphylococcus aureus that Colonize and Infect Skin Harbor Mutations in Metabolic Genes. *iScience*. **19**, 281–290 (2019).

258. S. J. Gabryszewski, T. Wong Fok Lung, M. K. Annavajhala, K. L. Tomlinson, S. A. Riquelme, I. N. Khan, L. P. Noguera, M. Wickersham, A. Zhao, A. M. Mulenos, D. Peaper, J. L. Koff, A.-C. Uhlemann, A. Prince, Metabolic Adaptation in Methicillin-Resistant Staphylococcus aureus Pneumonia. *Am. J. Respir. Cell Mol. Biol.* **61**, 185–197 (2019).

259. M. Wickersham, S. Wachtel, T. Wong Fok Lung, G. Soong, R. Jacquet, A. Richardson, D. Parker, A. Prince, Metabolic Stress Drives Keratinocyte Defenses against Staphylococcus aureus Infection. *Cell Rep.* **18**, 2742–2751 (2017).

260. K. L. Tomlinson, T. W. F. Lung, F. Dach, M. K. Annavajhala, S. J. Gabryszewski, R. A. Groves, M. Drikic, N. J. Francoeur, S. H. Sridhar, M. L. Smith, S. Khanal, C. J. Britto, R. Sebra, I. Lewis, A.-C. Uhlemann, B. C. Kahl, A. S. Prince, S. A. Riquelme, Staphylococcus aureus induces an itaconate-dominated immunometabolic response that drives biofilm formation. *Nat. Commun.* **12**, 1399 (2021).

261. C. E. Heim, M. E. Bosch, K. J. Yamada, A. L. Aldrich, S. S. Chaudhari, D. Klinkebiel, C. M. Gries, A. A. Alqarzaee, Y. Li, V. C. Thomas, E. Seto, A. R. Karpf, T. Kielian, Lactate production by Staphylococcus aureus biofilm inhibits HDAC11 to reprogramme the host immune response during persistent infection. *Nat. Microbiol.* **5**, 1271–1284 (2020).

262. W. Abu-Ashour, L. Twells, J. Valcour, A. Randell, J. Donnan, P. Howse, J.-M. Gamble, The association between diabetes mellitus and incident infections: a systematic review and meta-analysis of observational studies. *BMJ Open Diabetes Res. Care*. **5**, e000336 (2017).

263. W. Abu-Ashour, L. K. Twells, J. E. Valcour, J.-M. Gamble, Diabetes and the occurrence of infection in primary care: a matched cohort study. *BMC Infect. Dis.* **18**, 67 (2018).

264. B. A. Lipsky, Y. P. Tabak, R. S. Johannes, L. Vo, L. Hyde, J. A. Weigelt, Skin and soft tissue infections in hospitalised patients with diabetes: culture isolates and risk factors associated with mortality, length of stay and cost. *Diabetologia*. **53**, 914–923 (2010).

265. J. Smit, M. Søgaard, H. C. Schønheyder, H. Nielsen, T. Frøslev, R. W. Thomsen, Diabetes and risk of community-acquired Staphylococcus aureus bacteremia: a population-based case-control study. *Eur. J. Endocrinol.* **174**, 631–639 (2016).

266. C. W. Farnsworth, E. M. Schott, A. Benvie, S. L. Kates, E. M. Schwarz, S. R. Gill, M. J. Zuscik, R. A. Mooney, Exacerbated Staphylococcus aureus Foot Infections in Obese/Diabetic Mice Are Associated with Impaired Germinal Center Reactions, Ig Class Switching, and Humoral Immunity. *J. Immunol.* **201**, 560–572 (2018).

267. F. Hanses, S. Park, J. Rich, J. C. Lee, Reduced neutrophil apoptosis in diabetic mice during staphylococcal infection leads to prolonged Tnfα production and reduced neutrophil clearance. *PLoS ONE*. **6**, e23633 (2011).

268. K. T. Nguyen, A. K. Seth, S. J. Hong, M. R. Geringer, P. Xie, K. P. Leung, T. A. Mustoe, R. D. Galiano, Deficient cytokine expression and neutrophil oxidative burst contribute to impaired cutaneous wound healing in diabetic, biofilm-containing chronic wounds. *Wound Repair Regen.* **21**, 833–841 (2013).

269. S. Park, J. Rich, F. Hanses, J. C. Lee, Defects in innate immunity predispose C57BL/6J-Leprdb/Leprdb mice to infection by Staphylococcus aureus. *Infect. Immun.* **77**, 1008–1014 (2009).

270. D.-F. Zhang, X.-Y. Zhi, J. Zhang, G. C. Paoli, Y. Cui, C. Shi, X. Shi, Preliminary comparative genomics revealed pathogenic potential and international spread of Staphylococcus argenteus. *BMC Genomics*. **18**, 808 (2017).

271. M. Thoendel, J. S. Kavanaugh, C. E. Flack, A. R. Horswill, Peptide signaling in the staphylococci. *Chem. Rev.* **111**, 117–151 (2011).

272. B. Wang, A. Zhao, Q. Xie, P. D. Olinares, B. T. Chait, R. P. Novick, T. W. Muir, Functional plasticity of the agrc receptor histidine kinase required for staphylococcal virulence. *Cell Chem. Biol.* **24**, 76–86 (2017).

273. B. Kelly, L. A. J. O'Neill, Metabolic reprogramming in macrophages and dendritic cells in innate immunity. *Cell Res.* **25**, 771–784 (2015).

274. A. J. Freemerman, A. R. Johnson, G. N. Sacks, J. J. Milner, E. L. Kirk, M. A. Troester, A. N. Macintyre, P. Goraksha-Hicks, J. C. Rathmell, L. Makowski, Metabolic reprogramming of macrophages: glucose transporter 1 (GLUT1)-mediated glucose metabolism drives a proinflammatory phenotype. *J. Biol. Chem.* **289**, 7884–7896 (2014).

275. M. Bischoff, B. Wonnenberg, N. Nippe, N. J. Nyffenegger-Jann, M. Voss, C. Beisswenger, C. Sunderkötter, V. Molle, Q. T. Dinh, F. Lammert, R. Bals, M. Herrmann, G. A.

Somerville, T. Tschernig, R. Gaupp, CcpA Affects Infectivity of Staphylococcus aureus in a Hyperglycemic Environment. *Front. Cell. Infect. Microbiol.* **7**, 172 (2017).

276. K. Seidl, M. Stucki, M. Ruegg, C. Goerke, C. Wolz, L. Harris, B. Berger-Bächi, M. Bischoff, Staphylococcus aureus CcpA affects virulence determinant production and antibiotic resistance. *Antimicrob. Agents Chemother.* **50**, 1183–1194 (2006).

277. E. K. Sully, N. Malachowa, B. O. Elmore, S. M. Alexander, J. K. Femling, B. M. Gray, F. R. DeLeo, M. Otto, A. L. Cheung, B. S. Edwards, L. A. Sklar, A. R. Horswill, P. R. Hall, H. D. Gresham, Selective chemical inhibition of agr quorum sensing in Staphylococcus aureus promotes host defense with minimal impact on resistance. *PLoS Pathog.* **10**, e1004174 (2014).

278. A. J. Loughran, D. N. Atwood, A. C. Anthony, N. S. Harik, H. J. Spencer, K. E. Beenken, M. S. Smeltzer, Impact of individual extracellular proteases on Staphylococcus aureus biofilm formation in diverse clinical isolates and their isogenic sarA mutants. *Microbiologyopen*. **3**, 897–909 (2014).

279. L. R. Thurlow, G. S. Joshi, A. R. Richardson, Peroxisome Proliferator-Activated Receptor γ Is Essential for the Resolution of Staphylococcus aureus Skin Infections. *Cell Host Microbe*. **24**, 261-270.e4 (2018).

280. A. W. Maresso, O. Schneewind, Iron acquisition and transport in Staphylococcus aureus. *Biometals*. **19**, 193–203 (2006).

281. J. E. Cassat, E. P. Skaar, Metal ion acquisition in Staphylococcus aureus: overcoming nutritional immunity. *Semin. Immunopathol.* **34**, 215–235 (2012).

282. J. L. Hine, S. de Lusignan, D. Burleigh, S. Pathirannehelage, A. McGovern, P. Gatenby, S. Jones, D. Jiang, J. Williams, A. J. Elliot, G. E. Smith, J. Brownrigg, R. Hinchliffe, N. Munro, Association between glycaemic control and common infections in people with Type 2 diabetes: a cohort study. *Diabet. Med.* **34**, 551–557 (2017).

283. D. Schuster, J. Rickmeyer, M. Gajdiss, T. Thye, S. Lorenzen, M. Reif, M. Josten, C. Szekat, L. D. R. Melo, R. M. Schmithausen, F. Liégeois, H.-G. Sahl, J.-P. J. Gonzalez, M. Nagel, G. Bierbaum, Differentiation of Staphylococcus argenteus (formerly: Staphylococcus aureus clonal complex 75) by mass spectrometry from S. aureus using the first strain isolated from a wild African great ape. *Int. J. Med. Microbiol.* **307**, 57–63 (2017).

284. A. D. Yeap, K. Woods, D. A. B. Dance, B. Pichon, S. Rattanavong, V. Davong, R. Phetsouvanh, P. N. Newton, N. Shetty, A. M. Kearns, Molecular Epidemiology of Staphylococcus aureus Skin and Soft Tissue Infections in the Lao People's Democratic Republic. *Am. J. Trop. Med. Hyg.* **97**, 423–428 (2017).

285. S. R. Somarajan, J. H. Roh, K. V. Singh, G. M. Weinstock, B. E. Murray, CcpA is important for growth and virulence of Enterococcus faecium. *Infect. Immun.* **82**, 3580–3587 (2014).

286. L. A. Vega, H. Malke, K. S. McIver, in *Streptococcus pyogenes : Basic Biology to Clinical Manifestations*, J. J. Ferretti, D. L. Stevens, V. A. Fischetti, Eds. (University of Oklahoma Health Sciences Center, Oklahoma City (OK), 2016).

287. N. S. Kumar, E. M. Dullaghan, B. B. Finlay, H. Gong, N. E. Reiner, J. Jon Paul Selvam, L. M. Thorson, S. Campbell, N. Vitko, A. R. Richardson, R. Zoraghi, R. N. Young, Discovery and optimization of a new class of pyruvate kinase inhibitors as potential therapeutics for the treatment of methicillin-resistant Staphylococcus aureus infections. *Bioorg. Med. Chem.* **22**, 1708–1725 (2014).

288. J. M. Yarwood, J. K. McCormick, P. M. Schlievert, Identification of a novel two-component regulatory system that acts in global regulation of virulence factors of Staphylococcus aureus. *J. Bacteriol.* **183**, 1113–1123 (2001).

289. M. E. Wörmann, N. T. Reichmann, C. L. Malone, A. R. Horswill, A. Gründling, Proteolytic cleavage inactivates the Staphylococcus aureus lipoteichoic acid synthase. *J. Bacteriol.* **193**, 5279–5291 (2011).

290. L. R. Thurlow, M. L. Hanke, T. Fritz, A. Angle, A. Aldrich, S. H. Williams, I. L. Engebretsen, K. W. Bayles, A. R. Horswill, T. Kielian, Staphylococcus aureus biofilms prevent macrophage phagocytosis and attenuate inflammation in vivo. *J. Immunol.* **186**, 6585–6596 (2011).

291. P. L. Graham, S. X. Lin, E. L. Larson, A U.S. population-based survey of Staphylococcus aureus colonization. *Ann. Intern. Med.* **144**, 318–325 (2006).

292. V. Vella, I. Galgani, L. Polito, A. K. Arora, C. B. Creech, M. Z. David, F. D. Lowy, N. Macesic, J. P. Ridgway, A.-C. Uhlemann, F. Bagnoli, Staphylococcus aureus Skin and Soft Tissue Infection Recurrence Rates in Outpatients: A Retrospective Database Study at 3 US Medical Centers. *Clin. Infect. Dis.* **73**, e1045–e1053 (2021).

293. A. Schmidt, S. Bénard, S. Cyr, Hospital Cost of Staphylococcal Infection after Cardiothoracic or Orthopedic Operations in France: A Retrospective Database Analysis. *Surg Infect (Larchmt).* **16**, 428–435 (2015).

294. T. Horino, S. Hori, Metastatic infection during Staphylococcus aureus bacteremia. *J. Infect. Chemother.* **26**, 162–169 (2020).

295. H. F. L. Wertheim, D. C. Melles, M. C. Vos, W. van Leeuwen, A. van Belkum, H. A. Verbrugh, J. L. Nouwen, The role of nasal carriage in Staphylococcus aureus infections. *Lancet Infect. Dis.* **5**, 751–762 (2005).

296. S. Bhakdi, J. Tranum-Jensen, Alpha-toxin of Staphylococcus aureus. *Microbiol. Rev.* **55**, 733–751 (1991).

297. J. Deutscher, E. Küster, U. Bergstedt, V. Charrier, W. Hillen, Protein kinase-dependent HPr/CcpA interaction links glycolytic activity to carbon catabolite repression in gram-positive bacteria. *Mol. Microbiol.* **15**, 1049–1053 (1995).

298. A. K. Crooke, J. R. Fuller, M. W. Obrist, S. E. Tomkovich, N. P. Vitko, A. R. Richardson, CcpA-independent glucose regulation of lactate dehydrogenase 1 in Staphylococcus aureus. *PLoS ONE*. **8**, e54293 (2013).

299. K. Seidl, M. Bischoff, B. Berger-Bächi, CcpA mediates the catabolite repression of tst in Staphylococcus aureus. *Infect. Immun.* **76**, 5093–5099 (2008).

300. C. D. Majerczyk, P. M. Dunman, T. T. Luong, C. Y. Lee, M. R. Sadykov, G. A. Somerville, K. Bodi, A. L. Sonenshein, Direct targets of CodY in Staphylococcus aureus. *J. Bacteriol.* **192**, 2861–2877 (2010).

301. C. P. Montgomery, S. Boyle-Vavra, A. Roux, K. Ebine, A. L. Sonenshein, R. S. Daum, CodY deletion enhances in vivo virulence of community-associated methicillin-resistant Staphylococcus aureus clone USA300. *Infect. Immun.* **80**, 2382–2389 (2012).

302. A. Roux, D. A. Todd, J. V. Velázquez, N. B. Cech, A. L. Sonenshein, CodY-mediated regulation of the Staphylococcus aureus Agr system integrates nutritional and population density signals. *J. Bacteriol.* **196**, 1184–1196 (2014).

303. C. D. Majerczyk, M. R. Sadykov, T. T. Luong, C. Lee, G. A. Somerville, A. L. Sonenshein, Staphylococcus aureus CodY negatively regulates virulence gene expression. *J. Bacteriol.* **190**, 2257–2265 (2008).

304. S. R. Brinsmade, CodY, a master integrator of metabolism and virulence in Gram-positive bacteria. *Curr. Genet.* **63**, 417–425 (2017).

305. A. R. Richardson, G. A. Somerville, A. L. Sonenshein, Regulating the Intersection of Metabolism and Pathogenesis in Gram-positive Bacteria. *Microbiol. Spectr.* **3** (2015), doi:10.1128/microbiolspec.MBP-0004-2014.

306. A. L. Sonenshein, CodY, a global regulator of stationary phase and virulence in Gram-positive bacteria. *Curr. Opin. Microbiol.* **8**, 203–207 (2005).

307. L. R. Thurlow, A. C. Stephens, K. E. Hurley, A. R. Richardson, Lack of nutritional immunity in diabetic skin infections promotes Staphylococcus aureus virulence. *Sci. Adv.* **6** (2020), doi:10.1126/sciadv.abc5569.

308. P. A. Pattee, D. S. Neveln, Transformation analysis of three linkage groups in Staphylococcus aureus. *J. Bacteriol.* **124**, 201–211 (1975).

309. K. L. Krausz, J. L. Bose, Bacteriophage Transduction in Staphylococcus aureus: Broth-Based Method. *Methods Mol. Biol.* **1373**, 63–68 (2016).

310. M. R. Grosser, A. Weiss, L. N. Shaw, A. R. Richardson, Regulatory Requirements for Staphylococcus aureus Nitric Oxide Resistance. *J. Bacteriol.* **198**, 2043–2055 (2016).

311. H. S. Sader, R. E. Mendes, R. N. Jones, R. K. Flamm, Antimicrobial susceptibility patterns of community- and hospital-acquired methicillin-resistant Staphylococcus aureus from

United States Hospitals: results from the AWARE Ceftaroline Surveillance Program (2012-2014). *Diagn. Microbiol. Infect. Dis.* **86**, 76–79 (2016).

312. D. P. Calfee, Trends in Community Versus Health Care-Acquired Methicillin-Resistant Staphylococcus aureus Infections. *Curr. Infect. Dis. Rep.* **19**, 48 (2017).

313. M. Melzer, C. Welch, Thirty-day mortality in UK patients with community-onset and hospital-acquired meticillin-susceptible Staphylococcus aureus bacteraemia. *J. Hosp. Infect.* **84**, 143–150 (2013).

314. M. L. Jones, J. G. Ganopolsky, A. Labbé, C. Wahl, S. Prakash, Antimicrobial properties of nitric oxide and its application in antimicrobial formulations and medical devices. *Appl. Microbiol. Biotechnol.* **88**, 401–407 (2010).

315. C. Bogdan, Nitric oxide synthase in innate and adaptive immunity: an update. *Trends Immunol.* **36**, 161–178 (2015).

316. H. Rosenberg, R. G. Gerdes, K. Chegwidden, Two systems for the uptake of phosphate in Escherichia coli. *J. Bacteriol.* **131**, 505–511 (1977).

317. N. N. Rao, A. Torriani, Molecular aspects of phosphate transport in Escherichia coli. *Mol. Microbiol.* **4**, 1083–1090 (1990).

318. Y. Qi, Y. Kobayashi, F. M. Hulett, The pst operon of Bacillus subtilis has a phosphate-regulated promoter and is involved in phosphate transport but not in regulation of the pho regulon. *J. Bacteriol.* **179**, 2534–2539 (1997).

319. G. R. Willsky, M. H. Malamy, Characterization of two genetically separable inorganic phosphate transport systems in Escherichia coli. *J. Bacteriol.* **144**, 356–365 (1980).

320. R. M. Harris, D. C. Webb, S. M. Howitt, G. B. Cox, Characterization of PitA and PitB from Escherichia coli. *J. Bacteriol.* **183**, 5008–5014 (2001).

321. M. Lebens, P. Lundquist, L. Söderlund, M. Todorovic, N. I. A. Carlin, The nptA gene of Vibrio cholerae encodes a functional sodium-dependent phosphate cotransporter homologous to the type II cotransporters of eukaryotes. *J. Bacteriol.* **184**, 4466–4474 (2002).

322. R. Cunin, N. Glansdorff, A. Piérard, V. Stalon, Biosynthesis and metabolism of arginine in bacteria. *Microbiol. Rev.* **50**, 314–352 (1986).

323. J. Makhlin, T. Kofman, I. Borovok, C. Kohler, S. Engelmann, G. Cohen, Y. Aharonowitz, Staphylococcus aureus ArcR controls expression of the arginine deiminase operon. *J. Bacteriol.* **189**, 5976–5986 (2007).

324. S. M. Carvalho, A. de Jong, T. G. Kloosterman, O. P. Kuipers, L. M. Saraiva, The Staphylococcus aureus α-Acetolactate Synthase ALS Confers Resistance to Nitrosative Stress. *Front. Microbiol.* **8**, 1273 (2017).

325. S.-J. Ahn, K. Deep, M. E. Turner, I. Ishkov, A. Waters, S. J. Hagen, K. C. Rice, Characterization of LrgAB as a stationary phase-specific pyruvate uptake system in Streptococcus mutans. *BMC Microbiol.* **19**, 223 (2019).

326. J. L. Endres, S. S. Chaudhari, X. Zhang, J. Prahlad, S.-Q. Wang, L. A. Foley, S. Luca, J. L. Bose, V. C. Thomas, K. W. Bayles, The Staphylococcus aureus CidA and LrgA Proteins Are Functional Holins Involved in the Transport of By-Products of Carbohydrate Metabolism. *MBio*, e0282721 (2022).

327. M. R. Grosser, A. R. Richardson, Method for Preparation and Electroporation of S. aureus and S. epidermidis. *Methods Mol. Biol.* **1373**, 51–57 (2016).

328. I. Bekeredjian-Ding, C. Stein, J. Uebele, The Innate Immune Response Against Staphylococcus aureus. *Curr. Top. Microbiol. Immunol.* **409**, 385–418 (2017).

329. J. Purves, A. Cockayne, P. C. E. Moody, J. A. Morrissey, Comparison of the regulation, metabolic functions, and roles in virulence of the glyceraldehyde-3-phosphate dehydrogenase homologues gapA and gapB in Staphylococcus aureus. *Infect. Immun.* **78**, 5223–5232 (2010).

330. T. Doan, S. Aymerich, Regulation of the central glycolytic genes in Bacillus subtilis: binding of the repressor CggR to its single DNA target sequence is modulated by fructose-1,6-bisphosphate. *Mol. Microbiol.* **47**, 1709–1721 (2003).

331. C. Condon, D. H. Bechhofer, Regulated RNA stability in the Gram positives. *Curr. Opin. Microbiol.* **14**, 148–154 (2011).

332. M.-P. Caron, D. A. Lafontaine, E. Massé, Small RNA-mediated regulation at the level of transcript stability. *RNA Biol.* **7**, 140–144 (2010).

333. G. R. Hartmann, P. Heinrich, M. C. Kollenda, B. Skrobranek, M. Tropschug, W. Weiß, Molecular mechanism of action of the antibiotic rifampicin. *Angew. Chem. Int. Ed. Engl.* **24**, 1009–1014 (1985).

334. R. K. Carroll, A. Weiss, W. H. Broach, R. E. Wiemels, A. B. Mogen, K. C. Rice, L. N. Shaw, Genome-wide Annotation, Identification, and Global Transcriptomic Analysis of Regulatory or Small RNA Gene Expression in Staphylococcus aureus. *MBio*. **7** (2015), doi:10.1128/mBio.01990-15.

335. S. Carleton, S. J. Projan, S. K. Highlander, S. M. Moghazeh, R. P. Novick, Control of pT181 replication II. Mutational analysis. *EMBO J.* **3**, 2407–2414 (1984).

336. P. Z. Wang, V. B. Henriquez, S. J. Projan, S. Iordanescu, R. P. Novick, The effect of plasmid copy number mutations on pT181 replication initiator protein expression. *Plasmid*. **25**, 198–207 (1991).